IDENTIFICATION AND CHARACTERIZATION OF NOVEL ACTIVITIES FROM PLANT STEM CELL EXTRACTS REGULATING EPIDERMAL CELL PROLIFERATION AND HOMEOSTASIS

Orsola di Martino

Dottorato in Scienze Biotecnologiche 27° ciclo
Dottorato in azienda
Indirizzo Biotecnologie Molecolari ed Industriali
Università di Napoli Federico II

Dottorato in Scienze Biotecnologiche 27°ciclo
Indirizzo Biotecnologie Molecolari ed Industriali
Università di Napoli Federico II

IDENTIFICATION AND CHARACTERIZATION OF NOVEL ACTIVITIES FROM PLANT STEM CELL EXTRACTS REGULATING EPIDERMAL CELL PROLIFERATION AND HOMEOSTASIS

Orsola di Martino

Dottorando: Orsola di Martino

Relatore: Viola Calabrò

Tutor aziendale: Dott.ssa Annalisa Tito

Coordinatore: Prof. Giovanni Sannia

INDICE

Riassunto

La mia attività di dottorato si è articolata in due fasi distinte, la prima svolta presso il laboratorio di Genetica Molecolare dell'Università di Napoli "Federico II", sotto la supervisione della Prof.ssa Viola Calabrò, la seconda improntata sulla ricerca applicativa e svolta presso i laboratori dell'azienda Arterra Bioscience Srl. Questa parte del mio percorso formativo mi ha dato l'opportunità di avere un reale ed effettivo contatto con quelli che sono gli aspetti che caratterizzano la ricerca di tipo aziendale.

L'Arterra Bioscience Srl è un'azienda italiana basata sulla ricerca biotecnologica con una forte conoscenza di base nel settore della biologia e una vasta esperienza nella ricerca di molecole bio-attive.

Il filo conduttore della mia attività di dottorato è stato quello di studiare i processi di proliferazione, rigenerazione e differenziamento dell'epidermide, attraverso differenti approcci sperimentali. Per questo motivo la mia attività di ricerca aziendale è stata finalizzata alla identificazione di nuovi principi attivi derivanti da estratti di cellule staminali vegetali che svolgessero un'attività di controllo sui processi di idratazione, rigenerazione e differenziamento della pelle. L'azienda Arterra Bioscience Srl rappresenta una valida fonte di prodotti bioattivi già utilizzati nel settore della cosmetica per i loro benefici effetti nei processi di protezione, idratazione e rigenerazione della pelle.

La pelle rappresenta il più grande organo del corpo dei mammiferi e costituisce la principale barriera difensiva del corpo da fattori esterni di differente natura. Lo strato più superficiale della pelle è l'epidermide, un epitelio pluristratificato composto principalmente da strati di cheratinociti, ma anche da altri tipi cellulari, quali: i melanociti, le cellule di Langerhans e le cellule di Merkel. I cheratinociti a loro volta si dividono in cheratinociti proliferanti nello strato basale ed in cheratinociti differenziati nello strato sopra-basale (Candi E. et al. 2005). Nello strato basale sono immerse anche delle cellule staminali a cui si deve la capacità della pelle di auto-rigenerarsi. La capacità autorigenerativa della pelle richiede un corretto equilibrio tra il programma di proliferazione, differenziamento e morte cellulare (Fuchs et al. 2002). Tuttavia, fattori ambientali e genetici possono alterare il normale turnover dei cheratinociti, e determinare la comparsa di differenti condizioni patologiche, quali: proliferazione incontrollata (carcinoma delle cellule basali e squamose), infiammazione dell'epidermide (dermatite atopica e psioriasi) ed invecchiamento prematuro.

Ad Arterra erano già presenti colture di cellule staminali di *Hibiscus syriacus* e *Betula pendula* in quanto queste due piante, dai dati presenti in letteratura, sembravano avere benefici effetti sui meccanismi di controllo dell'omeostasi cellulare. Infatti, l'acido betulinico (3β, hydroxyl-lup-20(29)-en-28oic acid) è un prodotto naturale con un ampio spettro di attività biologiche, tra cui l' attività antitumorale (Fulda 2008). In più è stato dimostrato che l'olio ottenuto dalla corteccia di Betula pendula è già utilizzato nel trattamento di patologie infiammatorie, quali l'eczema e la psoriasi. Invece, la corteccia radicale di *Hibiscus syriacus* è nota in Asia per le sue attività

antipiretiche, antielmintiche e antifungine mentre l'estratto di *Hibiscus syriacus* è noto per la sua capacità antiossidante (Kwon SW et al. 2003) e mostra effetti antiproliferativi sui carcinomi polmonari umani (Cheng YL et al. 2008) .

Nella prima fase del mio periodo in azienda, mi sono occupata della preparazione di due tipologie di estratti da culture di cellule staminali vegetali, ottenendo un estratto alcolico ed uno idrosolubile per ciascuna coltura. Infatti, nella produzione industriale la possibilità di usare differenti solventi e procedure di estrazione risulta vantaggiosa per produrre estratti con contenuti differenti di alcuni principi bio-attivi sulla base della loro differente solubilità. Ho poi caratterizzato in base alle loro proprietà biochimiche le due diverse tipologie di estratto, determinando per ciascuna la quantità totale di proteine, la quantità totale di zuccheri, la quantità totale di polifenoli ed infine la loro capacità antiossidante mediante un saggio ORAC. Ho infine determinato la concentrazione di utilizzo di tali estratti nei sistemi cellulari da me selezionati, quali i cheratinociti umani immortalizzati ma non trasformati (cellule HaCaT) ed in fibroblasti umani primari (cellule HDF) mediante un saggio MTT che mi ha permesso di valutare l'effetto citotossico o pro-proliferativo delle differenti concentrazioni di estratto.

Nella fase successiva ho valutato gli effetti degli estratti alcolici e idrosolubili di *Betula p.* e *Hybiscus s*. sulla regolazione dell'espressione di geni coinvolti nell'idratazione dell'epidermide, ed in particolare sul gene dell'aquaporina 3 (AQP3) e della filagrina (FLG). Le aquaporine sono una famiglia di proteine transmembrana, che funzionano da canali per il trasporto di acqua ed altri soluti attraverso la membrana plasmatica, risultando fondamentali per l'idratazione dell'epidermide (Verkman AS et al. 2012). In particolare, l'Aquaporina-3 (AQP3) è la più abbondante nella pelle dei mammiferi. La filagrina è una proteina strutturale responsabile dell'integrità degli strati superiori della pelle e della loro capacità di trattenere l'acqua (Pereda MCV et al. 2010). I risultati ottenuti mediante PCR semi-quantitativa, indicano chiaramente che il trattamento delle cellule HaCaT con entrambi gli estratti, ma in particolare con gli estratti di *Betula p*., promuove la trascrizione di AQP3 e FLG suggerendo quindi che tali estratti possano trovare applicazione in tutti i processi che richiedano riequilibrio della idratazione cutanea.

La rigenerazione della pelle è un processo patologico dinamico e finemente regolato da segnali intra ed extra- cellulari, che sono fondamentali per la sostituzione dei tessuti danneggiati con nuovi tessuti (H. Sinno et al. 2013). Mediante un saggio di *Wound Healig* ho osservato che gli estratti di *Betula p*. non hanno mostrato effetti considerevoli sul fenomeno della rigenerazione sia su cellule HaCaT che sui fibroblasti HDF, mentre l'estratto alcolico di *Hibiscus s*. si è dimostrato efficace nel favorire il processo di riparo in ambedue i contesti cellulari. In particolare, mediante saggi ELISA, ho dimostrato che l'estratto alcolico di *Hibiscus s*. è in grado di favorire la produzione della fibronectina, una proteina adesiva che gioca un ruolo fondamentale nel processo di rigenerazione della matrice extracellulare (ECM).

In seguito, ho analizzato la capacità dell'estratto alcolico di *Hibiscus s.* di incrementare la contrattilità dei fibroblasti mediante un saggio tridimensionale di contrazione del collagene. Infatti, i fibroblasti giocano un ruolo fondamentale nel processo di rigenerazione della pelle, poiché secernono chemochine, fattori di

crescita e proteine dell'ECM che sono necessarie per l'infiltrazione delle cellule nei processi di infiammazione e neo-angiogenesi (Singer AJ et al 1999). La contrazione del collagene è un fenomeno fondamentale in questo processo perché può ridurre la dimensione della ferita e facilitare il suo riparo (Martin P. 1997). Anche in questo caso, l'estratto alcolico di *Hibiscus s*. si è rivelato efficace ad incrementare la contrazione del collagene in cellule HDF.

Lo sviluppo ed il mantenimento dell'integrità e del riparo della pelle dipende anche dall'equilibrio tra la produzione ed la degradazione del pro-collagene di tipo I (Verrecchia F 2005). Mediante un saggi ELISA ho analizzato la produzione del pro-collagene di tipo I in cellule HDF in seguito al trattamento con l'estratto alcolico di *Hibiscus s*. osservando un incremento della sua produzione.

Infine, mediante PCR semi-quantitativa, ho analizzato l'effetto degli estratti di Betula p. ed *Hibiscus s*. sull'espressione dei geni che codificano per le laminine che giocano un ruolo fondamentale nell'architettura della membrana basale (Senyürek I et al. 2014). Ho osservato che sia *Betula p*. che *Hibiscus s*. incrementano l' espressione genica di LAM B che codifica per la catena β della laminina 5. Viceversa, non ho avuto risultati sull'espressione genica di LAM C che codifica per la catena γ della laminina 5.

I dati ottenuti durante il periodo trascorso in Arterra indicano chiaramente che l'estratto di *Betula p*. può essere un valido prodotto bioattivo da usare nel settore cosmetico per migliorare l'idratazione della pelle, mentre l'estratto alcolico di Hibiscus s. si è rivelato essere efficace nella stimolazione dei processi di rigenerazione della cute.

I processi di rigenerazione e riparo dell'epidermide sono un settore affascinante anche per la ricerca di base poiché coinvolge settori quali quello farmacologico, della genetica del differenziamento o del cancro. Durante la seconda fase della mia tesi, nel laboratorio della prof.ssa Viola Calabrò, ho avuto modo di studiare i meccanismi molecolari che governano i processi di rigenerazione e differenziamento dell'epidermide. Come detto in precedenza, l'omeostasi dell'epidermide dipende dall'equilibrio tra i processi di differenziamento, proliferazione e morte cellulare. I cheratinociti dello strato basale dell'epidermide mostrano un elevato potenziale proliferativo ed esprimono elevati livelli della proteina ΔNp63α. Durante il differenziamento dei cheratinociti l'espressione della proteina ΔNp63α decresce fino a scomparire (Barbieri et al. 2006).

Nel laboratorio della prof.ssa Viola Calabrò è stato dimostrato che ΔNp63α interagisce fisicamente col l'oncoproteina YB-1 (Di Costanzo et al. 2012). La proteina YB1 è fattore trascrizionale e traduzionale coinvolto in un ampio spettro di funzioni cellulari inclusi I processi di proliferazione, migrazione, riparo del DNA, resistenza ai farmaci e risposta allo stress (Annette LASHAM et al. 2013). La proteina YB1 svolge le sue funzioni sia nel nucleo che nel citoplasma (Evdikomova et al. 2009). L'incremento della quantità di YB-1 nella cellula o la sua traslocazione dal citoplasma al nucleo sono tipiche della trasformazione tumorale. Tuttavia, i meccanismi che governano la localizzazione subcellulare della proteina YB-1 e la sua stabilità sono ancora in gran parte sconosciuti. Dato il grande potenziale che YB-1 potrebbe avere

nel controllare il differenziamento e la proliferazione dei cheratinociti, ho esaminato dettagliatamente la relazione funzionale tra YB-1 e ΔNp63α.

Ho proceduto analizzando il pattern di espressione di YB-1 durante il processo di differenziamento indotto da Ca_2^+, sia nei cheratinociti umani primari (NHEK) che nelle cellule HaCaT, ed ho osservato che sia i livelli di ΔNp63α che di YB-1 decrescono bruscamente con l'avanzare del differenziamento. In seguito, portando le cellule HaCaT a confluenza ed inducendo un blocco della crescita mediante privazione del siero, ho osservato che i livelli di espressione di YB-1 e di ΔNp63α decrescono, e che tale diminuzione è associata ad un'uscita dal ciclo cellulare dimostrata da una riduzione della ciclina D1 e dall'induzione dell'inibitore del ciclo cellulare p21WAF. Contemporaneamente, nel mio laboratorio è stato dimostrato che il silenziamento di YB-1 nelle HaCaT e in cellule di cheratinociti trasformati porta ad una immediata e drammatica risposta apoptotica (Troiano et al. 2015). Questi dati dimostrano che YB-1 è essenziale per sostenere la proliferazione e la sopravvivenza dei cheratinociti basali.

In seguito, poichè ΔNp63α e YB-1 sono abbondantementi espressi nei cheratinociti basali proliferanti e ΔNp63α promuove l'accumulo della forma di 50kDa di YB-1 nel nucleo (Di Costanzo et al. 2012), ho ipotizzato che ΔNp63α potesse controllare la stabilità di YB-1. Mediante esperimenti condotti in presenza di cicloesimmide, un inibitore della traduzione, in cellule trasfettate e non con ΔNp63α ho osservato che ΔNp63α riduce il turnover della proteina YB-1.

Inoltre, ho osservato che la proteina YB-1 presenta una notevole quantità di forme ad alto peso molecolare. Per di più, in seguito alla trasfezione di quantità crescenti della proteina ΔNp63α in cellule MDA-MB 231 ho osservato un aumento della forma da 50 kDa e delle forme ad alto peso molecolare. Tali forme ad alto peso sono state riscontrate in tutte le linee cellulari testate (A431, SCC011, e HaCaT), ed inoltre sono state visualizzate utilizzando anticorpi anti-YB-1 diretti contro diversi epitopi della proteina.

Dopo aver verificato l'identità di queste forme modificate di YB-1 mediante esperimenti di silenziamento genico, ho dimostrato che esse sono localizzate prevalentemente nel compartimento nucleare e che l'espressione di ΔNp63α ne determina un ulteriore accumulo in tale compartimento subcellulare.

A questo punto ho proceduto valutando un possibile coinvolgimento del proteasoma sul turnover della proteina YB-1. Il trattamento delle cellule HaCaT con l'inibitore del proteasoma MG132 dimostra che la la proteina YB-1 è sottoposta all'attività proteolitica del proteasoma.

In letteratura è stato precedentemente dimostrato che YB-1 è poli-ubiquitinata (Lutz M. et al. 2006). Inoltre, la sequenza aminoacidica di YB-1 è ricca di lisine che sono potenziali siti di ubiquitinazione o sumoilazione. A tale scopo, ho trasfettato in cellule A431 ubiquitina coniugata all'epitopo HA e mediante esperimenti di immunoprecipitazione ho dimostrato che le forme ad alto peso di YB-1 sono poli-ubiquitinate. Sulla base dei miei dati non è possibile ancora escludere che la proteina possa subire ulteriori modifiche quali la sumoilazione o l'acetilazione. Infine,

ho dimostrato che in cellule MDA-MB 231 le forme ad alto peso molecolare di YB-1 incrementano significativamente in seguito alla co-trasfezione di ΔNp63α e ubiquitina, suggerendo un ruolo fondamentale di ΔNp63α non solo nell'accumulo della forma da 50 kDa di YB-1 ma anche delle sue forme modificate.

Tutti questi dati nel loro insieme indicano che YB-1 svolge un ruolo fondamentale nel processo di proliferazione dei cheratinociti basali e che ΔNp63α ne influenza significativamente la stabilità ed il "*turnover*".

Durante la mia attività di dottorato ho avuto anche la possibilità di trascorrere quattro mesi in Germania presso il Karlsruhe Institute of Technology (KIT) sotto la supervisione del Professore Nickolaus Foulkes, uno dei maggiori esperti della biologia di zebrafish (*danio rerio*). In questo periodo, ho avuto la possibilità di imparare a lavorare con un sistema modello come zebrafish e di caratterizzare l'espressione di YB-1 in questo organismo modello ed in colture cellulari di fibroblasti derivanti da zebrafish. Ho ottenuto chiare evidenze sperimentali che la localizzazione nucleare della proteina YB-1 in zebrafish è fortemente regolata dal ritmo circadiano, con un massimo picco di espressione all'inizio della fase luminosa e un minino durante la notte.

Il mio percorso formativo è stato estremamente interessante poiché mi ha dato l'opportunità, di poter studiare un solo processo biologico guardandolo da differenti prospettive ed usando approcci sperimentali diversi ma sicuramente complementari. Tale esperienza mi consentirà di effettuare le mie scelte future con una maggiore consapevolezza.

Summary

My PhD program included two phases, the first was carried out in the laboratory of Molecular Genetics, under the supervision of Professor Viola Calabrò, and the latter in the laboratory of Arterra Biosciene Srl.
Arterra Bioscience is an Italian research-based biotech company with a strong know-how in biological science and an extensive experience in screening for the discovery of active molecules.
The opportunity to join these two different scientific groups allows me to gain a more comprehensive experience including molecular biology and industrial biotechnology.
During my period in Arterra Bioscience Srl, I investigated whether *Betula pendula* and *Hybiscus syriacus* plant stem cells could have beneficial effects on several aspects of skin homeostasis. Surprisingly, I found that *Betula p*. extract can be a valuable bioactive ingredient to use in cosmetic field for improving skin hydration, on other hand *Hibiscus s.* extract turned out to be more efficient in stimulating skin regeneration.
The research about skin regeneration and differentiation is not only an appealing topic for biotechnological company, but also for molecular basic investigation. Indeed, in the laboratory of the professor Viola Calabrò, I had the possibility to study the molecular mechanisms governing skin regeneration and differentiation.
The epidermis is the outermost layer of the skin, a multistratified epithelium whose homeostasis depends on a balance between cell proliferation and differentiation. ΔNp63α is a critical pro-proliferative factor and a marker of epidermal stemness. We had previously shown that ΔNp63α physically interacts with YB-1 a multifunctional protein with a well assessed oncogenic potential (Di Costanzo et al. 2012).
Given the great potential that YB-1 may have in the control of keratinocyte proliferation, I have investigated in more details the functional relationships between YB-1 and ΔNp63α and provided clear evidences indicating that ΔNp63α plays a role in the control of YB-1 protein stability and turnover (di Martino et al. 2015 *in submission*).
Finally, I spent a period of four months abroad at the Karlsruhe Institute of Technology (KIT), Karlsruhe, Germany (April 2014- July 2014) under the supervision of Professor Nicholas S. Foulkes, one of the major expert in zebrafish biology.
During this period I demonstrated that YBX-1 protein is expressed in adult zebrafish fins and in the embryonic cell line (Pac2). Moreover, I obtained consistent evidences that YBX-1 nuclear localization and protein expression level is a circadian regulated protein. Indeed, under a light-dark cycle it shows a maximum peak of nuclear protein at the beginning of the light phase and a minimum trough during the beginning of the dark phase.
All these working experiences gave me the possibility to study different aspects of skin proliferation and differentiation, developing new bioactive molecules to use in the cosmetics field and studying more in detail the molecular mechanisms that regulate keratinocyte proliferation and differentiation.

Chapter 1

1.1 Aim of the thesis

In the last years, cosmetic industry is constantly looking for innovative products to use especially in skincare sector that amounts for approximately 80% of the total U.S. and European cosmeceutical market.

In particular, the cosmetics research field is focused on the discovery of natural compounds able to excite beneficial effects on skin hydration, elasticity or to counteract molecular pathways leading to skin damage and aging. For this reason the plant kingdom has been already selected as preferred source of natural products.

I spent part of my Ph.D project in Arterra Bioscience Srl an Italian research-based biotech company with a strong know-how in biological science and an extensive experience in screening for the discovery of active molecules. Arterra Bioscience Srl represents a valuable source of bioactive products that are already used in the cosmetic sector for their positive effect on skin protection, hydration and regeneration.
The principal aim of this work was then to first identify novel activities from plant stem cell extracts and subsequently to determine their biological properties particularly on skin proliferation, differentiation and hydration.

1.2 Introduction:

1.2.1 Epidermis: structure and function.

Skin is the largest organ of the mammalian organism and its direct defence from external factors (Elias PM et al. 2008). Healthy skin provides protection of the body from environmental factors: physical (mechanical trauma, thermal injury, radiation etc.), chemical (destructive agents, surface active substances, xenobiotics, allergens) and biological (bacteria, viruses, etc.), (Elias PM et al. 2005).The epidermis is a stratified epithelium that forms the outer layer of the skin, serving as the physical and chemical barrier between the interior body and exterior environment; it is mainly composed of layers of keratinocytes but also contains melanocytes, Langerhans cells and Merkel cells.

The formation of the different layers of the epidermis (stratification) occurs during the embryonic development, so that animals at birth already present a functional barrier (Pangiota et al. 2012).

The self-renewing ability of the epidermis requires an appropriate proliferation and differentiation program in the basal layer (Fuchs et al. 2002).

Basal stem cells proliferate to produce daughter transit amplifying (TA) cells having a limited proliferative potential, TA cells migrate upwards through the epidermis layers and begin to differentiate producing the external skin components (Koster MI et al. 2010).

Recent studies have established an important developmental role for p63 in formation of stratified epithelia. p63 is a transcription factor driving expression of proteins controlling cell proliferation, adhesion and apoptosis (Makoto Senoo et al. 2007). Moreover, it also induces tissue specific proteins such as keratins, involucrin and loricrin (Vigano MA et al.2009).

The relevance of p63 in skin development was mainly supported by the observation of the phenotype of knockout mice, that at birth lacked multilayered epithelia and skin appendages, such as teeth, hair follicles and mammary glands (McKeon F 2004).

Studies on mature epidermis led to the conclusion that p63 plays a dual role: initiating epithelial stratification during development and maintaining proliferative potential of basal keratinocytes in mature epidermis (Maranke I. Koster et 2004).

Environmental and genetic factors can alter normal keratinocytes turnover, and this alteration can generate different pathological conditions such as: uncontrolled hyper-proliferation (squamous and basal cell carcinoma), skin inflammation and premature aging (atopic dermatitis and psoriasis).

1.2.2 Epidermal Hydration: Role of AQP3 and FLG in skin hydration

The main function of the skin is to act as a barrier that maintains homeostasis by preventing the uncontrolled loss of water, ions and serum proteins from the organism into the environment (R. Darlenski. et al 2011). Water retention contributes to the skin elasticity and is a fundamental to have a healthy skin. In fact, water is one of the basic element of physiological processes in living organisms. In particular, the uncontrolled passage of water to the external environment is limited by the stratum corneum (SC) whose integrity acts as a barrier (Elias PM et al. 2006). The mechanical resistance of the epidermal barrier is mainly due to the corneocytes embedded in the so-called cornified envelope that is composed of keratins, corneodesmosin and the dynamically linked loricrin, involucrin and filaggrin (Elias PM et al. 2006).

The keratins form the intermediate filaments of the corneocyte cytoskeleton. The major keratins, expressed in the suprabasal layers are keratins 1, 2f and 10, representing about 80% of the corneocyte weight (Elias PM et al. 2006). Keratins 1 and 10 forming the corneocyte cytoskeleton are connected with desmoglein 1 and desmocollin 1 through desmosomal plaque proteins – plakoglobin and desmoplakins (Sprecher E et al.2001). The keratins are attached to the cornified envelope proteins surrounding the corneocyte, thus contributing to the stability of the epidermal barrier. Mutations in the gene responsible for the synthesis of keratin 1 in ichthyosis hystrix, leads to incomplete formation of intermediate filaments and impaired barrier function (Sprecher E et al.2001).

Filaggrin belongs to the family of the S100 Ca2+-binding proteins. The enzymatic transformation of profilaggrin located in keratohyalin granules in stratum granulosum, leads to the formation of two products filaggrin and N-terminal peptide (Elias PM et al. 2006). Filaggrin provides the formation of keratin filaments into macrofibrils in the lowest layers of stratum corneum (SC) (R. Darlenski. et al 2011). The filaggrin is an important source for maintaining skin moisture (Rawlings AV et al. 2005). By reaching the skin surface, filaggrin is degraded to free amino acids – the basic components of a highly absorbent complex called natural moisturizing factor (NMF) (Rawlings AV et al. 2006).
A small part of filaggrin binds to loricrin forming the corneocyte envelope (Candi et al. 2005). The N-terminal peptide is involved in regulation of the corneocyte programmed cell differentiation (Pearton DJ et al.2002).The enzymatic degradation of filaggrin is dependent also on the water content in SC (Casper PJ et al. 2003) . The reduced hydration of SC activates the filaggrin degradation to hygroscopic amino acids (the composition of the natural moisturizing factor) which retain water in the stratum corneum (Scott IR et al. 2006).

Impairment of this regulatory mechanism in ichthyosis vulgaris is associated with reduced levels of natural moisturizing factor and impaired skin barrier function (Madison KC et al. 2003). Mutations in the filaggrin gene are

associated with impaired barrier function in diseases such as ichthyosis vulgaris and atopic dermatitis (O'Regan GM et al. 2009).
Other proteins fundamental for the epidermal hydration are the aquaporins, a family of transmembrane channels transporting water and in some cases, small solutes across the plasma membrane driven by osmotic gradients (Verkman AS et al. 2012).
Aquaporin-3 (AQP3) is the predominant and most widely studied aquaporin in mammalian skin. It is an aquaglyceroporin which transports water, glycerol and small solutes across the plasma membrane (Verkman AS et al. 2012). Its functions are not limited to fluid transport but also involve the regulation of cell proliferation, migration, skin hydration, wound healing and tumorigenesis (Liogiong Guo et al. 2013).
The functions of AQP3 in skin have been defined from studies in AQP3-deficient mice. AQP3-mediated transport of glycerol plays an important role in hydration of stratum corneum, skin elasticity, barrier recovery, wound healing and cell proliferation whereas AQP3-mediated water transport is critical for cell migration (Hara-Chikuma M et al 2008).

1.2.3 Epidermal regeneration: Proteins involved in Wound Healing

Skin is always exposed to the external environment, therefore it is subjected to mechanical stress and injuries. The regeneration process by which the skin repairs itself after injury is named Wound healing (H. Sinno et al. 2013).The restoration of tissue integrity is the result of the interaction of neutrophils, monocytes/macrophages, fibroblasts, endothelial cells, and keratinocytes as well as extracellular matrix (ECM) components, such as fibronectin, glycosaminoglycans, proteoglycans, thrombospondins, tenascin, vitronectin, or collagens (K.S. Midwood et al. 2004).

ECM components play a significant role in each stage of the healing process. It concerns the structural biomechanical aspect of the process because they create a "scaffolding" (a temporary matrix, granulation tissue, and scar), which is indispensable in the repairing process, providing in this way a structural integrity of the matrix during each stage of the healing process (Pawel Olczyk et al 2013). Moreover, other functions are connected with stimulating the adhesion and migration of cells during the healing process as well as interactions among cells, between cells and the matrix, or between ECM proteins (Pawel Olczyk et al 2013).

Collagens, the main structural element of the ECM, provide tensile strength, regulate cell adhesion, support chemotaxis and migration, and direct tissue development (Rozario and DeSimone, 2010).

The bulk of interstitial collagen is transcribed and secreted by fibroblasts that either reside in the stroma or are recruited to it from neighbouring tissues (De Wever et al., 2008). By exerting tension on the matrix, fibroblasts are able to organize collagen fibrils into sheets and cables and, thus, can dramatically influence the alignment of collagen fibers. Although within a given tissue, collagen fibers are generally a heterogeneous mix of different types, one type

of collagen usually predominates (Christian Frantz et al 2010). Collagen associates with elastin, another major ECM fiber. Elastin fibers provide recoil to tissues that undergo repeated stretch. Importantly, elastin stretch is crucially limited by tight association with collagen fibrils (Wise and Weiss, 2009).

Fibronectin is an adhesive molecule that plays a crucial role in wound healing, particularly in extracellular matrix (ECM) formation and also in re-epithelialisation (Lenselink EA et al. 2013). Fibronectin plays many different roles in the wound healing process because of the presence of specific functional domains and binding sites in its structure (Lenselink EA et al. 2013). The main role of fibronectin is ECM formation. First, plasma fibronectin forms a provisional fibrin-fibronectin matrix, which will later be replaced by the mature ECM-containing tissue fibronectin (Lenselink EA et al. 2013). Moreover, Fibronectin can interact with different cell types and cytokines.

The laminins are a family of glycoproteins that provide an integral part of the structural scaffolding of basement membranes in almost every animal tissue Laminins contribute to the structure of the extracellular matrix (ECM), each laminin is a heterotrimer made of α, β, and γ chain subunits, secreted and incorporated into cell-associated extracellular matrices (Holly Colognato and Peter D. Yurchenco 2000).The laminins can self-assemble, bind to other matrix macromolecules, and have unique and shared cell interactions mediated by integrins, dystroglycan, and other receptors and through these interactions, laminins critically contribute to cell differentiation, cell shape and movement, maintenance of tissue phenotypes, and promotion of tissue survival (Holly Colognato and Peter D. Yurchenco 2000).

Since ancient times, search is on for suitable materials which may restore or reproduce a favourable and a natural milieu required for skin regeneration, so as to prevent infections, and make the process fast and less painful. The journey started with the use of natural materials with a simple function of covering or dressing the wounds. Advances in the field of biotechnology research has made it possible to produce more advanced materials and scaffolds, which are designed for specific and extraordinary functions. Natural and modified or synthetic polymers; alone or in combination are commonly used as dressing (couture) materials for wound healing.

1.2.4 Plant cell cultures as source of cosmetic active ingredients

Plants are notable for their high synthetic versatility: the spectrum of chemical structures synthesized by the plant kingdom is broader than that of any other group of organisms, which makes the plants the biggest source of natural remedies in the fields of pharmacy, food and cosmetics (Fowler 1984).

The two characteristics that most distinguish plants among all living organisms and are fundamental to understand plant tissue culturing are plasticity and totipotency. Plasticity is the capacity of the plants to change their metabolism, adapting their growth and development to the surrounding environmental conditions. In nature, plant cells are able to initiate cell division from almost

any tissue, to regenerate and switch on different biosynthetic and developmental pathways according to stress conditions.

Plant cell cultures provide useful alternatives for the production of active ingredients for cosmetic industry, since they represent standardized, contaminant-free and bio-sustainable systems, which allow the production of desired compounds on an industrial scale. Moreover, thanks to their totipotency, plant cells grown as liquid suspension cultures can be used as “biofactories” for the production of commercially interesting secondary metabolites, which are in many cases synthesized in low amounts in plant tissues and differentially distributed in the plant organs, such as roots, leaves, flowers or fruits (Barbulova et al. 2014).

In vitro plant cells have very high levels of plasticity as well, and are able to regenerate tissues, organs and even entire plants by a process of dedifferentiation and subsequent differentiation (Barbulova et al.2014). In addition, some undifferentiated totipotent cells are always present in the meristems located in the tips of shoots and roots or inside the vascular system, in order to obtain a fast cell division under proper stimuli (Lee, E. et al 2010). As Barbulova said, even though scientifically correct, it is generally redundant to use the term “stem” when talking about plants, since the totipotency is an intrinsic feature of each differentiated plant tissue belonging to adult plants and not only to embryonic developmental stages.

For this reasons, plant cell cultures certainly represent a valid alternative for the production of cosmetic active ingredients, since they always provide standardized, contaminant-free and bio-sustainable products, whose production can be easily extended to an industrial scale (Barbuolova et al. 2014).

1.2.5 Plant stem cell culture

The plant tissue culture technique is based on propagation of plant stem cells either to produce a whole plant, a tissue or just a single type of cells in culture to harvest plant metabolites. This practice allows the production of plant material under sterile and standardized conditions independent of season and other environmental restraints. Plant tissue cultures can be initiated from nearly all type of plant tissue called explant. As a kind of wound reaction, new cells are formed on the cut surfaces of the explant. The cells slowly divide to form a color-less cell mass which is called callus. Callus cells are stem cells comparable to those in the meristem regions. They are dedifferentiated and lack the distinctive features of normal plant cells. For high yield production callus cells can be cultured as individual cells or small cell clusters in a liquid culture (D. Schmid et al. 2008) The callus could be maintained in vitro practically for unlimited time using the appropriate growth medium. In practical terms though, identifying the culture conditions and stimuli required to manifest this totipotency can be extremely difficult and often entirely depends on the responsiveness of a certain plant species, thus it can be largely an empirical process (Barbulova et al. 2014). When callus cells are cultured in

liquid medium, they form a fast growing suspension culture of single cells or small clusters of cells (Moscatiello, R et al. 2013). Plant cell cultures grown in liquid media can now be up-scaled to much bigger volumes and employed for the production of commercially interesting compounds for industrial applications, including cosmetics.

1.2.6 Plant stem cell extracts

Different types of bio-active ingredients can be developed and produced from plant grown as a liquid suspension. As known, 55% of the plant cell volume consists of cell wall and membranes. The remaining is cytosol that consists of 90% water and contains the different cellular organelles. Various metabolites, with different chemical natures (for example, oil-soluble or water-soluble), are produced during the life cycle of the plants and then are stored in different cell compartments.
For this reason it's critical to select the appropriate plant cell extraction method in order to enrich the amount of the desired compounds with efficient activity. Using different solvents and extraction procedures allows to obtain more than one active ingredient from the same culture, resulting really advantageous in the industrial production scale (Barbulova et al 2014).
Generally, it's possible to obtain two different type of extracts from the same culture: water soluble (hydrosoluble) and oil-soluble (liposoluble). Each kind of extracts is enriched of different bio-active compounds with different properties.

1.3 Results

1.3.1 Identification and characterization of novel activitiesIdentification of *Betula pendula* and *Hibiscus syriacus*

In Arterra Bioscience Srl my PhD project partner are available a wide range of plant stem cell cultures. Moreover, Arterra Bioscience Srl is an Italian research-based biotech company with a strong know-how in biological science and an extensive experience in screening for the discovery of active molecules. In Arterra were already present *Betula pendula* and *Hibiscus syriacus* plant cell cultures, because these two species appear to be very interesting from a dermatological point of view.
In fact, the Betulinic acid (3β, hydroxyl-lup-20(29)-en-28oic acid), present in *Betula p*. is a natural product with a range of biological effects, for example potent antitumor activity. This anticancer property is linked to its ability to induce apoptotic cell death in cancer cells by triggering the mitochondrial pathway of apoptosis. In contrast to the cytotoxicity of betulinic acid against a variety of cancer types, normal cells and tissue are relatively resistant to betulinic acid, pointing to a therapeutic window for antitumor activity (Fulda 2008). In addition, oil obtained from the *Betula pendula* bark are already used for the treatment of skin inflammatory diseases, such as eczema and psoriasis. The root bark of *Hibiscus syriacus* is known in Asia for antipyretic, anthelmintic, and antifungal properties. Moreover, the *Hibiscus syriacus* extract shows antiproliferative effect on human lung cancer cells (Cheng YL et al. 2008) and antioxidant capacity of have been already demonstrated (Kwon SW et al. 2003).

1.3.2 Chemical characterization of *Betula pendula* and *Hibiscus syriacus* stem cells extract.

I prepared two different type of extracts from the plant cell cultures: water soluble (hydrosoluble) and ethanolic (liposoluble) extracts. In this way it is possible to have two kind of extracts enriched of different bio-active compounds with different characteristics.

The extracts thus obtained were analysed by several assays aimed to characterize some properties of each kind of extract.
For each extract it was determined the total protein content (Bradford assay), the total sugar amount (phenol/H2SO4 method) and the quantity of total polyphenol content in extract (Folin Denis Method), as described in materials and methods.
Finally, I measured the total antioxidant capacity of the *Betula p*. and *Hibiscus s.* cell extracts using the ORAC (Oxygen Radical Absorbance Capacity) assay. Table 1 shows that *Betula pendula* Ethanolic Extract preparation has a lower protein content than Hydrosoluble Extract preparation, and a lower total polyphenol amount (indicated as ug Gallic acid/ ug powder).
However, it shows a higher sugar content and antioxidant capacity expressed as μmol Trolox Equivalent/g. Remarkably, the results obtained with *Hybiscus*

siriacus shows the same trend (Table 2). However, the antioxidant capacity of *Hybiscus siriacus* Alcohol Extract seems to be almost twice in comparison with *Hybiscus siriacus* Hydrosoluble extract (Table 2).

Betula pendula **Hydrosoluble extract**		***Betula pendula*** **Ethanolic extract**	
ORAC	52 µmol Trolox Eq/g	ORAC	68 µmol Trolox Eq/g
POLYPHENOL	0,413 µg Gallic acid/ µg	POLYPHENOL	0,336 µg Gallic acid/ µg
SUGARS	23,46%	SUGARS	39,96%
PROTEINS	3,13%	PROTEINS	0,04%

Table 1. Chemical characterization of Betula pendula Hydrosoluble and Ethanolic stem cells extract. The total protein content was determined by Biorad assay. The total sugar amount by the phenol/H2SO4 method while the quantity of total polyphenol content in extract was determided by Folin Denis Method. Finally, I measured the total antioxidant capacity of the Betula p. using the ORAC (Oxygen Radical Absorbance Capacity) assay.

Hibiscus syriacus **Hydrosoluble extract**		***Hibiscus syriacus*** **Ethanolic extract**	
ORAC	69 µmol Trolox Eq/g	ORAC	113 µmol Trolox Eq/g
POLYPHENOL	0,82 µg Gallic acid/ µg	POLYPHENOL	0,54 µg Gallic acid/ µg
SUGARS	20%	SUGARS	53,89%
PROTEINS	2,375%	PROTEINS	0,041%

Table 2. Chemical characterization of Hibiscus syriacus Hydrosoluble and Ethanolic stem cells extract. The total protein content was determined by Biorad assay. The total sugar amount by the phenol/H2SO4 method while the quantity of total polyphenol content in extract was determided by Folin Denis Method. Finally, I measured the total antioxidant capacity of the Betula p. using the ORAC (Oxygen Radical Absorbance Capacity) assay.

1.3.3 Analysis of cell vitality after treatment with *Betula pendula* and *Hibiscus syriacus* stem cells extracts.

Viable cells with active metabolism convert MTT (3-(4,5-dimetiltiazol-2-il)-2,5-difeniltetrazolio) into a purple coloured formazan product, thus colour formation serves as convenient marker of cells viability.
I have established the extract use concentrations showing nether cytotoxic nor hyper-proliferative effect by a MTT assay in primary fibroblasts (HDF) and HaCaT cells (immortalized but not transformed keratinocytes).
The results of MTT assay performed in HaCaT cells after 24 hours of treatment show the absence of both the effects. (Figura 1). As shown in figure 2 a similar result was obtained with a long term treatment (8 days).

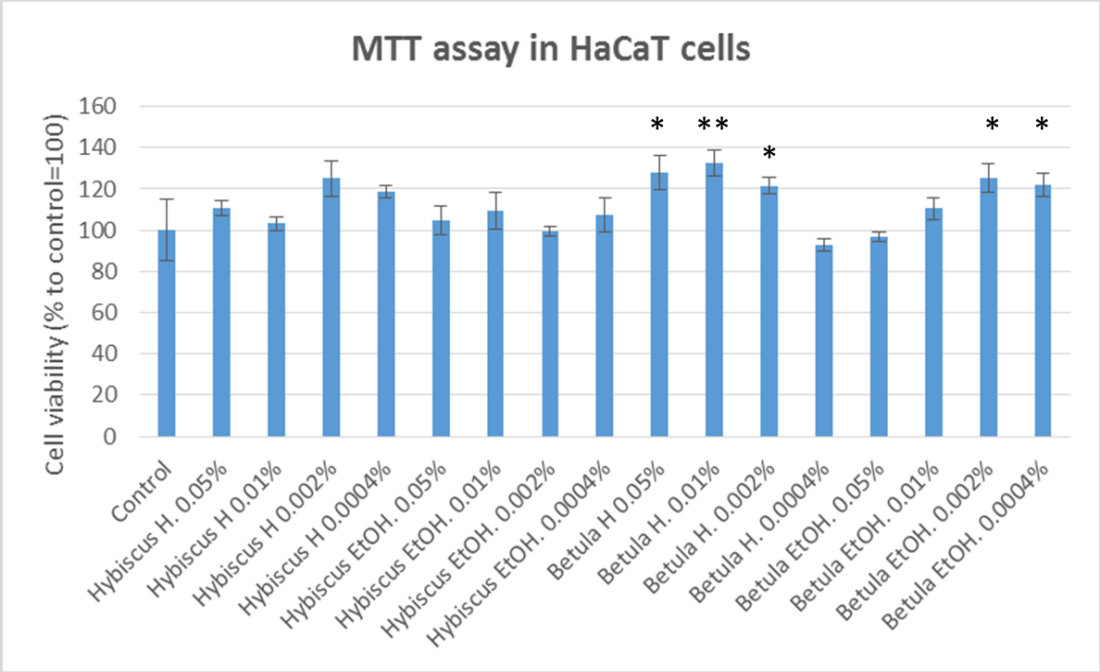

Figure1. Analysis of cell vitality in HaCaT cells after treatment with Betula pendula and Hibiscus syriacus stem cells extract. A total of HaCaT keratinocytes cells were plated into 96-well plates at a density of 1.3×103 cells/well, grown for 8 hrs and treated for 12h with different concentrations of the extracts (from 0.05% w/v to 0.0004% w/v). After treatments, the percentage of vital cells was measured for each sample by using MTT dye. The number of healthy cells is directly proportional to the level of the formazan product created. The values are means of five independent measures obtained from one representative experiment among three, and the P-value < 0.05 is represented by *; P-value < 0.01 is represented by **.

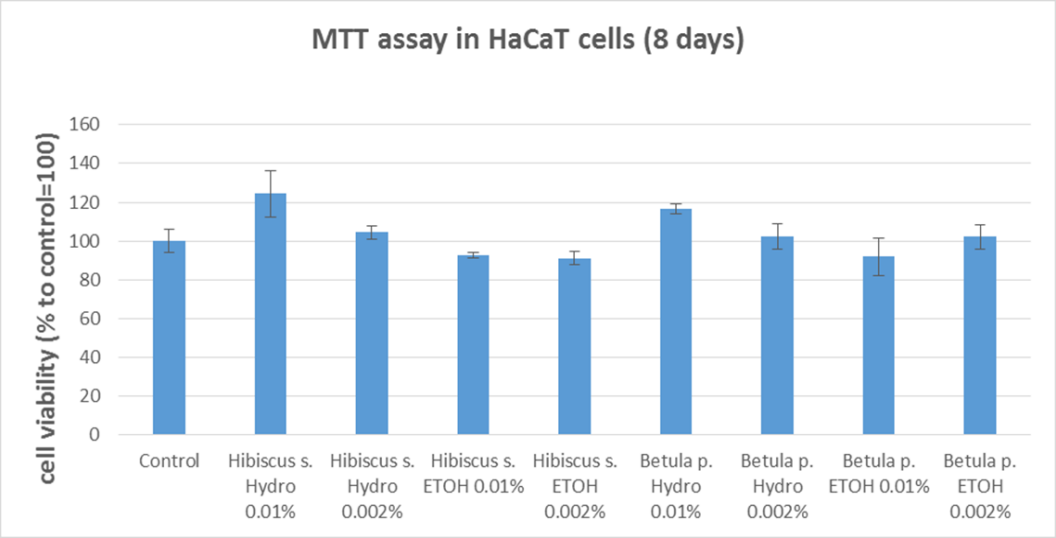

Figure 2. Analysis of cell vitality in HaCaT cells after long term treatment (8 days) with Betula pendula and Hibiscus syriacus stem cells extract. A total of HaCaT keratinocytes cells were plated into 96-well plates at a density of 1.3×103 cells/well, grown for 8 hrs and treated for 8 days with two different concentrations of the extracts (0,01% and 0,002% w/v). After treatments, the percentage of vital cells was measured for each sample by using MTT dye. The number of healthy cells is directly proportional to the level of the formazan product created. The values are means of five independent measures obtained from one representative experiment among three.

1.3.5 Effect of *Betula pendula* and *Hibiscus syriacus* stem cells extracts in epidermal hydration.

1.3.6 Regulation of AQP3 and FLG genes after treatment with *Betula pendula* and *Hibiscus syriacus* stem cells extracts

I investigated whether these extracts could improve skin hydration by stimulating biosynthesis of aquaporins and filaggrin, proteins specifically involved in the maintenance of water balance in human skin cells.
As previously described aquaporins are channel proteins that facilitate the transport of water and other solutes across the cell membrane and AQP3 is the most abundant in skin.
Filaggrin is a structural protein, responsible for the water-proofing capacity and integrity of the upper skin layers (Pereda MCV et al. 2010). In fact, filaggrin (FLG) is a protein which interacts with keratins intermediate filaments into the corneum stratum causing their aggregation into macrofibrils. This process contributes to form highly insoluble keratin matrix, and for this reason, filaggrin monomers are fundamental for the skin barrier function (Sandilands et al. 2009).
Using semi quantitative RT-PCR I demonstrated that HaCaT cells treatment with *Betula pendula* ethanolic extract (at concentration of 0,002% w/v) or with *Hibiscus syriacus* hydrosoluble and ethanolic extracts (at concentration of 0,002% w/v) increased the expression of AQP3 by 80% and 20%, respectively (Figure 3).

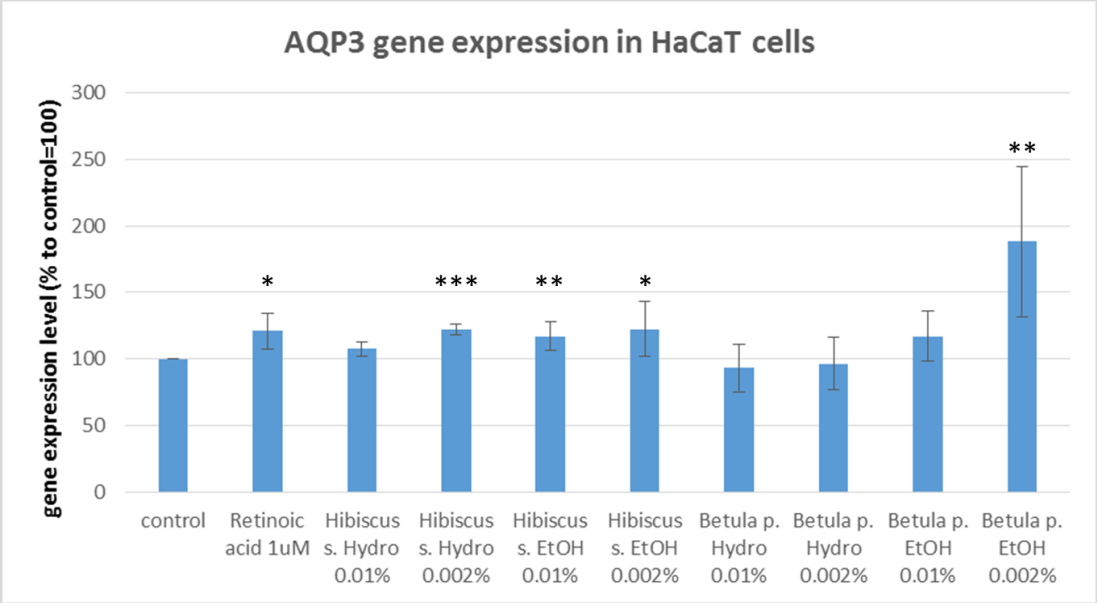

Figure 3. AQP3 gene expression analysis in HaCaT cells cells treated with *Betula p*. and *Hibiscus s.* extracts at the indicated concentrations. HaCat cells were seeded at concentration of $1.5x10^5$ cells in 35mm dishes. After 24 hours, cells were treated with the extracts for six hours and total RNA were collected. cDNA obtained was used to evaluate AQP3 gene expression by performing a semi-quantitative RT- PCR. Retinoic acid at concentration of 1 μM/ ml was used as positive control. The values were normalized to rRNA18S. Each column value represents the average of four experiments and error bars indicate standard deviations. P-value < 0.05 is represented by *; P-value < 0.01 is represented by **. P-value < 0.001 is represented by ***.

Next, using semi quantitative PCR, I demonstrated that treatment of HaCaT cells with *Betula pendula* hydrosoluble extracts or *Hibiscus syriacus* ethanolic extracts increased FLG gene expression by about 60% (Figure 4).
Instead, as shown in figure 4 treatment of HaCaT cells with *Betula pendula* ethanolic at concentration of 0,002% increased FLG gene expression by 100%.

Taken together these data strongly suggest that both extracts, and especially that from *Betula pendula,* are able to improve skin hydration by promoting FLG and AQP3 biosynthesis.

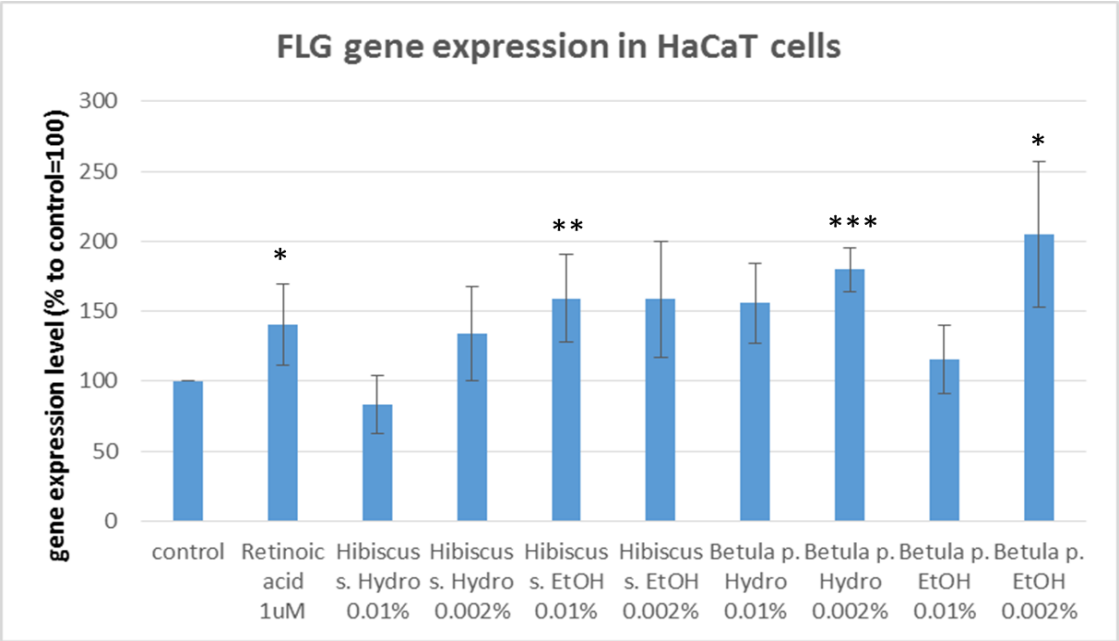

Figure 4. FLG gene expression analysis in HaCaT cells cells treated with *Betula p*. and *Hibiscus s.* extracts at the indicated concentrations. HaCat cells were seeded at concentration of $1.5x10^5$ cells in 35mm dishes. After 24 hours, cells were treated with the extracts for six hours and total RNA were collected. cDNA obtained was used to evaluate FLG gene expression by performing a semi-quantitative RT- PCR. Retinoic acid at concentration of 1 μM/ ml was used as positive control. The values were normalized to rRNA18S. Each column value represents the average of four experiments and error bars indicate standard deviations. P-value < 0.05 is represented by *; P-value < 0.01 is represented by **. P-value < 0.001 is represented by ***.

1.3.7 Effect of *Betula pendula* and *Hibiscus syriacus* stem cells extracts on skin regeneration.

1.3.8 Effect of *Betula pendula* and *Hibiscus syriacus* stem cells extracts during Wound Healing process

Next, I investigated whether *Betula pendu*la and *Hibiscus syriacus* stem cells extracts could improve epidermal regeneration process.
Wound healing is a complex and dynamic pathological process, finely regulated by intracellular signaling and extracellular components, which concerns replacing damaged tissue by a living one (H. Sinno et al. 2013). Preliminary data showed that *Betula p.* had no effect the wound healing process (data not shown), thus I continued my experiments only with *Hibiscus s*.
Wound healing assay in HaCaT cells clearly showed that ethanolic extract of *Hibiscus syriacus* (0,002% and 0,001% w/v) increased the wound repair by 50% and 20%, respectively (Figure 5).

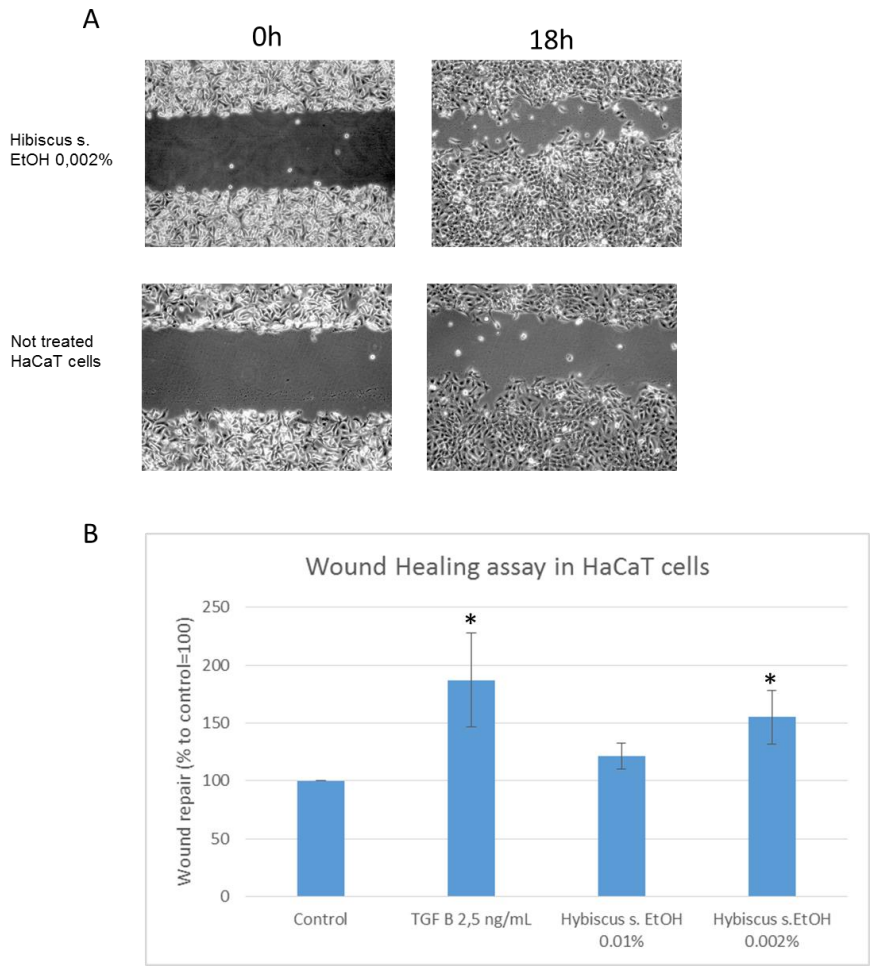

Figure 5. Effect of and Hibiscus syriacus ethanolic extracts during Wound Healing process in HaCaT cells. (A) Cells seeded at confluence were wound and then treated with Hibiscus S. extracts at indicated concentrations for 7 h in 0.5% FBS-containing medium. At 0, 18h, phase-contrast pictures of the wounds at four different locations were taken. (B) To estimate the relative migration of the cells, for each condition was compared the unclosed cell-free areas at time 0 and eighteen hours after treatments by using the software Image J. TGF β at concentration of 2,5 ng/ml had used as positive control. Each column value represents the average of three experiments and error bars indicate standard deviations. P-value < 0.05 is represented by *.

As shown in figure 5 in human dermal fibroblast (HDF cells) treatment with *Hibiscus syriacus* ethanolic extract (0,01% and 0,002% w/v) resulted in an increase of healing of 18% and 30%, respectively.

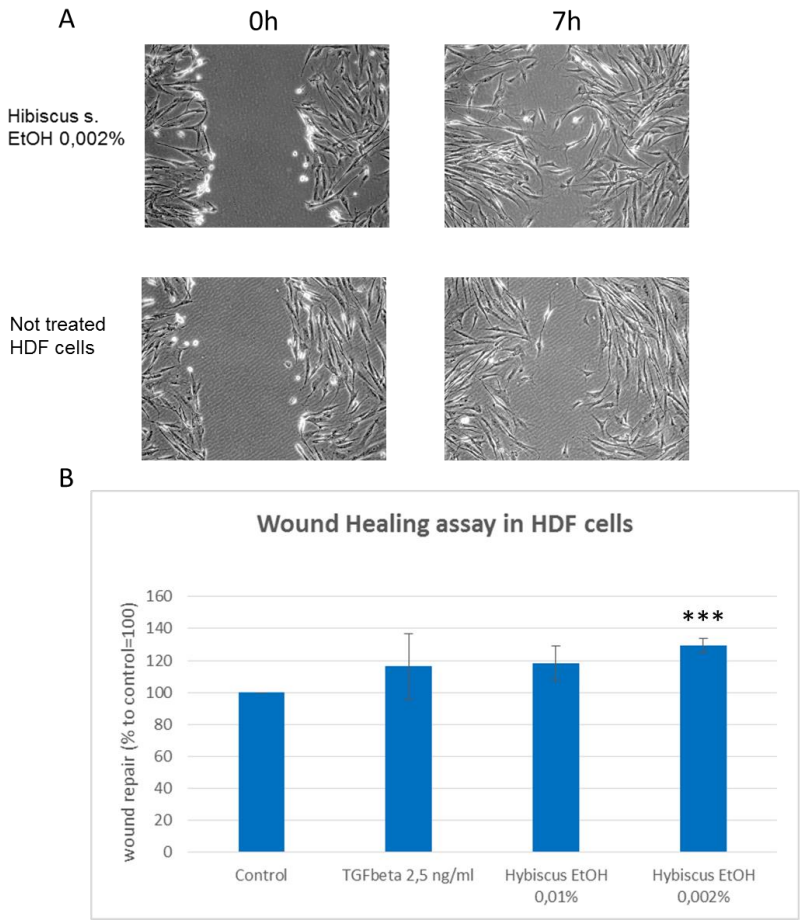

Figure 6. Effect of and Hibiscus syriacus ethanolic extracts during Wound Healing process in HDF cells. (A) Cells seeded at confluence were wound and then treated with Hibiscus S. extracts at indicated concentrations for 7 h in 0.5% FBS-containing medium and Mytomycin C (10 μg/ml) is included in the media to prevent cell proliferation. At 0, 7h, phase-contrast pictures of the wounds at four different locations were taken. (B) To estimate the relative migration of the cells, for each condition was compared the unclosed cell-free areas at time 0 and seven hours after treatments by using the software Image J. TGF β at concentration of 2,5 ng/ml had used as positive control. Each column value represents the average of three experiments and error bars indicate standard deviations. P-value < 0.001 is represented by ***.

1.3.9 Effect of *Hibiscus syriacus* ethanolic extracts on Fibronectin production.

Fibronectin is an adhesive molecule that plays a crucial role in wound healing, particularly in extracellular matrix (ECM) formation. To investigate the molecular mechanisms by which *Hibiscus syriacus* enhances wound healing, I evaluated in HDF cells fibronectin neo-synthesis upon Hibiscus treatment by Elisa. In fact, I carried out an Elisa assay and measured the amount of fibronectin produced by fibroblast (HDF cells) under cell extract stimulation. The results show that 0,002% w/v of *Hibiscus syriacus* ethanolic extract caused an increase in fibronectin of about 30% (Figure 6).

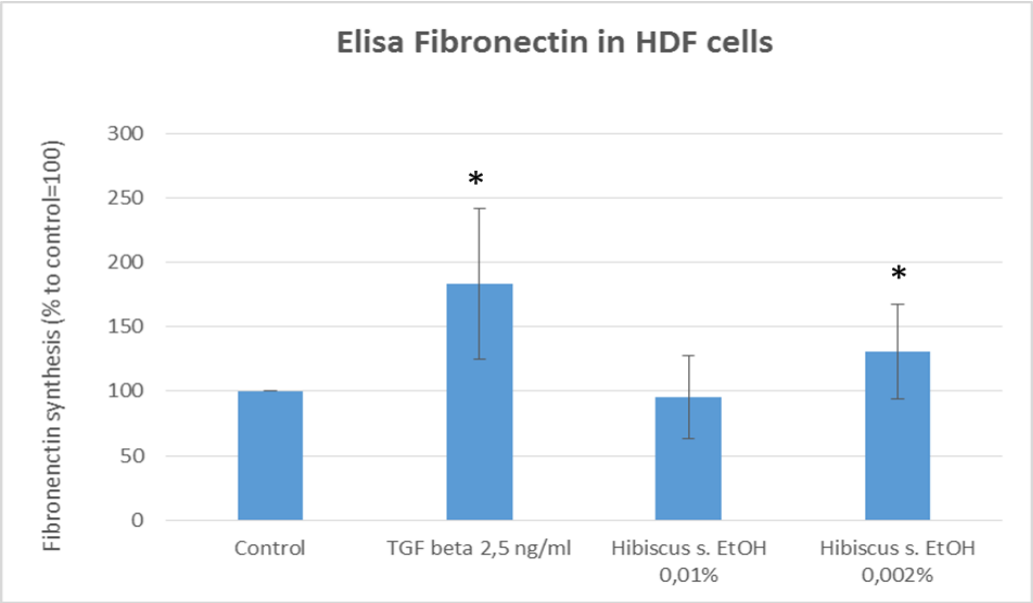

Figure 6. Effect of Hibiscus syriacus ethanolic extracts on Fibronectin production. HDF cells are seeded in 96-well plates at density of 9 x 103 per well, and treated with compounds at indicate concentrations for 72h without changing the medium. Each condition is run in quadruplicate. TGF β at concentration of 2,5 ng/mL was used as positive control. Each column value represents the average of four experiments and error bars indicate standard deviations. P-value < 0.05 is represented by *.

1.3.10 Effect of *Hibiscus syriacus* ethanolic extracts on Collagen contraction.

Next, I proceeded to examine the effect of the Hibiscus syriacus ethanolic extracts on fibroblast contractility by three-dimensional collagen gel contraction assay. Fibroblasts play a fundamental role in wound healing by secreting chemokines, growth factors and ECM proteins that are necessary for inflammatory cells infiltration and neo-angiogenesis (Singer AJ et al 1999). Collagen contraction can shrink the size of the wound facilitating its repair, so that it is a crucial event in this process (Martin P. 1997). 3D collagen gel contraction assay simulates the 3D collagen-riched environment of wound granulation tissue, so it is a useful in vitro model for studying wound contraction (Carlson MA et al. 2004). The result of 3D collagen gel contraction assay proved that HDF cells after treatment with 0,01% w/v *Hibiscus syriacus* promotes about 30% wound contraction (Figure 7).

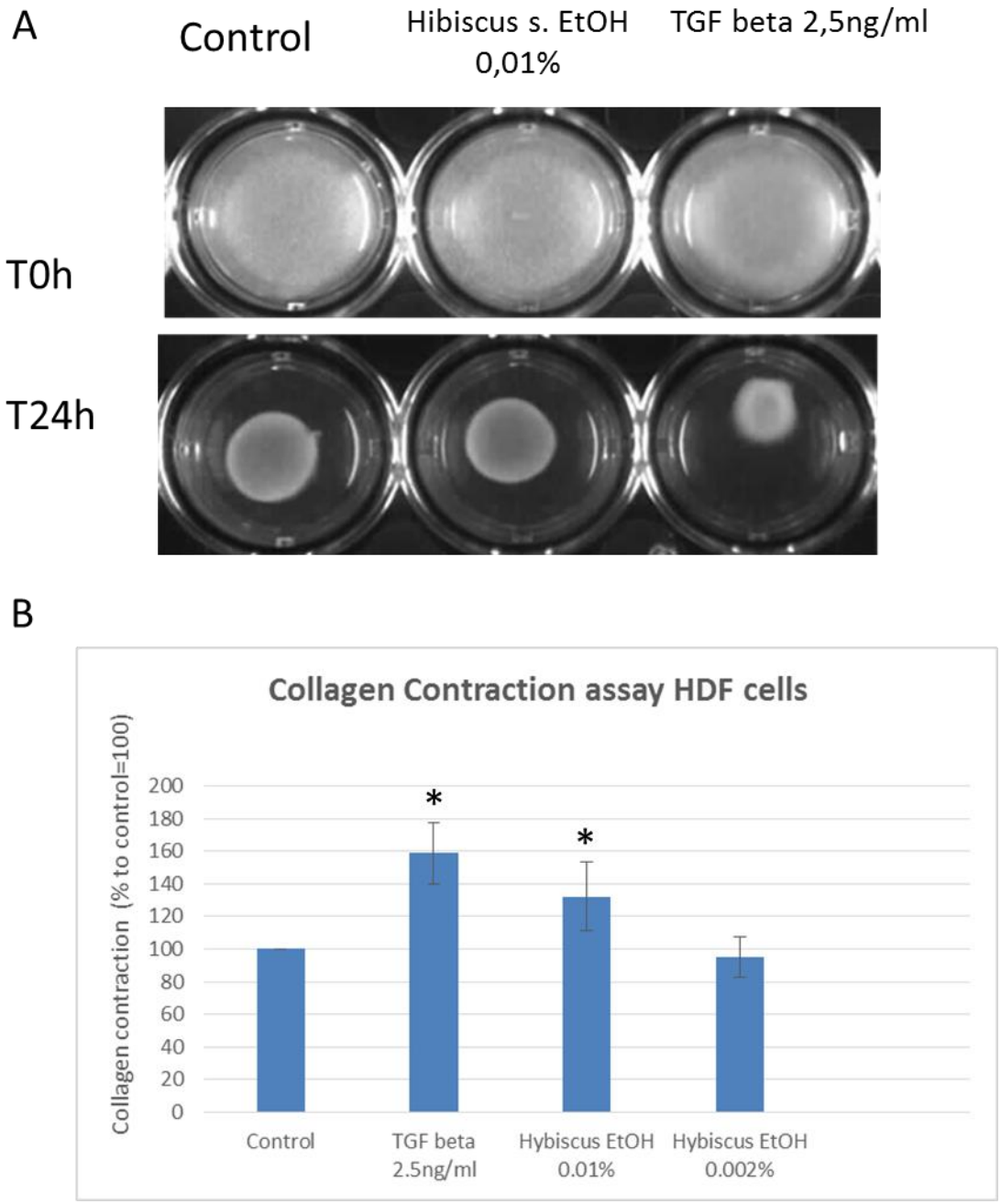

Figure 7. Effect of Hibiscus syriacus ethanolic extracts on Collagen contraction. (A) $2x10^5$ HDF are seeded in 24 well mixed with 2mg/ml of collagen solution .The plate is incubated at 37°C for 30' in way to induce collagen gel formation. TGF β at concentration of 2,5 ng/ml had used as positive control At the end of incubation the medium with treatment is added and the plate is incubated for the night. The next day the gel is released from the bottom of the well in way to induce collagen gel contraction. Pictures at different times are taken and the best time is 24 hours after the release. Each column value represents the average of four experiments and error bars indicate standard deviations. . P-value < 0.05 is represented by *.

1.3.11 Effect of *Hibiscus syriacus* ethanolic extracts on Pro-Collagen type I production

Development and maintenance of skin integrity and repair is also dependent on the balance between production and degradation of type I collagen (Verrecchia F 2005). Collagen is a major structural protein in the skin, it contributes to make skin compact and healthy.
For this reason considering the positive effect of *Hibiscus s.* on wound healing, fibronectin biosynthesis and collagen contraction I have investigated whether the treatment with this extract improve also the Pro-collagene type I biosynthesis by Elisa in HDF cells.
I carried out an Elisa assay and measured the amount of new Pro-Collagen I type produced by fibroblast (HDF cells).
The result shows that under stimulation with 0,01% and 0,002% w/v of *Hibiscus syriacus* ethanolic extract, the synthesis of Pro-Collagen type I increased by 60%.

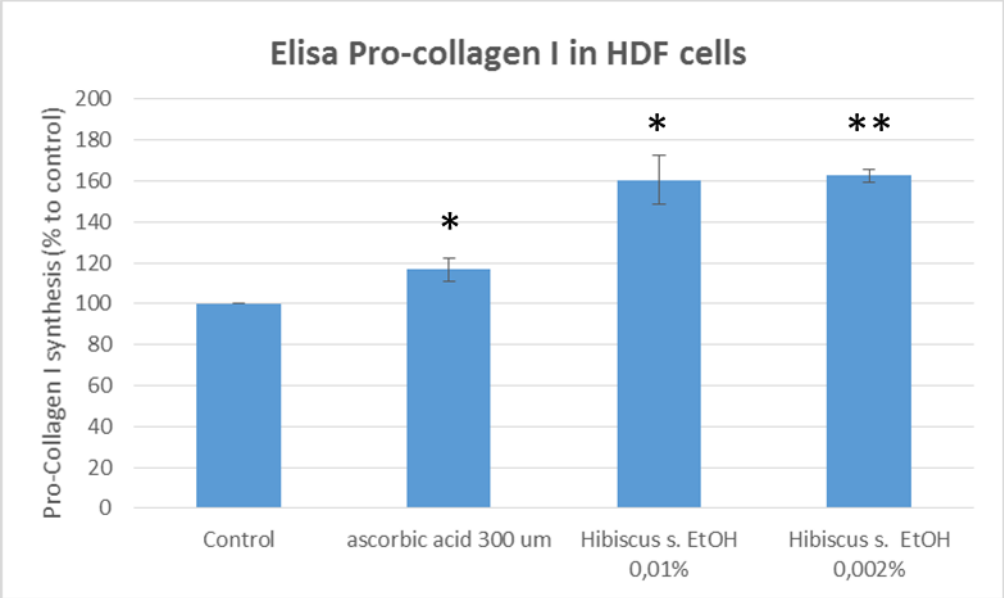

Figure 8. Effect of Hibiscus syriacus ethanolic extracts on Pro-Collagen I production. HDF cells are seeded in 96-well plates at density of 1,5 x 10^4 per well, and treated with compounds at indicate concentrations for 24h without changing the medium. Each condition is run in quadruplicate. Ascorbic acid at concentration of 300/mL was used as positive control. Each column value represents the average of three experiments and error bars indicate standard deviations. . P-value < 0.05 is represented by *. P-value < 0.01 is represented by **.

1.3.12 Regulation of LAM B and C genes after treatment with *Betula pendula* and *Hibiscus syriacus* stem cells extracts.

Laminins play a fundamental role in skin basement membrane architecture and function (Senyürek I et al. 2014). I also evaluated if *Betula pendula* or *Hibiscus syriacus* extracts could improve biosynthesis of β chain (LAM B) and γ chain (LAM C) of laminin 5 protein.

Using semi quantitative RT-PCR I demonstrated that both *Betula* and *Hibiscus syriacus* hydrosoluble and ethanolic extracts increased the expression of LAM B in HaCaT cells, of about 40%.(Figure 9)

Conversely, LAM C gene expression was not regulated by *Betula p*. and *Hibiscus s*. treatment (data not shown).

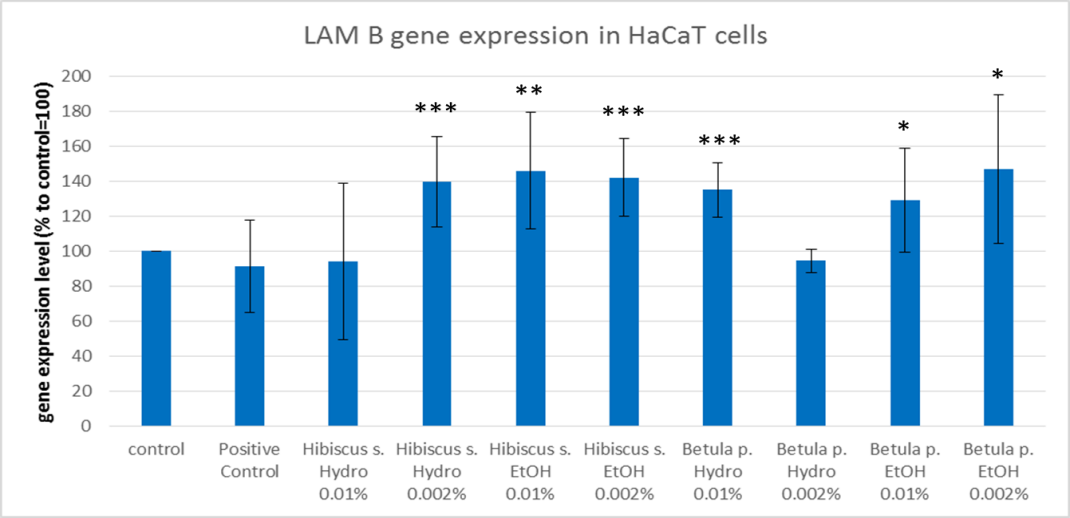

Figure 9. LAM B gene expression analysis in HaCaT cells cells treated with Betula p. and Hibiscus s. extracts at the indicated concentrations. HaCat cells were seeded at concentration of $1.5x10^5$ cells in 35mm dishes. After 24 hours, cells were treated with the extracts for six hours and total RNA were collected. cDNA obtained was used to evaluate FLG gene expression by performing a semi-quantitative RT- PCR. A compound known for stimulating LAM B biosynthesis was used as positive control. The values were normalized to rRNA18S. Each column value represents the average of four experiments and error bars indicate standard deviations. P-value < 0.05 is represented by *; P-value < 0.01 is represented by **; P-value < 0.001 is represented by ***.

1.4 Discussion

During my PhD I contributed to select novel plant-derived bio-active products and characterize their activity in epidermal homeostasis and skin self-renewal.
This project was aimed to discover new bio-active products that can be used as anti- aging dermo-cosmetics or pharmacological treatment for skin disorders associated to deregulated epidermal proliferation and/or differentiation.
For this reason I selected Arterra Bioscience Srl company as my PhD project partner. In Arterra, a wide range of plant stem cell cultures are available. They represents a valuable source of bioactive products with potential pro-regenerative and differentiative properties to be used in cosmetics and pharmaceuticals sector.
The selected plant stem cell extracts were *Betula pendula* and *Hibiscus syriacus*, on the othe hand Human Dermal Fibroblasts (HDF) and human keratinocytes (HaCaT) were chosen as cell model systems.

First, I produced two different type of extracts from each stem cell culture: ethanolic and hydrosoluble. I observed no cytotoxic and pro-proliferative effect of both extracts in our cell systems, also in long term, by performing a MTT assay, at selected concentrations. Then, I analysed in HaCaT cells the effect of the extracts on the expression of Aquaporin 3 (AQP3) and Filaggrin (FLG), two genes involved in water transport and retention. The results of my experiments clearly indicate that the *Betula p*. is more efficient than *Hibiscus s*. in the up regulating of both AQP3 and FLG gene expression.

Concerning the regeneration process, data from the wound healing assay in HaCaT and HDF cells strongly show that *Hibiscus syriacus* ethanolic extracts efficiently increases the wound repair and this was more evident at the 0,002% w/v concentration while Betula exhibited no detectable effects.
Accordingly, I observed a strong stimulation of fibronectin by *Hibiscus* in HDF cells further supporting the pro-regenerative potential of this extractNext, I concentrated my attention on the wound repair capacities.

When HDF cells were treated with the *Hibiscus syriacus ethanolic extract*, wound contraction significantly increased thereby demonstrating the efficacy of *Hibiscus syriacus* in promoting fibroblast activation. Moreover, *Hibiscus s*. was able to enhance Pro-Collagen I production in HDF fibroblasts. Remarkably, collagen production is fundamental for a healthy skin and especially Type I collagen fibrils that because of their enormous tensile strength can be stretched without being broken.

Finally, to corroborate data from Wound healing and Collagen contraction assays I investigated whether Hibiscus and/or Betula extracts could improve skin regeneration by stimulating biosynthesis of basal lamina genes, and in particular I examined laminin 5 β and γ chain transcription. Actually, laminins play a fundamental role in basement membrane architecture and function in human skin (Senyürek I et al. 2014).

Interestingly, when HaCaT cells were treated with the *Hibiscus syriacus and Betula pendula*, I observed an increase in LAM B genes expression but not LAM C. Further experiments should be performed to clarify this point.

Taken together my data suggest that *Betula p.* extract can be a valuable bioactive ingredient to use in cosmetic field for improving skin hydration, on other hand *Hibiscus s.* extract turned out to be more efficient in stimulating skin regeneration.

1.5 Material and Methods

1.5.1 Hydrosoluble extract preparation from plant stem cell.

Cells are harvested, verified for micro-organism contamination (37°C ON) and then frozen at -30°C or -80°C until processing. The cells are grinded (when still partially frozen) in PBS 3X pH 7.2 (1:1 w/v) in a mortar with pestle or mechanic grinder. Filter through a cloth filter and collect the soluble fraction in a sterile container placed in an ice bath.

1.5.2 Ethanol (liposoluble) extract preparation from plant stem cells

Cells are harvested, verified for micro-organism contamination (37°C ON) and then frozen at -30°C or -80°C until processing. 200ml of EtOH 96% is added. The mix is agitated for 1h at Room Temperature. Filter through a cloth filter and collect the lipo soluble fraction in a sterile container placed in an ice bath. The ethanol is eliminated by using the Rotavapor until 1/10 of the extract is obtained

1.5.3 Bradford assay

The Bradford assay is a protein determination method that involves the binding of Coomassie Brilliant Blue G-250 dye to proteins (Bradford 1976). a series of standards dilution of BSA (Bovine Serum Albumin) from 1ug/1ul to final concentrations of 0, is prepare in Bradford solution 1X. Serial dilutions of the unknown sample are also prepare to be measured. 5 µL of sample is added in each well of 96-well. 100 µL of Coomassie Blue is added to each well and mix, gently. After 5 minutes, the developed colour was quantified at 595 nm by a multiwell spectrophotometer Victor3 (PerkinElmer). Plot the absorbance of the standards vs. their concentration and calculate the concentrations of the unknown samples.

1.5.4 Folin Denis assay

Aliquot 50 µl dilutions of the samples to test in a 96 well plate (from 20ug/µl to 0). Prepare a solution of 1mg/ml of gallic acid and make several dilutions in 50 µl volume of water. The Folin-Denis reagent (sodium tungstate 10% w/v, phosphomolybdic acid 2% w/v, orthophosphoric acid 5% v/v) is diluted 1:20 in water and add 50 µl to all samples (both the extract dilutions and the standards). Leave 3-5 minutes at room temperature. Read at Victor by Bradford@595 program to obtain the blank. Add 50 µl of 1M Na_2CO_3 pH 8-9 to all wells and the plate is incubated 10-15 minutes until dark-blue color develops. Read at Victor by Bradford@595. Compare OD values of the sample extracts with those obtained from standard dilutions of gallic acid. Calculate total polyphenol amount present in the extract (% or mg/g).

1.5.5 Measure of sugar content with Phenol/H_2SO_4

It's prepared a standard curve with different concentrations of mannose or glucose (from 0 mM to 5mM) in 200 ul of water containing 30% phenol. 5-10 μl of sample solution is taken and mixed with water/30% phenol in 200 μl volume. All the samples are briefly vortexed and added 800 μl of concentrated H_2SO_4, and mix well. Wait until the red/orange color appears. The samples is transferred in to plastic cuvettes or 24 well plates and the OD at 490 nm (Victor) is taken. The concentrations of sugar in the samples is calculated comparing with those of the standard curve

1.5.6 ORAC assay

The Oxygen Radical Absorbance Capacity assay measures the total antioxidant power of a compound or extract and is based on the ability to inhibit the oxidation of a fluorophore, generally fluorescein, by a potent oxidant, 2,2'-Azobis(2-amidinopropane) dihydrochloride (AAPH). Twenty-five μL of the extract dilutions in phosphate buffer 100mM. pH 7.4, was aliquoted into 96-well plate, and 150 μL of a fluorescein solution (8nM in phosphate buffer) was added to each sample. After incubation at 37°C for 15 min, 25 μL of AAPH solution (153 mM in phosphate buffer) was pipetted into each well, and the progress of the reaction was monitored at 535 nm(excitation at 485 nm), using a fluorescence multiwall reader. The fluorescence was measured every minute for 50 min. Antioxidant power of the mixture was calculated according to the method described by Huang D et al. (2002). The standard curve was obtained by plotting Trolox concentrations against the average AUC (area Under Curve) of two measurements for each concentration. ORAC values of the samples were expressed as μmole of Trolox equivalents per g of extract.

1.5.7 Skin cell cultures

Spontaneously immortalized human keratinocyte (HaCaT) and Human Dermal Fibroblasts (HDF) were maintained in DMEM supplemented with 10% fetal bovine serum (FBS) or fetal calf serum (FCS) respectively 95% air, 5% CO_2 humidified atmosphere at 37°C.

1.5.8 MTT assay

A total of Human Dermal Fibroblasts (HDF) or HaCaT keratinocytes cells were plated into 96-well plates at a density of 1.3×10^3 cells/well, grown for 8 hrs and treated for 12h with different concentrations of the extracts. After treatments, cells were washed with PBS and incubated with 100 μL per well of reaction buffer (10 mM Hepes, 1.3 mM $CaCl_2$, 1 mM $MgSO_4$, 5mM glucose and 0.5 mg/mL of colorimetric substrate MTT 3-(4,5-dimethylthiazol-2-yl)-2,5-dipheny

ltetrazoliumbromide) in PBS buffer at pH 7.4. After 3 hrs, at 37°C, 5% CO_2, cells were solubilized by the addiction of 100 μL of solubilation solution (TritonX100, 0.1N HCl in 10% isopropanol), and the plate was incubated for 4 hrs at room temperature. The number of healthy cells is directly proportional to the level of the formazan product created. The developed colour was then quantified at 595 nm by a multiwall- plate reader Victor3 (Perkin Elmer).

1.5.9 Gene expression analysis

HaCaT or HDF cells were seeded in 6-well plates at density of 1.5 x 10^4 or 1.0 x 10^5, per well, respectively. The cells were incubated for 6 hours at 37°C, 5% CO_2 , with the extracts and with retinoic acid 1μm alone (control), and then collected for total RNA extraction. Total RNA was extracted with the GenElute Mammalian Total RNA Purification Kit (Sigma), according to the manufacture's instructions and treated with DNAse I at 37°C for 30 min to eliminate any contaminating genomic DNA. The first strand cDNA was synthesized from 1 μg using the RevertAid™ First Strand cDNA Synthesis Kit (Fermentas). RT-PCR was performed using gene specific primers and the Quantum RNATM 18S internal standard (Ambion) according to manufacturer's instructions. The Quantum RNA TM kit contains primers to amplify 18S rRNA along with competimers that reduce the amplified 18S rRNA product within the range to allow it to be used as endogenous standard. The amplification reactions are performed with the following general scheme: 2 min at 94°C followed by 35 cycles of 94°C for 30s, annealing temperature (specific for each gene) for 30s, and 72°C for 30-60s, with a 10 min final extension at 72°C. The PCR products obtained are loaded on 1.5 percent agarose gel, and the amplification bands are visualized and quantified with the Geliance 200 Imaging system (Perkin Elmer). The amplification band corresponding to the gene analyzed is normalized to the amplification band corresponding to the 18S. The values obtained are finally converted into percentage values by considering the measure of the untreated controls as 100 percent. All the semiquantitative RT-PCR_s were repeated three times, and the result of a representative experiment are reported in the graphs.

Gene Specific Primers used:

AQP3-FW: 5'GATCAAGCTGCCCATCTA 3'

AQP3-RV: 5'TGGGCCAGCTTCACATTCT 3'

FLG-FW: 5' AGAGCTGAAGGAACTTCTGG 3'

FLG-RV: 5' GTGTCATAGGCTTCATCC 3'

LAM5-β-FW: 5' AGACCTATGATGCGGACCT 3'

LAM5-β RV: 5' GAAGACATCTCCAGCCTCA 3'

LAM5-γ FW: 5 'ATCAACAGGTGAGCTATGG 3'

LAM5-γ RV: 5 ’CAATCTCCTGTGTCTGGAT 3’

1.5.10 ELISA assay

HDF cells are seeded in 96-well plates at density of 9 x 103 per well, and treated with test compounds for 24-72h without changing the medium. Each condition is run in quadruplicate. After the treatments, the medium is removed and the cells are washed with PBS 1X, fixed in para-formaldehyde (PFA) 4% for 10 min, washed three times with PBS 1X, and permeabilized with 1% TritonX-100 in PBS for 30 min. After permeabilization, the cells are treated for 30 min with 0.5% Tween, 5% BSA in PBS and incubated a 4°C with primary goat polyclonal antibody, raised against human fibronectin or Pro-Collagen type I (Santa Cruz Biotechnology), diluted 1:500 in PBS 1X, containing 0.5% Tween, 1% BSA. 16 hours later, samples are washed 3 times with PBS + 0.5% Tween, and incubated wi and incubated with anti-goat secondary antibody, labelled with Horse-Radish Peroxidase (HRP) (Santa Cruz Biotechnology), diluted 1:1000 in PBS 1X, containing 0.5% Tween, 1% BSA. One hour later, plates are washed 3 times with PBS 1X and the amount of fibronectin produced by the cells is measured by a colorimetric reaction, using a 0.5 mg/ml solution of o-phenylendiamin (OPD) (Sigma-Aldrich) 0.012% H2O2 in citrate buffer 50mM. The plate is incubated at room temperature for 60 min until the yellow color develops. The absorbance of each sample is measured at 490 nm by a Multi-well Plate reader Victor3 (Perkin Elmer).

1.5.11 Wound Healing assay

HaCaT or HDF cells were seeded in 6-well plates at density of 1 x 10^6, per well. 7hrs later, when the cells are confluent, same areas of each well are displaced by scratching a line through the cell layer by a pipet tip, simulating a wound. Floating cells are removed by PBS washing. Media containing 0.5% FBS with or without treatment is added and the cells incubated for 7 hours. Mytomycin C (10 μg/ml) is always included in the media to prevent cell proliferation. To estimate the relative migration of the cells, it’s compared, for each condition, the unclosed cell-free areas at time 0 and seven hours after treatments by using the software Image J. Means of left and right wound margins were calculated

1.5.12 Collagen Contraction assay

2x10^5 HDF are seeded in 24 well mixed with 2mg/ml of collagen solution .The plate is incubated at 37°C for 30’ in way to induce collagen gel formation. At the end of incubation the medium with treatment is added and the plate is incubated for the night. The next day the gel is released from the bottom of the well in way to induce collagen gel contraction. Pictures at different times are taken and the best time is 24 hours after the release.

1.5.13 Statistical analysis.

Unpaired t-test was performed using GraphPad softwere. Quantitative data were presented as mean ± standard deviation (SD). Comparison between data was analyzed using t-tests. Significant differences were accepted when P values is less than 0.05 $p<0.05$ was considered statistically significant.

1.6 References:

1. Elias PM: Skin barrier function. Curr Allergy Asthma Rep. 2008;8:299-305.
2. Elias PM, Choi EH: Interactions among stratum corneum defensive functions. Exp Dermatol. 2005;14:719-726.
3. Panagiota A. Sotiropoulou and Cedric Blanpain Development and Homeostasis of the Skin Epidermis. Cold Spring Harbor Perspectives in Biology 2012,
4. Fuchs E, Raghavans. Getting under the skin of epidermal morphogenesis. Nat Rev Genet 2002; 3(3): 199–209.
5. Koster MI. p63 in skin development and ectodermal dysplasias. J Invest Dermatol 2010; 130(10): 2352–2358.
6. Makoto Senoo, Filipa Pinto, Christopher P. Crum, Frank McKeon p63 Is Essential for the Proliferative Potential of Stem Cells in Stratified Epithelia. Cell 2007; Volume 129, Issue 3, p523–536.
7. Vigano Ma, Mantovani R. hitting the numbers: the emerging network of p63 targets. Cell Cycle 2007; 6(3:233-239)
8. McKeon F. p63 and the epithelial stem cell: more than status quo? Genes Dev 2004; 18(5): 465–469.
9. Maranke I. Koster, Soeun Kim, Alea A. Mills, Francesco J. DeMayo, and Dennis R. Roop. p63 is the molecular switch for initiation of an epithelial stratification program Genes Dev. 2004 Jan 15; 18(2): 126–131.
10. R. Darlenski, J. Kazandjieva, N. Tsankov. Skin barrier function: Morphological basis and regulatory mechanisms. JCM 2011.
11. Elias P, Feingold K: Permeability barrier homeostasis; in Elias P, Feingold K (eds): Skin barrier New York, Taylor & Francis Group, LCC, 2006, pp 337-361
12. Sprecher E, Ishida-Yamamoto A, Becker OM, Marekov L, Miller CJ, Steinert PM, Neldner K, Richard G: Evidence for novel functions of the keratin tail emerging from a mutation causing ichthyosis hystrix. J Invest Dermatol. 2001;116:511-519.
13. Rawlings AV, Matts PJ: Stratum corneum moisturization at the molecular level: An update in relation to the dry skin cycle. J Invest Dermatol. 2005;124:1099-1110.
14. Rawlings AV: Sources and role of stratum corneum hydration; in Elias PM, Feingold KR (eds): Skin barrier. New Yourk, Taylor & Francis Group, LCC, 2006, pp 399-425
15. Candi E, schmidt R, Melino G. The cornified envelope: amodel of cell death in the skin. Nat Rev Mol Cell biol 2005; 6(4): 328–340
16. Pearton DJ, Dale BA, Presland RB: Functional analysis of the profilaggrin n-terminal peptide: Identification of domains that regulate nuclear and cytoplasmic distribution. J Invest Dermatol. 2002;119:661-669.
17. Caspers PJ, Lucassen GW, Puppels GJ: Combined in vivo confocal raman spectroscopy and confocal microscopy of human skin. Biophys J. 2003;85:572-580

18. Scott IR, Harding CR: Filaggrin breakdown to water binding compounds during development of the rat stratum corneum is controlled by the water activity of the environment. Dev Biol. 1986;115:84-92
19. Madison KC: Barrier function of the skin: „La raison d'etre" Of the epidermis. J Invest Dermatol. 2003;121:231-241.
20. O'Regan GM, Sandilands A, McLean WH, Irvine AD: Filaggrin in atopic dermatitis. J Allergy Clin Immunol. 2009;124:R2R6.
21. Verkman AS (2012) Aquaporins in clinical medicine. Annu Rev Med 63: 303-316. doi:10.1146/annurev-med-043010-193843. PubMed: 22248325.
22. Liqiong Guo, Hongxiang Chen, Yongsheng Li, Qixing Zho. , Yang Sui5An Aquaporin 3-Notch1 Axis in Keratinocyte Differentiation and Inflammation (2013).
23. Hara-Chikuma M, Verkman AS (2008) Aquaporin-3 facilitates epidermal cell migration and proliferation during wound healing. J Mol Med 86: 221-231. doi:10.1007/s00109-007-0272-4. PubMed: 17968524.
24. H. Sinno and S. Prakash,"Complements and the wound healing cascade: an updated review," Plastic Surgery International, vol. 2013, Article ID146764, 7pages,2013
25. K.S.Midwood,L.V.Williams,andJ.E.Schwarzbauer,"Tissue repair and the dynamics of the extracellular matrix," International Journal of Biochemistry and Cell Biology, vol. 36, no. 6, pp.1031–1037,2004
26. Pawel Olczyk, Aukasz Mencner, and Katarzyna Komosinska-Vassev Hindawi. The Role of the Extracellular Matrix Components in Cutaneous Wound Healing Publishing Corporation BioMed Research International Volume 2014, Article ID 747584, 8 pages http://dx.doi.org/10.1155/2014/747584
27. Rozario, T. and DeSimone, D. W.(2010). The extracellular matrix in development and morphogenesis: a dynamic view. Dev. Biol. 341, 126-140.
28. De Wever, O., Demetter, P., Mareel, M. and Bracke, M. (2008). Stromal myofibroblasts are drivers of invasive cancer growth. Int. J. Cancer 123, 2229-2238.
29. Christian Frantz, Kathleen M. Stewart and Valerie M. Weaver. The extracellular matrix at a glance. Journal of Cell Science 123, 4195-4200 © 2010. Published by The Company of Biologists Ltd doi:10.1242/jcs.023820
30. Wise, S. G. and Weiss, A. S. (2009). Tropoelastin. Int. J. Biochem. Cell Biol. 41, 494-497.
31. Lenselink EA.Int Wound J. 2013 Jun 7;9999(9999). doi: 10.1111/iwj.12109Role of fibronectin in normal wound healing.
32. HOLLY COLOGNATO AND PETER D. YURCHENCO. Form and Function: The Laminin Family of Heterotrimers. DEVELOPMENTAL DYNAMICS 218:213–234 (2000)
33. Fowler, M. Plant cell culture: Natural products and industrial application. Biotechnol. Genet. Eng. Rev. 1984, 10, 41–67
34. Ani Barbulova, Fabio Apone and Gabriella Colucci. Plant Cell Cultures as Source of Cosmetic Active Ingredients. Cosmetics 2014
35. Lee, E.; Jin, Y.; Park, J.; Yoo, Y.; Hong, S.; Amir, Z.; Yan, Z.; Kwon, E.; Elfisk, A.; Tomlinson, S.; et al. Cultured cambial meristematic cells as a source of plant natural products. Nat. Biotechnol. 2010, 28, 1213–1217

36. D. Schmid, C. Schürch, P. Blum, E. Belser, F. Zülli* Plant Stem Cell Extract for Longevity of Skin and Hair COSMETICS. 2008
37. Moscatiello, R.; Baldan, B.; Navazio, L. Plant cell suspension cultures. Methods Mol. Biol. 2013, 953, 77–93.
38. Simone Fulda .Betulinic Acid for Cancer Treatment and Prevention Int J Mol Sci. 2008 Jun; 9(6): 1096–1107.Published online 2008 Jun 27. doi: 10.3390/ijms9061096.
39. Cheng YL1, Lee SC, Harn HJ, Huang HC, Chang WL The extract of Hibiscus syriacus inducing apoptosis by activating p53 and AIF in human lung cancer cells. Am J Chin Med. 2008;36(1):171-84.
40. Kwon SW1, Hong SS, Kim JI, Ahn IH Antioxidant properties of heat-treated Hibiscus syriacus. Izv Akad Nauk Ser Biol. 2003 Jan-Feb;(1):20-1.
41. Pereda MCV, Dieamant Gde C, Eberlin S, Werka RM, Colombi D, Queiroz ML, Di Stasi LC. Expression of differential genes involved in the maintenance of water balance in human skin by Piptadenia colubrina extract J Cosmet Dermatol. 2010 Mar;9(1):35-43. doi: 10.1111/j.1473-2165.2009.00458.x.
42. Sandilands A, Sutherland C, Irvine AD, McLean WH. Filaggrin in the frontline: role in skin barrier function and disease. J Cell Sci. 2009 May 1;122(Pt 9):1285-94. doi: 10.1242/jcs.033969.
43. Singer AJ, Clark RA (1999) Cutaneous wound healing. The New England journal of medicine 341: 738–746.
44. Martin P (1997) Wound healing - Aiming for perfect skin regeneration. Science 276: 75–81
45. Carlson MA, Longaker MT (2004) The fibroblast-populated collagen matrix as a model of wound healing: a review of the evidence. Wound Repair and Regeneration 12: 134–147.
46. Verrecchia F [Functional interactions between the TGF-beta signaling pathway via the Smads and TNF-alpha: implications for the regulation of type I collagen expression]. J Soc Biol. 2005;199(4):329-36. Review. French.
47. Senyürek I, Kempf WE, Klein G, Maurer A, Kalbacher H, Schäfer L, Wanke I, Christ C, Stevanovic S, Schaller M, Rousselle P, Garbe C, Biedermann T, Schittek B. Processing of laminin α chains generates peptides involved in wound healing and host defense. J Innate Immun. 2014;6(4):467-84. doi: 10.1159/000357032. Epub 2014 Jan 18.
48. Huang D, Ou B, Hampsch-Woodill M, Flanagan JA, Prior RL.High-throughput assay of oxygen radical absorbance capacity (ORAC) using a multichannel liquid handling system coupled with a microplate fluorescence reader in 96-well format. J Agric Food Chem. 2002 Jul 31;50(16):4437-44.
.

Chapter 2

2.1 Aim of the thesis

The evidence that YB-1 interacts with ΔNp63α and accumulates into the nuclear compartment following ΔNp63α overexpression raises the interesting question of what could be the biological role of YB-1 in normal epidermis.

Furthermore, multiple stimuli trigger YB-1 protein nuclear localization but the mechanisms governing YB-1 protein subcellular localization and turnover are still largely unknown.

My PhD thesis was aimed to elucidate the physiological role of ΔNp63α/YB-1 interaction given the potential relevance that this association might have in skin biology.

During my Ph.D project I have analysed the expression pattern of YB-1 and ΔNp63α in several cell contexts contribuiting to the knowledge that ΔNp63α plays a role in YB-1 protein post-translational modification and turnover.

In the first part I have shown that ΔNp63α and YB-1 are highly expressed in proliferating keratinocytes and are both down-regulated under differentiating conditions.

In the second part of my work I have established that ΔNp63α reduces YB-1 protein turnover and induces the accumulation of poly-ubiquitinated forms of YB-1 into the nucleus.

Taken together, my data indicate, that the control of YB-1 protein stability by ΔNp63α contributes to the proliferative potential of basal keratinocytes while the ubiquitination process can regulate YB-1 protein abundance into the nuclear compartment.

ΔNp63α protects YB-1 oncoprotein from proteasome-dependent proteolysis

2.2 Introduction:

2.2.1 Epidermal differentiation and proliferation

I spent part of my PhD in the laboratory of Molecular Genetics under the supervision of Prof. Viola Calabrò. Her main field of interest is to study the molecular mechanisms governing skin regeneration and differentiation.
The epidermis is the outermost layer of the skin, a multistratified epithelium whose homeostasis depends on a balance between cell proliferation and differentiation. Several molecular pathways impinge on epidermal regeneration and their deregulation often results in the development of cancer.
The epidermis is composed of four layers of keratinocytes: basal, spinosum, granulosum and corneum but it also cells of a different ontogenic derivation such as melanocytes, Langerhans and Merkel cells. During epidermal differentiation the actively proliferating basal keratinocytes move towards the surface of the skin and differentiate generating the so-called stratum corneum made of flattened dead cells (Blanpain et al. 2009).
Keratinocyte differentiation is characterized by subsequent steps of expression of distinct keratins: K5 and K14 are found in the basal layer while K1 and K10 in the suvrabasal more differentiated ones.
Keratinocytes of the basal layer show high proliferative potential and express high level of ΔNp63α, one of the products of the TP63 locus. During the differentiation process the level of ΔNp63α decreases (Barbieri et al. 2006).
In embrionic development, ΔNp63α is crucial for epidermal commitment while in mature epidermis it controls skin regeneration and differentiation (Yang et al. 1999).
In a collaborative study of functional proteomics, the Y-box binding protein 1(YB-1, NSEP1) was identified among a pool of 50 potential ΔNp63α protein partners in human keratinocytes (Amoresano et al. 2010).
YB-1 is a multifunctional protein with a well assessed oncogenic potential. Its interaction with ΔNp63α was further validated by several experimental approaches (Di Costanzo et al. 2012).
Given the great potential that YB-1 may have in the control of keratinocyte proliferation, I have investigated in more details the functional relationships between YB-1 and ΔNp63α and provided clear evidences indicating that ΔNp63α plays a role in the control of YB-1 protein stability and turnover (di Martino et al. 2015; *in submission*).

2.2.2 The controversial role of ΔNp63α protein

ΔNp63α is encoded by the TP63 locus, the ancestral gene of the p53 gene family (Calabrò et al. 2004). Originally, it was thought that p63 was another tumor-suppressor as p53. Studies on p63 knockout mice have clearly demonstrated that p63 plays a fundamental role in skin homeostasis, regeneration and proliferation (Yang et al. 1999). ΔNp63-null mice die within hours after birth, are unable to develop a mature stratified epidermis and show severe abnormalities including limb truncations and craniofacial malformations (Romano RA et al 2012).

Using two alternative start sites the TP63 gene generates two functionally different protein isoforms: TA isoforms with an acidic transactivation domain and ΔN isoforms lacking this domain.

Alternative splicing at the carboxy-terminal (C-terminal) generates at least three p63 variants (α, β and γ) in each class (Rossi et al. 2006). Among the six p63 isoforms, only ΔNp63α and TAp63α hold a sterile alpha motif (SAM domain) that is involved in protein-protein interactions (Lee E. Finlan et al. 2007).

ΔNp63α isoform is the most predominantly expressed isoform in the skin. ΔNp63α is a critical pro-proliferative factor and a marker of epidermal stemness. It's essential for morphogenesis of organs/tissues developing by epithelial-mesenchimal interactions such as the epidermis, teeth, hair and glands (Yang et al. 1999).

ΔNp63α is highly expressed in embryonic ectoderm while in adults is found in the nuclei of basal regenerative cells of stratified epithelia including skin, breast, myoepithelium, oral epithelium, prostate and urothelia (Mc Keon 2004).

Finally, according to its pro-proliferative role ΔNp63α is the most abundant isoform over-expressed in squamous cell carcinomas (Nylander K et al. 2000) suggesting that ΔNp63α also plays a role in squamous carcinogenesis.

2.2.3 Y Box Binding protein 1: structure and function

Y Box Binding protein 1 (YB-1) encoded by the YBX1 gene, belongs to the superfamily of cold-shock proteins characterized by a highly conserved motif, the "cold shock domain" (CDS) that binds to both DNA and RNA. This motif is located within a central region of the protein encompassing about 65 amino acids (Annette LASHAM et al. 2013).

Human YB-1 consists of 324 amino acid residues, the most abundant are Arg (11.7%), Gly (12%), Pro (11%), and Glu (8.3%). Based on amino acid sequence, YB-1 molecular mass was estimated to be 35.9 kDa. However in SDS-PAGE YB1 migrates as a protein of 50 kDa showing a peculiar behavior (I. A. Eliseeva et al.2011).

YB1 protein is a transcription/translation regulator factor involved in a wide variety of cellular functions including cell proliferation and migration, DNA repair, multidrug resistance and stress response to extracellular signals (Annette LASHAM et al. 2013).

YB1 protein performs its functions both in the cytoplasm and in the cell nucleus (I. A. Eliseeva et al. 2011). YB-1 peptides can be secreted from kidney mesangial cells and can activate mitogenic signaling by binding to Notch 3 receptor (I. A. Eliseeva et al. 2011).

Under physiological conditions, YB-1 localizes in the nucleus at certain steps of the cell cycle (Jurchott K etr al. 2003). Cytokines (Tsujimura et al. 2004) and Serine 102 phosphorylation in response to MAPK and PI3K/AKT signaling (Sinneberg et al. 2012; Sepe et al. 2011) also promote YB-1 nuclear translocation.

In the cytoplasm, YB-1 inhibits translation of pro-proliferative proteins and acts as a positive translation factor of pro-metastatic genes including Snail1 (Evdokimova et al. 2009). In the nucleus, YB-1 induces the transcription of several pro-proliferative genes, such as cyclins, DNA pol α and PIK3CA and the multidrug resistance (MDR1) (Jurchott K etr al. 2003; En-Nia et al 2005; Astanahe et al. 2009).

The plethora of functions fulfilled by YB-1 necessitates sub-cellular protein shuttling. Specific protein domains, denoted nuclear localization (NLS) and cytoplasmic retention signals (CRS), coordinate YB-1 multifunctional shuttling and tasking (Van Roeyen et al. 2013). Changes in the abundance of YB-1 in the cell or YB-1 translocation from the cytoplasm to the nucleus is characteristic of malignant cell growth. However, the mechanisms governing YB-1 protein subcellular localization and stability are still largely unknown.

In clinical studies, it has been shown that YB-1 is highly expressed in several type of tumors (Shibao et al 1999). Nuclear accumulation of YB-1 was shown to be associated with tumor progression, multidrug resistance and poor prognosis in ovarian cancer (Yahata et al. 2002), glioblastoma (Fotovati et al. 2011), melanoma (Sinneberg et al. 2012) and non-small cell lung cancer (Shibahara et al. 2001). For this reason, in the last years, YB1 has been considered one of the most important tumor markers and a potential therapeutic target gene for several types of malignancies.

YB-1 is targeted by several post-translational modifications, including phosphorylation, and acetylation. Data from literature indicate that YB1 protein undergoes limited proteolysis by the 20S proteasome (Sorokin et al. 2005). On the other hand, Lutz et al. have demonstrated that YB1 can be completely degraded by the 26S proteasome after ubiquitination by the F-Box protein (FBX33), a ubiquitin ligase induced during programmed cell death (Lutz et al. 2006). Later on, Moredreck et al. in 2008 discovered a new E3 ligase capable of ubiquitinating YB-1 named RBBP6 (Retinoblastoma binding protein 6) (Moredreck et al. 2008). Taken together, these observations suggest that YB-1 protein levels have to be finely tuned during cell proliferation and differentiation. However, molecular players and signaling controlling YB-1 protein turnover are remain largely unknown.

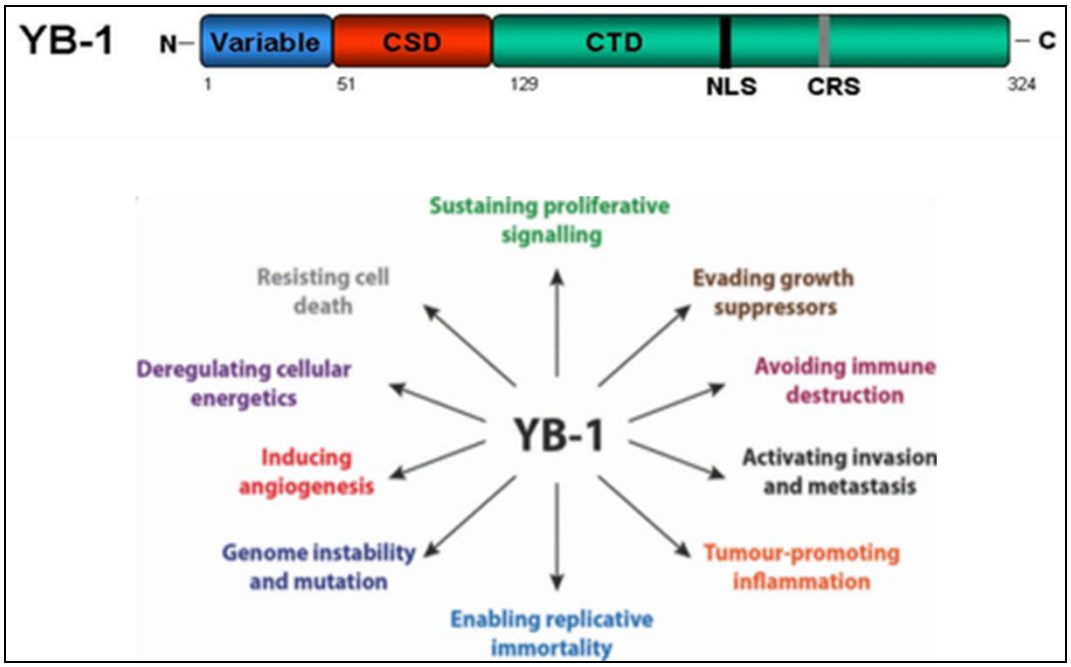

Image modified by Lasham et al. 2013

Figure 1. The Y-box-binding protein (YB-1). YB-1 represents the most evolutionary conserved nucleic-acid-binding protein currently known. YB-1 is a member of the cold-shock domain (CSD) protein superfamily. It performs a wide variety of cellular functions, including transcriptional regulation, translational regulation, DNA repair, drug resistance and stress responses to extracellular signals. As a result, YB-1 expression is closely associated with cell proliferation

2.2.4 Ubiquitination function in different biological process.

Ubiquitination is a critical modification for several biological processes, such as cell survival, differentiation and innate and adaptive immunity. Usually, ubiquitin–proteasome proteolysis pathway is used to label proteins for rapid degradation. Ubiquitin (Ub) is covalently coupled to lysine residues on target proteins by four critical enzymes that acts in succession: a ubiquitin-activating enzyme (E1), a ubiquitin-conjugating enzyme (E2 or UBC), a ubiquitin ligase (E3), and the 26S proteasome. Ub is first activated by E1 in an ATP-dependent manner via a thiolester bond and then transferred to an E2.

E3 Ubiquitin ligases concomitantly interact with a Ub-loaded E2 and the substrate protein and mediate isopeptide bond formation between the C terminus of Ubiquitin and a substrate lysine (Hershko, A. & Ciechanover, A. 1998). The 26S proteasome rapidly detects and degrades the polyubiquitinated conjugates resulting from covalent ubiquitination.

Proteins can be modified through the conjugation of monoubiquitin or polyubiquitin chains of variable length on any of the seven Lys residues (Lys6, Lys11, Lys27, Lys29, Lys33, Lys48 or Lys63) or the amino-terminal Met (Met1) of the ubiquitin monomer (Grabbe et al.2011).

Ubiquitination was shown to regulate several biological processes such as protein turnover, receptor internalization, assembling of multiprotein complexes, intracellular trafficking, inflammatory signaling, autophagy, DNA repair and regulation of enzymatic activity (Popovic d. et al 2014).

For this reason, deregulation of the ubiquitination pathway can have dramatic consequences on cell physiology. For example it could entail to up-regulation or down-regulation of metabolic pathways, incorrect assembly of protein complexes, accumulation of misfolded proteins or mislocalization of proteins (Popovic d. et al 2014).
Finally, ubiquitination can influence cancer development. However, this aspect is still difficult to understand the role of ubiquitination since ubiquitination might equally control tumor-suppressor and tumor-promoting pathways. Therefore, depending on the nature of the targeted substrate, a single Ub ligase can act as both as an oncogene or a tumor suppressor (Hoeller D. et al 2009).
My work experience stemmed from previous data showing that ΔNp63α protein physically associates with YB-1 promoting its nuclear accumulation (Di Costanzo et al. 2012). I have focused my attention on YB-1 post-translational modification and demonstrated that ΔNp63α plays a role in the control of YB-1 protein ubiquitination and turnover.

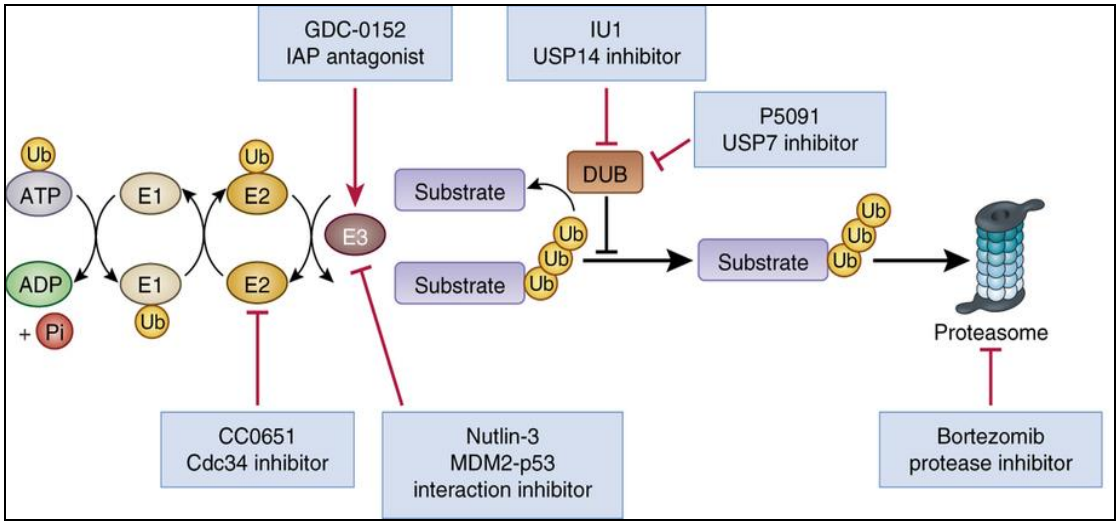

Popovic et al. 2014

Figure 2. Ubiquitination machinery. (Ub) is covalently coupled to lysine residues on target proteins by four critical enzymes that acts in succession: a ubiquitin-activating enzyme (E1), a ubiquitin-conjugating enzyme (E2 or UBC), a ubiquitin ligase (E3), and the 26S proteasome. Ub is first activated by E1 in an ATP-dependent manner via a thiolester bond and then transferred to an E2. E3 Ubiquitin ligases concomitantly interact with a Ub-loaded E2 and the substrate protein and mediate isopeptide bond formation between the C terminus of Ubiquitin and a substrate lysine (Hershko, A. & Ciechanover, A. 1998). The 26S proteasome rapidly detects and degrades the polyubiquitinated conjugates resulting from covalent ubiquitination.

2.3 Results

2.3.1 YB1 and ΔNp63α are down-regulated during keratinocyte differentiation

ΔNp63α is highly expressed in proliferating keratinocytes and decreases abruptly when cells start to differentiate (Barbieri et al. 2006). Since ΔNp63α and YB-1 are co-expressed in proliferating HaCaT keratinocytes (Di Costanzo et al. 2012), I investigated the pattern of YB1 expression in Normal Human Epidermal (NHEK) and HaCaT keratinocytes during Ca2+ induced differentiation. I cultured keratinocytes in calcium-free medium, and treated them with Ca2+ for the indicated time points. Then, I prepared whole cell extracts to perform immunoblot analysis. As shown in Figures 1A and 1B as differentiation proceeds, the level of YB1 protein decreased suggesting that, similar to ΔNp63α, YB1 must be down-regulated to allow differentiation of keratinocytes.

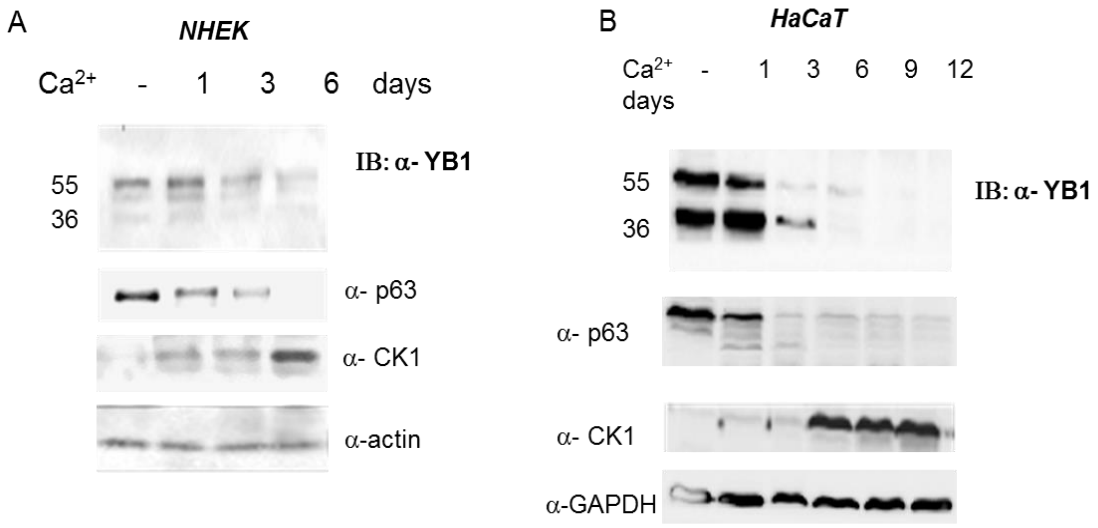

Figure 1. YB1 and ΔNp63α are down-regulated during keratinocyte differentiation.
(A) NHEK were induced to differentiate, for the indicated days, in 1.5 mM Ca2+. Whole cell extracts were analyzed by immunoblotting using antibodies against p63, YB-1, Cytokeratin 1 (CK1). Actin was used as loading control. (B) HaCaT cells were induced to differentiate for the indicated days with 2.0 mM calcium. Cell extracts were analyzed by immunoblotting with p63, YB- 1 and CK1 antibodies, as indicated. Undifferentiated HaCaT, grown in absence of calcium, were used as negative control. GAPDH was used as loading control.

2.3.2 YB-1 and ΔNp63α down-regulation is associated to cell cycle exit.

Next, I induced growth arrest in HaCaT keratinocytes by confluency and serum starvation as cell cycle exit is an integral part of keratinocyte differentiation. My aim was to examine YB1 and ΔNp63α expression under normal and serum-starvation conditions. HaCaT keratinocytes were grown to confluence and serum starved for 24 hours. I prepared nuclear and cytoplasmic extracts to perform immunoblot analysis. As shown in Figure 2A, both YB1 and ΔNp63α were down-regulated under growth arrest conditions as demonstrated by reduction of cyclin D1 expression and induction of the cell cycle inhibitor p21WAF (Figure 2A). While I was doing my experiments, results from Dr. A. Troiano in my laboratory revealed that YB1 silencing in proliferating HaCaT and transformed keratinocytes triggers a dramatic and fast apoptotic response (Troiano et al. 2015). All together these results indicate that YB1 is essential for sustaining proliferation and survival of basal keratinocytes. Remarkably, I noticed that calcium-dependent differentiation protects from apoptotic death induced by decrease of YB-1 protein level.

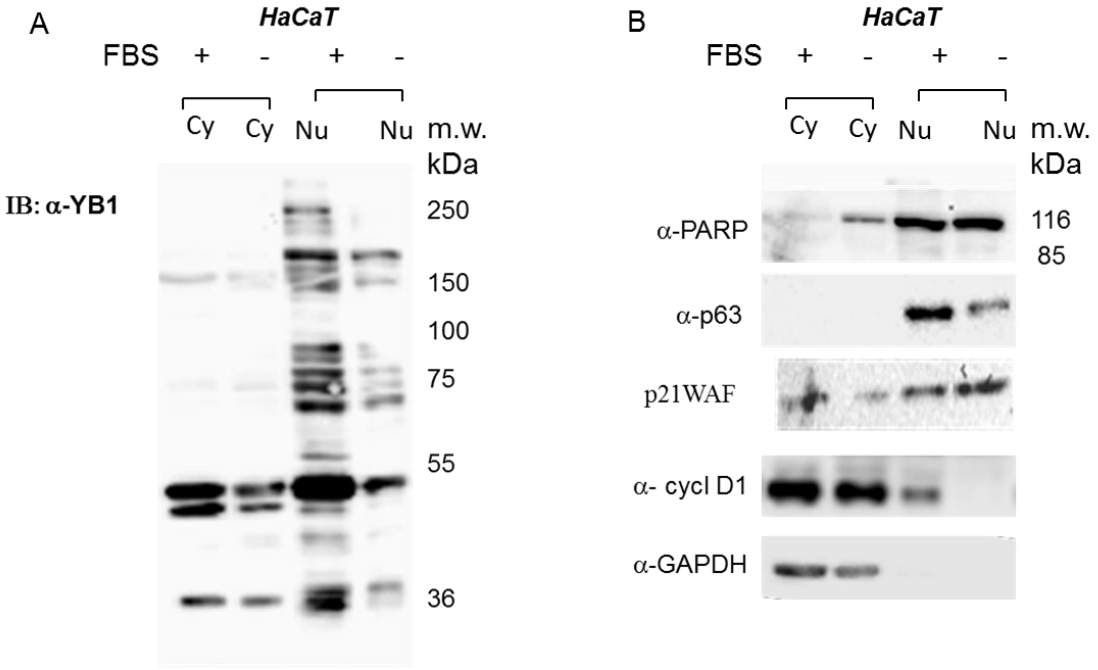

Figure 2. YB-1 sustains the proliferative activity of keratinocytes. (A-B) HaCaT keratinocytes were cultured in DMEM medium with (+ FBS) or without FBS (- FBS), as indicated. After 48 hours, cells were harvested. Nuclear (Nu) and cytoplasmic (Cy) extracts were subjected to immunoblot using p63, YB-1, P21WAF, Cyclin D1 antibodies. GAPDH and PARP antibodies were used as loading controls and to check for cross-contamination between the fractions.

2.3.3 ΔNp63α regulates YB1 stability

Since ΔNp63α and YB-1 are abundantly expressed in proliferating basal keratinocytes and ΔNp63α promotes accumulation of full length YB1 protein in the nuclear compartment (Di Costanzo et al. 2012), I postulated that ΔNp63α control YB1 protein stability. Therefore, I first investigated whether the increase of YB1 protein level, induced by ΔNp63α, was due to reduced YB1 protein turnover. Thus, I compared YB1 protein half-life in mock and ΔNp63α transfected MDA-MB231 cells. 24 hrs after transfection, cells were treated with cycloheximide to block protein synthesis. At the indicated times of drug exposure, cells were harvested, and whole extracts were analyzed by Western blot and probed with anti-YB1 antibody. As shown in Figure 3, in mock transfected cells, YB1 exhibited a very peculiar byphasic response to cycloheximide, indeed the amount of YB1 protein was reduced to 40% after 4 hours, but then it remained constant up to 16 hours of incubation. Strikingly, in presence of ΔNp63α 80% of YB1 protein persisted after 24 hours of incubation with CHX thereby indicating that ΔNp63α reduces YB1 protein turnover.

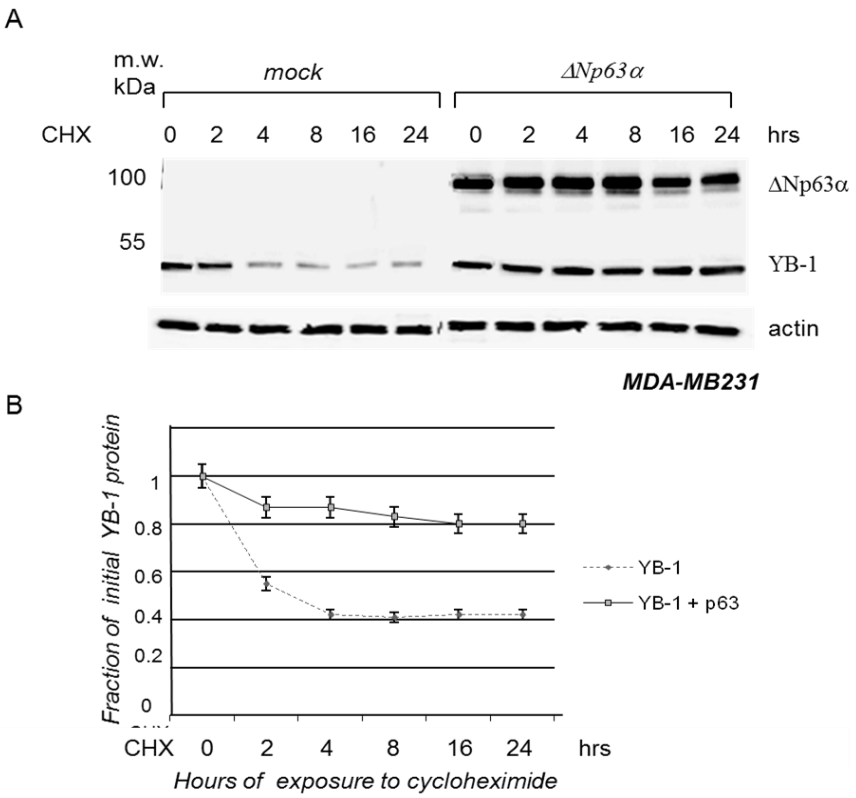

Figure 3. ΔNp63α reduces YB-1 protein turnover. (A) A representative immunoblot analysis of YB-1 protein level in MDA-MB231 cells treated with 10 µg/ml cycloheximide (CHX), for the indicated times. Cells were seeded at 60% confluency in 100-mm dishes. 24 hours after, cells were transfected with an empty vector or a ΔNp63α expressing plasmid. Equal amounts of proteins were subjected to immunoblot analysis with YB-1 or p63 antibodies. Actin was used as loading control. (B) Protein half-life was expressed in the plot as the fraction of the initial protein. Data are presented as the mean value obtained from three independent experiments. YB-1 bands (50 kDa) were quantified by densitometric scanning and Quantity-ONE software.

2.3.4 ΔNp63α expression increase the amount of YB1 slow migrating forms

Next, I transfected increasing amount of ΔNp63α expression plasmid in p63 null MDA-MB231 cells. In addition to the expected accumulation of full length YB1 protein (p50/YB1), ΔNp63α expression caused an increase of slow migrating YB1 immunoreactive bands (sm/YB1) and a concomitant reduction of faster migrating YB1 forms (Figure 4A). In particular, I observed the reduction of a 36 KDa band of YB-1 previously reported to be a product of YB-1 50 kDa limited proteolysis by proteosome 26S (Sorokin et al. 2005).Then, I performed immunoblot analyses of whole-cell extracts obtained from ΔNp63α proficient HaCaT, A431, and SCC011 cells to further investigate on the observed high molecular forms of YB1. In all cell lines tested, I observed slow migrating bands immunoreactive to YB1 antibodies raised against a peptide encompassing aminoacids 1 to 100 of human YB1 (Figure 4B). I obtained similar results with a different commercial antibody directed against a peptide encompassing aminoacids 167 to 264 of YB1 (data not shown).

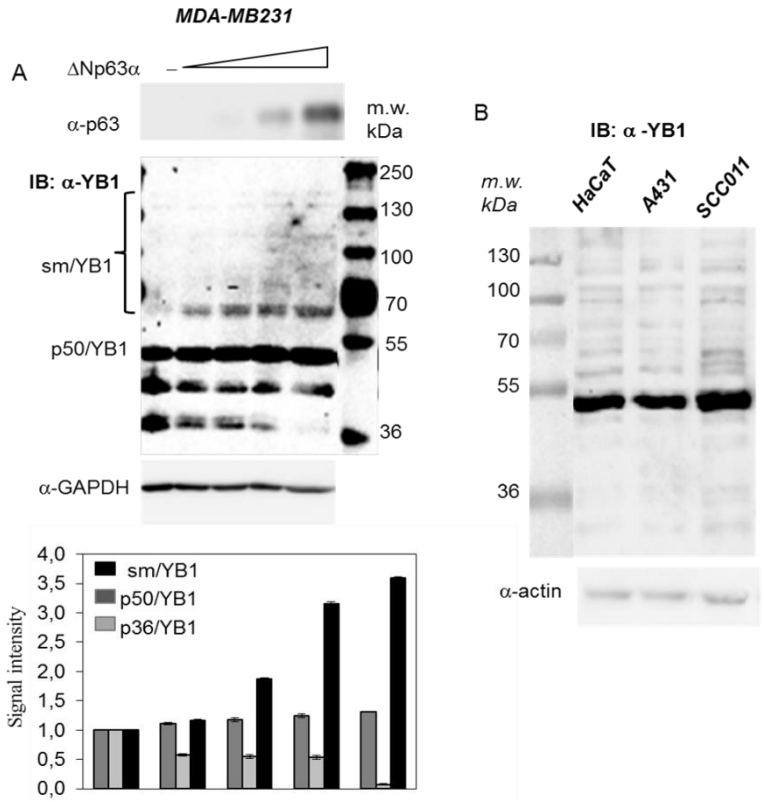

Figure 4. ΔNp63α expression increase the amount of YB1 slow migrating forms. (A) Immunoblotting (upper panel) and densitometric analysis (lower panel) of MDA-MB231 cells transiently transfected with increasing amounts of ΔNp63α expression plasmid (0.5, 1.0, 1.5, 2.0 μg). Whole extracts were analysed with YB-1 and p63 antibodies. Glyceraldehyde 3-phosphate dehydrogenase (GAPDH) was used as loading control. (B) Immunoblot analysis of YB-1 in HaCaT, A431 and SCC011 cells with YB-1 antibody (ab12148, Abcam). The 50 kDa band corresponding to unmodified YB-1 protein is indicated by arrow. Actin was used as loading control.

2.3.5 p63 depletion by siRNA induces a reduction of YB1 slow migrating forms

To check the identity of the observed slow migrating bands, I depleted p63 proficient A431 cells of endogenous YB1 by RNA interference. 48 hrs after YB1 silencing, whole cell extracts were subjected to immunoblots with YB1 antibodies. Some of the slow migrating bands disappeared or were reduced along with full length YB1 implying that they were YB1 modified forms (Figure 5A, black arrows). Next, I depleted SCC011 cells of endogenous ΔNp63α, to finally prove the effect of ΔNp63α on YB1 protein modification. As shown in Figure 5B, I observed a significant reduction of full length and slow migrating YB1 bands in the nuclear compartment. As expected, the p36/YB1 form became clearly detectable thus confirming my previous observations (Figure 5B).

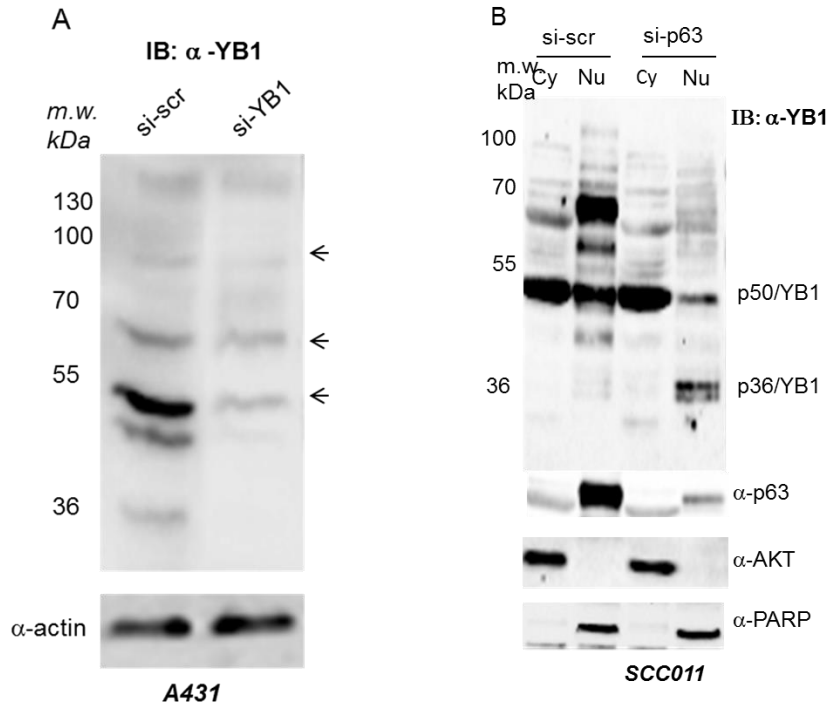

Figure 5. p63 and YB-1 depletion by siRNA induces a reduction of YB1 slow migrating forms (A) Immunoblot analysis of YB-1 in YB-1 depleted A431 cells 48 hours after silencing. YB-1 protein was detected using the YB-1 antibody. Actin was used as loading control. (B) SCC011 cells were silenced with IBONI p63-siRNA pool or scrambled oligos. 48 h after silencing, cells were fractionated to obtain cytoplasmic (Cy) and nuclear (Nu) fractions. Filters were incubated with YB-1 and p63 antibodies. To check for cross-contamination, PARP and total AKT were used as nuclear and cytoplasmic control, respectively.

2.3.6 YB1 slow migrating forms are accumulated in the nuclear compartment

Next, I performed western blot analysis of nuclear and cytoplasmic fractions of MDA-MB231, A431 and SCC01 carcinoma cells (Figure 3A). These experiments revealed that slow migrating YB1-immunoreactive bands were enriched in the nuclear compartment. Interestingly, I also detected distinct several YB1 forms, smaller than 50 kDa, likely generated by proteasome-mediated limited cleavage (Sorokin et al. 2005) (Figure 6A, black arrow). I analyzed the effect of proteasome inhibition, by treating HaCaT cells with

MG132. I prepared nuclear/cytoplasmic fractions to perform immunoblot with YB1 antibodies. As shown in Fig 3B, I observed high molecular forms of YB1 into the nucleus of not transformed HaCaT keratinocytes. Following MG132 treatment, full length YB1 accumulated and nuclear YB1 fragments smaller than 50 kDa either decreased or disappeared. Remarkably, proteasome inhibition also reduced high molecular forms of YB1 suggesting that they were generated upon endoproteolytic cleavage of YB1 probably by the 20S proteasome (Figure 6B).

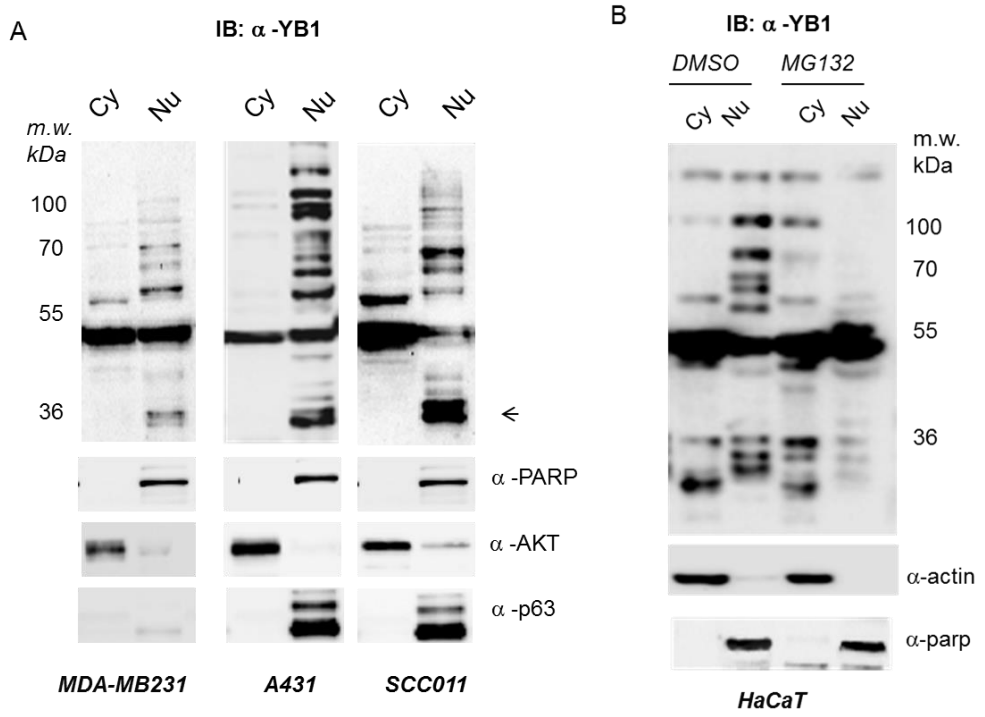

Figure 6.YB1 slow migrating forms are accumulated in the nuclear compartment. (A) Immunoblot analysis of MDA-MB231, A431 and SCC011 cytoplasmic (Cy) and nuclear (Nu) 361 fractions. YB-1 and p63 were detected with ab12148 (Abcam) and D9 (Santa Cruz Biotechnology) antibodies, respectively. The filters were blotted with antibodies against PARP and total AKT to check for cross-contamination between the fractions. (Note the presence of YB-1 36 kDa band exclusively in the nuclear compartment). (B) Immunoblot analysis of HaCaT cytoplasmic (Cy) and nuclear (Nu) fractions after 5 hrs of MG132 treatment (5μM final concentration). YB-1 was detected with ab12148 (Abcam). Note the decrease of slow and fast migrating YB-1 forms following MG132 treatment into the nucleus and the accumulation of full length YB-1 50 kDa. The filters were blotted with antibodies against PARP and actin to check for cross-contamination between the fractions.

2.3.7 YB1 slow migrating forms are poli-ubiqitinated

It was previously reported that YB1 is poly-ubiquitinated and degraded via the ubiquitin-proteasome pathway (Lutz M. et al. 2006). Indeed, in MDA-MB231 cells transfected with Ubi-Ha, ubiquitin-containing complexes, immunoprecipitated with anti-HA antibodies, included endogenous YB1 and p63 proteins (Figure 7A, lanes 5 and 6). By specifically looking at the pattern of high-molecular weight YB1 forms in MB-MDA231 cells, I found that it was enhanced by ubiquitin or ΔNp63α transfection (Figure 7B, lanes 1 and 3 and

Figure 7C, lane 2) and even more by ubiquitin and ΔNp63α co-transfection (Figure 7B lane 4 and Figure 7C lane 4) resulting very similar to that observed in ΔNp63α proficient A431 cells (Figure 7B, lane 5). Moreover, I observed a reduction of the YB1 36 kDa forms in cells expressing ΔNp63α (Figure 7C, lanes 2 and 4). MG132 addition to cells overexpressing ubiquitin and ΔNp63α, instead, stabilized full length YB1 and reduced ubi-conjugated forms of YB1, particularly those migrating between 50 and 70 kDa, again suggesting that they are generated following limited YB1 cleavage (Figure 7C, compare lanes 3 and 4).

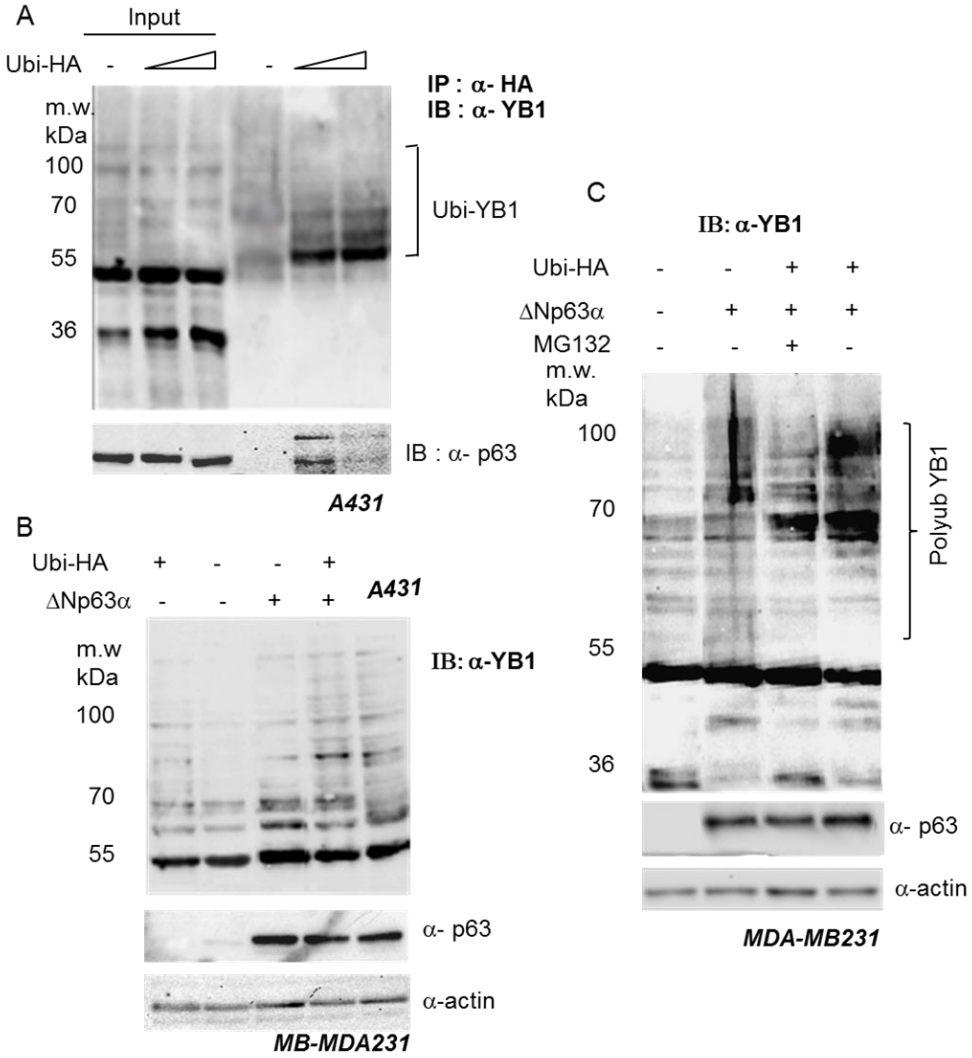

Figure 7. YB1 slow migrating forms are poli-ubiqitinated. (A) A431 cells were transiently transfected with Ubi-HA expression plasmids. After 24 hrs, extracts were immunoprecipitated (IP) with anti-HA antibody and the immunocomplexes were subjected to immunoblot (IB) with YB-1 or p63 antibodies, as indicated. (B) MDA-MB231 cells were transiently transfected with an empty vector (mock), a ΔNp63α and/or Ubi-HA plasmid, asindicated. Whole cell extracts were analysed by immunoblotting with YB-1 and p63 antibodies. Actin was used as loading control. A431 are p63 proficient cells. (C) MDA-MB231 cells were transiently transfected with Ubiquitin and/or ΔNp63α expression plasmid. Cells were treated with MG132, as indicated. Whole extracts were analysed by immunoblotting with YB-1 and p63antibodies. Actin was used as loading control.

2.4 Discussion

In the second part of my PhD work I contributed to understand the functional mechanism by which ΔNp63α is involved in the regulation of YB-1 protein turnover.

My first observation was that YB-1 protein exhibits a quite reproducible pattern of high molecular weight forms. Moreover, the expression pattern of those bands was quite reproducible and similar in all cell lines tested.

Inspection of YB-1 aminoacid sequence revealed the presence of many lysines that are potential target of ubiquitin and sumo modifications.

Transfection of HA-tagged Ubiquitin followed by immunoprecipitation with HA antibodies confirmed that at least some of the observed YB1 slow migrating forms are poly-ubiquitinated although we cannot exclude that other modifications such as sumoylations or acetylations can also be present. Further experiments are needed to clarify this point.

This observation suggested a role for the proteasome 26S in YB-1 degradation. However, since I have observed accumulation of full length YB-1 and reduction of YB-1 slow-migrating Y-1 forms following treatment with MG132, we hypothesized that a 20S proteasome-dependent YB-1 endoproteolityc cleavage occurs before YB-1 poli-ubiquitination. It is important to remind that it was previously demonstrated that YB-1 undergoes a proteasome-dependent limited cleavage under DNA damage stimuli (Sorokin et al).

Next, I established that the ectopic expression of ΔNp63α in p63 null MDA-MB231cells significantly increases full length YB1 protein half-life and reduces the level of the p36 YB-1 fragment. This last experiment demonstrates that ΔNp63α expression can protect full length YB-1 from specific endoproteolysis.

Moreover, the increase of poli-ubiquitinated YB-1 upon ΔNp63α enforced expression suggests that ΔNp63α might either reduce their export from the nuclear to the cytoplasmic compartment or increase the rate of YB-1 ubiquitination. At these stage, however, I have not clear experimental evidences to distinguish between these two hypotheses.

Ubiquitination is a critical modification for several biological processes, such as cell survival, differentiation and innate and adaptive immunity (Popovic et al. 2014). Usually, ubiquitin-conjugation is used to label proteins for rapid degradation. By the 26 proteasome. However, considering my results I cannot exclude that addition of polyubiquitin chain to YB-1 can confer to the protein new functionalities such as the ability to interact with target proteins via ubiquitin binding domains or assemble into multimeric complexes (O'Neil LA 2009).

In my system I have not identified a specific ubiquitin ligase/s involved YB-1 post- translational modification. However, the F-box Protein 33 (FBX33) (Lutz

et al.2006) and the ring finger Retinoblastoma Binding Protein 6 (RBBP6) (Moredreck Chibi et al. 2008) are potential candidates as they have already demonstrated to specifically target YB-1.

Generation of YB-1 mutant proteins that that cannot be ubiquitinated will largely help to understand the physiological role of such YB-1 modification.

YB-1 expression in basal keratinocytes can be functionally critical for skin proliferation and survival. Accordingly, ΔNp63α a well assessed marker of basal keratinocyte proliferation acts by preserving full length YB-1 integrity. I have observed that YB-1 levels are higher in response to growth stimuli and rapidly down-regulated during cell cycle such as upon serum deprivation and differentiating stimuli. A relevant issue, is whether YB-1 expression can exert a selective control upon ΔNp63α transcriptional functions and what might the effect of mutant p63 on YB-1 functions.

A further hypothesis to explore is that by binding YB-1 into the nuclear compartment, ΔNp63α might recruit the YB-1 protein on the promoter of pro-proliferative genes. ΔNp63α gene silencing followed by Chromatin immunoprecipitation and deep sequencing can provide the answer to this question. However, we cannot exclude that ΔNp63α might reduce the pool of cytoplasmic YB-1 thereby influencing the translation regulatory functions of YB-1.

At this stage, although it needs to be confirmed *in vivo*, YB-1 can be considered a reliable marker of keratinocyte proliferation and a pro-survival factor.

2.5 Materials and Methods

2.5.1 Plasmids

cDNA encoding human ΔNp63α was previously described (Di Costanzo et al. 2012). cDNA encoding human Ubi-HA were provided by Dr. V Orsini.

2.5.2 Cell culture

MDA-MB231 cells were derived from metastatic breast carcinoma and A431 cells were established from an epidermoid carcinoma of the vulva. Cutaneous squamous carcinoma cells SCC011 were described in Di Costanzo et al. 2012 and cultured in RPMI supplemented with 10% fetal bovine serum at 37°C 42 and 5% CO2. A431, HaCaT and MDA-MB231 were purchased from Cell Line Service (CLS, Germany) and cultured at 37°C and 5% CO2. A431 and HaCaT cells were maintained in DMEM supplemented with 10% FBS. MDA-MB231 cells were maintained in DMEM supplemented with5% FBS. NHEK cells were obtained from PromoCell (Heidelberg; Germany) and cultured M2 medium under the manufacturer's recommendations For differentiation, NHEK (2.3×10^5) cells, seeded at 60% confluence in 60 mm dishes were cultured for the indicated days in 1.5 mM Ca2+. For HaCaT differentiation, cells (2.5×10^5) were seeded in 35 mm dishes and grown until 80% confluence. The medium was then replaced with DMEM without FBS and 2 mM calcium.

2.5.3 Transient transfection

Lipofections were performed with Lipofectammine 2000 (Invitrogen), according to the manufacturer's recommendations. YB1 transient silencing was carried out with RIBOXX (IBONI YB-1siRNA pool) and RNAiMAX reagent (Invitrogen), according to the manufacturer's recommendations. Briefly, cells were seeded at 60% confluence (1.5×10^6) in 100-mm dishes and transiently silenced with IBONI YB1-siRNA at 20 nm final concentration.

YB-1 guide sequences: UUUAUCUUCUUCAUUGCCGCCCCC; UUAUUCUUCUUAUGGCAGCCCCC; UUCAACAACAUCAAACUCCCCC; UCAUAUUUCUUCUUGUUGGCCCCC.

ΔNp63α transient silencing was carried out with RIBOXX (IBONI p63-siRNA pool) at 20 nm (final concentration) and RNAiMAX reagent (Invitrogen).

p63 guide sequences: UUAAACAAUACUCAAUGCCCCC; UUAACAUUCAAUAUCCCACCCCC; AUCAAUAACACGCUCACCCCC; AUGAUUCCUAUUUACCCUGCCCCC.
"All Star Negative Control siRNA", provided by Quiagen, was used as negative control.

2.5.4 Protein turnover analysis

For half-life studies MDA-MB231 cells were transfected with mock or ΔNp63α plasmids. 24 hours after transfection, cells were replated in 6-well dishes, allowed to adhere overnight, and treated with cycloheximide (Calbiochem) at a final concentration of 10 μg/ml. Cells were harvested at the indicated time points. Total cell extracts were prepared and 20 μg of each sample was probed, in Western blot, with anti YB-1 antibody and, as control, with anti-actin.

2.5.5 Antibodies and chemical reagents

Anti-p63 (4A4), anti-cytokeratin 1 (4D12B3), anti-p21WAF (F-5), anti-GAPDH (6C5), and anti- actin (1-19) were purchased from Santa Cruz (Biotechnology Inc.). Cyclin D1, PARP and AKT antibodies were from Cell Signaling Technology (Beverly, Massachussets). Rabbit polyclonal YB1(Ab12148) antibody was purchased from Abcam. (Cambridge, UK). Mouse monoclonal anti-HA(12CA5) antibody was purchased from Roche Applied Science. Proteasome inhibitor MG132 and Cycloheximide (CHX) were purchased from Sigma-Aldrich. MG132 treatment was carried out as previously described (22).

2.5.6 Western blotting

At 48 h after transfection cells were lysed in 10 mM Tris-HCl (pH 7.5), 1 mM EDTA, 150 mM NaCl, 1 mM dithiothreitol, 1 mM phenylmethylsulfonyl fluoride, 0.5% sodium deoxycholate, and protease inhibitors. Cell lysates were incubated on ice for 30 min, and the extracts were centrifuged at 13,000 rpm for 10 min to remove cell debris. Protein concentrations were determined by the Bio-Rad protein assay. After the addition of 4× loading buffer (2% sodium dodecyl sulfate [SDS], 30% glycerol, 300 mM β-mercaptoethanol, 100 mM Tris-HCl [pH 6.8]), the samples were incubated at 95°C for 5 min and resolved by SDS-polyacrylamide gel electrophoresis. To detect YB-1 poli-ubiquitinated forms, in MDA- MB231 cells (p63 -/-), 2 $\times 10^6$ cells were plated in 100 mm dishes and transfected with plasmids encoding human ΔNp63α and Ubi-HA. 30 □g of whole extracts were separated by SDS-PAGE and subjected to immunoblot.

2.5.7 Nuclear-cytoplasmic fractionation

The cells were seeded at 60% confluence (1.5 × 106) in 100 mm dishes. 24 h after seeding, cell lysates were fractionated to obtain cytoplasmic and nuclear fractions. 10 □g of nuclear and 30 □g of cytoplasmic extracts (1:3 rate) were separated by SDS-PAGE and subjected to immunoblot. All images were acquired with CHEMIDOC (Bio Rad) and analyzed with the Quantity-ONE 100 software.

2.5.8 Immunoprecipitation

To detect YB-1 poli-ubiquitinated forms in A431 cells, 2 ×10^6 cells were seeded in 100 mm dishes and transfected with Ubi-HA plasmid vector. Lysates containing 1 mg of proteins were precleared with 30 µl of protein A-agarose (50% slurry; Roche) and then incubated overnight at 4℃ with 3µg of anti-p63 (anti-HA; Roche). The immunocomplexes were collected by incubating with protein A-agarose (Roche) at 4℃ for 4 hrs. The beads were washed vigorously seven times with Co-IP buffer (50 mM Tris-HCl pH 7.5; 150 mM NaCl; 5 mM EDTA; 0.5% NP40; 10% glycerol). The beads were then resuspended in 4X loading buffer, loaded directly onto an SDS-8% polyacrylamide gel and subjected to western blot with the indicated primary antibodies.

2.6 References:

1. Cédric Blanpain and Elaine Fuchs. Epidermal homeostasis: a balancing act of stem cells in the skin. Nat Rev Mol Cell Biol. 2009 Mar; 10(3): 207–217.
2. Barbieri CE, Tang LJ, Brown KA,Pietenpol JA. (2006) Loss of p63 leads to increased cell migration and up-regulation of genes involved in invasion and metastasis. Cancer Res. 321 66(15):7589-97.
3. Yang A, Schweitzer R, Sun D, Kaghad M, Walker N, Bronson RT, Tabin C, Sharpe 307 A, Caput D, Crum C, McKeon F. (1999) p63 is essential for regenerative proliferation in 308 limb, craniofacial and epithelial development. Nature. 398: 714-718.
4. Amoresano A., Di Costanzo A., Leo G., Di Cunto F., La Mantia G., Guerrini L. et al. (2010) Identification of ΔNp63α Protein Interactions by Mass Spectrometry. J. Proteome Res. 9: 2042-48.
5. Calabrò V, Mansueto G, Santoro R, Gentilella A, Pollice A, Ghioni P, Guerrini L, La 301 Mantia G. (2004). Inhibition of p63 transcriptional activity by p14ARF: Functional and 302 physical link between human ARF tumor suppressor and a member of the p53 family. 303 M.C.B. 24:8529-8540
6. Romano RA, Smalley K, Magraw C, Serna VA, Kurita T, Raghavan S, Sinha S. ΔNp63 knockout mice reveal its indispensable role as a master regulator of epithelial development and differentiation. Development. 2012 Feb;139(4):772-82. doi: 10.1242/dev.071191.
7. Rossi M, De Simone M, Pollice A, Santoro R, La Mantia G, Guerrini L, Calabrò V. (2006) 305 Itch/AIP4 associates with and promotes p63 protein degradation. Cell Cycle. 5(16):1816-22.
8. Lee E. Finlan and Ted R. Hup p63: The Phantom of the Tumor Suppressor Cell Cycle 2007; Vol.6 Issue 9 Review 1062-1071
9. McKeon F. p63 and the epithelial stem cell: More than status quo? Genes dev. 2004. 18:4659.
10. Nylander K, Coates PJ, Hall PA. Characterization of the expression pattern of p63 alpha and delta Np63 alpha in benign and malignant oral epithelial lesions. Int J Cancer 2000; 87:368-72.
11. Annette LASHAM, Cristin G. PRINT, Adele G. WOOLLEY, Sandra E. DUNN and Antony W. BRAITHWAITE. REVIEW ARTICLE YB-1: oncoprotein, prognostic marker and therapeutic target? Biochem.J.(2013)449,11–23) doi:10.1042/BJ20121323 11
12. I. A. Eliseeva, E. R. Kim, S. G. Guryanov, L. P. Ovchinnikov*, and D. N. Lyabi Y-Box Binding Protein 1 (YB-1) and Its Functions. 2011. Published in Russian in Uspekhi Biologicheskoi Khimii, 2011, Vol. 51, pp. 65-132.
13. Jurchott K., Bergmann S., Stein U., Walther W., Janz M., Manni I., Piaggio et al. (2003) YB1 as a cell cycle-regulated transcription factor facilitating cyclin A and cyclin B1 gene expression. J Biol Chem. 278: 27988-96.
14. Tsujimura S, Saito K, Nakayamada S, Nakano K, Tsukada J, Kohno K et al. (2004) Transcriptional regulation of multidrug resistance-1 gene by interleukin-2 in lymphocytes. Genes Cells.; 9(12):1265-73.

15. Sinnberg T, Sauer B, Holm P, Spangler B, Kuphal S, Bosserhoff A et al. (2012) MAPK and PI3K/AKT mediated YB-1 activation promotes melanoma cell proliferation which is counteracted by an autoregulatory loop. Exp Dermatol. 21(4):265-70; e-pub ahead of print doi: 10.1111/j.1600-0625.2012.01448.x.
16. Sepe M., Festa L., Tolino F., Bellucci L., Sisto L., Alfano D., Ragno P., Calabrò V., de Franciscis V., La Mantia G., Pollice A. (2011) A regulatory mechanism involving TBP-1/Tat-Binding Protein 1 and Akt/PKB in the control of cell proliferation. PLoS One. 6(10) e-pub ahead of print Oct 4. doi: 10.1371/journal.pone.0022800.
17. Evdokimova V, Tognon C, Ng T, Ruzanov P, Melnyk N, Fink D et al. (2009) Translational activation of snail1 and other developmentally regulated transcription factors by YB-1 promotes an epithelial-mesenchymal transition. Cancer Cell. 5;15(5):402-15; e-pub ahead of print doi: 10.1016/j.ccr.2009.03.017.
18. En-Nia A, Yilmaz E, Klinge U, Lovett DH, Stefanidis I, Mertens PR. (2005) Transcription factor YB-1 mediates DNA polymerase alpha gene expression. J Biol Chem. 280(9):7702-11.
19. Astanehe A, Finkbeiner MR, Hojabrpour P, To K, Fotovati A, Shadeo A et al. (2009) The transcriptional induction of PIK3CA in tumor cells is dependent on the oncoprotein Y-box binding protein-1. Oncogene. 28(25):2406-18; e-pub ahead of print doi: 10.1038/onc.2009.81.
20. Van Roeyen CR, Scurt FG, Brandt S, Kuhl VA, Martinkus S, Djudjaj S et al. (2013) Cold shock Y-box protein-1 proteolysis autoregulates its transcriptional activities. Cell Commun Signal. 27;11(1):63-70.
21. Shibao, K., Takano, H., Nakayama, Y., Okazaki, K., Nagata, N., Izumi, H., Uchiumi, T., Kuwano, M., Kohno, K., and Itoh, H. (1999) Int. J. Cancer, 83, 732-737.
22. Yahata H., Kobayashi H., Kamura T., Amada S., Hirakawa T., Kohno K., Kuwano M., Nakano H. (2002) Increased nuclear localization of transcription factor YB-1 in acquired cisplatin-resistant ovarian cancer. J Cancer Res Clin Oncol. 128(11):621-6.
23. Fotovati A, Abu-Ali S, Wang PS, Deleyrolle LP, Lee C, Triscott J et al. (2011) YB-1 bridges neural stem cells and brain tumor-initiating cells via its roles in differentiation and cell growth. Cancer Res. 71(16):5569-78; e-pub ahead of print doi: 10.1158/0008-5472.CAN-10-2805.
24. Shibahara K, Sugio K, Osaki T, Uchiumi T, Maehara Y, Kohno K et al. (2001) Nuclear expression of the Y-box binding protein, YB-1, as a novel marker of disease progression in non-small cell lung cancer. Clin Cancer Res. 7(10):3151-5.
25. Sorokin AV, Selyutina AA, Skabkin MA, Guryanov SG, Nazimov IV, Richard C, Th'ng 294 J, Yau J, Sorensen PH, Ovchinnikov LP, Evdokimova V. (2005) Proteasome-mediated 295 cleavage of Y-box-binding protein 1 is linked to DNA damage response. The EMBO 296 Journal 24: 3602-3612.
26. Lutz, M., Wempe, F., Bahr, I., Zopf, D., and von Melchner, H. Proteasomal degradation of the multifunctional regulator YB-1 is mediated by an F-Box

protein induced during programmed cell death (2006) FEBS Lett., 580, 3921-3930.
27. Moredreck Chibi, Mervin Meyer, Amanda Skepu, D. Jasper G, Johanna C. Moolman-Smook, David J.R. Pugh RBBP6 Interacts with Multifunctional Protein YB-1 through Its RING Finger Domain, Leading to Ubiquitination and Proteosomal Degradation of YB-1Rees Journal of Molecular Biology. Volume 384, Issue 4, 26 December 2008, Pages 908–91
28. Hershko, A. & Ciechanover, A. The ubiquitin system. Annu. Rev. Biochem. 67, 425–479 (1998).
29. Caroline Grabbe, Koraljka Husnjak,and Ivan Dikic. The spatial and temporal organization of ubiquitin networks Nat Rev Mol Cell Biol. 2011 May; 12(5): 295–307.
30. Popovic D, Vucic D, Dikic I Ubiquitination in disease pathogenesis and treatment. Nat Med. 2014 Nov;20(11):1242-53. doi: 10.1038/nm.3739. Epub 2014 Nov 6.
31. Hoeller, D. & Dikic, I. Targeting the ubiquitin system in cancer therapy. Nature 458, 438–444 (2009).
32. Di Costanzo A, Troiano A, di Martino O, Cacace A, Natale CF, Ventre M et al. (2012) The p63 protein isoform ΔNp63α modulates Y-box binding protein 1 in its subcellular distribution and regulation of cell survival and motility genes. J Biol Chem. 287(36):30170-80; e-pub ahead of print doi: 10.1074/jbc.M112.349951.
33. O'Neil LA. (2009) Regulation of Signaling by non-degradative ubiquitination. J.Biol. Chem. 326 284(13):8209.

Chapter 3

3. Zebrafish as a model to study YBX-1 protein expression and function

3.1 Aim of the visit

As part of my PhD degree program I spent four months abroad at the Karlsruhe Institute of Technology (KIT), Karlsruhe, Germany (April 2014- July 2014) under the supervision of Professor Nicholas S. Foulkes, one of the major expert in zebrafish biology.

The aim of my visit was to study YBX-1 gene expression and function *in vivo* using zebrafish (Danio rerio) as a model organism. The use of Zebrafish present several benefits, such as the small size, fecundity and the optical transparency of its embryos. Zebrafish has become a widely used model organism because of its morphological and physiological similarity to mammals (Graham et al. 2007), the existence of many genomic tools and the amenability to genetic and chemical phenotype-based screening. Because of these attributes, zebrafish can largely contribute to drug developmental process, including target identification, disease modeling and toxicology. The Karlsruhe Institute of technology (KIT institute, Germany) has one of the biggest European fish facility (European Zebrafish Resource Center of Karlsruhe) therefore is one of the best place to gain experience on this model.

As previously mentioned the relevance of YBX-1 in the control of cell proliferation is well assessed. However, the specific role played by YBX-1 in the molecular mechanisms regulating cell proliferation and differentiation remains undefined.

In zebrafish, cell cycle is under the control of the light and circadian rhythms. Remarkably, this is also observed in established zebrafish cell lines (Dekens et al., 2003). I took advantage of these properties to investigate the expression pattern of YB-1 under light-dark conditions in epidermal cells.

3.2 Introduction

3.2.1 Circadian rhythmicity and timing in cell proliferation.

Almost every aspect of plant and animal biology shows day - night rhythms. Rhythmicity is observed in transcriptional expression of a wide range of genes that regulate a variety of normal cell functions, such as cell division and proliferation. De-synchrony of this rhythmicity seems to be implicated in several pathologic conditions, including tumorigenesis and progression of cancer (Christos Savvidis and Michael Koutsilieris 2012).

Central to the circadian timing system is a pacemaker that oscillates with a period of circa 24 hours (Idda et al. 2012). Thus, to remain synchronized with the day-night cycle, environmental timing signals (*zeitebergs*) such as light or

temperature, reset this pacemaker via input pathways. Importantly, clock output pathways subsequently convey this timing information to almost every aspect of physiology in the organism (Idda et al. 2012). At the core of the circadian clock are transcription-translation feedback loops that take approximately 24 hours to complete one cycle (Vatine et al 2011). (Figure 1)

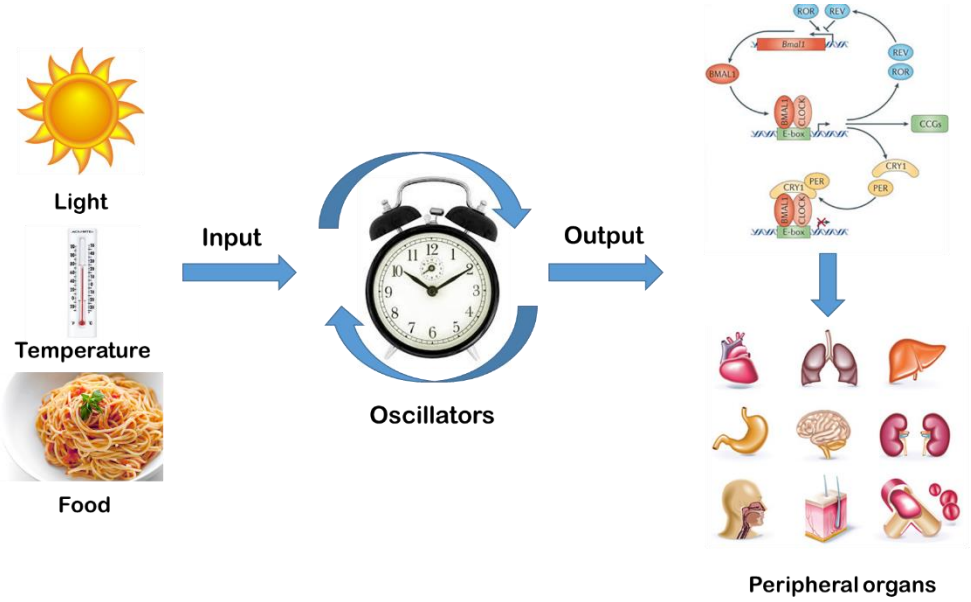

Figure 1. Circadian clock system. Central to the circadian timing system is a pacemaker that oscillates with a period of circa 24 hours (Idda et al. 2012). Thus, to remain synchronized with the day-night cycle, environmental timing signals (*zeitebergs*) such as light or temperature, reset this pacemaker via input pathways. Importantly, clock output pathways subsequently convey this timing information to almost every aspect of physiology in the organism (Idda et al. 2012).

Within the vertebrate clock, the bHLH PAS domain transcription factors CLOCK and BMAL (positive elements) bind as heterodimers to E-box enhancer elements (CACGTG) up-regulating the expression of negative elements (PERIOD and CRYPTOCHROME) that thereby down-regulate their own transcription.

One of the key outputs of the clock is the timing of cell cycle progression. From cyanobacteria to higher vertebrates, there is evidence that the circadian clock gates regulatory steps in DNA synthesis and mitosis (Mori T et al. 2000). Circadian rhythms of cell cycle and cyclins mRNA expression have been reported in many vertebrate peripheral tissues included skin. (Bjarnason GA et al. 2000).

3.2.2 Zebrafish as excellent model organism to study circadian clock

The zebrafish represents a fascinating model for studying key aspects of the vertebrate circadian timing system (Vatine et al. 2011). As in other vertebrates, most zebrafish tissues contain independent circadian clocks (so-called peripheral clocks) (Whitmore et al.1998). While in mammals, light entrainment of peripheral clocks occurs indirectly via the retina and the central clock of the suprachiasmatic nucleus (Bailes et al.2010), in zebrafish the peripheral clocks are directly entrained by exposure to light (Whitmore et al. 2000). In zebrafish organs, exposure to light directly activates the transcription of two clock genes per2 and cry1a in tissues and cultured cells. This is predicted to lead to the entrainment of the circadian clock (Mracek et al. 2012).

3.3 Results

3.3.1 Analysis of YBX-1 protein expression in Pac2 cells and adult Zebrafish fins.

One limitation of the zebrafish model is the lack of high-quality primary antibodies to detect zebrafish proteins. Zebrafish literature is plenty of studies that rely on reverse transcription-PCR to measure gene-expression, although it is well known that gene function can also be regulated at protein level, in a non-negligible part.

Because YBX-1 is evolutionarily well-conserved protein, I tested whether primary antibodies directed against aa 1-100 of human YBX-1 (1-100 epitope) were able to detect zebrafish YB-1 (zYBX-1). Figure 2 shows the alignment sequence of Human and Zebrafish YBX-1 aminoacids, the alignment shows that Human YB1 is 67% identical to Zebrafish YBX-1 protein. The region encompassing residues 29 to 132 of zYB-1 is 100% identical to the correspondent region of human YBX-1.

```
Human  1    MSSEAETQQPPAAPPAAPALSAADTKPGTTGSGAGSGGPGGLTSAAPAGGDKKVIATKVL  60\
            MSSEAETQQPP   PAA A S +                   +AA   GDKKVIATKVL\
Zebraf 1    MSSEAETQQPPQ--PAADAESPS-----------------SPAAAATAGDKKVIATKVL  40\
\
Query  61   GTVKWFNVRNGYGFINRNDTKEDVFVHQTAIKKNNPRKYLRSVGDGETVEFDVVEGEKGA  120\
            GTVKWFNVRNGYGFINRNDTKEDVFVHQTAIKKNNPRKYLRSVGDGETVEFDVVEGEKGA\
Sbjct  41   GTVKWFNVRNGYGFINRNDTKEDVFVHQTAIKKNNPRKYLRSVGDGETVEFDVVEGEKGA  100\
\
Query  121  EAANVTGPGGVPVQGSKYAADRNHYRRYPRRRGPPRNYQQNYQN---SESGEKNEGSESA  177\
            EAANVTGPGGVPVQGSKYAADRN YRRYPRRR PPR+YQ+NYQ+   +E  EK EG+ESA\
Sbjct  101  EAANVTGPGGVPVQGSKYAADRNRYRRYPRRRAPPRDYQENYQSDPEAEPREKREGAESA  160\
\
Query  178  PEG--QAQQRRPYR--RRRFPPYYMRRPYGRRPQYSNP--PVQGEVMEGADNQGAGEQG-  230\
            PEG  Q QQRRP    RRR+PPY++RR YGRRP Y+N       E  EG +NQG  +QG \
Sbjct  161  PEGEMQQQQRRPTYPGRRRYPPYFVRRRYGRRPPYTNSQRGEMTEGGEGEENQGGPDQGN  220\
\
Query  231  RPVRQNMYRGYRPRFRRGPPRQRQPREDGNEEDKENQGDETQGQQPPQRRYRRNFNYRRR  290\
            +P+RQN YRG+RP   RGP R R P  DG EEDKENQ +  Q Q+P QRRYRRNFNYRRR\
Sbjct  221  KPMRQNYYRGFRP--SRGPSRPR-PVRDG-EEDKENQSESGQNQEPRQRRYRRNFNYRRR  276\
\
Query  291  RPENPKPQDGKETKAADPPAENSSAPEAEQGGAE  324\
            RP+  KPQDGK++KAAD  A+ S+APEAEQGGA+\
Sbjct  277  RPQTTKPQDGKDSKAADASADKSAAPEAEQGGAD  310\
```

Figure 2. Alignment sequence of Human and Zebrafish YBX-1 aminoacids. The alignment shows that Human YB1 is 67% identical to Zebrafish YBX-1 protein.

I first performed immunoblot using the human YBX-1 antibody to detect zYB-1 protein in whole extract from adult zebrafish fins collected at different time after injury. An aliquot of extract from human squamous carcinoma cells (SCC022) was loaded as positive control. As shown in Figure 3.A specific

band at about 50 kDa was detected. Interestingly, YBX-1 expression appeared to oscillate in a time-dependent manner.
Notably, the same band was detected with a different mouse antibody direct against the full length aminoacid sequence of human YBX-1 (aa 1-324) suggesting that the observed signal was specific (data not shown).

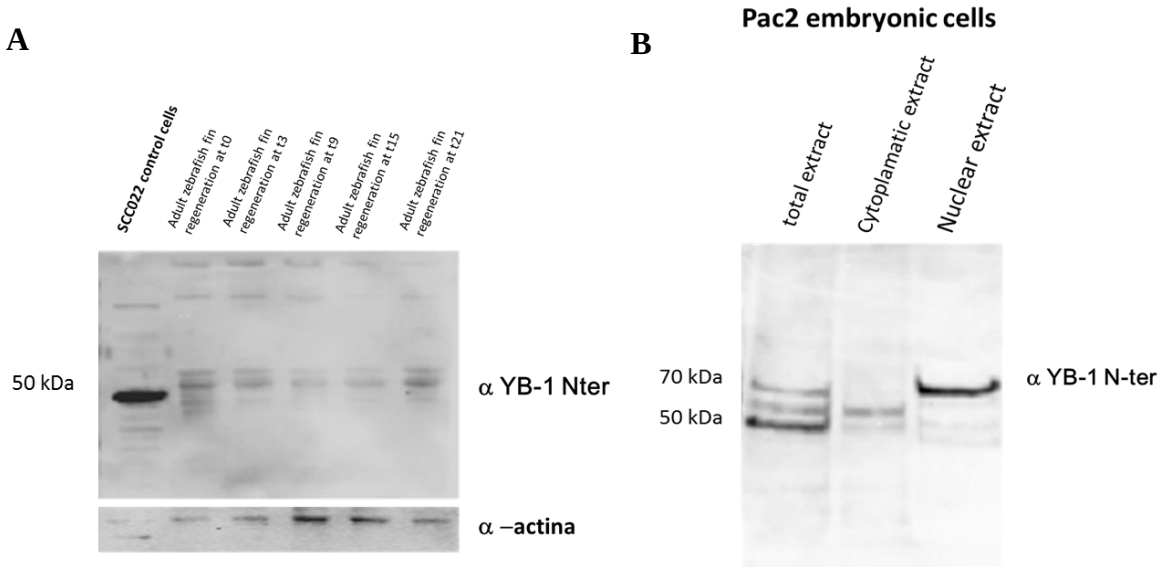

Figure3. Analysis of YBX-1 protein expression during adult Zebrafish fin regeneration and in Pac 2 cells. (A)Extracts of adult zebrafish fin were collected at different time after injury, an aliquot of extract from human squamous carcinoma cells (SCC022) was loading as positive control. Proteins were detected with specific antibodies, as indicated. Actin was used as loading control. Images were acquired with CHEMIDOC (Bio-Rad) and analyzed with the Quantity-ONE software. (B) Pac2 fibroblast cells were seeded at 60% confluency (5×10^5) in 35-mm dishes. 24 h after seeding, cells were collected and part of cell lysates were fractionated to obtain cytoplasmic (cy) and nuclear (nu) fractions. Total and Nuclear/cytoplasmic extracts were separated by SDS-PAGE and subjected to immunoblot. Proteins were detected with specific antibodies, as indicated. . Images were acquired with CHEMIDOC (Bio-Rad) and analyzed with the Quantity-ONE software.

Next, I prepared whole and nuclear/cytoplasmatic fractions of zebrafish Pac2 fibroblasts to analyze them by immunoblot with YBX1 antibodies. Surprisingly, in addition to the expected 50 kDa form, a 70 KDa band of YBX-1 was observed and it was enriched in the nuclear compartment (Figure 3.B).

3.3.2 Analysis of YBX-1 protein expression in the nuclei of adult zebrafish fin in Light-Dark cycle 14:10.

To deeply investigate if YBX-1 protein expression is under a time-dependent control, I proceeded to collect samples from adult zebrafish fins kept in a permanent light-dark cycle 14:10 (14 h of light and 10 h of darkness) at different time points (*zeitebergs*=ZT). Nuclear/cytoplasmic extracts were prepared and subjected to immunoblots with YBX-1 antibodies. As shown in

Figure 4, right panel, I observed a peak and trough of nuclear YBX-1 protein at the beginning of the light phase (ZT3).
The same experiment, performed in amputated adult fin, gave a very similar results suggesting that the phenomenon was not influenced by the regeneration process (Figure 4.A, left panel). I never observed differences of YBX-1 in cytoplasmic fractions (data not shown).

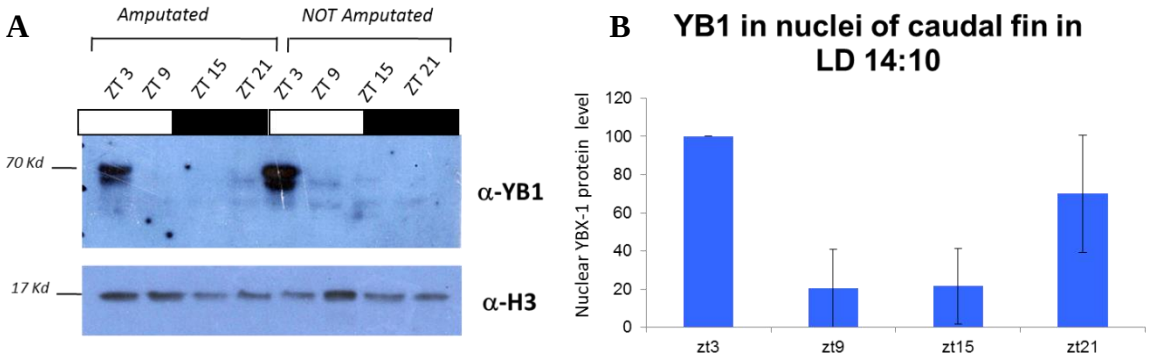

Figure 4. Analysis of YB-1 protein expression in the nuclei of adult zebrafish fin in Light-Dark cycle 14:10. (A) Fins derived from adult zebrafish kept permanently in Light-Dark cycle 14:10 were collected at different time points (ZT). The samples were fractionated to obtain cytoplasmic (cy) and nuclear (nu) fractions. Nuclear extracts were separated by SDS-PAGE and subjected to immunoblot. Proteins were detected with specific antibodies, as indicated. H3 was used as loading control. (B) Histograms of protein expression were measured using Image, and proportions normalized against the mean of H3 for each individual blot. The values are means of six independent measures obtained from three experiments.

3.3.3 Analysis of YBX-1 expression in the Nuclear extract of Pac2 cells in LD 14:10

Pac2 is a zebrafish-derived fibroblast cell line widely used for *in vitro* studies on circadian clock regulation. I explored the pattern of YBX-1 expression, in zebrafish Pac2 fibroblasts kept in light-dark cycle (14:10) for 24 h. 24 h after circadian clock induction, nuclei of Pac2 cells were collected at different time points (ZT) and subjected to immunoblot with YBX-1 antibodies. As shown in Figure 5, YBX-1 nuclear levels were strongly regulated by the light-dark cycle with a peak of nuclear protein during the light phase and a trough during the dark phase showing that YBX-1 protein expression was subjected to a similar regulation both *in vitro* and *in vivo.*

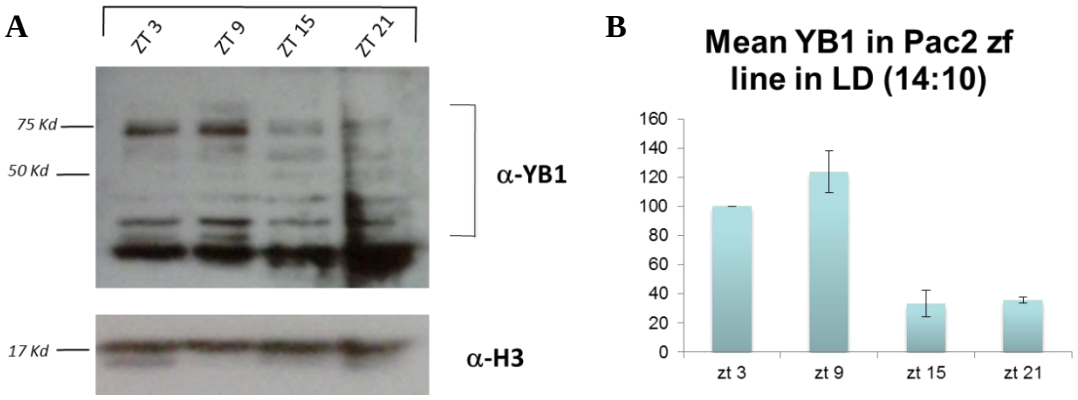

Figure 5. **Analysis of YBX-1 expression in the Nuclear extract of Pac2 cells in LD 14:10.** (A) Pac2 fibroblast cells were seeded at 60% confluency (5 × 105) in 35-mm dishes and kept in light-dark cycle for 24 hours to induce circadian regulation. 24 h after circadian clock induction, cells were collected and cell lysates were fractionated to obtain cytoplasmic (cy) and nuclear (nu) fractions. Nuclear extracts were separated by SDS-PAGE and subjected to immunoblot. Proteins were detected with specific antibodies, as indicated. . H3 was used as loading control. (B) Histograms of protein expression were measured using Image, and proportions normalized against the mean of H3 for each individual blot. The values are means of six independent measures obtained from three experiments.

3.3.4 High resolution of YBX-1 expression in the Nuclear extract of Caudal Fin in LD 14:10

Comparison of data showed that YBX-1 expression, in PAC2 and fin tissues, peaked at slightly different time points. To determine exactly the peak and trough of nuclear YBX-1 protein I performed a high resolution curve of YBX-1 protein expression by collecting samples of fin tissues from adult zebrafish kept permanently in light-dark (14:10) conditions.
Nuclei of adult Zebrafish fin in light-dark cycle 14:10 (14 hours of light and 10 hours of darkness), were collected at different time points (ZT) and subjected to immunoblots with YB1 antibodies. Histone H3 was used as loading control. Figure 6 shows that the level of YBX-1 in nuclear extracts peaked after 3 hours of light exposure, and trough after 7 hours of light exposure.

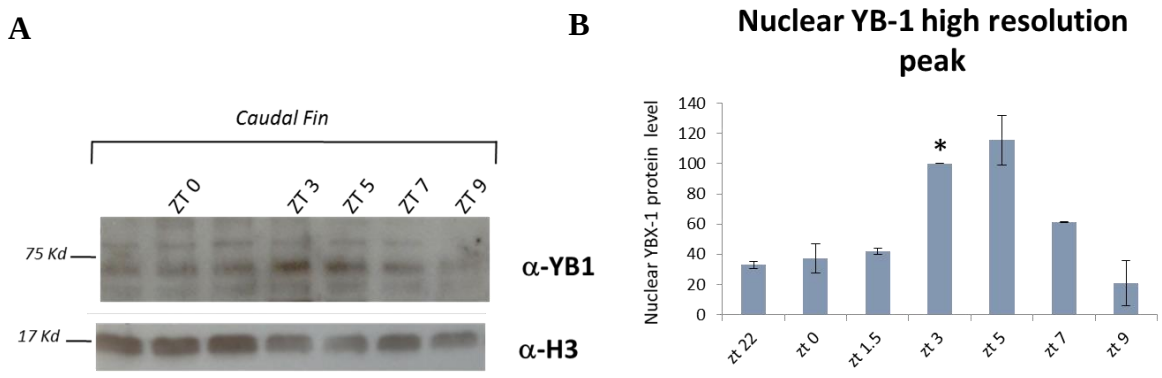

Figure 6. High resolution of YB1 expression in the nuclear extract of Caudal Fin in LD 14:10. (A) Fins derived from adult zebrafish kept permanently in Light-Dark cycle 14:10 were collected at different time points (ZT). The samples were fractionated to obtain cytoplasmic (cy) and nuclear (nu) fractions. Nuclear extracts were separated by SDS-PAGE and subjected to immunoblot. Proteins were detected with specific antibodies, as indicated. H3 was used as loading control. (B) Histograms of protein expression were measured using Image J, and proportions normalized against the mean of H3 for each individual blot. The values are means of three independent measures obtained from one representative experiment and the asterisk indicates statistically significant value, P <0.01.

3.3.5 YBX-1 Immunofluorescence in Zebrafish caudal fin

Next, I carried out an immune-fluorescence assay in zebrafish caudal fin taking two different time points, corresponding at the observed peak (ZT3) and trough (ZT9) of YBX-1 nuclear protein. The samples of fins were collected from adult zebrafish kept permanently in light-dark cycle. Incubation of fin samples with YB-1 antibody showed that at ZT3 YBX-1 protein was mainly localized into nuclear compartment while at ZT9 it was localized mostly in the cytoplasm (Figure 7).
Thus, the immunofluorescence confirmed the data obtained by Western blot analysis thus leading to the conclusion that YBX-1 nuclear expression is clock regulated.

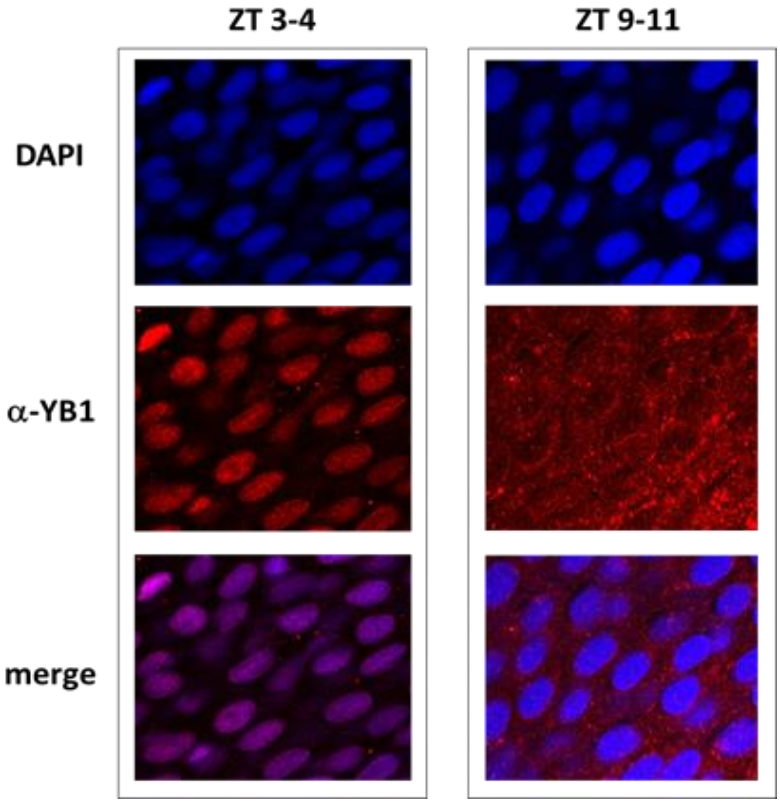

Figure 7. YB-1 Immunofluorescence in Zebrafish caudal fin. Caudal fin collected from adult zebrafish kept permanently in light-dark cycle 14:10 were fixed and subjected to double immunofluorescence using rabbit primary YB-1 antibody and Cy3-conjugated secondary antibodies (red). DAPI was used to stain nuclei. Images of merge (yellow) show the co-expression of YBX-1 protein and the nuclei.

3.3.6 YBX-1 mRNA expression in adult caudal fins in LD cycle (14L:10D)

Next, it was of interest to determine if clock-dependent regulation of YBX-1 expression was regulated at transcript or protein level. Therefore, I analyzed the level of YBX-1 mRNA from caudal fin of adult zebrafish, permanently kept in light- dark cycle 14L:10D. Samples were collected at different time points (ZT), mRNA was purified and subjected to quantitative RT-PCR analysis using oligonucleotides designed to specifically amplify YBX-1 transcript mRNA. β-actin was used to normalize the samples. As shown in Figure 8, the level of YBX-1 mRNA fluctuates during the light-dark cycle but its behaviour did not reflect the observed pattern of YBX-1 protein expression thereby suggesting that regulation of YBX-1 expression was at protein level.

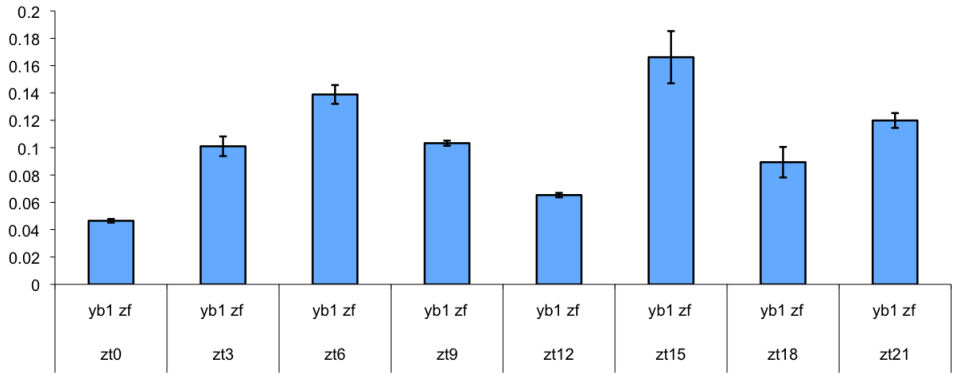

Figure 8. RT-PCR analysis of YBX-1 mRNA expression in adult caudal fins in LD cycle (14L:10D). Real-time PCR was used to quantify YBX-1 mRNA expression in adult caudal fins in LD cycle (14L:10D). mRNA levels were normalized to β-actin. The values are the means ± S.D. of three biological replicates.

3.3.7 YBX-1 in the nuclei has a circadian oscillation in deep darkness (DD) with a shift of peak between CT3 and CT9

To further elucidate if YBX-1 protein peak in the nuclei was light inducible, I performed experiments in deep darkness on adult zebrafish fin and Pac2 cells. For this reason, adult zebrafish caudal fins and Pac2 cells were held in deep darkness for 48 hours, in order to eliminate any light-related stimulus.
After 48 hours nuclei of adult Zebrafish fin and Pac2 in deep darkness, were collected at different time points (CT) and subjected to immunoblots with YB1 antibodies. H3 was used as loading control.
As is shown in Figure 9, interestingly, nuclear YBX-1 exhibited the same pattern of expression shown under the light-dark cycle. This experiment confirmed that YBX-1 expression in the nuclei is not light-inducible but is dependent on the circadian clock.

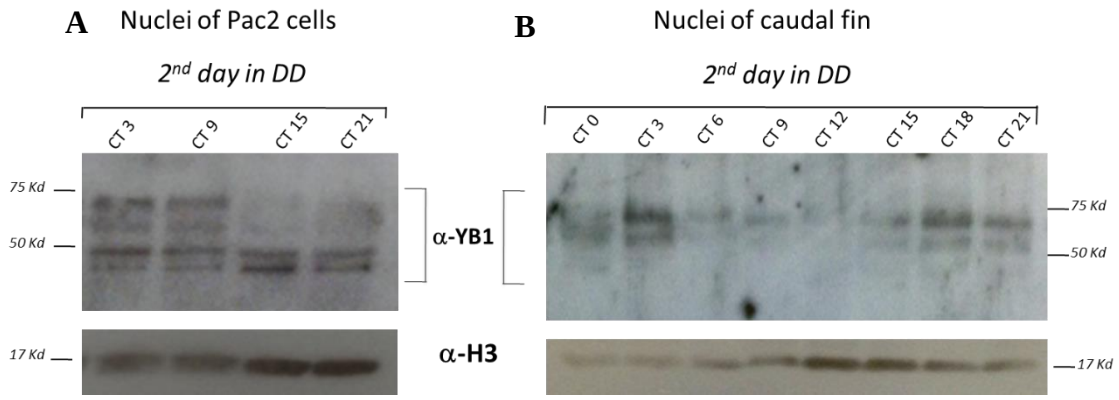

Figure 9. Analysis of YBX-1 nuclear protein expression in deep darkness. (A) Pac2 fibroblast cells were seeded at 60% confluency (5 × 105) in 35-mm dishes and kept in deep darkness for 48 hours to eliminate stimuli light related. After 48 hours, cells were collected and cell lysates were fractionated to obtain cytoplasmic (cy) and nuclear (nu) fractions. Nuclear extracts were separated by SDS-PAGE and subjected to immunoblot. Proteins were detected with specific antibodies, as indicated. H3 was used as loading. (B) Fins derived from adult zebrafish kept in deep darkness for 48 hours to eliminate stimuli light related were collected at different time points (CT). The samples were fractionated to obtain cytoplasmic (cy) and nuclear (nu) fractions. Nuclear extracts were separated by SDS-PAGE and subjected to immunoblot. Proteins were detected with specific antibodies, as indicated. H3 was used as loading control.

3.4 Discussion

During my training in the laboratory of Professor Nicholas Foulkes, I had the opportunity to learn the use of a model organism as zebrafish.First, I demonstrated that YBX-1 is expressed in adult zebrafish fins and in the embryonic cell line (Pac2).

Moreover, I obtained consistent evidence that YBX-1 nuclear localization and protein expression level is strongly regulated by the light-dark cycle with a maximum peak of nuclear protein at the beginning of the light phase and a minimum trough during the beginning of the dark phase.

The oscillation of YBX-1 nuclear localization persists also when the fishes are transferred in constant darkness conditions showing that YBX-1 is regulated by the circadian clock.

Finally, I observed that YBX-1 mRNA doesn’t present a clear circadian regulation. In addition, the nuclear form of YBX-1 shows an increased molecular weight consistent with post-translation modification However, this point needs to be further investigated. All these data taken together represent a solid starting point to further investigate the potential involvement of YBX-1 in regulating the cell time proliferation, a mechanism clock regulated.

3.5 Materials and Methods

3.5.1 Zebrafish cell culture

A subline derived from the zebrafish embryonic cell line PAC-2 (Lin, Gaiano et al. 1994) was propagated at 25^{o}C in L-15 (Leibovitz) medium (Gibco BRL) supplemented with 15% Fetal Calf Serum (Biochrom KG), 100 units/ml penicillin, 100 µg/ml streptomycin and 50 µg/ml gentamycin (Gibco BRL) in an atmospheric CO_2, non-humidified cell culture incubator. These fibroblast-like cells grow optimally as an adherent monolayer culture on normal tissue culture-treated plastic substrates (Greiner). Cells were typically subcultured once every week by trypsinization of the cells followed by dilution in culture medium at a ratio of 1:4 and then seeding in fresh culture flasks.

3.5.2 Adult Fish treatment and ethical statements

The zebrafish Tübingen strain were raised according to standard procedures in a re-circulating water system under 14 hours light and 10 hours dark cycles at 28°C and fed twice per day. Before each experiment adult zebrafish (6–12 months of age) were adapted for a minimum of 3 days at a constant 28°C under a 14-h light: 10-h dark cycle (LD) (light intensity, 20 uW/cm^2), or in constant darkness (DD). The caudal fins were amputated using razor blades following anesthesia with 0.02% MS222 (3-aminobenzoate methanesulfonic acid, Sigma Aldrich). In the regeneration experiments, the control fish (non-amputated) were anesthetized and handled in the same way and at the same times as the amputated fish.

3.5.3 RNA extraction and reverse transcription

Total RNA was extracted from t zebrafish fins by adding Trizol Reagent (Gibco, BRL). Addition of chloroform and subsequent centrifugation lead to phase separation under conditions where RNA remained water-soluble and proteins or DNA were partitioned in the lower, organic phase or at its interface. Total RNA was subsequently isolated from the aqueous phase by isopropanol precipitation followed by centrifugation and then rinsing the pellet using 75% ethanol. Reverse transcription was performed with the extracted total RNA to produce cDNA using Superscript III RT (Invitrogen), according to the manufacturer's recommendations.

3.5.4 Quantitative RT-PCR (qRT-PCR)

For qRT-PCR analysis, 4µl of 1:20 diluted cDNA was pipetted in each well of a 96well plate together with the SYBRgreen-Primer-MasterMix (Promega). qRT-PCR was performed in an ABI StepOnePlus Real-Time RT-PCR machine (Applied Biosystems) with a standard temperature cycle programme, according to the manufacturer's conditions. The relative levels of each mRNA were calculated by the $2^{-\Delta\Delta CT}$ method (CT indicating the cycle number at which the signal reaches the threshold of detection). Relative expression levels were normalized using zebrafish β-*actin* mRNA. For each gene the RT-PCR primer sequences are listed as follows:

β-actin (Forward): 5'GCCTGACGGACAGGTCAT 3'

β-actin (Reverse): 5' ACCGCAAGATTCCATACCC 3'

zYBX-1 (Forward):5' TACCCACCATACTTCGTGCG 3'

zYBX-1 (Reverse): 5'GCGGTAGTTGAAGTTGCGAC 3'

3.5.5 Protein analysis by Western blots

For western blot analysis, whole fin protein extracts were prepared from fins of zebrafish adult fish or from confluent Pac2 cell monolayers $5x10^5$ in 35 mm dishes. The extracts were prepared by direct addition of 200µl of Laemmli solution including a cocktail of phosphatase inhibitors (Sigma Aldrich) into an eppendorf where 3 amputated fins were added. For the Pac2 200µl of Laemmli solution was added for each 35 mm dish.including a cocktail of phosphatase inhibitors (Sigma Aldrich). Lysate samples were boiled for 5 min to denature the proteins before storage at –20°C. A miniprotean III gel system (BioRad) was used for all subsequent electrophoresis and transfer steps according to the manufacturer's instructions. Samples were loaded on 10% polyacrylamide-SDS gels for electrophoresis and subsequently transferred to an Immobilon-P membrane (Millipore). Transferred membranes were then blocked for two hours at room-temperature by incubation in 1x Tris Buffer saline supplemented with 0, 1% Tween20 and either non-fat dry milk or BSA. Histone H3 and YB-1 antibodies were used at dilution 1:1000 in 1x Tris Buffer saline supplemented with 0,1% Tween20 and 5% BSA. Immunoreactive bands were visualized by using either anti-rabbit secondary antibodies (1:5000). Signals were then detected using the Pierce-ECL detection system (Thermo Scientific).

3.5.6 Immunochemestry

Adult zebrafish (6–12 months of age) were adapted for a minimum of 3 days at a constant 28°C under a 14-h light: 10-h dark cycle (LD) (light intensity, 20 uW/cm2), or in constant darkness (DD). The caudal fins were amputated using razor blades following anesthesia with 0.02% MS222 (3-aminobenzoate methanesulfonic acid, Sigma Aldrich). Fins were fixed 4% PFA for 20 to 30 minutes in 6-multiwell. After the fixation the fins were permeabilized, denatured (PBST) and blocked PBST+BSA .As the primary antibody we used the YBX1 (Abcam ab 12148) at 1:1000 diluition. The incubation of the antibodies was overnight at 4°C .The next step involved repeated washing and blocking before the next second antibody 1.1000 was added (codice Cy-3) for 1h in the dark. The antibody staining was followed by DAPI 1:10000 to

visualize the nuclei for 30 minutes at RT in the dark. The next day the slides were examined using a Confocal Microscope SPE (Leica).

3.5.7 Statistical analysis.

Unpaired t-test was performed using Microsoft Excel. All the results were expressed as means +/− SD. $p<0.05$ was considered statistically significant.

3.6 References:

1. Dekens MP, Santoriello C, Vallone D, Grassi G, Whitmore D, Foulkes NS. Light regulates the cell cycle in zebrafish. Curr Biol. 2003 Dec 2;13(23):2051-7
2. .Graham J. Lieschke1 & Peter D. Currie Animal models of human disease: zebrafish swim into view. Nature Reviews Genetics 8, 353-367 (May 2007) | doi:10.1038/nrg2091
3. Savvidis C, Koutsilieris M. Circadian rhythm disruption in cancer biology.Mol Med. 2012 Dec 6;18:1249-60. doi: 10.2119/molmed.2012.00077.
4. M. Laura Idda, Elena Kage, Jose Fernando Lopez-Olmeda, Philipp Mracek, Nicholas S. Foulkes and Daniela Vallone. Circadian timing of injury-induced cell proliferation in zebrafish. PLoS One. 2012
5. Mori T, Johnson CH Circadian control of cell division in unicellular organisms. Prog Cell Cycle Res. 2000; 4():185-92.
6. Bjarnason GA, Jordan R Circadian variation of cell proliferation and cell cycle protein expression in man: clinical implications. Prog Cell Cycle Res. 2000; 4():193-206
7. Gad Vatine, Daniela Vallone Yoav GothilfNicholas S. Foulkes. It's time to swim! Zebrafish and the circadian clock. Febs Letter 2011. Volume 585, Issue 10, Pages 1485–1494
8. Whitmore D, Foulkes NS, Strahle U, Sassone-Corsi P (1998) Zebrafish Clock rhythmic expression reveals independent peripheral circadian oscillators. Nat Neurosci 1: 701–707. doi: 10.1038/3703
9. Bailes HJ, Lucas RJ (2010) Melanopsin and inner retinal photoreception. Cell Mol Life Sci 67: 99–111. doi: 10.1007/s00018-009-0155-7.
10. Whitmore D, Foulkes NS, Sassone-Corsi P (2000) Light acts directly on organs and cells in culture to set the vertebrate circadian clock. Nature 404: 87–91. doi: 10.1038/35003589.
11. Philipp Mracek, Cristina Santoriello, M. Laura Idda, Cristina Pagano Zohar Ben-Moshe, Yoav Gothilf, Daniela Vallone , Nicholas S. Foulkes Regulation of per and cry Genes Reveals a Central Role for the D-Box Enhancer in Light-Dependent Gene Expression. Plos one(2012)

Appendix:

Personal publication:

1. Di Costanzo A, Troiano A, di Martino O, Cacace A, Natale CF, Ventre M, Netti P, Caserta S, Pollice A, La Mantia G, Calabrò V.The p63 protein isoform ΔNp63α modulates Y-box binding protein 1 in its subcellular distribution and regulation of cell survival and motility genes. J Biol Chem. 2012 Aug 31;287(36):30170-80.
2. Troiano A., Lomoriello IS., di Martino O., Fusco S., Pollice A., Vivo M., La Mantia G., Calabrò V. "Y-box binding protein-1 is part of a complex molecular network linking ΔNp63α to the PI3K/AKT pathway in cutaneous squamous cell carcinoma". J. Cell Physiol. 2015 DOI: 10.1002/jcp.24934.
3. O. di Martino, A. Troiano, L. Addi, A. Guarino, S. Calabrò, R. Tudisco, N. Murru, M.I.Cutrignelli, F. Infascelli and V. Calabrò. "Regulation of Stearoyl Coenzyme A Desaturase 1 gene promoter in bovine mammary cells Animal Biotechnology 2015 in press.
4. O. di Martino, A. Troiano, A.M. Guarino, Alessandra Pollice, Maria Vivo, Girolama La Mantia, Viola Calabrò ΔNp63α protects YB-1 oncoprotein from proteasome-dependent proteolysis" Febs Letters submitted January 2015.

Abstract:

1. Troiano, DI MARTINO O., I. Schiano Lomoriello, M. Vivo, A. Pollice, G. La Mantia, V. Calabrò (2014). YB-1 and DNp63a cross-talk in the control of squamous carcinoma cell adhesion and survival. In: XII FISV Congress 2014. Pisa, 24th-27th September 2014.
2. DI MARTINO O., Annaelena Troiano, I. Schiano Lomoriello, Daniela Di Girolamo, Maria Vivo, Enzo Di Iorio, Alessandra Pollice, Girolama La Mantia, Viola Calabrò (2013). DNp63a and YB-1 Dependent regulation of keratinocyte adhesion and survival. In: Cortona AGI Congress 25 th -27 th September 2013.
3. V. Calabrò, A. Troiano, DI MARTINO O., I. Schiano Lomoriello, M. Vivo, A. Pollice, G. La Mantia (2013). Cooperation between YB-1 and DNp63a in the control of cell proliferation and survival. In: ABCD 2013 Programme and Abstracts. Ravenna, 12th -14th September 2013
4. DI MARTINO O., Annaelena Troiano, Alessandra Pollice, Girolama La Mantia, Viola Calabrò (2012). The DNp63a protein interacts with Y-box binding protein 1 and promotes its ubiquitination. In: 12th FISV Congress . Roma, 24-27 Settembre, 2012, vol. unico, p. 101-101
5. A. Troiano, DI MARTINO O., A. Pollice, M. Ventre, C. Natale, G. La Mantia, V. Calabrò (2012). The p63 protein as a regulator of Y Box binding protein 1 subcellular distribution and functions. In: 12th FISV Congress. Roma, 24-27 Settembre 2012, vol. unico, p. 103-104

Karlsruhe Institute of Technology

Institut für Toxikologie und Genetik
ITG

Leiter/in: Prof. Dr. Uwe Strähle
Prof. Dr. Stefan Bräse

Hermann-von-Helmholtz-Platz 1
76344 Eggenstein-Leopoldshafen

Telefon: 0721 608-2-6233
Fax: 0721 608-2-3544
E-Mail: sandra.schneider@kit.edu
Web: http://www.itg.kit.edu

KIT-Campus Nord | ITG| Postfach 3640 | 76021 Karlsruhe

Bearbeiter/in: Dr. Sandra Schneider
Unser Zeichen:
Datum: 28.08.2014

To whom it might concern

Certificate of attendance

We hereby confirm that Orsola di Martino, born 04.02.1988 in Aversa (Italy), has been visiting the Institute of Toxicology and Genetics at the KIT starting from 10th of April 2014 until 30th of July 2014.
She was working as a guest PhD student in the laboratory of Professor Nicholas Foulkes on an independent project in order to characterize the expression of YB1 in Zebrafish and to determinate if it is a clock regulated gene.

Yours sincerely

Schneider

Dr. Sandra Schneider

Acceptance Letter

19-Feb-2015

Dear Professor Calabrò:

Ref: Regulation of Stearoyl Coenzyme A Desaturase 1 gene promoter in bovine mammary cells

Our referees have now considered your paper and have recommended publication in Animal Biotechnology. We are pleased to accept your paper in its current form which will now be forwarded to the publisher for copy editing and typesetting. The reviewer comments are included at the bottom of this letter, along with those of the editor who coordinated the review of your paper.

You will receive proofs for checking, and instructions for transfer of copyright in due course.

The publisher also requests that proofs are checked and returned within 48 hours of receipt.

Thank you for your contribution to Animal Biotechnology and we look forward to receiving further submissions from you.

Sincerely,
Dr Schook
Editor, Animal Biotechnology
schook@illinois.edu

Reviewer(s)' Comments to Author:

Reviewer: 1

Comments to the Author
I have no further comments

Regulation of Stearoyl Coenzyme A Desaturase 1 gene promoter in bovine mammary cells

Journal:	*Animal Biotechnology*
Manuscript ID:	LABT-2014-0097.R1
Manuscript Type:	Articles
Date Submitted by the Author:	20-Dec-2014
Complete List of Authors:	di Martino, Orsola; Università di Napoli Federico II, Troiano, Annaelena; Università di Napoli Federico II, Addi, Laura; Università di Napoli Federico II, Guarino, Andrea; Università di Napoli Federico II, Calabrò, Serena; Università di Napoli Federico II, Tudisco, Raffaella; Università di Napoli Federico II, Murru, Nicoletta; Università di Napoli Federico II, Cutrignelli, Monica; Università di Napoli Federico II, Infascelli, Federico; Università di Napoli Federico II, Calabrò, Viola; Università di Napoli Federico II,
Keywords:	stearoyl coenzyme A desaturase, regulation of gene expression, bovine mammary cells, fatty acids, insulin

Regulation of Stearoyl Coenzyme A Desaturase 1 gene promoter in bovine mammary cells

O. Di Martino , A. Troiano[§], L. Addi[#], A. Guarino[§], S. Calabrò[#], R. Tudisco[#], N. Murru[#], M.I.Cutrignelli[#] F. Infascelli[#] and V.Calabrò[§*].

[§]Department of Biology, University of Naples "Federico II", Via Cinzia, Monte S. Angelo, 80126 Naples, Italy.

[#]Department of Veterinary Medicine and Animal Production, University of Naples "Federico II", Via F. Delpino 1, 80137 Naples, Italy.

*** Corresponding author**: Viola Calabrò, e-mail address: vcalabro@unina.it.

Running head: SCD1 gene promoter activity in bovine mammary cells

Acknowledgement

We thank Prof. Antonella Baldi of the Laboratory of Cell Culture-Department of Veterinary Science and Technologies for Food safety at the Veterinary Medicine Faculty (University of Milan) for providing the BME-UV1 cells.

This work was supported by Progetto "Bovlac" - PSR 124 2007-2013 "Cooperazione per lo sviluppo di nuovi prodotti, Processi e tecnologie nei settori agricolo e alimentare e settore forestale" Regione Campania.

Conflict of Interest

The authors declare that they have no competing interests.

ABSTRACT

Stearoyl-Coenzyme A desaturase 1 (SCD1) belongs to the fatty acid family of desaturases. In lactating ruminants, the SCD1 protein is highly expressed in the mammary gland and is relevant for the fatty acid composition of milk and dairy products. Bovine mammary epithelial cells (BME-UV1), cultured in vitro, have been proposed as a model to reproduce the biology of the mammary gland. The present study was designed to investigate the responsiveness of bovine SCD1 promoter to serum, insulin, oleic acid and NFY transcription factor in BME-UV1 cells. A luciferase-based reporter assay was used to monitor the transcriptional activity of the SCD1 promoter region in BME-UV1 cells treated or not with insulin and/or oleic acid. The level of endogenous SCD1 mRNA was evaluated by Real time PCR. Insulin (20 ng/mL) induced a 2.0 to 2.5-fold increase of SCD1 promoter activity. Additionally, the effect of insulin was inhibited by oleic acid, serum components, and NFY enforced expression. Serum and NFY showed no synergistic or additive effect on SCD1 promoter activity suggesting that they repress SCD1 transcription through the same responsive element.

Key words: stearoyl coenzyme A desaturase; regulation of gene expression; bovine mammary cells; fatty acids; insulin.

INTRODUCTION

Understanding the basis of lipid homeostasis is fundamental for developing new strategies to combat obesity, diabetes and other diseases of abnormal lipid metabolism. Stearoyl CoA desaturase 1 **(SCD1**, also called Δ^9-desaturase**)** (EC 1.14.99.5) is a short-lived endoplasmic reticulum-bound enzyme that catalyzes the Δ^9-*cis* desaturation of saturated fatty acyl-CoA substrates **(SFAs)** to monounsaturated fatty acids **(MUFAs)**, primarily palmitoyl-CoA and stearoyl-CoA into palmitoleoleyl-CoA and oleyl-CoA, respectively (1). Oleic acid, the main product of SCD1 reaction, is the predominant fatty acid of human adipose tissue triacylglycerols, associating SCD1 with the development of obesity and metabolic syndrome. Moreover, as the SFA/MUFA ratio affects membrane phospholipid composition and fluidity; it has been implicated in obesity, diabetes, neurological disease, skin disorders and cancer (2). Stearoyl CoA desaturase 1 gene homologs have been identified in a range of species, many of which express multiple isoforms, with SCD1 being the most abundant isoform in lipogenic tissues (3; 4). The SCD1 gene plays an important role in converting *trans-11* C18:1 vaccenic acid into *cis-9, trans-11* C18:2 CLA (5) and is highly expressed in the mammary gland of lactating ruminant (6). Early after parturition, the SCD1 activity in adipose tissue decreases while increasing in mammary gland (7).

Activity and expression of SCD1 have been reported to be regulated by fatty acids, although the responses appear to vary among the species. For instance, oleic acid was shown to reduce rat and bovine SCD1 promoter activity (8; 9) but had no effect on

human SCD1 mRNA synthesis (10). Promoter elements that are responsible for the PUFA repression localize with the promoter elements for SREBP-mediated regulation of the SCD gene (11). In *Bos Taurus,* the PUFA response region (PUFA-RE, 60 bp) is essential for the control of SCD1 expression by PUFA (12). This region encompasses the binding sites for Sp1 and NFY transcription factors and the Sterol Response Element (SRE) which is the binding site for the SREBP1 protein. Recently, it has been demonstrated that SREBP1 cooperates extensively with NFY in the control of genes involved in lipid metabolism. Moreover, promoters of genes involved in lipid metabolism were preferentially occupied by the combination of SREBP1 and NFY factors while genes involved in carbohydrate metabolism were enriched among targets of SREBP1 alone (13). In the present study, we have explored the ability of oleic acid and serum to repress SCD1 promoter activity in control and insulin-stimulated BME-UV1 immortalized cells that can mimic the in vivo response of bovine mammary cells. Moreover, since oleic acid was reported to have no effect on human SCD1 mRNA synthesis (10) we performed similar experiments in MCF7 cells, a human breast cancer cell line previously defined as a model for the study of insulin action on mammalian cell metabolism (14).

MATERIALS AND METHODS

Cell Culture

The BME-UV1 cell line was established from primary bovine mammary epithelial cells by stable transfection with a plasmid, carrying the sequence of the simian virus 40 early region mutant tsA58, encoding the thermolabile large T antigen (15). BME-UV1 cells were provided to us by the Laboratory of Cell Culture-Department of Veterinary Science and Technologies for Food safety at the Veterinary Medicine Faculty (University of Milan) and cultured according to Cheli et al., 1999. Human breast cancer MCF7 cells were purchased from Cell Line Service (CLS, Germany). MCF7 cells were routinely grown into 100 cm^2 plates (Corning Life Science, Corning, NY, USA) as a monolayer culture in Dulbecco's modified Eagle's medium (DMEM) (EuroClone, Pero, MI) supplemented with 10% (v/v) fetal bovine serum (FBS) (EuroClone), in humidified incubator with 5% CO_2 at 37° C.

Construction of SCD1_PGL3 reporter plasmid containing the bovine SCD1 promoter

A 600 bp genomic fragment containing the SCD1 proximal promoter region, -590 from the transcription start site (+1) was amplified by PCR. The amplified region is shown in Figure 1A and contains the SP1, SRE and NFY binding sites (Figure 1A and B). Whole genomic DNA was isolated from leucocytes of cow peripheral blood and used as template for PCR using bovine SCD1-promoter specific primers: *Forward* 5'**GCATGGTA**CCCCAGTGCCCATC and *Reverse*

*5'*GGTACCGCGCTGCACGGTGC. The primers included a 8 extra-bases (indicated by small caps) to generate protected *XhoI* or *KpnI* restriction sites. The PCR conditions are given as follows: 94°C for 30 s, 40 cycles of 57°C for 1 min and a final extension step at 72°C for 1 min. The PCR fragment was gel purified and appropriately digested with *XhoI* or *KpnI* restriction enzyme (Roche diagnostics, MI, Italy) to produce cohesive ends. After a step of purification, the digested DNA insert was directionally cloned into the promoter-less luciferase reporter vector, pGL3-Basic (Promega, Madison USA), using *XhoI* and *KpnI* cloning sites. Ligation reaction was set up at a vector to insert ratio of 1:5, using 50 ng of pGL3-Basic vector. T4 DNA ligase and 1X ligase buffer were used according to manufacturer's instructions. Positive clones were first selected for the presence of the *XhoI* and *KpnI* 600 bp restriction fragment, by agarose gel electrophoresis, and then sequenced.

The 2.4 Kb fragment containing the p21WAF promoter was retrieved from the p21WAF-CAT plasmid (16) and ligated into the HindIII site of pGL3-basic Vector (Promega) to obtain the p21WAF-Luciferase reporter construct.

cDNAs encoding human NFYA, NFYB and NFYC proteins cloned in pBK-CMV expression vector (Stratagene) were provided to us by Dr. Maria Morasso (NIH, Bethesda).

Transient transfections and luciferase assay

MCF-7 or BME-UV1 cells were counted and seeded in 6-well plates at a density of $2.5X10^5$ cells/well in 4 mL of complete medium. For luciferase assay, each

experimental point was transfected with 1 µg of PGL plasmid (SCD1_PGL3, p21WAF_PGL3 or PGL3 basic vector). Briefly plasmid DNA was diluted in 250 µl of DMEM serum free and mixed with 2,5 µl of Lipofectamine 2000 (Life Technologies, CA, USA) in 250 µl DMEM serum free. Transfection master mixtures were incubated at room-temperature for 20 min, prior to drop-wise addition to MCF7/BME-UV1 cells. Complexes were added to the cells containing 1 mL of DMEM and 0, 5 or 10% FBS/FCS). After 24 h transfection, the medium was removed, cells were washed twice with PBS and then lysed using the Lysis Buffer (Promega) according to manufacturer's instructions. *Firefly* luciferase activity in cell lysates was measured using Dual Luciferase Assay kit (Promega), according to the manufacturer's instructions. Results were normalized against protein concentration (Bradford Assay, Biorad).

To evaluate the effect of NFY transcription factor, MCF7 cells were co-transfected with 0.5 γ of SCD1_PGL3 basic construct and 0.5 γ of each NFY subunit (NFY-A, NFY-B, NFY-C). Four hours after transfection, the cells were incubated with 0%, 5% or 10% FBS, for 24 h. The promoter activity was evaluated by Luciferase assay.

To evaluate the effect of insulin on SCD1 promoter activity, insulin was added to MCF7 and BME-UV1 cells, at a concentration of 20 ng/mL (3.4 10^{-9} M), 4 h after transfection. Physiologic concentrations of insulin range between 10^{-8} and 10^{-11} (14) therefore treatment with 3.4 10^{-9} M insulin is expected to induce a physiological response in mammalian cells.

Cells were then incubated for 24 hours. To evaluate the promoter response to MUFA, oleic acid (≥ 99% purity, Calbiochem) was added to a concentration of 30 and 50 μM according to a previously published manuscript (17).

Immunoblot

Immunoblots (IB) was performed as previously described (18). NF-YA (G2, sc-17753) and NF-YB (FL207, sc13045) antibodies (Santa Cruz Biotechnology Inc.) were used to specifically detect expression of NFYA or B subunits and used at 1:200 dilution. The anti-GAPDH (6C5) was purchased from Santa Cruz (Biotechnology Inc.).

mRNA quantification by qPCR

SCD1 specific transcript was amplified by quantitative PCR. The primers designed for qPCR reaction are: *Forward* TCCGACCTAAGAGCCGAGAA and *Reverse* AGCACAACAACAGGACACCA (NCBI Reference Sequence: NM_173959.4, from 751 to 823, amplified fragment 72 bp). Total RNA was extracted from BME-UV1 cells maintained in culture with FCS 0% or 10%, with or without insulin (20 ng/mL) (Sigma-Aldrich, St. Louis, MO) using Cells to Ct™ kit (Ambion, Life Technologies), according to the manufacturer's instructions. To evaluate the response of SCD1 endogenous gene in BME-UV1 cells to MUFA, oleic acid ≥ 99% purity (Calbiochem, Millipore, Germany) was added to a concentration of 30 and 50 μM.

For PCR analysis total RNA was isolated using the RNA Extraction Kit from Qiagen (Hilden, Germany) according to the manufacturer's instructions. RNA (2-

5µg) was treated with DNAse I (Promega, Madison USA) and used to generate reverse transcribed cDNA using SuperScript III (Life Technologies, CA, USA) and random examers in 20 µl of total reaction volume. All samples in each experiment were reverse transcribed at the same time and the resulting cDNA diluted 1:5 in nuclease-free water and stored in aliquots at –80°C until used.

Real Time PCR with SYBR green detection was performed with a 7500 RT-PCR Thermo Cycler (Applied Biosystem, Foster City, USA). The thermal cycling conditions were composed of 50ºC for 2 min followed by an initial denaturation step at 95ºC for 10 min, 45 cycles at 95ºC for 30s, 60ºC for 30s and 72ºC for 30s. For the qPCR the relative quantification in gene expression was determined using the $2^{-\Delta\Delta Ct}$ method (19). As previously suggested, Eukaryotic translation initiation factor 3 subunit K (EIF3K) and Glyceraldehyde-3-phosphate dehydrogenase (GAPDH) were used as an internal controls to normalize all data (20). After normalization, the data were presented as fold change relative to the control sample. Appropriate no-RT and non-template controls were included in each 96-well PCR reaction and dissociation analysis was performed at the end of each run to confirm the specificity of the reaction.

Statistical analysis

All experiments were performed in triplicate and repeated at least two times. Quantitative data were presented as mean ± standard deviation (SD). Comparison between data was analyzed using t-tests. Significant differences were accepted when P values is less than 0.05

RESULTS

The effect of Fetal Bovine Serum and Insulin on SCD1 promoter activity

The sequence of full length SCD1 promoter in *Bos Taurus* (1880 base pairs) is annotated in the (EMBL BANK) with the accession number AY241932 while a partial promoter region of *Bubalus bubalis* SCD1 is included in the ENA database (EMBL gene BANK) with the accession number FM876222. Comparison of the SCD1 proximal promoter region of several mammalian species, using the TFBIND and the TRANSFAC (ver.3.4) software, reveals high homology. The SCD1 proximal promoter sequences of *Bos Taurus* and *Bubalus bubalis* share 97% of identity. Figure 1a shows the PUFA-responsive SCD1 promoter region encompassing the perfectly conserved binding sites for Sp1, the SREBP-1c and NF-Y transcription factors, as previously described (8).

To evaluate bovine SCD1 promoter activity we generated the SCD1_PGL3 luciferase reporter construct. The bovine SCD1 promoter region including the PUFA-RE was PCR amplified from genomic cow DNA and appropriate primers (see Materials and Methods). The 600 bp amplified fragment was cloned upstream of the luciferase gene in the PGL3 promoter-less vector (Promega) to generate the SCD1_PGL3 reporter construct.

Cell culture conditions can have a profound impact on intracellular signaling cascade and may be a fondamental source of variability accounting, at least in part, for the conflicting results in the SCD1 litterature. For instance, oleic acid was reported to

reduce rat and bovine SCD1 promoter activity (8; 9) while having no effect on human SCD1 mRNA synthesis (10). To determine the extent to which serum affects SCD1 promoter activity, MCF7 cells were grown in serum-free or serum-supplemented medium (5-10% FBS) and transiently transfected with the SCD1_PGL3 construct or the p21WAF_PGL3 plasmid, containing a serum-independent promoter (our previous observations). The promoter-less pGL3 basic vector was used to evaluate the background signal. At 24 hrs after transfection, cells were collected, whole cell extracts were prepared and subjected to luciferase assay. As shown in Fig. 2a, in presence of serum, the p21WAF promoter activity was unaffected while the SCD1 promoter activity was significantly reduced ($p < 0.02$). In 10% FBS the SCD1 promoter activity was about 4.3 folds lower than in serum-free medium, with a residual activity ranging between 15 and 25 %. The background activity of pGL3 basic construct was negligible in both serum conditions (4.3 +/- 1.5 RLU, arbitrary units of luciferase activity).

Next, we monitored the effect of insulin on SCD1 promoter activity. The experiments were performed in serum-free condition or 10% serum as this is the most commonly used condition for the growth of mammalian cell lines. Insulin was added to the medium at the concentration of 20 ng/mL. In serum-free medium, insulin treatment caused a 2.5-fold induction of the SCD1 promoter reporter (Fig. 2b). After FBS-supplementation, the SCD1 promoter basal activity was reduced and insulin treatment was unable to evoke any response (Fig. 2b). The results demonstrate that serum components exert a strong repression on the SCD1 promoter and that insulin appears to be unable to overcome this repression.

Role of NFY transcription factor in the regulation of SCD1 promoter activity.

NFY factor has been suggested to be a PUFA-specific transcription factor for SCD1 gene repression (11). The transcription factor NFY is a hetero-trimeric protein, composed of three subunits NFY-A, NFY-B and NFY-C. NF-YB and NF-YC must interact and dimerize for association with NF-YA and consequent binding to CCAAT motifs in the promoter regions of a variety of genes. NFY interacts with the Sterol Regulatory Element-Binding Proteins (SREBPs). SREBPs, indeed, are weak transcriptional activators on their own and interact with their target promoters in cooperation with additional regulators, most commonly including one or both NFY and SP1 transcription factors. To investigate the effect of NFY enforced expression on SCD1 promoter activity, we transiently transfected the SCD1_PGL3 reporter construct into MCF7 cells along with an equal amount of each plasmid encoding NFY subunit A, B or C. Four hours after transfection, the culture medium was replaced and cells were maintained in serum-free, 5% or 10% FBS-supplemented medium for 24 h. The expression of transfected NFY subunit A and B was monitored by immunoblot analysis using NFY specific antibodies (Figure 3A). The SCD1_PGL3 activity was then evaluated by Luciferase assay. As expected, in serum-supplemented media the basal activity of SCD1 promoter was lower than in serum-free medium (Fig. 3A). However, both in absence and 5% serum NFY expression causes a significant decline of luciferase activity ($p < 0.02$) indicating that NFY is a transcriptional repressor of SCD1 gene. However, in 10% serum the residual activity of SCD1 promoter was 50% of the control and NFY caused only a

15 % reduction thereby suggesting that serum and NFY compromise SCD1 promoter activity by acting at the same regulatory element.

Regulation of SCD1 promoter activity in bovine mammalian cells

The regulation of SCD1 expression in bovine mammary cells affects milk yield and fatty acid profile (21). SCD1 is induced by insulin (22). It was interesting to study the effect of insulin on SCD1 gene expression in BME-UV1 cells, immortalized, but not transformed, bovine mammary cells that closely mimic the *in vivo* mammary epithelial cells. The promoter reporter construct was transiently transfected into BME-UV1 grown in serum-free, 5% or 10% FCS with or without insulin (20 ng/mL). BME-UV1 cells were transiently transfected with SCD1_PGL3 construct and after 24 hours whole cell extracts were prepared and subjected to the luciferase assay. According to what observed in MCF7 cells, serum-addition repressed SCD1 activity in bovine mammary cells (Fig. 4A). Again, we observed a 2.5 fold promoter activation by insulin only in serum-starved cells showing that the repressive activity of serum is dominant over the inductive effect of insulin. To corroborate these data, we decided to examine the level of SCD1 endogenous mRNA in BME-UV1 cells by quantitative Real Time PCR. Cells were grown in serum-free or 10% FCS medium and treated or not with insulin (20 ng/mL), for 24 hours. Total RNA was isolated and subjected to quantitative PCR using primers to specifically amplify bovine SCD1 mRNA. The level of SCD1 specific transcript was normalized against the 18S ribosomal RNA and expressed as relative amount respect to the sample obtained in

serum and insulin-free medium. As shown in Fig. 4B, we confirmed that insulin treatment enhanced SCD1 mRNA expression level only in serum-deprived cells.

Regulation of SCD1 promoter by oleic acid is still controversial. Oleic acids concentrations up to 100 μM were previously demonstrated do not affect MCF7 cell proliferation and viability (23). However, we performed preliminary test by treating MCF7 and BME-UV1 with increasing amount of oleic acid (15, 30, 50, 80 and 100 μM) for 24 and 48 hours. In each experimental point the cells behave healthy. Moreover, cells lysates were analyzed by immunoblot with antibodies against Caspase3 and PARP and we did not detect signs of apoptosis neither in terms of Caspase 3 induction nor Poli ADP-ribose polymerase cleavage.

(data not shown). To check the effect of oleic acid in the control of bovine SCD1 promoter we transiently transfected BME-UV1 cells with the SCD1 promoter-luciferase reporter in serum-free medium supplemented or not with 30 or 50 μM oleic acid.

The combined effect of insulin and oleic acid was checked by adding insulin at a concentration of 20 ng/mL in cells treated or not with oleic acid. 24 hours after transfection, whole cell extracts were prepared and subjected to the luciferase assay.

As shown in Fig. 5A, oleic acid alone did not significantly changed the basal activity of SCD1 promoter which was instead efficiently activated by insulin. Interestingly, insulin-dependent activation was almost completely abolished by oleic acid addition to the culture medium showing that, similar to serum, the repressive activity of oleic acid overrides the inductive effect of insulin. To substantiate these data, we decided to examine the level of SCD1 endogenous mRNA in BME-UV1 cells by quantitative

Real Time PCR. Cells were grown in serum-free medium supplemented or not with 30 or 50 μM oleic acid for 24 hours. The combined effect of insulin and oleic acid was checked by adding insulin at a concentration of 20 ng/mL. Total RNA was isolated and subjected to quantitative PCR using primers to specifically amplify bovine SCD1 mRNA. The level of SCD1 specific transcript was normalized against the EIF3K and GAPDH RNA and expressed as relative amount respect to the sample obtained in oleic acid and insulin-free medium. As shown in Fig. 5B, we confirmed the induction of SCD1 endogenous gene transcription by insulin which was completely suppressed by oleic acid.

DISCUSSION

Alignment of the highly conserved region of bovine SCD1 promoter region shows the expected high homology of the putative PUFA-RE between different farm animal species. This region is known to be involved in the response of SCD promoter to insulin, fatty acids and sterols (24). The PUFA-RE contains binding sites for SREBP1, NFY and SP1 transcription factors. Genome-wide analysis of promoter co-occupancy, in human liver cells, have recently shown that SREBP1 cooperates extensively with NFY and SP1 throughout the genome, thereby suggesting that the regulatory circuitry among SREBP, NFY and SP1 is highly interconnected. Concerning the metabolic pathways, combination of all three factors was reported to be involved in the control of cholesterol biosynthesis and aminoacid activation while the combination of SREBP1 and NFY alone was shown to regulate lipid metabolism and RNA processing (13).

The expression of the SCD 1 gene is under complex control mechanisms such as hormones and, possibly, intermediates of carbohydrate and fat metabolism therefore it is difficult to dissect all the agents that regulate SCD1 gene transcription by *in vivo* models. The aim of this study was to investigate the responsiveness of bovine SCD1 promoter to insulin, oleic acid and NFY in BME-UV1 cells, a potential in vitro model for studying biotransformation in bovine mammary gland.

In the mammary gland of ruminants, SCD1 is known to be responsible for the production of about 63-97% of c9t11 CLA coming from vaccenic acid as estimated using either direct (13C-labelled fatty acids) or indirect methods (inhibition of SCD

by sterculic acid or duodenal and milk FA flows) (25). SCD1 activity can be measured by comparing the product/substrate ratios of certain fatty acids. There are four main products of SCD1 activity in the mammary gland of ruminants: c9C14:1, c9C16:1, c9C18:1 and CLA, which are produced from C14:0, C16:0, C18:0 and trans11 C18:1, respectively. According to Lock and Garnsworthy (26), the best indicator of SCD1 activity is the c9C14:1/C14:0 ratio because all of the C14:0 in milk fat is produced via de novo synthesis in the mammary gland; consequently, desaturation is the only source of C14:1. Increasing c9C14:1/C14:0 ratio values would indicate an increase of SCD1 activity.

The regulation of SCD1 by dietary factors has been largely investigated in rodents (11), while in ruminants the results are conflicting. Ahnadi et al. (27) and Harvatine and Bauman (28) found a depression of mammary SCD1 mRNA abundance when lactating cows were fed protected PUFA. Researches effected on goats showed that the supplementation of sunflower seed oil (29) and linseed oil (30) did not affect both SCD1 expression and/or activity in maize silage-based diets while the same supplementation to diets based on grass hay decreased only the SCD1 activity (31). Similar results have been reported supplementing soya beans to lucerne hay-based diets (32). Finally, supplementing grass hay-based diets with formaldehyde-treated linseed decreased mammary SCD1 mRNA without effect on the SCD1 activity (32). Tudisco et al (33) reported higher SCD1 expression in the somatic cells of milk yielded from goats bred according either organic system than those bred in stable. The authors justify the results for the a higher amount of both C18:2 and C18:3

ingested by organic group than the stable group, as registered in previous researches (34; 35) thus probably resulting in an up-regulation of the SCD expression.

Bernard et al. (36) suggest to evaluate the importance of interactions between the composition of the basal diet and lipid supplement with the implication that specific PUFA escaping metabolism in the rumen or specific biohydrogenation intermediates may inhibit SCD1 activity via transcriptional or post- transcriptional regulatory mechanisms.

More recently, Tudisco et al (37) reported that the grazing season as well as lactation stage can affect the SCD1 mRNA abundance determined from milk somatic cells with values that progressively decreased from April until June, increased in July and decreased again in August.

In keeping with previous findings (38), we found that insulin treatment induces a significant increase of SCD 1 gene promoter activity in BME-UV1 cells, providing further evidence of its pro-lipogenic role. However, attention must be paid to the evaluation of SCD1 promoter regulation in serum-supplemented cell culture as the repressive effect of serum on SCD1 promoter activity overcomes induction by insulin and this was consistently shown both in human MCF7 and bovine BME-UV1 cells. Remarkably, oleic acid was also able to repress SCD1 promoter activation only in insulin treated cells thereby providing a possible explanation of the controversial literature about the inhibitory effect of oleic on SCD1 expression (11). We confirmed our data on SCD1 endogenous transcription of BME-UV1 cells, thereby demonstrating that our reporter system truly reflects the response of the endogenous SCD1 gene promoter and can be a useful tool to investigate the modulation of SCD1

promoter activity by nutrients and extracellular stimuli. Finally, our study provides evidences that NFY enforced expression represses SCD1 promoter activity. It has to be mentioned that Tabor and coworkers (22) reported that NFY transcription factor is a SCD1 transcriptional activator in adipocytes; our data are in contrast with Tabor conclusion and this might depend on the specific cell type and growing condition used. However, whether NFY works in cooperation or not with other transcription factors, deserves more attention and will be the subject of further investigations.

References

1. Ntambi, J. M. The regulation of stearoyl-CoA desaturase (SCD). Prog. Lipid Res. 1995; 34, 139-150.
2. Paton, C.M., Ntambi, J.M. Biochemical and Physiological Function of Stearoyl-CoA Desaturase. Am J Physiol Endocrinol Metab. 2009; 297:28-37.
3. Flowers, M. T., Groen A. K., Oler, A. T., Keller, M. P., Choi, Y. J., Schueler, K.L., Richards O.C., Lan, H., Miyazaki M., Kuipers, Kendziorski C. M., J. M. Ntambi and A. D. Attie. Cholestasis and hypercholesterolemia in SCD1-deficient mice fed a low-fat, highcarbohydrate diet. J. Lipid Res. 2006; 47:2668-2680.
4. Bionaz, M. and Loor J. Gene networks driving bovine milk fat synthesis lactation cycle. BMC Genomics 9(1). 2008; 366. doi:10.1186/1471-2164-9-366
5. Bauman, D. E., L. H. Baumgard, B. A. Corl, and J. M. Griinari. Biosynthesis of conjugated linoleic acid in ruminants. Proc Am. Soc. Anim. Sci. 1999; Available at: http://jas.fass.org/cgi/content/abstract/77/E-Suppl/1-ae. Accessed Dec. 5, 2005.
6. Ward, R. J., M. T. Travers, S. E., Richards, R. G. Vernon, A. M., Salter, P. J. Buttery, and M. C. Barber. Stearoyl coenzyme A desaturase mRNA is transcribed from a single gene in the ovine genome. Biochim. Biophys. Acta.1998; 1391:145–156.
7. Griinari, J. M., B. A. Corl, S. H. Lacy, P. Y. Chouinard, K. V. Nurmela and D. E. Bauman. Conjugated linoleic acid is synthesized endogenously in lactating dairy cows by Δ9-desaturase. J. Nutr. 2000; 130:2285-2291.

8. Zulkifli R.M., Parr T., Salter A.M. and Brameld J. Salter and John M. 2010. Regulation of ovine and porcine stearoyl coA desaturase gene promoters by fatty acids and sterols. J.Anim.Sci. M. 2010; 88: 2565-2575

9. Keating, A.F., Kennelly J.J., and F. Zhao. Characterization and regulation of the bovine stearoyl-CoA desaturase gene promoter. Biochem. Biophys. Res. Commun. 2006; 200:763-768.

10. Bené, H., Lasky D. and J.M. Ntambi. Cloning and characterization of the human steroyl-CoA desaturase gene promoter: Transcriptional activation by sterol regulatory element binding protein and repression by polyunsaturated fatty acids and cholesterol. Biochem. Biophys. Res. Commun. 2001; .284:1194-1198.

11. Ntambi, J.M.,. Regulation of stearoyl-CoA desaturase by polyunsaturated fatty acids and cholesterol. J. Lipid Res. 1999; 40, 1549–1558.

12. Waters, K.M., Miller, C.W., Ntambi, J.M.. Localization of a polyunsaturated fatty acid response region in stearoyl-CoA desaturase gene 1. Biochim. Biophys. Acta. 1997; 1349(1):33-42.

13. Reed, B.D., Charos, A.E., Szekeley, A.M., Weissman, S.M., Snyder M. Genome-Wide occupancy of SREBP1 and its partners NFY and Sp1 reveals novel functional roles and combinatorial regulation of distinct class of genes. PLOS Genetics. 2008; DOI: 10.1371/journal.pgen.1000133

14. Osborne, C.K., Bolan, G., Monaco, M.E., Lippman, M.E. Hormone responsive human breast cancer in long-term tissue culture. Effect of insulin. Proc. Natl. Acad. Sci USA 1976; 73(12): 4536-4540.

15. Cheli F, Zavizion B, Todoulou O, Politis I. The effect of calcium on mammary epithelial cell proliferation and plasminogen activating system. Can.J. Anim. Sci. 1999; 277-283.

16. Calabrò, V., Mansueto, G., Parisi, T., Vivo, M., Calogero, R.A., La Mantia, G. The human MDM2 oncoprotein increases the transcriptional activity and protein level of the p53 homolog p63. J. Biol. Chem. 2002; 277(4): 2674-81.

17. Harvey, KA, Walker CL, Xu, Z., Whitley, P., Pavlina, T.M., Hise, M., Zaloga, G.P., Siddiqui, R.A. Oleic acid inhibits stearic-induced inhibition of cell growth and pro-inflammatory responses in human aortic endothelial cells. J. Lipid Res. 2010(12): 3470-80.

18. Rossi, M., De Simone, M., Pollice, A., Santoro, R., La Manti, G., Guerrini, L., Calabrò, V. Itch/AIP4 associates with and promotes p63 protein degradation. Cell Cycle. 2006; 5(16):1816-22.

19. Livak, K.J., Schmittgen, T.D. Analysis of relative gene expression data using Real-Time 436 Quantitative PCR and the 2-DDCT method. Methods. 2011(25): 402-408.

20. Kadegowda, A.K.G., Bionaz, M., Thering, B., Piperova, L.S., Erdman, R.A., Loor, J.J. Identification of internal control genes for quantitative polymerase chain reaction in mammary tissue of lactating cows receiving lipid supplements. J Dairy Sci. 2009; 92(5): 2007–2019.

21. Pauciullo A, Cosenza G, Steri R, Coletta A, La Battaglia A, Di Berardino D, Macciotta NP, Ramunno L. A single nucleotide polymorphism in the promoter region of river buffalo stearoyl CoA desaturase gene (SCD) is associated with milk yield. J Dairy Res. 2012; 79(4):429-35.

22. Tabor, D.E., Kim, J.B., Spiegelman B.M. and Edwards P.A. Identification of conserved cis-elements and transcription factors required for sterol-regulated transcription of stearoyl-CoA desaturase 1 and 2. J. Biol. Chem. 1999; 274:20603-20610.

23. Dailey, O.D. Jr, Wang, X., Chen, F., Huang, G. Anticancer activity of branched-chain derivatives of oleic acid. Anticancer Res 2011, 31 (10):3165-9 .

24. Biddinger, S., Miyazaki, M., Boucher, J., Ntambi, J. and Kahn, C.R. Leptin Suppresses Stearoyl-CoA Desaturase 1 by Mechanisms Independent of Insulin and Sterol Regulatory Element–Binding Protein-1c. Diabetes. 2006; 55, 2032-2041

25. Bernard, L., Leroux, C., Chilliard, Y. Nutritional regulation of mammary lipogenesis and milk fat in ruminant: contribution to sustainable milk production. Revista Colombiana de Ciencias Pecuarias 2013; 26, 292-302.

26. Lock, A.L., Garnsworthy, P.C. Seasonal variation in milk conjugated linoleic acid and D9-desaturase activity in dairy cows. Livestock Production Science. 2003; 79, 47–59.

27. Ahnadi, C.E., Beswick, N., Delbecchi, L., Kennelly, J.J., Lacasse, P. Addition of fish oil to diets for dairy cows. II. Effects on milk fat and gene expression of mammary lipogenic enzymes. J. Dairy Res. 2002; 69, 521–531.

28. Harvatine, K.J., Bauman, D.E. SREBP1 and thyroid hormone responsive spot 14 (S14) are involved in the regulation of bovine mammary lipid synthesis during diet-induced milk fat depression and treatment with CLA. J. Nutr. 2006; 136, 2468–2474.

29. Bernard, L., Rouel, J., Leroux, C., Ferlay, A., Faulconnier, Y., Legrand, P., Chilliard, Y. Mammary lipid metabolism and milk fatty acid secretion in alpine goats fed vegetable lipids. Journal of Dairy Science. 2005; 88, 1478–1489.

30. Bernard, L., Bonnet, M., Leroux, C., Shingfield , K. J., Chilliard, Y. Effect of sunflower-seed oil and linseed oil on tissue lipid metabolism, gene expression, and milk fatty acid secretion in alpine goats fed maize silage–based diets. Journal of Dairy Science. 2009;92, 6083–6094.

31. Bernard, L., Leroux, C., Faulconnier, Y., Durand, D., Shingfield, K.J., Chilliard, Y. Effect of sunflower-seed oil or linseed oil on milk fatty acid secretion and lipogenic gene expression in goats fed hay-based diets. Journal of Dairy Research 2009;76, 241–248.

32. Bernard, L., Leroux, C., Bonnet, M., Rouel, J., Martin, P., Chilliard, Y. Expression and nutritional regulation of lipogenic genes in mammary gland and adipose of lactating goats. Journal of Dairy Research. 2005; 72, 250–255

33. Tudisco, R., Calabrò, S., Cutrignelli, M.I., Moniello, G., Grossi, M., Gonzalez, O.J., Piccolo, V., Infascelli, F. Influence of organic systems on Stearoyl-CoA-Desaturase in goat milk. Small Ruminant Research. 2012; 106, 37-42.

34. D'Urso, S., Cutrignelli, M.I., Calabrò, S., Bovera, F., Tudisco, R., Piccolo, V., Infascelli, F. Influence of pasture on fatty acid profile of goat milk. Journal of Animal Physiology and Animal Nutrition 2008; 92, 405-10

35. Tudisco, R., Cutrignelli, M.I., Calabrò, S., Piccolo, G., Bovera, F., Guglielmelli, A., Infascelli, F. Influence of organic systems on milk fatty acid profile and CLA in goats. Small Ruminant Research. 2010; 88: 151-155.

36. Bernard , L., Leroux , C., Chilliard. Expression and Nutritional Regulation of Stearoyl-CoA Desaturase Genes in the Ruminant Mammary Gland: Relationship with Milk Fatty Acid Composition. In: Ntambi, J.M. (Ed.), Stearoyl-CoA Desaturase Genes in Lipid Metabolism, Springer Science+Business Media New York. Y.2013;161-193.

37. Tudisco, R., Grossi, M., Calabrò, S., Cutrignelli, M.I., Musco, N., Addi, L., Infascelli F. Influence of pasture on goat milk fatty acids and Stearoyl-CoA desaturase expression in milk somatic cells. Small Ruminant Research. 2014; DOI: 10.1016/j.smallrumres.2014.07.016.

38. Mauvoisin, D., Rocque, G., Arfa, O., Radenne A., Boissier P., Mounier C. Role of the PI3-kinase/mTor pathway in the regulation of the stearoyl CoA desaturase (SCD1) gene expression by insulin in liver. J Cell Commun Signal. 2007 ; 1(2), 113-125.

Legends to figures

Figura 1. **The SCD1 gene promoter**. **(A)** Sequence alignment of the PUFA-RE sequence in the SCD1 proximal promoter region underlined the sequences corresponding to the Sp1 protein binding site, the Sterol Responsive Element and the NF-Y/NFI consensus. **(B)** The SCD1 proximal promoter region. The primers used for PCR and subsequent cloning are indicated in italic. Underlined are highlighted the sequences corresponding to the Sp1 protein binding site, the Sterol Responsive Element and the NF-Y/NFI consensus. The transcription start site (+1) is indicated in capital.

Figure 2. Effect of FBS on SCD1 promoter activity. (A) The SCD1_PGL3 or p21WAF_PGL3 promoter constructs were transfected into MCF7 cells and treated with different concentrations of serum (0%, 5%,10%). After 24 h the luciferase assay was performed. The p21WAF_PGL3 promoter, was used as a serum independent control. The basal activity of the promoters at 0% FBS was fixed as 100%. Each experimental point was done in triplicate and the results are presented as the mean of three biological replicates. **(B)** The SCD1_PGL3 promoter construct was transfected into MCF7 cells grown in serum-free or 10% Fetal Bovine Serum. Insulin was added at a concentration of 20 ng/ml. After 24 hr the luciferase assay was performed. The basal activity of the promoters at 0% FBS was fixed as 100%. Each experimental point was done in triplicate and the results are presented as the mean of three biological replicates.

Fig.3 Effect of NFY transcription factor and on SCD1 promoter activity into MCF7 cells.

MCF7 cells were co-trasfected with 0.5 μg of SCD-1-PGL3 construct along with 0.5 μg of each plasmid encoding NFY-A, NFY-B and NFY-C subunits. Cells were grow in serum-free medium or media supplemented with 5 or 10% FBS for 24 hrs. **(A)** Expression of transfected NFYA and NFYB protein was evaluated by immunoblot analysis with specific antibodies. **(B)** Promoter activity was evaluated by luciferase assay. Each experimental point was done in triplicate and the results are presented as the mean of three biological replicates.

Figure 4. Effect of serum and Insulin on SCD1 promoter activity. (A) SCD1_PGL3 promoter construct was transfected into BME-UV1 cells treated with the indicated concentrations of serum (0%, 5%, 10%) with or without insulin (20 ng/mL), as indicated. After 24 hr, the promoter activity was evaluated by luciferase assay. Each experimental point was done in triplicate and the results are presented as the mean of three biological replicates.

(B) BME-UV1 cells were treated with the indicated concentrations of serum (0%, 10%) with or without insulin (20 ng/mL), for 24 h. The SCD1 specific transcript was quantified by Real Time PCR and expressed as the relative amount respect to the level expressed in cells grown in serum and insulin-free medium. The results are presented as the mean of three experimental replicates

Figure 5. Effect of insulin and oleic acid on SCD1 promoter activity

(A) SCD1_PGL3 promoter construct was transfected into BME-UV1 cells cultured in serum-free medium with or without insulin (20 ng/mL), as indicated. Oleic acid (30 and 50 μM) was supplemented to the medium as indicated. After 24 hr, the promoter activity was evaluated by luciferase assay. Each experimental point was done in triplicate and the results are presented as the mean of three biological replicates.

(B) BME-UV1 cells were treated as indicated in (A) for 24 h. The SCD1 specific transcript was quantified by Real Time PCR and expressed as the relative amount respect to the level expressed in cells grown in serum-free medium without insulin and oleic acid. The results are presented as the mean of three experimental replicates.

Figure 1

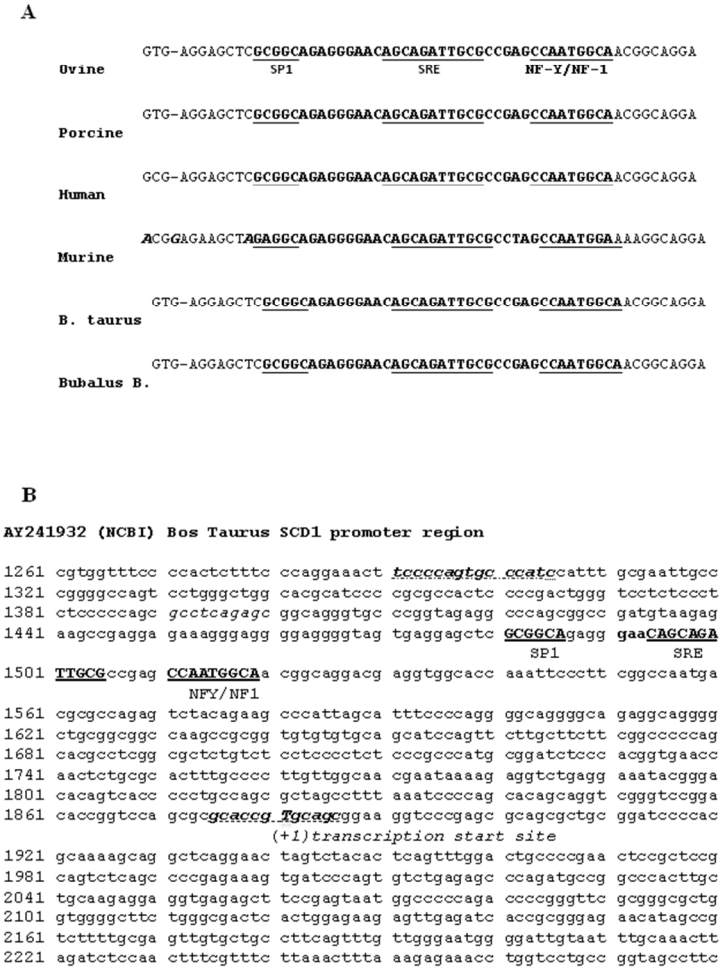

The SCD1 gene promoter. (A) Sequence alignment of the PUFA-RE sequence in the SCD1 proximal promoter region underlined the sequences corresponding to the Sp1 protein binding site, the Sterol Responsive Element and the NF-Y/NFI consensus. (B) The SCD1 proximal promoter region. The primers used for PCR and subsequent cloning are indicated in italic. Underlined are highlighted the sequences corresponding to the Sp1 protein binding site, the Sterol Responsive Element and the NF-Y/NFI consensus. The transcription start site (+1) is indicated in capital.
190x275mm (96 x 96 DPI)

Figure 2

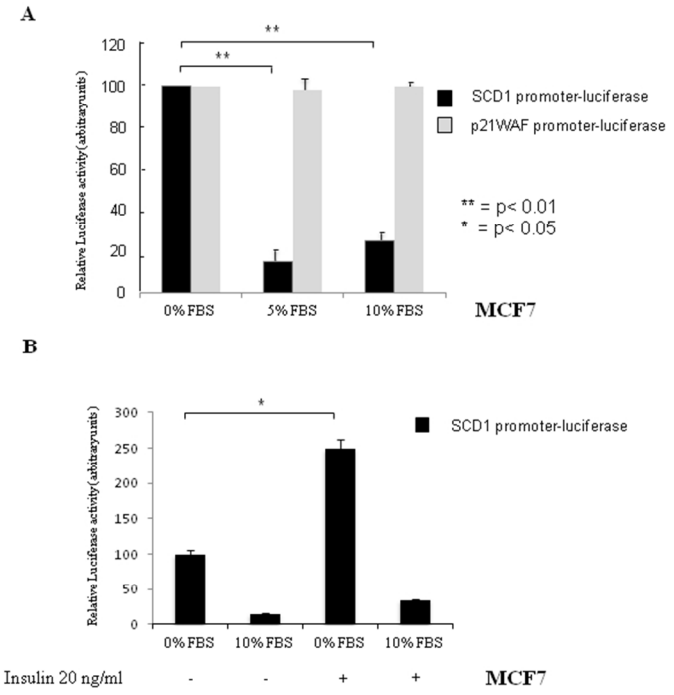

Effect of FBS on SCD1 promoter activity. (A) The SCD1_PGL3 or p21WAF_PGL3 promoter constructs were transfected into MCF7 cells and treated with different concentrations of serum (0%, 5%,10%). After 24 h the luciferase assay was performed. The p21WAF_PGL3 promoter, was used as a serum independent control. The basal activity of the promoters at 0% FBS was fixed as 100%. Each experimental point was done in triplicate and the results are presented as the mean of three biological replicates. (B) The SCD1_PGL3 promoter construct was transfected into MCF7 cells grown in serum-free or 10% Fetal Bovine Serum. Insulin was added at a concentration of 20 ng/ml. After 24 hr the luciferase assay was performed. The basal activity of the promoters at 0% FBS was fixed as 100%. Each experimental point was done in triplicate and the results are presented as the mean of three biological replicates.
190x275mm (96 x 96 DPI)

Figure 3

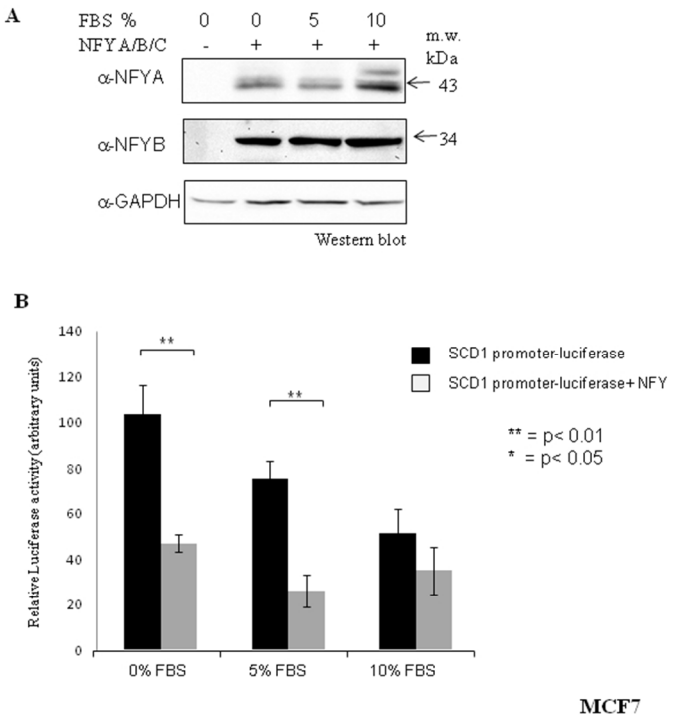

Effect of NFY transcription factor and on SCD1 promoter activity into MCF7 cells.
MCF7 cells were co-trasfected with 0.5 µg of SCD-1-PGL3 construct along with 0.5 µg of each plasmid encoding NFY-A, NFY-B and NFY-C subunits. Cells were grow in serum-free medium or media supplemented with 5 or 10% FBS for 24 hrs. (A) Expression of transfected NFYA and NFYB protein was evaluated by immunoblot analysis with specific antibodies. (B) Promoter activity was evaluated by luciferase assay. Each experimental point was done in triplicate and the results are presented as the mean of three biological replicates.

190x275mm (96 x 96 DPI)

Figure 4

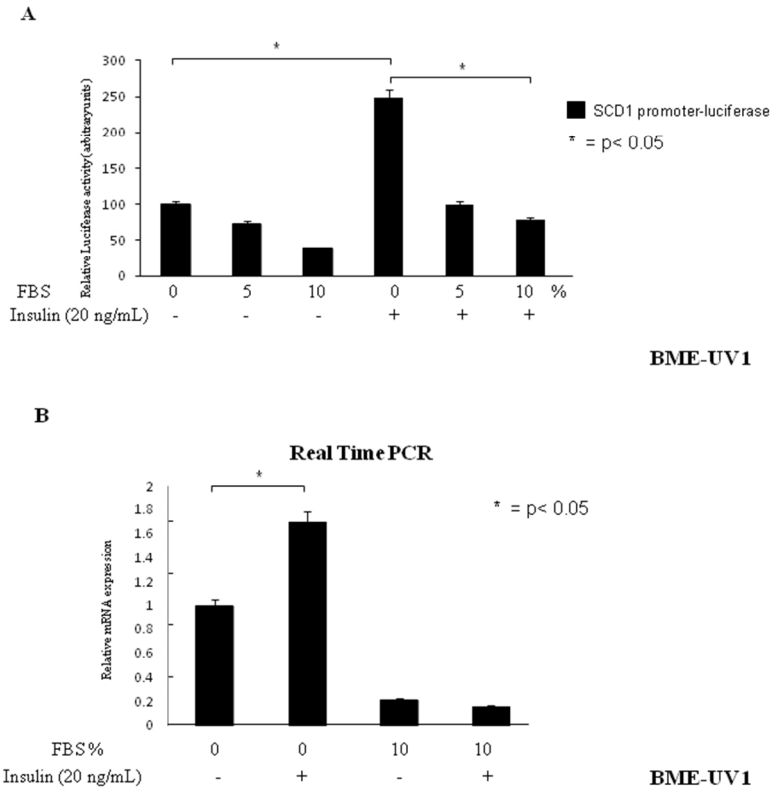

Effect of serum and Insulin on SCD1 promoter activity. (A) SCD1_PGL3 promoter construct was transfected into BME-UV1 cells treated with the indicated concentrations of serum (0%, 5%, 10%) with or without insulin (20 ng/mL), as indicated. After 24 hr, the promoter activity was evaluated by luciferase assay. Each experimental point was done in triplicate and the results are presented as the mean of three biological replicates.
190x275mm (96 x 96 DPI)

Figure 5

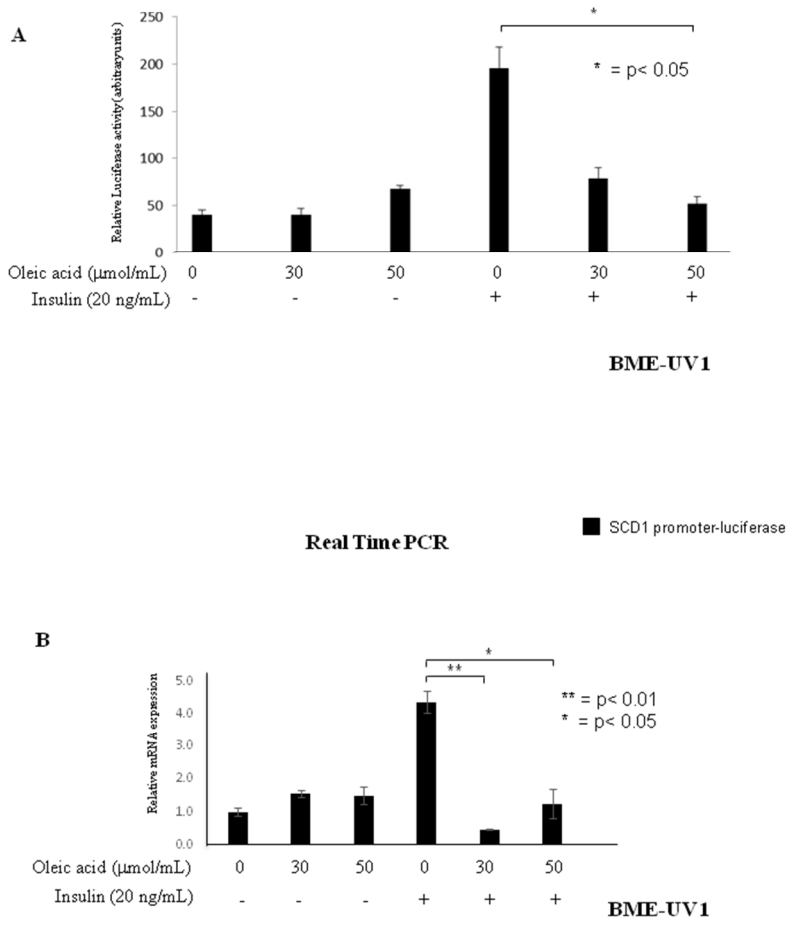

Effect of insulin and oleic acid on SCD1 promoter activity

(A) SCD1_PGL3 promoter construct was transfected into BME-UV1 cells cultured in serum-free medium with or without insulin (20 ng/mL), as indicated. Oleic acid (30 and 50 µM) was supplemented to the medium as indicated. After 24 hr, the promoter activity was evaluated by luciferase assay. Each experimental point was done in triplicate and the results are presented as the mean of three biological replicates.

(B) BME-UV1 cells were treated as indicated in (A) for 24 h. The SCD1 specific transcript was quantified by Real Time PCR and expressed as the relative amount respect to the level expressed in cells grown in serum-free medium without insulin and oleic acid. The results are presented as the mean of three experimental replicates.

190x275mm (96 x 96 DPI)

Elsevier Editorial System(tm) for FEBS Letters
Manuscript Draft

Manuscript Number:

Title: ΔNp63α protects YB-1 oncoprotein from proteasome-dependent proteolysis

Article Type: Research Letter

Keywords: p53 protein family; Y-box binding protein; keratinocytes; ubiquitination; protein stability; cell proliferation.

Corresponding Author: Prof. Viola Calabrò, Ph.D.

Corresponding Author's Institution: University of Naples

First Author: Orsola di Martino

Order of Authors: Orsola di Martino; Annaelena Troiano; Andrea Maria Guarino; Alessandra Pollice; Maria Vivo; Girolama La Mantia; Viola Calabrò, Ph.D.

Manuscript Region of Origin: ITALY

Abstract: Y-box binding protein 1 (YBX-1 or YB-1) is an oncoprotein that promotes replicative immortality, tumor cell invasion and metastasis. A change in YB-1 abundance or nuclear localization is characteristic of malignant cell growth. YB-1 interacts with ΔNp63α a master regulator of epidermal morphogenesis. Here, we report that ΔNp63α reduces YB-1 protein turnover and induces the accumulation of polyubiquitinated YB-1 into the nucleus. We show that ΔNp63α and YB-1 are highly expressed in proliferating keratinocytes and are both down-regulated under differentiating conditions. This suggests that the control of YB-1 protein stability by ΔNp63α contributes to the proliferative potential of basal keratinocytes.

Suggested Reviewers: Peter Mertens Professor
Otto-von-Guericke-Universität Magdeburg
peter.mertens@med.ovgu.de
Expert in YB-1 protein studies

Apollonia Tullo Dr.
Istituto Tecnologie Biomediche Bari, Italy
apollonia.tullo@ba.itb.cnr.it
Expert in p53 family protein

Opposed Reviewers:

Cover Letter

Dear Dr. Wieland,

we would like to submit the research article: **ΔNp63α protects YB-1 oncoprotein from proteasome-dependent proteolysis** by Orsola di Martino, Annaelena Troiano, Andrea Maria Guarino, Alessandra Pollice, Maria Vivo, Girolama La Mantia, Viola Calabrò for publication in **FEBS Letters**.

We have previously demonstrated a physical and functional association between ΔNp63α and YB-1 oncoproteins in squamous carcinoma cell lines. Moreover, we have demonstrated that ΔNp63α and YB-1 association cooperates in gene promoter activation (Di Costanzo et al. *J.Biol.Chem. 2012*). Recently, we have shown that YB-1 regulates ΔNp63α protein levels at transcriptional level (Troiano et al. *J. Cell Physiol. 2015*) In the present study, we show that ΔNp63α controls YB-1 protein turnover. Moreover, we show that YB-1 and ΔNp63α are highly co-expresses in actively proliferating keratinocytes and are both down-regulated under differentiating conditions suggesting that the control of YB-1 protein stability by ΔNp63α can contribute to the proliferative potential of basal keratinocytes.

The material reported in the present manuscript is original research, it has not been published previously and it is not under consideration for publication elsewhere. Its publication is approved by all authors. Author Contributions: VC conceived and supervised the study and wrote the manuscript. O. di M., A. T., A. M. G. performer experiments, M. V. and A. P. analyzed data, G. L. M. made manuscript revision. The authors declare that they have no conflict of interest.

Sincerely

Viola Calabrò

Corresponding author:
Viola Calabrò
Associate Professor of Genetics
Dipartimento di Biologia
Università di Napoli, "Federico II",
Edificio 7, Via Cinzia, Monte S. Angelo
80126 Naples, Italy. Telephone: +39 081 679069 or 679070. Fax +39 081 679233. Email: vcalabro@unina.it

ΔNp63α protects YB-1 oncoprotein from proteasome-dependent proteolysis

Orsola di Martino*, Annaelena Troiano*, Andrea Maria Guarino, Alessandra Pollice, Maria Vivo, Girolama La Mantia, Viola Calabrò§

Department of Biology, University of Naples "Federico II", 80126 Naples, Italy

*O. di M. and A.T. have equally contributed to this work.

§Corresponding author: Prof. Viola Calabrò, PhD. Dipartimento di Biologia, Università di Napoli, "Federico II", Viale Cinzia, Monte S Angelo, 80126 Napoli, Italy. Phone: +39 081 679069. Fax +39 081 679033. E-mail: vcalabro@unina.it

Abstract

Y-box binding protein 1 (YBX-1 or YB-1) is an oncoprotein that promotes replicative immortality, tumor cell invasion and metastasis. A change in YB-1 abundance or nuclear localization is characteristic of malignant cell growth. YB-1 interacts with ΔNp63α, a master regulator of epidermal morphogenesis. Here, we report that ΔNp63α reduces YB-1 protein turnover and induces the accumulation of polyubiquitinated YB-1 into the nucleus. We show that ΔNp63α and YB-1 are highly expressed in proliferating keratinocytes and are both down-regulated under differentiating conditions. This suggests that the control of YB-1 protein stability by ΔNp63α contributes to the proliferative potential of basal keratinocytes.

Highlights

- ΔNp63α expression protects full length YB-1 from specific endoproteolysis.
- ΔNp63α induces the accumulation of polyubiquitinated YB-1 into the nucleus.
- YB-1 and ΔNp63α sustains the proliferative potential of basal keratinocytes.

Introduction

Y Box Binding protein 1 (YBX-1 also known as YB-1) is a transcription/translation factor involved in a wide variety of cellular functions including cell proliferation and migration, DNA repair, multidrug resistance and stress response to extracellular signals (1; 2; 3). In clinical studies, YB-1 is associated with tumor progression, chemoresistance and poor prognosis in ovarian cancer (4), glioblastoma (5), melanoma (6) and non small cell lung cancer (7).

In physiological conditions, YB-1 is predominantly cytoplasmic and it appears to localize in the nucleus only at certain steps of the cell cycle (8). Cytokines (9), cytotoxic agents (10) and stimuli exerted by hyperthermia (11) and hypoxia (12) alter YB-1 cytoplasmic localization to a nuclear preponderance. YB-1 phosphorylation at Serine 102 in response to MAPK and PI3K/AKT signaling, also promotes YB-1 translocation in the nucleus (6) where it activates pro-proliferative genes such as cyclins, DNA pol α, PCNA and PIK3CA (8; 13; 14).

The plethora of functions fulfilled by YB-1 requires its sub-cellular shuttling. Specific protein domains, denoted nuclear localization (NLS) and cytoplasmic retention (CRS) signals, coordinate YB-1 multifunctional shuttling and tasking (15).

Changes in the abundance of YB-1 in the cell or YB-1 translocation from the cytoplasm to the nucleus is characteristic of malignant cell growth. The mechanisms governing YB-1 protein localization and stability are still largely unknown. YB-1 was reported to be fully degraded by 26S proteasome or endoproteolitically cleaved by the 20S proteasome. YB-1 limited proteolysis releases YB-1 fragments that localize to the nucleus and play pro-survival functions (3; 16).

We have previously identified YB-1 as a ΔNp63α molecular partner (17). ΔNp63α is encoded by the TP63 locus, the ancestral gene of the p53 gene family (17). By alternative promoters usage, the TP63 locus gives rise to multiple isoforms that can be placed in two categories: TA isoforms with an acidic transactivation domain and ΔN isoforms that lack this domain. Alternative splicing at the carboxy-terminal (C-terminal) generates at least three p63 variants (α, β and γ) in each class (18).

ΔNp63α is a critical pro-proliferative factor. It is essential for morphogenesis of organs/tissues developing by epithelial-mesenchimal interactions such as the epidermis, teeth, hair and glands (19). In adults, ΔNp63α is robustly expressed in progenitor cells within the basal layer of stratified epithelia, such as the skin, breast and prostate where it is required for both the proliferative and differentiation potential of developmentally mature cells (20).

Recently, we have demonstrated that YB-1 silencing affects ΔNp63α expression and viability of human immortalized keratinocytes (21). Here, we show evidence that ΔNp63α controls YB-1 protein stability suggesting that ΔNp63α/YB-1 cross-talk is relevant for survival of basal keratinocytes in stratified epithelia.

Materials and Methods

Plasmids

cDNA encoding human ΔNp63α was previously described (1). cDNA encoding human Ubi-HA were provided by Dr. V Orsini.

Cell culture

MDA-MB231 cells were derived from metastatic breast carcinoma and A431 cells were established from an epidermoid carcinoma of the vulva. Cutaneous squamous carcinoma cells SCC011 were previously described (1) and cultured in RPMI supplemented with 10% fetal bovine serum at 37°C and 5% CO_2 (1). A431, HaCaT and MDA-MB231 were purchased from Cell Line Service (CLS, Germany) and cultured at 37°C and 5% CO_2. A431 and HaCaT cells were maintained in DMEM supplemented with 10% FBS. MDA-MB231 cells were maintained in DMEM supplemented with 5% FBS. NHEK cells were obtained from PromoCell (Heidelberg; Germany) and cultured M2 medium under the manufacturer's recommendations.

For differentiation, NHEK (2.3×10^5) cells, seeded at 60% confluence in 60 mm dishes were cultured for the indicated days in 1.5 mM Ca^{2+}. For HaCaT differentiation, cells (2.5×10^5) were seeded in 35 mm dishes and grown until 80% confluence. The medium was then replaced with DMEM without FBS and 2 mM calcium.

Transient transfection

Lipofections were performed with Lipofectammine 2000 (Invitrogen), according to the manufacturer's recommendations.

YB1 transient silencing was carried out with RIBOXX (IBONI YB-1siRNA pool) and RNAiMAX reagent (Invitrogen), according to the manufacturer's recommendations. Briefly, cells were seeded

at 60% confluence (1.5×10^6) in 100-mm dishes and transiently silenced with IBONI YB1-siRNA at 20 nm final concentration.

YB-1 guide sequences: UUUAUCUUCUUCAUUGCCGCCCCC; UUAUUCUUCUUAUGGCAGCCCCC; UUCAACAACAUCAAACUCCCCC; UCAUAUUUCUUCUUGUUGGCCCCC.

ΔNp63α transient silencing was carried out with RIBOXX (IBONI p63-siRNA pool) at 20 nm final concentration and RNAiMAX reagent (Invitrogen).

p63 guide sequences: UUAAACAAUACUCAAUGCCCCC; UUAACAUUCAAUAUCCCACCCCC; AUCAAUAACACGCUCACCCCC; AUGAUUCCUAUUUACCCUGCCCCC.

"All Star Negative Control siRNA", provided by Quiagen, was used as negative control.

Protein turnover analysis

For half-life studies MDA-MB231 cells were transfected with mock or ΔNp63α plasmids. 24 hours after transfection, cells were replated in 6-well dishes, allowed to adhere overnight, and treated with cycloheximide (Calbiochem) at a final concentration of 10 μg/ml. Cells were harvested at the indicated time points. Total cell extracts were prepared and 20 μg of each sample was probed, in Western blot, with anti YB-1 antibody and, as control, with anti-actin.

Antibodies and chemical reagents

Anti-p63 (4A4), anti-cytokeratin 1 (4D12B3), anti-p21WAF (F-5), anti-GAPDH (6C5), and anti-actin (1-19) were purchased from Santa Cruz (Biotechnology Inc.). Cyclin D1, PARP and AKT antibodies were from Cell Signaling Technology (Beverly, Massachussets). Rabbit polyclonal YB1 (Ab12148) antibody was purchased from Abcam. (Cambridge, UK). Mouse monoclonal anti-HA(12CA5) antibody was purchased from Roche Applied Science. Proteasome inhibitor MG132

and Cycloheximide (CHX) were purchased from Sigma-Aldrich. MG132 treatment was carried out as previously described (22).

Immunoblot analyses and coimmunoprecipitation

Immunoblots (IB) and coimmunoprecipitations (Co-IP) were performed as previously described (18; 19). To detect YB-1 poli-ubiquitinated forms in A431 cells, 2 $\times 10^6$ cells were seeded in 100 mm dishes and transfected with Ubi-HA plasmid vector. For Co-IP, cell extracts, precleared with 30 μl of protein A-agarose (50% slurry; Roche, Manheim, Germany), were incubated overnight at 4°C with anti-HA (3 μg) or α-rabbit IgG (3 μg). To detect YB-1 poli-ubiquitinated forms, in MDA-MB231 cells (p63 -/-), 2 $\times 10^6$ cells were plated in 100 mm dishes and transfected with plasmids encoding human ΔNp63α and Ubi-HA. 30 μg of whole extracts were separated by SDS-PAGE and subjected to immunoblot.

Nuclear-cytoplasmic fractionation was performed as previously described (21); briefly cells were seeded at 60% confluence (1.5×10^6) in 100 mm dishes. 24 h after seeding, cell lysates were fractionated to obtain cytoplasmic and nuclear fractions. 10 μg of nuclear and 30 μg of cytoplasmic extracts (1:3 rate) were separated by SDS-PAGE and subjected to immunoblot.

All images were acquired with CHEMIDOC (Bio Rad) and analyzed with the Quantity-ONE software.

Results

ΔNp63α regulates YB-1 stability

We have previously shown that ΔNp63α promotes accumulation of full length YB-1 protein in the nuclear compartment (1). To investigate whether the increase of YB-1 protein abundance, induced by ΔNp63α, was due to reduced YB-1 protein turnover, we compared the half-life of YB-1 in mock

and ΔNp63α transfected MDA-MB231 cells. 24 hrs after transfection, cells were treated with cycloheximide to block protein synthesis. At the indicated times of drug exposure, cells were harvested, and whole extracts were analyzed by Western blot and probed with anti-YB1 antibody. As shown in Figure 1, in mock transfected cells, YB-1 exhibited a very peculiar byphasic response to cycloheximide, indeed the amount of YB1 protein was reduced to 40% after 4 hours, but then it remained constant up to 16 hours of incubation (Figure 1). Strikingly, in presence of ΔNp63α, 80% of YB-1 protein persisted after 24 hours of incubation with CHX thereby indicating that ΔNp63α reduces YB-1 protein turnover.

ΔNp63α stabilizes Ubi-conjugated forms of YB-1

Next, we transfected increasing amount of ΔNp63α expression plasmid in p63 null MDA-MB231 cells. In addition to the expected accumulation of full length YB-1 protein (p50/YB1), ΔNp63α expression caused an increase of slow migrating YB-1 immunoreactive bands (sm/YB1) and a concomitant reduction of faster migrating YB-1 forms (Figure 2A).

To further investigate on the observed high molecular forms of YB-1 we performed immunoblot analyses of whole-cell extracts obtained from ΔNp63α proficient HaCaT, A431, and SCC011 cells. In all cell lines tested, we observed slow migrating bands immunoreactive to YB-1 antibodies raised against a peptide encompassing aminoacids 1 to 100 of human YB-1 (Figure 2B). Similar results were obtained with a different commercial antibody directed against a peptide encompassing aminoacids 167 to 264 of YB-1 (data not shown).

To check the identity of the observed slow migrating bands, we depleted p63 proficient A431 cells of endogenous YB-1 by RNA interference. 48 hrs after YB-1 silencing, whole cell extracts were subjected to immunoblots with YB-1 antibodies. Some of the slow migrating bands either

disappeared or were reduced along with full length YB-1 implying that they were YB-1 modified forms (Figure 2C, black arrows).

Western blot analysis of nuclear and cytoplasmic fractions of MDA-MB231, A431 and SCC011 carcinoma cells (Figure 3A) revealed that slow migrating YB-1 immunoreactive bands were enriched in the nuclear compartment. Interestingly, we also detected distinct YB-1 forms, smaller than 50 kDa, probably generated by proteasome-mediated limited cleavage (16) (Figure 3A, black arrow).

To analyze the effect of proteasome inhibition, we treated HaCaT cells with MG132. Nuclear/cytoplasmic extracts were prepared and subjected to immunoblot with YB-1 antibodies. As shown in Fig 3B high molecular forms of YB-1 were clearly observed into the nucleus of non-transformed HaCaT keratinocytes. Following MG132 treatment, full length YB-1 accumulated and nuclear YB-1 proteolytic fragments smaller than 50 kDa either decreased or disappeared. Remarkably, proteasome inhibition also reduced high molecular forms of YB-1 suggesting that they were generated following YB-1 endoproteolytic cleavage (Figure 3B).

It was previosly reported that YB-1 is polyubiquitinated and degraded via the ubiquitin-proteasome pathway (23). Indeed, in MDA-MB231 cells transfected with Ubi-Ha, ubiquitin-containing complexes, immunoprecipitated with anti-HA antibodies, included endogenous YB-1 and p63 proteins (Figure 4A, lanes 5 and 6). By looking specifically at the pattern of high-molecular weight YB-1 forms in MB-MDA231 cells, we found that it was enhanced by ubiquitin or ΔNp63α transfection (Figure 4B, lanes 1 and 3 and Figure 4C, lane 2) and even more by ubiquitin and ΔNp63α co-transfection (Figure 4B lane 4 and Figure 4C lane 4) resulting very similar to that observed in ΔNp63α proficient A431 cells (Figure 4B, lane 5). Moreover, we observed a reduction of the YB-1 36 kDa forms in cells expressing ΔNp63α (Figure 4C, lanes 2 and 4).

MG132 addition to cells overexpressing ubiquitin and ΔNp63α, instead, stabilized full length YB-1 and reduced ubi-conjugated forms of YB-1, particularly those migrating between 50 and 70 kDa, again suggesting that they are generated following limited YB-1 cleavage (Figure 4C, compare lanes 3 and 4).

Next, we depleted SCC011 cells of endogenous ΔNp63α, to finally prove the effect of ΔNp63α on YB-1 protein modification. As shown in Figure 4D, we observed a significant reduction of full length and slow migrating YB-1 bands in the nuclear compartment. As expected, the p36/YB1 form became clearly detectable thus confirming our previous observations (Figure 4 D).

YB-1 and ΔNp63α dowregulation are associated to cell cycle exit

ΔNp63α is highly expressed in proliferating keratinocytes and decreases abruptly when cells undergo differentiation (24). As our results strongly indicate that ΔNp63α stabilizes YB-1 protein into the nucleus, we wondered whether we could establish a functional link between their cross-talk and the proliferation of keratinocytes.

To this aim, we examined Normal Human Epidermal (NHEK) and HaCaT keratinocytes for YB1 expression during Ca^{2+} induced differentiation. Keratinocytes were cultured in calcium-free medium, treated with Ca^{2+} for the indicated time points and subjected to immunoblot analysis. As differentiation proceeds, the level of YB-1 protein decreased suggesting that, similar to ΔNp63α, YB-1 must be downregulated to allow keratinocyte differentiation (Figures 5A and 5B). Then, as cell cycle exit is an integral part of keratinocyte differentiation, we induced growth arrest of HaCaT keratinocytes by confluency and serum starvation. HaCaT keratinocytes were grown to confluence and serum starved for 24 hours. Nuclear and cytoplasmic extracts were prepared and subjected to immunoblot to examine YB1 and ΔNp63α expression under normal and serum-starvation conditions. As shown in Figure 5C, both YB1 and ΔNp63α were downregulated under growth

178 arrest conditions as demonstrated by reduction of cyclin D1 expression and induction of the cell
179 cycle inhibitor p21WAF (Figure 5C). Finally, we have recently published that YB-1 silencing
180 causes apoptotic death of immortalized and transformed keratinocytes (21). All together our results
181 strongly indicate that YB-1 and ΔNp63α cooperation is essential for sustaining proliferation and
182 survival of basal keratinocytes.
183

Discussion

While not frequently mutated, p63, and in particular the ΔNp63α subclass, is commonly overexpressed in human squamous cell cancers, however, whether it actively plays a role in skin tumor formation or is a bystander is still unclear.

We have recently demonstrated that ΔNp63α physically interact with YB-1, a proliferation-dependent factor that is up-regulated in several forms of cancer (1). We have already shown that ΔNp63α contributes to YB-1 accumulation into the nucleus where YB-1 is known to play a major role in enhanced cell survival and drug resistance (11). Herein, we present data indicating that ΔNp63α is involved in the regulation of YB-1 protein turnover.

The mechanisms governing YB-1 protein stability are still undefined. Sorokin et al. (16) described that YB-1 is endoproteolitically processed by the 20S proteasome after the negatively charged glutamic acid residue E219. The released N-terminal protein fragment was found to accumulate in the nucleus after thrombin stimulation of endothelial cells (25) or following treatment of cells with DNA damaging drugs (3). Recently, van Roeyen et al. demonstrated that cell stress-dependent YB-1 cleavage is followed by the nuclear shuttling of the C-terminal domain of the protein (15). Intriguingly, using an antibody against the YB-1 epitope (aa 21-37), the authors were unable to detect the N-terminal fragment of YB-1 suggesting that it was either post-translationally modified, thus masking the epitope, or rapidly degraded (15). Moreover, it has also been reported that YB-1 is polyubiquitinated and degraded via the ubiquitin-proteasome pathway (23).

Our first observation was that YB-1 protein exhibits a quite reproducible pattern of high molecular forms, although there are notable variations among different cell lines. Immunoprecipitation with HA antibodies, specifically targeting HA-ubiquitin tagged proteins, revealed the presence of YB-1 thus indicating that the ubiquitin-proteasome pathway is involved in the control of YB-1 protein turnover. On the other hands, according to Sorokin (16), we found that YB-1 undergoes a proteasome-dependent limited cleavage. Interestingly, following treatment with MG132 that

inhibits the proteolytic activity of the proteasome, we found accumulation of full length YB-1 and reduction of YB-1 modified forms thus suggesting that many of them are generated following YB-1 limited cleavage.

The relevant outcome of our work is the demonstration that ΔNp63α expression protects full length YB-1 from specific endoproteolysis. Accordingly, ΔNp63α significantly increases the half-life of p50 YB-1 protein and reduces the level of the p36 YB-1 fragment. However, ΔNp63α enforced expression also causes an increase of poli-ubiquitinated YB-1. Historically, the function of poly-ubiquitination was to cause protein degradation in the 26 proteasome. However, we cannot exclude that addition of polyubiquitin chain to YB-1 can confer to the protein new functionalities such as the ability to interact with target proteins via ubiquitin binding domains or assemble into multimeric complexes (26).

In our system we have not yet identified a specific ubiquitin ligase/s involved YB-1 post-translational modification. However, the F-box Protein 33 (FBX33) (23) and the ring finger Retinoblastoma Binding Protein 6 (RBBP6) (27) are potential candidates as they have already demonstrated to specifically target YB-1.

In normal conditions, full length YB-1 exists simultaneously in the nucleus with the truncated form, although their relative amount can be modulated by several stimuli such as stress and/or DNA damage (3). However, the exact biological function of p36/YB-1 and p50/YB-1 is not fully understood. The nuclear accumulation of YB-1 is believed to impart pro-survival advantages to cells (7; 28; 29).

Concerning the physiological role of YB-1 and ΔNp63α association in keratinocytes, we can speculate that YB-1 expression in basal keratinocytes can be functionally critical for skin homeostasis. Although it needs to be confirmed in an *in vivo* system, our observations suggest that ΔNp63α may increase the proliferative potential of basal keratinocytes by preserving full lenght

YB-1 integrity into the nucleus. Remarkably, we have show that YB-1 level are higher in response to growth stimuli and rapidly downregulated on cell cycle arrest conditions such as serum deprivation and differentiative stimuli. A relevant issue is whether YB-1 expression can exert a selective control upon ΔNp63α transcriptional functions and what might the effect of mutant p63 on YB-1 functions. We are currently addressing these relevant questions.

Acknowledgements

We thank R.T. Hay for providing plasmids. The authors have no conflict of interest to declare.

This work was supported by Progetto "Campania Research in Experimental Medicine" (CREME), POR Campania FSE 2007-2013 to V. C. and Regione Campania L R N°5/2007 to G. L. M.

References

1. Di Costanzo A, Troiano A, di Martino O, Cacace A, Natale CF, Ventre M, Netti P, Caserta S, Pollice A, La Mantia G, Calabrò V. (2012) The p63 protein isoform ΔNp63α modulates Y-box binding protein 1 in its subcellular distribution and regulation of cell survival and motility genes. J Biol Chem. 287(36):30170-80.

2. Lasham A, Print CG, Woolley AG, Dunn SE, Braithwaite AW. (2013) YB-1: oncoprotein, prognostic marker and therapeutic target? Biochem J 449(1):11-23.

3. Kim ER, Selyutina AA, Buldakov IA, Evokimova V, Ovchinnikov LP, Sorokin AV. (2013) The proteolytic YB-1 fragment interacts with DNA repair machinery and enhances survival during DNA damaging stress. Cell Cycle 12(24): 3791-3803.

4. Yahata H, Kobayashi H, Kamura T, Amada S, Hirakawa T, Kohno K, Kuwano M, Nakano H. (2002) Increased nuclear localization of transcription factor YB-1 in acquired cisplatin-resistant ovarian cancer. J Cancer Res Clin Oncol. 128(11):621-6.

5. Fotovati A, Abu-Ali S, Wang PS, Deleyrolle LP, Lee C, Triscott J Chen JY, Franciosi S, Nakamura Y, Sugita Y, Uchiumi T, Kuwano M, Leavitt BR, Singh SK, Jury A, Jones C, Wakimoto H, Reynolds BA, Pallen CJ, Dunn SE. (2011) YB-1 bridges neural stem cells and brain tumor-initiating cells via its roles in differentiation and cell growth. Cancer Res. 71(16):5569-78.

6. Sinnberg T, Sauer B, Holm P, Spangler B, Kuphal S, Bosserhoff A, Schittek B. (2012) MAPK and PI3K/AKT mediated YB-1 activation promotes melanoma cell proliferation which is counteracted by an autoregulatory loop. Exp Dermatol. 21(4):265-70.

7. Shibahara K, Sugio K, Osaki T, Uchiumi T, Maehara Y, Kohno K Yasumoto K, Sugimachi K, Kuwano M. (2001) Nuclear expression of the Y-box binding protein, YB-1, as a novel marker of disease progression in non-small cell lung cancer. Clin Cancer Res. **7**(10):3151-5.

8. Jurchott K, Bergmann S, Stein U, Walther W, Janz M, Manni I, Piaggio G, Fietze E, Dietel M, Royer HD. (2003) YB1 as a cell cycle-regulated transcription factor facilitating cyclin A and cyclin B1 gene expression. J Biol Chem. 278: 27988-96.

9. Tsujimura S, Saito K, Nakayamada S, Nakano K, Tsukada J, Kohno K Tanaka Y. (2004) Transcriptional regulation of multidrug resistance-1 gene by interleukin-2 in lymphocytes. Genes Cells: 9(12):1265-73.

10. Ohga T, Koike K, Ono M, Makino Y, Itagaki Y, Tanimoto M, Kuwano, M, Kohno K. (1996) Role of the human Y box-binding protein YB-1 in cellular sensitivity to the DNA-damaging agents cisplatin, mitomycin C, and ultraviolet light. Cancer Res. 56(18):4224-8.

11. Stein U, Jurchott K, Walther W, Bergmann S, Schlag PM, Royer HD. (2001) Hyperthrmia-induced nuclear translocation of transcription factor YB-1 leads to enhanced expression of multidrug resistance-related ABC transporters. J. Biol. Chem. 276(30): 28562-9.

12. Comerford K M, Wallace T J, Karhausen J,Louis N A, Montalto M C, Colgan S P. (2002) Hypoxia-inducible Factor 1-dependent Regulation of the Multidrug Resistance (MDR1) Gene 1. Cancer Research 62, 3387-339

13. En-Nia A, Yilmaz E, Klinge U, Lovett DH, Stefanidis I, Mertens PR. (2005) Transcription factor YB-1 mediates DNA polymerase alpha gene expression. J Biol Chem. 280(9):7702-11.

14. Astanehe A, Finkbeiner MR, Hojabrpour P, To K, Fotovati A, Shadeo A, Stratford AL, Lam WL, Berquin IM, Duronio V, Dunn SE. (2009) The transcriptional induction of PIK3CA in tumor cells is dependent on the oncoprotein Y-box binding protein-1. Oncogene. 28(25):2406-18.

15. van Roeyen CR, Scurt FG, Brandt S, Kuhl VA, Martinkus S, Djudjaj S, Raffetseder U, Royer HD, Stefanidis I, Dunn SE, Dooley S, Weng H, Fischer T, Lindquist JA, Mertens PR. (2013) Cold shock Y-box protein-1 proteolysis autoregulates its transcriptional activities. Cell Commun Signal. 11(1):63-70.

16. Sorokin AV, Selyutina AA, Skabkin MA, Guryanov SG, Nazimov IV, Richard C, Th'ng J, Yau J, Sorensen PH, Ovchinnikov LP, Evdokimova V. (2005) Proteasome-mediated cleavage of Y-box-binding protein 1 is linked to DNA damage response. The EMBO Journal 24: 3602-3612.

17. Amoresano A, Di Costanzo A, Leo G, Di Cunto F, La Mantia G, Guerrini L, Calabrò V. (2010) Identification of ΔNp63α Protein Interactions by Mass Spectrometry. J. Proteome Res. 9: 2042-48.

18. Calabrò V, Mansueto G, Santoro R, Gentilella A, Pollice A, Ghioni P, Guerrini L, La Mantia G. (2004). Inhibition of p63 transcriptional activity by p14ARF: Functional and physical link between human ARF tumor suppressor and a member of the p53 family. M.C.B. 24:8529-8540.

19. Rossi M, De Simone M, Pollice A, Santoro R, La Mantia G, Guerrini L, Calabrò V. (2006) Itch/AIP4 associates with and promotes p63 protein degradation. Cell Cycle. 5(16):1816-22.

20. Yang A, Schweitzer R, Sun D, Kaghad M, Walker N, Bronson RT, Tabin C, Sharpe A, Caput D, Crum C, McKeon F. (1999) p63 is essential for regenerative proliferation in limb, craniofacial and epithelial development. Nature. 398: 714-718.

21. Troiano A, Schiano Lomoriello I., di Martino O., Fusco S., Pollice A., Vivo M., La Mantia G. and Calabrò V. (2015) Y-box binding protein-1 is part of a complex molecular network linking ΔNp63α to the PI3K/AKT pathway in cutaneous squamous cell carcinoma. DOI: 10.1002/jcp.24934.

22. Sepe M, Festa L, Tolino F, Bellucci L, Sisto L, Alfano D, Ragno P, Calabrò V, de Franciscis V, La Mantia G, Pollice A. (2011) A regulatory mechanism involving TBP-1/Tat-Binding Protein 1 and Akt/PKB in the control of cell proliferation. PLoS One. 6(10) e22800.

23. Lutz M, Wempe F, Bahr I, Zopf D, von Melchner H. (2006) Proteasomal degradation of the multifunctional regulator YB-1 is mediated by an F-Box protein induced during programmed cell death. FEBS Letters 580(16):3921-3930.

24. Barbieri CE, Tang LJ, Brown KA,Pietenpol JA. (2006) Loss of p63 leads to increased cell migration and up-regulation of genes involved in invasion and metastasis. Cancer Res. 66(15):7589-97.

25. Stenina OI, Shaneyfelt KM, DiCorleto PE. (2001) Thrombin induces the release of the Y-box protein dpbB from mRNA: A mechanism of transcriptional activation. Proc. Natl. Acad. Sci. USA 98(13): 7277-7282.

326 26. O'Neil LA. (2009) Regulation of Signaling by non-degradative ubiquitination. J.Biol. Chem.
327 284(13):8209.

328 27. Chibi M, Meyer M, Skepu A, G Rees DJ, Moolman-Smook JC, Pugh DJ. (2008) RBBP6
329 interacts with multifunctional protein YB-1 through its ring finger domain, leading to
330 ubiquitination and proteasomal degradation of YB-1. J. Mol. Biol. 384 (4):908-916.

331 28. Gessner C, Woischwill C, Schumacher A, Liebers U, Kuhn H, Stiehl P, Jurchott K, Royer
332 HD, Witt C, Wolff G. (2004) Nuclear YB-1 expression as a negative prognostic marker in
333 nonsmall cell lung cancer. Eur. Respir. J. 23(1): 14-9.

334 29. Huang J., Tan PH, Li KB, Matsumoto K, Tsujimoto M, Bay BH. (2005) Y-box binding
335 protein, YB-1, as a marker of tumor aggressiveness and response to adjuvant chemotherapy
336 in breast cancer. Int. J. Oncol. 26(3): 607-13.

337

Figure Legends

Figure 1. ΔNp63α reduces YB-1 protein turnover. (**A**) A representative immunoblot analysis of YB-1 protein level in MDA-MB231 cells treated with 10 μg/ml cycloheximide (CHX), for the indicated times. Cells were seeded at 60% confluency in 100-mm dishes. 24 hours after, cells were transfected with an empty vector or a ΔNp63α expressing plasmid. Equal amounts of proteins were subjected to immunoblot analysis with YB-1 or p63 antibodies. Actin was used as loading control. **(B)** Protein half-life was expressed in the plot as the fraction of the initial protein. Data are presented as the mean value obtained from three independent experiments. YB-1 bands (50 kDa) were quantified by densitometric scanning and Quantity-ONE software.

Figure 2. ΔNp63α influences YB-1 stability and specific proteolysis

(A) Immunoblotting (upper panel) and densitometric analysis (lower panel) of MDA-MB231 cells transiently transfected with increasing amounts of ΔNp63α expression plasmid (0.5, 1.0, 1.5, 2.0 μg). Whole extracts were analysed with YB-1 and p63 antibodies. Glyceraldehyde 3-phosphate dehydrogenase (GAPDH) was used as loading control. (**B**) Immunoblot analysis of YB-1 in HaCaT, A431 and SCC011 cells with YB-1 antibody (ab12148, Abcam). The 50 kDa band corresponding to unmodified YB-1 protein is indicated by arrow. Actin was used as loading control. (**C**) Immunoblot analysis of YB-1 in YB-1 depleted A431 cells 48 hours after silencing. YB-1 protein was detected using the YB-1 antibody. Actin was used as loading control.

Figure 3. Posttranslationally modified YB-1 accumulates within the nucleus

(A) Immunoblot analysis of MDA-MB231, A431 and SCC011 cytoplasmic **(**Cy**)** and nuclear **(**Nu**)** fractions. YB-1 and p63 were detected with ab12148 (Abcam) and D9 (Santa Cruz Biotechnology) antibodies, respectively. The filters were blotted with antibodies against PARP and total AKT to check for cross-contamination between the fractions. (Note the presence of YB-1 36 kDa band exclusively in the nuclear compartment). (**B**) Immunoblot analysis of HaCaT cytoplasmic **(**Cy**)** and nuclear **(**Nu**)** fractions after 5 hrs of MG132 treatment (5μM final concentration). YB-1 was detected with ab12148 (Abcam). Note the decrease of slow and fast migrating YB-1 forms following MG132 treatment into the nucleus and the accumulation of full length YB-1 50 kDa. The filters were blotted with antibodies against PARP and actin to check for cross-contamination between the fractions.

Figure 4. YB-1 is ubiquitinated

(**A**) A431 cells were transiently transfected with Ubi-HA expression plasmids. After 24 hrs**,** extracts were immunoprecipitated (**IP**) with anti-HA antibody and the immunocomplexes were subjected to immunoblot (**IB**) with YB-1 or p63 antibodies, as indicated. (**B**) MDA-MB231 cells were transiently transfected with an empty vector (mock), a ΔNp63α and/or Ubi-HA plasmid, as indicated. Whole cell extracts were analysed by immunoblotting with YB-1 and p63 antibodies. Actin was used as loading control. A431 are p63 proficient cells. (**C**) MDA-MB231 cells were transiently transfected with Ubiquitin and/or ΔNp63α expression plasmid. Cells were treated with MG132, as indicated. Whole extracts were analysed by immunoblotting with YB-1 and p63 antibodies. Actin was used as loading control. (**D**) SCC011 cells were silenced with IBONI p63-siRNA pool or scrambled oligos. 48 h after silencing, cells were fractionated to obtain cytoplasmic (**Cy**) and nuclear (**Nu**) fractions. Filters were incubated with YB-1 and p63 antibodies. To check for

cross-contamination, PARP and total AKT were used as nuclear and cytoplasmic control, respectively.

Figure 5. YB-1 sustains the proliferative activity of keratinocytes

(A) NHEK were induced to differentiate, for the indicated days, in 1.5 mM Ca^{2+}. Whole cell extracts were analyzed by immunoblotting using antibodies against p63, YB-1, Cytokeratin 1 (CK1). Actin was used as loading control. (**B**) HaCaT cells were induced to differentiate for the indicated days with 2.0 mM calcium. Cell extracts were analyzed by immunoblotting with p63, YB-1 and CK1 antibodies, as indicated. Undifferentiated HaCaT, grown in absence of calcium, were used as negative control. GAPDH was used as loading control. (**C**) HaCaT keratinocytes were cultured in DMEM medium with (+ FBS) or without FBS (- FBS), as indicated. After 48 hours, cells were harvested. Nuclear (Nu) and cytoplasmic (Cy) extracts were subjected to immunoblot using p63, YB-1, P21WAF, Cyclin D1 antibodies. GAPDH and PARP antibodies were used as loading controls and to check for cross-contamination between the fractions.

Figure

Click here to download Figure: di Martino 2015.ppt

Figure 1

A

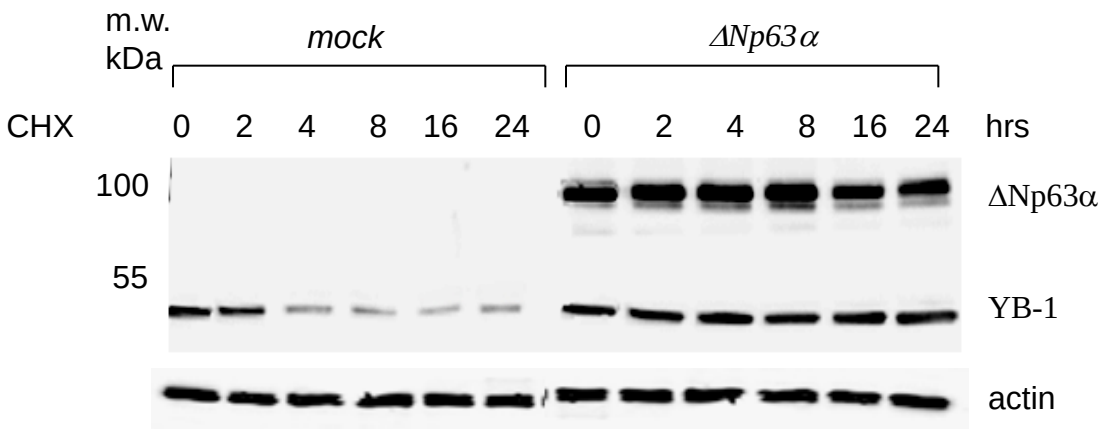

MDA-MB231

B

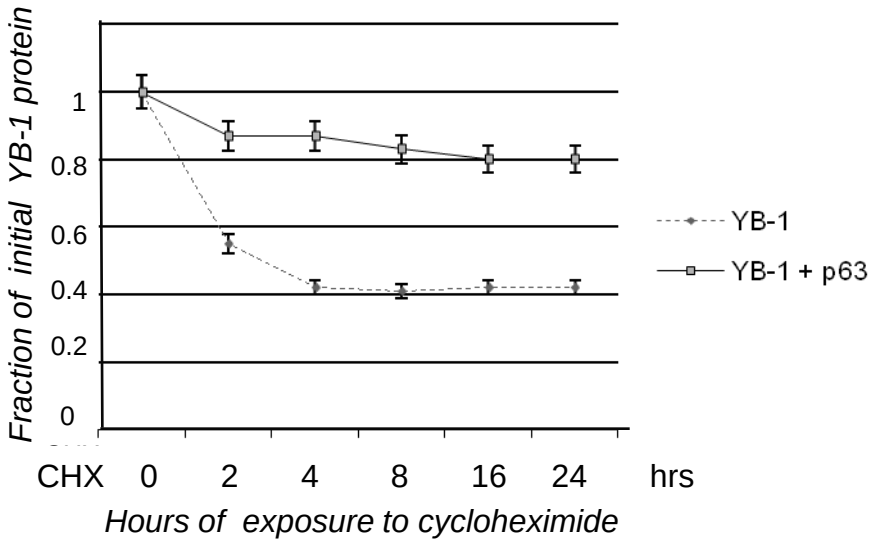

Figure 2

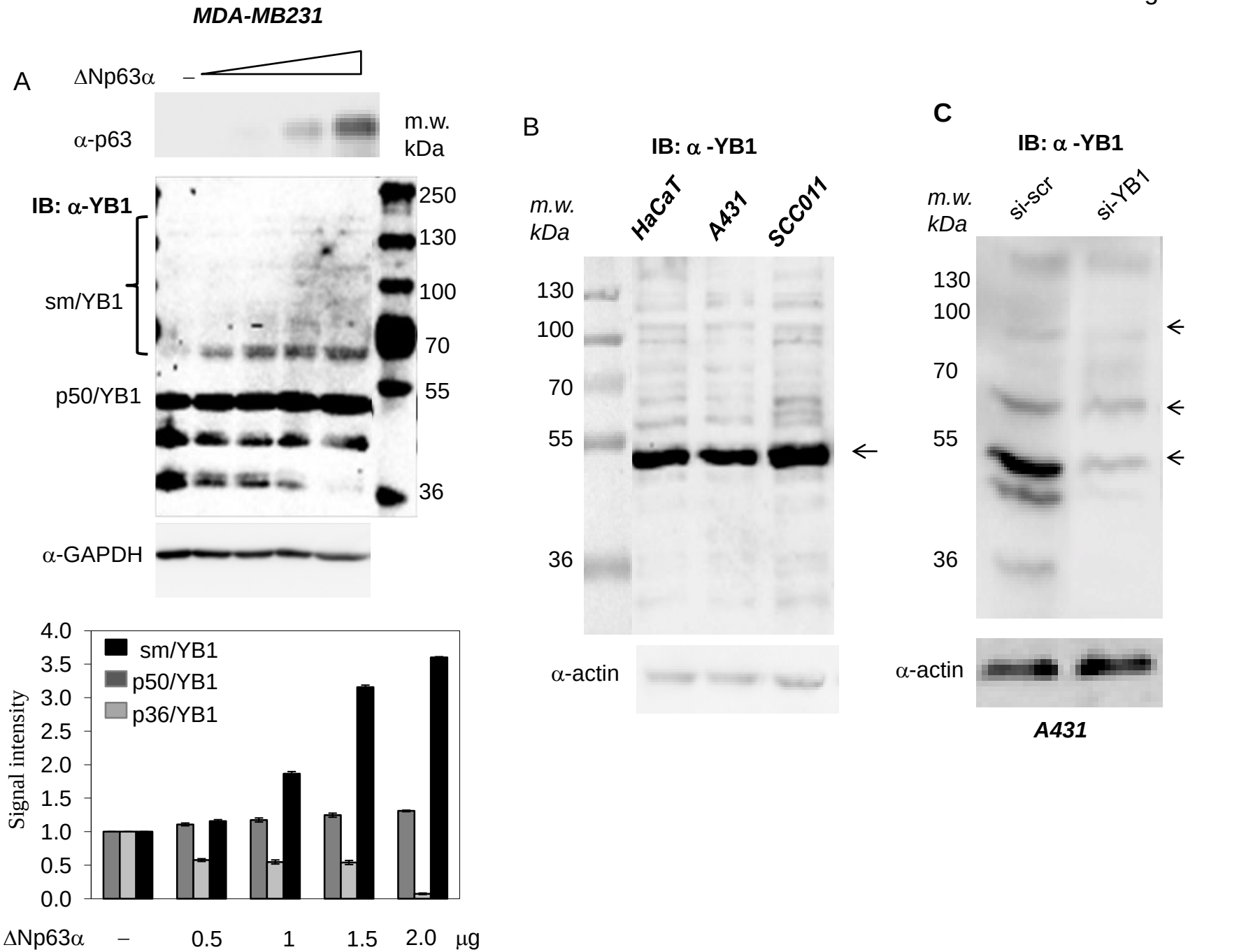
MDA-MB231
A
ΔNp63α
–
α-p63
m.w.
kDa
IB: α-YB1
sm/YB1
p50/YB1
250
130
100
70
55
36
α-GAPDH
4.0
3.5
3.0
2.5
2.0
1.5
1.0
0.5
0.0
Signal intensity
sm/YB1
p50/YB1
p36/YB1
ΔNp63α
–
0.5
1
1.5
2.0
μg
B
IB: α -YB1
m.w.
kDa
HaCaT
A431
SCC011
130
100
70
55
36
α-actin
C
IB: α -YB1
m.w.
kDa
si-Scr
si-YB1
130
100
70
55
36
α-actin
A431

Figure 3

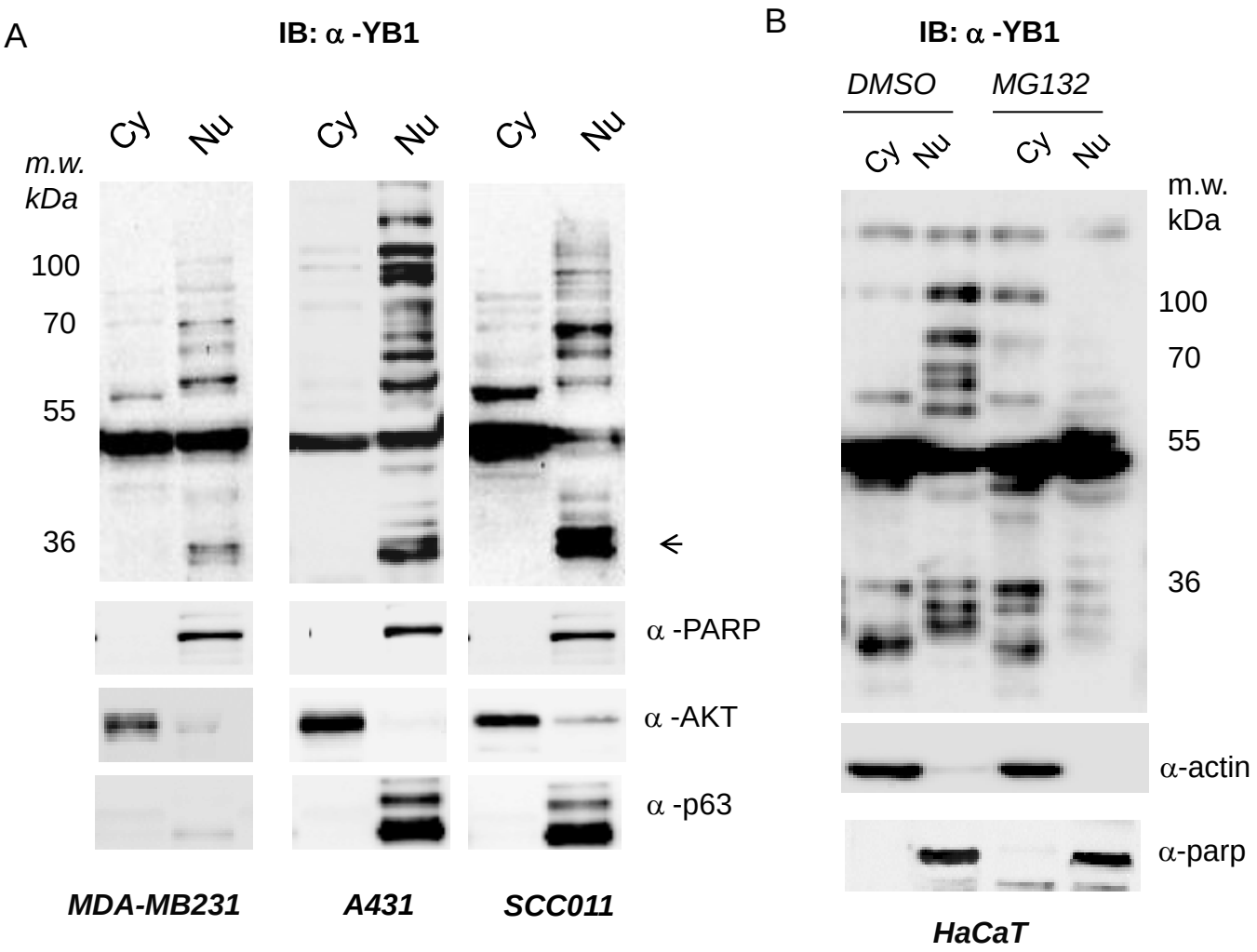
A
IB: α -YB1
Cy
Nu
m.w.
kDa
100
70
55
36
α -PARP
α -AKT
α -p63
MDA-MB231
A431
SCC011
B
IB: α -YB1
DMSO
MG132
α-actin
α-parp
HaCaT

Figure 4

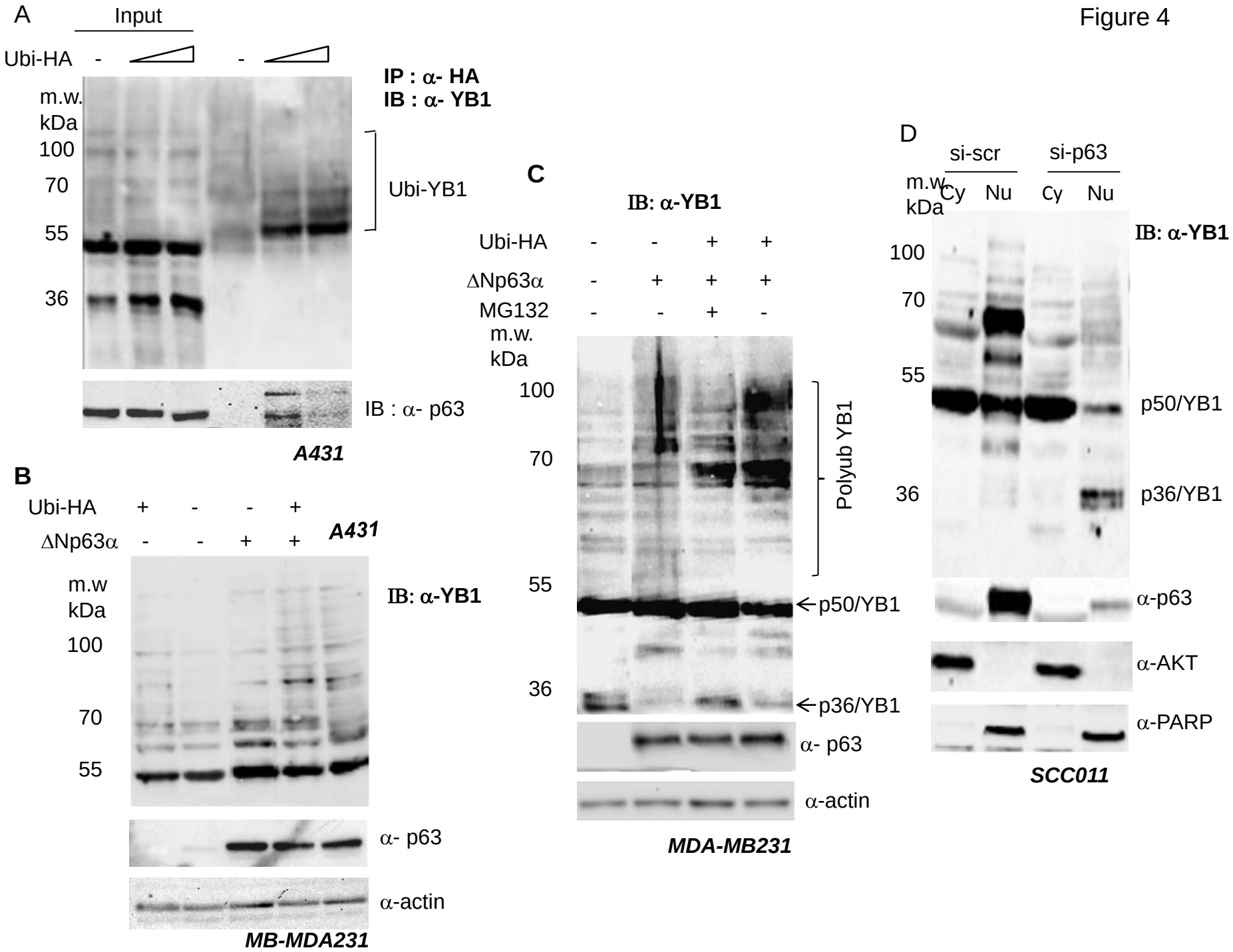
A
Input
Ubi-HA
IP : α- HA
IB : α- YB1
m.w.
kDa
100
70
55
36
Ubi-YB1
IB : α- p63
A431
B
Ubi-HA
ΔNp63α
A431
m.w
kDa
100
70
55
IB: α-YB1
α- p63
α-actin
MB-MDA231
C
IB: α-YB1
Ubi-HA
ΔNp63α
MG132
m.w.
kDa
100
70
55
36
Polyub YB1
p50/YB1
p36/YB1
α- p63
α-actin
MDA-MB231
D
si-scr
si-p63
m.w.
kDa
Cy
Nu
Cy
Nu
IB: α-YB1
100
70
55
36
p50/YB1
p36/YB1
α-p63
α-AKT
α-PARP
SCC011

Figure 5

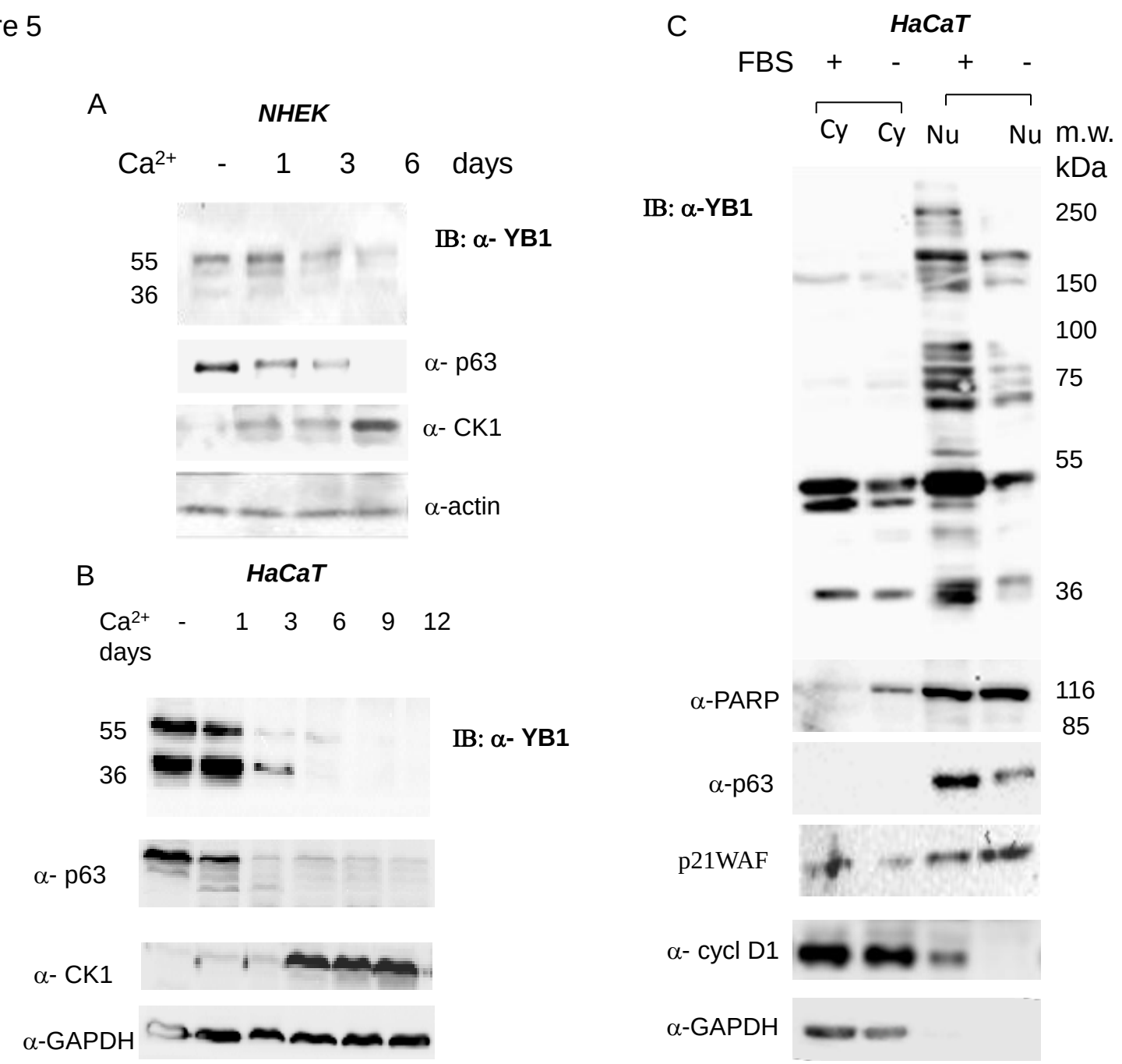
A
NHEK
Ca2+ - 1 3 6 days
55
36
IB: α- YB1
α- p63
α- CK1
α-actin
B
HaCaT
Ca2+ - 1 3 6 9 12
days
55
36
IB: α- YB1
α- p63
α- CK1
α-GAPDH
C
HaCaT
FBS + - + -
Cy Cy Nu Nu
m.w.
kDa
IB: α-YB1
250
150
100
75
55
36
α-PARP
116
85
α-p63
p21WAF
α- cycl D1
α-GAPDH

Original Research Article

Y-Box binding protein-1 is part of a complex molecular network linking ΔNp63α to the PI3K/AKT pathway in cutaneous squamous cell carcinoma[†]

Annaelena Troiano, Irene Schiano Lomoriello, Orsola di Martino, Sabato Fusco§, Alessandra Pollice, Maria Vivo, Girolama La Mantia, Viola Calabrò*

Department of Biology, University of Naples "Federico II", 80128 Naples, Italy

§Center for Advanced Biomaterials for Health Care@CRIB, Istituto Italiano di Tecnologia, Naples, Italy.

Running Title: YB-1, ΔNp63α and the PI3K pathway cross-talk

Keywords: **p53 protein family, Y-box binding protein, PI3K/AKT/PTEN, cell proliferation, squamous carcinoma, skin cancer**.

This work was supported by Progetto "Campania Research in Experimental Medicine" (CREME), POR Campania FSE 2007-2013 to V. C. and Regione Campania L R N°5/2007 to G. L. M.

Corresponding author: Prof. Viola Calabrò, PhD. Dipartimento di Biologia, Università di Napoli, "Federico II", Viale Cinzia, Monte S Angelo, 80126 Napoli, Italy. Phone: +39 081 679069. Fax +39 081 679033. E-mail: vcalabro@unina.it

Additional Supporting Information may be found in the online version of this article.

Received 28 October 2014; Revised 19 December 2014; Accepted 16 January 2015
Journal of Cellular Physiology

DOI 10.1002/jcp.24934

Abstract

Cutaneous squamous cell carcinomas (SCCs) typically lack somatic oncogene-activating mutations and most of them contain p53 mutations. However, the presence of p53 mutations in skin premalignant lesions suggests that these represent early events during tumor progression and additional alterations may be required for SCC development. SCC cells frequently express high levels of ΔNp63α and Y-box binding 1 (YB-1 or YBX1) oncoproteins. Here, we show that knockdown of YB-1 in spontaneously immortalized HaCaT and non-metastatic SCC011 cells led to a dramatic decrease of ΔNp63α, cell detachment and death. In highly metastatic SCC022 cells, instead, YB-1 silencing induces PI3K/AKT signaling hyperactivation which counteracts the effect of YB-1 depletion and promotes cell survival. In summary, our results unveil a functional cross-talk between YB-1, ΔNp63α and the PI3K/AKT pathway critically governing survival of squamous carcinoma cells.

This article is protected by copyright. All rights reserved

Introduction

Squamous cell carcinoma (SCC) is a treatment-refractory malignancy arising within the epithelium of different organs, that is frequently associated with overexpression of ΔNp63α oncoprotein (Rocco et al., 2006, Hibi et al., 2000). ΔNp63α is encoded by the TP63 locus, the ancestral gene of the p53 gene family that gives rise to multiple isoforms that can be placed in two categories: TA isoforms with an acidic transactivation domain and ΔN isoforms that lack this domain. Alternative splicing at the carboxy-terminal (C-terminal) generates at least three p63 variants (α, β and γ) in each class (Rossi et al., 2006, Yang et al., 1999). ΔNp63α is essential for the maintenance of the proliferative capacity of epithelial cell progenitors (Senoo et al., 2004); as these cells start to differentiate, ΔNp63α protein level gradually drops and those that no longer express ΔNp63α, loose the proliferative capacity (Koster, 2010).

In squamous carcinoma, ΔNp63α up-regulation causes skin hyperplasia and abnormal keratinocyte differentiation predisposing to malignant transformation (Hibi et al., 2000; Moll and Slade, 2004). Despite its undisputed relevance in epithelial cancer, the mechanisms through which ΔNp63α executes its pro-oncogenic functions are not fully understood. However, ΔNp63α expression was shown to be induced by activation of downstream targets of EGFR activation including STAT3 (Ripamonti et al., 2013) and the phosphoinositide-3-kinase (PI3K) pathway (Barbieri et al., 2003).

We have recently shown that ΔNp63α interacts with the YB-1 oncoprotein and promotes accumulation of YB-1 into the nuclear compartment (Di Costanzo et al., 2012; Amoresano et al., 2010). YB-1, also named YBX1, is a member of the cold shock domain (CSD) protein family, which is found in the cytoplasm and nucleus of mammalian cells, being able to shuttle between the two compartments (Eliseeva et al., 2011). The YB-1 gene, located on chromosome 1p34 (Toh et al., 1998), encodes a 43 kDa protein having three functional domains: a variable NH2-terminal Alanine/Proline rich tail domain (aa 1-51), involved in transcriptional regulation, a highly conserved nucleic acid binding domain (CSD, aa 51-171), and a COOH-terminal tail (B/A repeat) for RNA/ssDNA binding and protein dimerization (129-324).

YB-1 is a major downstream target of Twist (Shiota et al., 2008) and c-Myc-Max complexes by recruitment to the E-box consensus sites in YB-1 promoter (Uramoto et al., 2002). YB-1 regulates genes promoting cancer cell growth such as EGFR, Her-2, PI3KCA and MET (To et al., 2010) as well as genes linked to cancer stem cells such as those encoding the hyaluronan receptor CD44, CD49f (integrin α6) and CD104 (β4 integrin), implying that YB-1 plays a key role as oncogene by transactivating genes associated with a cancer stem cell phenotype (To et al., 2010). YB-1 protein level drastically increases during progression of several types of tumors including squamous carcinoma, thereby suggesting a role for this protein in the pathogenesis of human epithelial malignancy (Di Costanzo et al., 2012, Kolk et al., 2011).

To mediate gene regulation, YB-1 translocates into the nucleus and interacts with the proximal promoter regions of its target genes (Sutherland et al., 2005; Shiota et al., 2011). Phosphorylation of serine 102 in response to MAPK and PI3K/AKT signaling promotes YB-1 nuclear translocation (Sinnberg et al., 2012). Moreover, YB-1 translocates to the nucleus when cells are exposed to cytokines, anticancer agents, hyperthermia, or UV light irradiation (Schittek et al., 2007).

Herein, we present data showing the existence of a functional cross-talk between YB-1, ΔNp63α and the PI3K/AKT signaling pathway critically governing survival of squamous carcinoma cells.

MATERIALS AND METHODS

Plasmids

The 1.1 Kb EGFR promoter luciferase plasmid was provided by Dr. A.C. Johnson (US National Cancer Institute, Massachusetts, USA). The cDNA encoding human ΔNp63α and ΔNp63α F518L were previously described (Lo Iacono et al., 2006).

Cell lines, transfection and antibodies

SCC011 and SCC022 cell lines were established from cutaneous squamous carcinomas (Lefort et al., 2007). SCC011 and SCC022 cells were cultured in RPMI supplemented with 10% fetal bovine serum at 37°C and 5% CO_2. HaCaT and MDA-MB231 cells were purchased from Cell Line Service (CLS, Germany) and cultured at 37°C and 5% CO_2. HaCaT cells were maintained in DMEM supplemented with 10% FBS. MDA-MB231 cells were maintained in DMEM supplemented with 5% FBS.

Transient transfection

Lipofections were performed with Lipofectammine 2000 (Life Technologies, CA, USA), according to the manufacturer's recommendations.

YB1 transient silencing was carried out with IBONI YB-1siRNA pool (RIBOXX GmbH, Germany) and RNAiMAX reagent (Life Technologies, CA, USA), according to the manufacturer's recommendations. Briefly, cells were seeded at 60% confluence (1.5×10^6) in 100-mm dishes and transiently silenced with IBONI YB1-siRNA at 20 nM final concentration.

YB-1 guide sequences:

UUUAUCUUCUUCAUUGCCGCCCCC;

UUAUUCUUCUUAUGGCAGCCCCC;

UUCAACAACAUCAAACUCCCCC;

UCAUAUUUCUUCUUGUUGGCCCCC.

ΔNp63α transient silencing was carried out with IBONI p63-siRNA pool (RIBOXX GmbH, Germany) at 20 nM final concentration and RNAiMAX reagent (Life Technologies, CA, USA).

p63 guide sequences:

UUAAACAAUACUCAAUGCCCCC;

UUAACAUUCAAUAUCCCACCCCC;

AUCAAUAACACGCUCACCCCC;

AUGAUUCCUAUUUACCCUGCCCCC.

"All Star Negative Control siRNA", provided by Quiagen (Hilden, Germany), was used as negative control.

Transfection efficiency of siRNA was quantified using BLOCK-iT™ Control Fluorescent Oligo (Life Technologies, CA, USA) at a final concentration of 20 nM using Lipofectamine RNAiMAX (Life Technologies, CA, USA). Cells were stained with Hoechst and transfected cells detected by direct immunofluorescence. Transfection efficiency ranged between 70 and 80% .The percentage of transfected cells was estimated as the average of counts performed on 100 cells in five independent fields.

Immunoblot analyses and coimmunoprecipitation

Immunoblots (IB) were performed as previously described (Di Costanzo et al., 2012). Briefly, 30 μg of whole cell extracts were separated by SDS-PAGE, subjected to immunoblot and incubated overnight at 4°C with antibodies.

For nuclear-cytoplasmic fractionation 10 μg of nuclear and 30 μg of cytoplasmic extracts (1:3 rate) were separated by SDS-PAGE and subjected to immunoblot.

All images were acquired with CHEMIDOC (Bio Rad, USA) and analyzed with the Quantity-ONE software.

Coimmunoprecipitation was performed as previously described (Rossi et al., 2006). Briefly, whole HaCaT cell extracts, precleared with 30 μl of protein A-agarose (50% slurry; Roche, Manheim,

Germany), were incubated overnight at 4°C with anti-p63 (2 μg) or α-mouse IgG. The reciprocal experiment was performed with anti-YB-1(3 μg) or α-rabbit IgG (3 μg).

Antibodies and chemical reagents

Anti-p63 (4A4), anti-cytokeratin 1 (4D12B3), anti-GAPDH (6C5), and anti-actin (1-19) were purchased from Santa Cruz (Biotechnology Inc. CA, USA). PARP, PTEN, AKT, pAKT ^{S473}, EGFR and STAT3 antibodies were from Cell Signaling Technology (Beverly, Massachusetts). Rabbit polyclonal YB1 (Ab12148) antibody was purchased from Abcam (Cambridge, UK). Proteasome inhibitor MG132 were purchased from Sigma-Aldrich (St Louis, MO) and used at 10 μM final concentration in DMSO (Sigma-Aldrich, St Louis, MO). LY294002 was purchased from Calbiochem (CA, USA) and used at 50 μM final concentration in DMSO.

Cell Viability assay

Cell viability was determined by the MTT 3-(4,5-dimethylthiazol-2-yl)-2,5-diphenyl tetrazolium bromide assay (Sigma-Aldrich, St Louis, MO). Briefly, cells were seeded in 96-well plates at 2 x 10^3 and transfected with scrambled or YB-1 siRNA oligos, 48h after silencing MTT solution (5mg/ml in PBS, 20 μl/well) was added to cells to produce formazan crystals. MTT solution was substituted by 150 μl DMSO 30 minutes later to solubilize the formazan crystals. The optical absorbance was determined at 570 nm using an iMark microplate reader (Bio-Rad, USA). The experiments were carried out in triplicate for each knockdown and compared to scrambled control (value set at 1.0).

Quantitative Real Time-PCR

For PCR analysis total RNA was isolated using the RNA Extraction Kit from Qiagen (Hilden, Germany) according to the manufacturer's instructions. RNA (2-5μg) was treated with DNAse I (Promega, Madison USA) and used to generate reverse transcribed cDNA using SuperScript III

(Life Technologies, CA, USA), according to the manufacturer's instructions. All samples in each experiment were reverse transcribed at the same time, the resulting cDNA diluted 1:5 in nuclease-free water and stored in aliquots at –80°C until used.

Real Time PCR with SYBR green detection was performed with a 7500 RT-PCR Thermo Cycler (Applied Biosystem, Foster City, USA). The thermal cycling conditions were composed of 50ºC for 2 min followed by an initial denaturation step at 95ºC for 10 min, 45 cycles at 95ºC for 30s, 60ºC for 30s and 72ºC for 30s. Experiments were carried out in triplicate. The relative quantification in gene expression was determined using the $2^{-\Delta\Delta Ct}$ method (Livak and Schmittgen, 2011). Using this method, we obtained the fold changes in gene expression normalized to an internal control gene and relative to one control sample (calibrator). 18S was used as an internal control to normalize all data and the siCtrl was chosen as the calibrator.

Appropriate no-RT and non-template controls were included in each 96-well PCR reaction and dissociation analysis was performed at the end of each run to confirm the specificity of the reaction.

YB1(F):5'CGCAGTGTAGGAGATGGAGAG

YB1(R):5'GAACACCACCAGGACCTGTAA

ΔNp63 (F):5'GGTTGGCAAAATCCTGGAG

ΔNp63 (R):5'GGTTCGTGTACTGTGGCTCA

EGFR (F) :5'TTCCTCCCAGTGCCTGAA

EGFR (R):5'GGGTTCAGAGGCTGATTGTG

STAT3 (F) :5'CCTCTGCCGGAGAAACAG

STAT3 (R):5'CTGTCACTGTAGAGCTGATGGAG

GADD45A (F): 5' TTTGCAATATGACTTTGGAGGA

GADD45A (R): 5' CATCCCCCACCTTATCCAT

18S (F):5'TCGAGGCCCTGTAATTGGAA

18S (R):5'CTTTAATATACGCTATTGGAGCTG

Luciferase reporter assay

MDA-MB231 cells were co-transfected with ΔNp63α, ΔNp63α F518L and EGFR promoter-luciferase reporter vector. Transfections were performed in triplicate in each assay. At 24h after transfection, cells were harvested in 1x PLB buffer (Promega, Madison, USA) and luciferase activity was measured using Dual Luciferase Reporter system (Promega, Madison, USA) using pRL-TK activity as internal control. FireFly-derived luciferase activity was normalized for transfection efficiency. Successful transfection of p63 was confirmed by immunoblotting. The average values of the tested constructs were normalized to the activity of the empty construct.

Immunofluorescence and bright -field images acquisition

HaCaT cells (2.5 x 10^5) were plated in 35 mm dish, grown on micro cover glasses (BDH). At 24 hours after seeding, cells were washed with cold phosphate-buffered saline (PBS) and fixed with 4% paraformaldehyde (PFA) (Sigma-Aldrich, St. Louis, MO) for 15 min at 4°C. Cells were permeabilized with ice-cold 0.1% Triton X-100 for 10 min, washed with PBS and incubated with Thermo Scientific Hoechst 33342 (2'-[4-ethoxyphenyl]-5-[4-methyl-1-piperazinyl]-2,5'-bi-1H-benzimidazole trihydrochloride trihydrate) for 3 min. Images were digitally acquired at 470 nm using Nikon TE Eclipse 2000 microscope and processed using Adobe Photoshop software CS.

SCC022 cells (2.5 x 10^5) were plated in 35 mm dish and grown on micro cover glasses (BDH). At 24 hours after seeding, cells were transfected with scramble , YB-1 or p63 siRNA oligos. 48 hrs after silencing cells were washed with cold phosphate-buffered saline (PBS) and fixed with 4% paraformaldehyde (PFA) (Sigma-Aldrich, St. Louis, MO) for 15 min at 4°C. Cells were permeabilized with ice-cold 0.1% Triton X-100 for 10 min and then washed with PBS. P63 was detected using a 1:200 dilution of the monoclonal antibody D9 (Santa Cruz, Biotechnology Inc., CA, USA). YB-1 was detected using 1:100 dilution of the YB1 antibody (Ab12148). After extensive washing in PBS, the samples were incubated with Cy3-conjugated anti-mouse (red) and Cy5-conjugated anti-rabbit IgGs (green) at room temperature for 30 min. Cells were incubated with

Hoechst 33342 (2'-[4-ethoxyphenyl]-5-[4-methyl-1-piperazinyl]-2,5'-bi-1H-benzimidazole trihydrochloride trihydrate) (Thermo Scientific) for 3 min. Images were digitally acquired and processed using Adobe Photoshop software CS.

Cell motility assay

SCC022 cells were cultured on 35-mm dishes (Corning, NY) at $2x10^4$ cells/dish density. ΔNp63α or YB1 transient silencing were performed as described above. After 24 h from silencing cell migration tests were performed via an Olympus IX81 inverted microscope equipped with a 10X objective and an integrated stage incubator (Okolab, Italy). Images of selected positions of the cell culture were collected in bright field for 16 h with 5-min frame intervals. All of the collected data were processed with the Olympus imaging software Cell^R. To quantify the cell speed (μm/min), time-lapse acquisitions were processed by the dedicated software add-in (TrackIT). The average speed per cell was calculated from the length of the path divided by time. An average number of 60 cells were analyzed for each condition.

Results

YB-1 knockdown in HaCaT cells

We have previously shown that ΔNp63α interacts with YB-1 in human squamous carcinoma cells and promotes accumulation of full length YB-1 protein (50 kDa) in the nuclear compartment (Di Costanzo et al., 2012). We first validated the interaction between YB-1 and ΔNp63α in non transformed HaCaT keratinocytes by co-immunoprecipitation assay (Supplementary Fig. 1). Then, we examined the effect of YB-1 silencing in mitotically active HaCaT keratinocytes. Interestingly, at 48 hrs of silencing we observed massive cell detachment (Figure 1A, upper panel) associated with a high proportion of condensed and fragmented nuclei (Figure 1A, lower panel). Western blot analysis showed a significant reduction of ΔNp63α protein level and PARP1 proteolytic cleavage (Figure 1B, left panel) indicating that YB-1 is critical for keratinocyte survival.

ΔNp63α is known to sustain survival in squamous cell carcinoma (Rocco et al., 2006, Hibi et al., 2000) and up-regulate cell adhesion-associated genes (Carrol et al., 2006). To rule out the possibility that YB-1 silencing induces cell death by merely reducing the level of ΔNp63α, we knocked down ΔNp63α expression in HaCaT cells by RNA interference. According to previous studies (Barbieri et al., 2006), we observed neither cell detachment (Figure 1A, upper panel) nor PARP1 activation (Figure 1B, right panel) clearly indicating that apoptosis, induced by YB-1 depletion, cannot be simply ascribed to the lack of ΔNp63α.

Next, we evaluated the level of ΔNp63α-specific transcript following YB-1 knockdown by Real Time quantitative PCR (RT-qPCR) and we found that it was drastically reduced (Figure 1C). After p63 silencing, instead, YB-1 transcript level was slightly enhanced (Figure 1D) while the mRNA of GADD45A, a gene induced by stressful conditions and used as control, was enhanced in both experiments (Figure 1C and D).

YB-1 knockdown in squamous carcinoma cells

Next, we used RNA interference to explore the function of YB-1 in squamous cell carcinoma (SCC). SCC011 and SCC022 are cell lines derived from cutaneous squamous carcinomas (Lefort et al., 2007). SCC022 are highly metastatic and, when subcutaneously injected in nude mice, form large tumors. SCC011 cells, instead, generate only keratin pearls (C. Missero, personal communication).

Similarly to what observed in HaCaT cells, YB1-depleted SCC011 cells detached from the plate generating abundant cellular debris (Figure 2A, upper panel) and exhibited a reduced level of ΔNp63α protein (Figure 2B). PARP1 cleavage was barely detectable (Figure 2B). On the other hand, we have previously demonstrated that p63 knockdown has no apparent effect on SCC011 cell viability (Di Costanzo et al., 2012).

Surprisingly, SCC022 cells looked healthy and tightly adherent to the plate after YB1 silencing (Figure 2A, lower panel). Moreover, as detected by immunoblot analysis, the expression level of ΔNp63α protein was significantly increased (Figure 2B). Interestingly, ΔNp63α transcript in SCC011 was reduced while in SCC022 it was 2.1-fold higher than control (Figure 2C).

Analysis of cell viability by the MTT assay showed that after 48 hrs of YB-1 knockdown the percentage of viability of SCC022 cells was 70% of the control, while it was reduced to 10% in HaCaT and SCC011 cells (Figure 4C).

We have also performed p63 knockdown in SCC022 cells and, as expected, we observed accumulation of YB-1 in the cytoplasm without any apparent effect on cell viability (Supplementary Fig. 2).

We also determined the influence of ΔNp63α or YB-1 silencing on SCC022 cell motility by time-lapse microscopy using siRNA-based silencing of endogenous proteins. According to our previous observations made on SCC011 cells (Di Costanzo et al., 2012) ΔNp63α silenced cells display higher speeds ($p < 0.01$) than control cells. Conversely, SCC022 cell motility was unaffected by YB-1 depletion (Supplementary Fig. 3).

YB-1 silencing hyper-activates the PI3K/AKT signaling pathway in SCC022 cells

ΔNp63α is a target of the phosphoinositide-3-kinase (PI3K) pathway downstream of the Epidermal Growth Factor Receptor (Barbieri et al., 2003). We hypothesized an involvement of the PI3K/AKT pathway in the upregulation of ΔNp63α observed in SCC022 cells following YB-1 silencing, and we looked for changes in the phosphorylation status of $AKT_{Ser473.}$ Interestingly, unlike HaCaT and SCC011, SCC022 cells exhibited constitutive phosphorylation of AKT_{Ser473} which was reproducibly potentiated following YB-1 depletion (Figure 3A and B) suggesting that YB-1 expression restrains AKT activation. To corroborate this result, we treated YB1-silenced SCC022 cells with Ly294002, a highly selective PI3K inhibitor. Remarkably, Ly294002 treatment counteracted AKT hyperphosphorylation and the increase of ΔNp63α protein level in response to YB-1 silencing (Figure 3B). Moreover, it resulted in cell death and detachment (data not shown). Importantly, Ly294002 treatment alone had no apparent effect on ΔNp63α level and SCC022 cell viability (Figure 3B and data not shown). Quantification of ΔNp63α transcript in YB-1 depleted SCC022 cells, treated or not with LY294002, showed that the increase of ΔNp63α transcription was strictly dependent on the PI3K/AKT pathway (Figure 3B). Moreover, inhibition of the proteasome activity with MG132 did not significantly enhance ΔNp63α protein level in YB1-silenced SCC022 cells, thereby confirming that ΔNp63α up-regulation was almost exclusively at transcriptional level (Supplementary Fig. 4).

The PI3K/AKT signaling pathway is negatively regulated by the phosphatase and tensin homologue PTEN (Song et al., 2012). To further investigate on the ability of SCC022 cells to escape from death following YB-1 depletion, we compared the protein level of PTEN among HaCaT, SCC011 and SCC022 cell lines. Compared to HaCaT and SCC011 cells, the level of PTEN protein in SCC022 cells was very low, accounting for their high basal level of AKT_{Ser473} phosphorylation (Figure 3E). Furthermore, YB-1 silencing resulted in increased levels of cytoplasmic PTEN in

HaCaT and SCC011 cells, while no effects on PTEN protein level was observed in YB-1 silenced SCC022 cells (Figure 3E).

Cross-talk of ΔNp63α and YB-1 with EGFR/STAT3 and PI3K/AKT signaling pathways

In pancreatic cancer cells, ΔNp63α expression was shown to induce the Epidermal Growth Factor Receptor (EGFR) (Danilov et al., 2011). As we observed a PI3K-dependent increase of ΔNp63α in SCC022 cells upon YB-1 silencing, we decided to evaluate the level of EGFR and its direct downstream target STAT3 in SCC022 cells upon YB-1 or ΔNp63α silencing. As shown in Figure 4, along with ΔNp63α, YB-1 depletion up-regulates EGFR and STAT3 both at protein (Figure 4A) and RNA level (Figure 4B). Real Time PCR assay in SCC022 cells clearly shows that YB-1 silencing results in about 2 and 3.5 fold induction of EGFR and STAT3 transcripts, respectively (Figure 4B). Following ΔNp63α silencing, instead, the expression of both EGFR and STAT3 was switched off although the level of YB-1 protein remained unaltered (Figure 4A). These results suggest that ΔNp63α is a major activator of the EGFR/STAT3 axis in squamous carcinoma cells. Accordingly, in SCC011 and HaCaT cells where YB-1 silencing reduces ΔNp63α, EGFR and STAT3 transcription was also reduced (Supplementary Fig. 5A and B).

To confirm the ability of ΔNp63α to regulate EGFR gene expression we performed transient transfection and luciferase reporter assays in MDA-MB231 breast cancer cells expressing no detectable p63. MDA-MB231 cells were transiently transfected with the EGFR promoter-luciferase vector and increasing amount of expression plasmid encoding wild type ΔNp63α or its mutant form bearing the F to L substitution at position 518 of the SAM domain. This mutant was previously described to be transactivation defective (Radoja et al., 2007). Remarkably, wild type but not mutant ΔNp63α protein induced luciferase activity, in a dose-dependent manner (Figure 4C and D). Moreover, Western blot analysis of extracts from MDA-MB231 breast cancer cells

transiently transfected with ΔNp63α showed induction of both EGFR and STAT3 endogenous proteins, confirming that EGFR and STAT3 expression are induced by ΔNp63α (Figure 4E).

DISCUSSION

YB-1 is a versatile protein associated with many malignancies. However, because of its multifunctional character, the role of YB-1 in neoplastic cell growth remains elusive (Bader et al., 2006).

Our previous (Di Costanzo et al., 2012) and present data show that ΔNp63α hyper-expression, as it occurs in squamous carcinoma cells, is associated with YB-1 nuclear localization where it is expected to play a pro-proliferative role. In the present manuscript we show that YB-1 depletion has a strong negative impact on cell survival of both immortalized HaCaT keratinocytes and non-metastatic SCC011 squamous carcinoma cells. Interestingly, in HaCaT and SCC011 cells, YB-1 knockdown causes a significant reduction of ΔNp63α transcription (Yang et al., 1999; Senoo et al., 2004). However, in HaCaT and SCC cells, ΔNp63α knockdown is not sufficient to trigger cell death thereby indicating that YB-1, in keratinocytes, plays additional p63-independent pro-survival functions.

Surprisingly, in highly metastatic SCC022 cells, YB-1 silencing does not result in cell death. Strikingly, in these cells, YB-1 silencing potentiates AKT activation suggesting that YB-1 can act as a negative regulator of the PI3K/AKT signaling pathway and its loss allows PI3K/AKT-dependent induction of pro-survival genes, including ΔNp63α. Interestingly, the low level of endogenous PTEN observed in SCC022 cells can likely explain the constitutive activation of the PI3K/AKT pathway observed in this cell line. Remarkably, we have observed only in HaCaT and SCC011 cells a strong activation of PTEN in response to YB-1 depletion. In SCC022 cells, instead, where PI3K/AKT hyper-activation sustains ΔNp63α protein level, we did not observe any increase

of PTEN after YB-1 depletion. However, at this stage, we can hypothesize that, in this cell line, PTEN cannot be up-regulated because of epigenetic or other inactivating mechanisms.

The evidence that PI3K/AKT hyperactivation in SCC022 cells is responsible for ΔNp63α transcriptional induction is in line with previous studies showing that ΔNp63α is positively regulated by the PI3K pathway (Barbieri et al., 2003). However, it is important to remind that ΔNp63α has been shown to repress the expression of PTEN (Leonard et al., 2011). Accordingly, in PTEN-proficient HaCaT and SCC011 cells, where YB-1 silencing causes a decrease of ΔNp63α, we observed an increase in the level of PTEN protein which is expected to restrain signaling by the PI3K pathway.

In summary, our results indicate that, being able to sustain ΔNp63α gene expression, YB-1 is part of a complex molecular network linking ΔNp63α to the PI3K/AKT/PTEN pathway and that establishment of a positive feedback loop coupling induction of ΔNp63α expression with PI3K/AKT activation may be a relevant step in progression of squamous carcinogenesis.

An important finding of our work is the observation that ΔNp63α controls the expression of the Epidermal Growth Factor Receptor switching-on the entire EGFR/STAT3 axis. Accordingly, in normal adult epidermis, the EGFR is predominantly expressed in basal keratinocytes and signaling events elicited by it are known to affect their proliferation and migration (Bito et al., 2011). ΔNp63α, therefore, represents an important molecular connection between YB-1, the PI3K/AKT and the EGFR/STAT3 signaling pathways. We can postulate that constitutive activation of PI3K/AKT, such as in PTEN-deficient cells, may likely cause persistence of ΔNp63α which can induce keratinocyte hyper-proliferation by impinging on the EGFR/STAT3 pathway. Interestingly, in physiological conditions EGF-dependent and PI3K/AKT pathways are both required for efficient skin wound re-epithelialization (Haase et al., 2003). Moreover, EGFR/STAT3 inhibition was shown to be unable to induce apoptosis (Bito et al., 2003) thereby providing a plausible explanation of why ΔNp63α silencing alone was not sufficient to induce cell death in our experimental settings.

In summary, we have presented clear evidences to suggest that YB-1 can play a role in skin carcinogenesis. However, the molecular basis of cancer can widely vary and the ability of YB-1 to control multiple and overlapping pathways raises concerns about the consideration of YB-1 as an attractive target for therapy against metastatic squamous cancer. In particular, our results indicate that YB-1 knockdown in cells whose oncogenic transformation depends on PI3K/AKT constitutive activation is expected to enhance rather than arrest metastatic progression. Association of YB1-targeted therapy with drugs that target the PI3K and/or EGFR pathway should be evaluated as a valuable strategy to treat squamous carcinoma. *In vivo* experiments will help to clarify this relevant point.

Conflict of interest

The authors declare that they have no conflict of interest.

References

1. Amoresano A, Di Costanzo A, Leo G, Di Cunto F, La Mantia G, Guerrini L, Calabrò V. 2010. Identification of ΔNp63α Protein Interactions by Mass Spectrometry. J. Proteome Res. 9: 2042-48.
2. Bader AG. 2006. YB-1 activities in oncogenesis: transcription and translation. Curr Cancer Ther Rev . 2: 31–39.
3. Barbieri CE, Barton CE, Pietenpol JA. 2003. ΔNp63α expression is regulated by the phosphoinositide 3-kinase pathway. J Biol Chem; 278(51): 51408-51414.
4. Barbieri CE, Tang LJ, Brown KA, Pietenpol JA. 2006. Loss of p63 leads to increased cell migration and up-regulation of genes involved in invasion and metastasis. Cancer Research, 66: 7589- 7597.
5. Bito T, Sumita N, Ashida M, Budiyanto A, Ueda M, Ichihashi M, Tokura Y, Nishigori C. 2011. Inhibition of epidermal growth factor receptor and PI3K/AKT signaling suppresses cell proliferation and survival through regulation of Stat3 activation in human cutaneous cell carcinoma. Journal of Skin Cancer. doi:10.1155/2011/874571.
6. Carrol DK, Carrol JS, Leong CO, Cheng F, Brown M, Mills AA, Brugge JS, Ellisen LW 2006. p63 regulates an adhesion programme and cell survival in epithelial cells. Nat Cell Biol, 8(6): 551-561.
7. Danilov AV, Neupane D, Nagaraja AS, Feofanova E, Leigh AH, Di Renzo J., Kork M. 2011. DeltaNp63alpha-mediated induction of epidermal growth factor promotes pancreatic cancer cell growth and chemoresistence. Plos one: 6(10) e26815.
8. Di Costanzo A, Troiano A, Di Martino O, Cacace A, Natale CF, Ventre M, Netti P, Caserta S, Pollice A, La Mantia G, Calabrò V. 2012. The p63 protein isoforms ΔNp63α modulates Y-box binding protein 1 in its subcellular distribution and regulation of cell survival and motility genes. J Biol Chem, 287(36):30170-80.

9. Eliseeva A, Kim ER, Guryanov SG, Ovchinnikov LP, Lyabin DN. 2011. Y-Box-Binding Protein 1 (YB-1) and its function. Biochemistry (Moscow), 76(13): 1402-1433.
10. Haase I, Evans R, Pofahl R, Watt FM. 2003. Regulation of keratinocytes shape, migration and wound epithelialization by IGF-1-and EGF-dependent signaling pathways. J Cell Sci . 116: 3227-3238.
11. Hibi K, Trink B, Patturajan M, Westra WH, Caballero OL, Hill DE, Ratoviski EA, Jen J, Sidransky D. 2000. Ais is an oncogene amplified in Squamous cell carcinoma. Proc. Natl. Acad. Sci. USA; 97: 5462-5467.
12. Leonard MK, Kommagani R, Payal V, Mayo LD, Shamma HN, Kadakia MP. 2011. ΔNp63α regulates keratinocytes proliferation by controlling PTEN expression and localization. Cell Death Differ. 18(12): 1924-1933.
13. Lefort K, Mandinova A, Ostano P, Kolev V, Calpini V, Kolfschoten I, Devgan V, Lieb J, Rafooul W, Hohl D, Neel V, Garlick J, Chiorino G, Dotto P. 2007. Notch 1 is a p53 target gene involved in human keratinocytes tumor suppression through negative regulation of ROCK1/2 and MRCKα kinases. Genes Dev, 21(5): 562-577.
14. Livak KJ, Schmittgen TD. 2011. Analysis of relative gene expression data using Real-Time Quantitative PCR and the $2^{-DDC}{}_{T}$ method. *Methods*. **25**: 402-408.
15. Lo Iacono M, Di Costanzo A, Calogero RA, Mansueto G, Saviozzi S, Crispi S, Pollice A, La Mantia G, Calabrò V. 2006. The Hay Wells Syndrome-Derived TAp63αQ540L Mutant has Impaired Transcriptional and Cell Growth Regulatory Activity. Cell Cycle, 5(1):78-87
16. Kolk A, Jubitz N, Mengele K, Mantwill K, Bissinger O, Schmitt M, Kremer M, Holm PS. 2011. Expression of Y-box-binding protein YB-1 allows stratification into long- and short-term survivors of head and neck cancer patients. Br J Cancer, 105(12):1864-1873.
17. Koster MI. 2010. p63 in skin development and ectodermal dysplasias. J Invest Dermatol; 130(10): 2352-2358.

18. Moll UM, Slade N. 2004. p63 and p73: roles in development and tumor formation. Mol Cancer Res; 2: 371-386.
19. Radoja N, Guerrini L, Lo Iacono N, Merlo GR, Costanzo A, Weinberg WC, La Mantia G, Calabro V, Morasso MI. 2007. Homeobox gene Dlx3 is regulated by p63 during ectoderm development: relevance in the pathogenesis of ectodermal dysplasias. Development 134(1): 13-18.
20. Ripamonti F, Albano L, Rossini A, Borrelli S, Fabris S, Mantovani R, Neri A, Balsari A, Magnifico A, Tagliabue E. 2013. EGFR through STAT3 modulates ΔNp63α expession to sustain tumor-initiating cell proliferation in squamous cell carcinomas. J Cell Physiol; 228(4): 871-8.
21. Rocco JW, Leong CO, Kuperwasser N, DeYoung MP, Ellisen LW. 2006. p63 mediates survival in squamous cell carcinoma by suppression of p73-dependent apoptosis. Cancer Cell; 9(1): 45-56.
22. Rossi M, De Simone M, Pollice A, Santoro R, La Mantia G, Guerrini L, Calabrò V. 2006. Itch/AIP4 associates with and promotes p63 protein degradation. Cell Cycle; 5(16):1816-22.
23. Schittek B, Psenner K, Sauer B, Meier F, Iftner T, Garbe C. 2007. The increased expression of Y box-binding protein 1 in melanoma stimulates proliferation and tumor invasion, antagonizes apoptosis and enhances chemoresistance. Int J Cancer, 120:2110–2118.
24. Senoo M, Manis JP, Alt FW, McKeon F. 2004. p63 and p73 are not required for the development and p53-dependent apoptosis of T cells. Cancer Cell; 6: 85-89.
25. Shiota M, Izumi H, Onitsuka T, Miyamoto N, Kashiwagi E, Kidani A, Yokomizo A, Naito S, Kohno K. 2008. Twist promotes tumor cell growth through YB-1 expression.Cancer Res, 68(1): 98-105.
26. Shiota M, Zoubeidi A, Kumano M, Beraldi E, Naito S, Nelson C, Sorensen P, Gleave M. 2011. Clusterin is a critical downstream mediator of stress-induced YB-1 transactivation in Prostate Cancer. Mol Cancer Res; 9:1755-1766.

27. Sinnberg T, Sauer B, Holm P, Spangler B, Kuphal S, Bosserhoff A, Schittek B. 2012. MAPK and PI3K/AKT mediated YB-1 activation promotes melanoma cell proliferation which is counteracted by an auto regulatory loop. Exp. Dermatol; 21(4):265-270.
28. Song MS, Salmena L, Pandolfi PP. 2012. The function and regulation of the PTEN tumor suppressor. Nature Reviews Molecular Cell Biology, 13: 283-296.
29. Sutherland BW, Kucab J, Wu J, Lee C, Cheang MC, Yorida E, Turbin D, Dedhar S, Nelson C, Pollak M, Leighton Grimes H, Miller K, Badve S, Huntsman D,Blake-Gilks C, Chen M, Pallen CJ, Dunn SE. 2005. AKT phosphorylates the Y-box binding protein 1 at Ser102 located in the cold shock domain and affects the anchorage-independent growth of breast cancer cells. Oncogene**,** 24(26):4281-4292.
30. To K, Fotovati A, Reipas KM, Jennifer HL, Hu K,Wang J, Astanehe A, Davies AH, Lee L, Stratford AL, Raouf A, Johnson P, Berquin IM, Royer HD, Eaves CJ, Dunn SE. 2010. YB-1 induces expression of CD44 and CD49f leading to enhanced self-renewal, mammosphere growth, and drug resistance. Cancer Res; 70(7): 2840-2851.
31. Toh S, Nakamura T, Ohga T, Koike K**,** Uchiumi T**,** Wada M**,** Kuwano M**,** Kohno K. 1998. Genomic organization of the human Y-box protein (YB-1) gene. *Gene*, 206:93 -97.
32. Uramoto H, Izumi H, Ise T, Tada M, Uchiumi T, Kuwano M, Yasumoto K, Keiko F, Kohno K. 2002. p73 interacts with c-Myc to regulate Y-box-binding protein-1 expression. J Biol Chem, 277: 31694-31702.
33. Yang A, Schweitzer R, Sun D, Kaghad M, Walker N, Bronson RT, Tabin C, Sharpe A, Caput D, Crum C, McKeon F. 1999. p63 is essential for regenerative proliferation in limb, craniofacial and epithelial development. Nature; 398: 714-71.

Figures Legend

Figure 1. YB-1 knockdown affects HaCaT cell survival. (**A) upper panel,** Phase-Contrast imaging and Hoechst staining (**lower panel**) showing HaCaT keratinocyte cells transfected with

scrambled, YB-1 or p63 siRNA oligos. (**B**) Representative immunoblot analyses of HaCaT keratinocytes transfected with YB1 (**upper panel**), p63 (**lower panel**) or scrambled (siCtrl) siRNA oligos, respectively. 48 hours after silencing whole cell extracts were immunoblotted with YB-1, p63 and PARP antibodies. Actin was used as a loading control. Bar graphs are quantitative densitometric analyses of four indipendent Western blots. The blots were normalized to actin and the fold-changes of protein levels are reported in comparison to control (value set at 1.0). P-value <0.05 is represented by *; P-value <0.01 is represented by **. (**C**) Quantitative real-time PCR analysis of HaCaT keratinocytes transfected with scrambled or YB-1 siRNA oligos. GADD45A mRNA level was measured as a control. (**D**) Quantitative Real-time PCR analysis of HaCaT keratinocytes transfected with scrambled or p63 siRNA oligos. In both experiments data were analyzed according to the fold-changes compared to scrambled control (value set at 1.0) using the $2^{-\Delta\Delta Ct}$ method. P-value <0.05 is represented by *; P-value <0.01 is represented by **.

Figure 2. YB-1 knockdown in SCC011 and SCC022 squamous carcinoma cells. (A) Phase-contrast imaging showing SCC011 (**upper panel**) and SCC022 (**lower panel**) cells at 48 hours post-YB1 silencing. (**B**) Representative immunoblot analysis of SCC011 or SCC022 cells transfected with scrambled or YB-1 siRNA oligos. 48 hours after silencing whole cell lysates were immunoblotted with YB-1, p63 and PARP antibodies. GAPDH was used as a loading control. Bar graph is a quantitative densitometric analysis of four indipendent Western blots. The blots were normalized to GAPDH and the fold-changes of protein levels are reported in comparison to control (value set at 1.0). P-value <0.05 is represented by *; P-value <0.01 is represented by **. (**C**) Quantitative Real-time PCR analysis of SCC011 (**left panel**) and SCC022 cells (**right panel**) transfected with scrambled or YB-1 siRNA oligos. Data were analyzed according to the fold-changes compared to scrambled control (value set at 1.0) using the $2^{-\Delta\Delta Ct}$ method. P-value <0.05 is represented by *; P-value <0.01 is represented by **. (**D**) Effect of

YB1 silencing on the viability of HaCaT and SCC cells. Cell viability was assessed by MTT assay following 48 hours of YB-1 silencing. Data are represented as the mean +/- SD from three independent experiments. The asterisk indicates P-value<0.05.

Figure 3. YB-1 knockdown enhances pAKT^{S473} in SCC022 squamous carcinoma. (A) Immunoblot analysis of HaCaT, SCC011 and SCC022 cells transfected with scrambled or YB1-siRNA oligos. 48 hours after silencing whole cell extracts were immunoblotted with YB-1, pAKT^{S473} and AKT antibodies. Actin was used as a loading control. **(B)** SCC022 cells were transfected with scrambled or YB-1 siRNA oligos transfection. After 42 hrs cells were treated with LY294002 for 6 hrs. Whole cell extracts were analyzed by immunoblotting with YB-1, pAKT^{S473}, p63 and AKT antibodies. Actin was used as loading control. (**C**) Quantitative Real-time PCR of ΔNp63 mRNA levels. ΔNp63 mRNA levels were analyzed according to the fold-changes compared to scrambled control (value set at 1.0) using the $2^{-\Delta\Delta Ct}$ method. P-value < 0.05 is represented by *; P-value < 0.01 is represented by **. DMSO was used as control (**D**) Immunoblot analysis of HaCaT, SCC011 and SCC022 cells. Whole cell extracts were immunoblotted with, PTEN, pAKT^{S47} , and AKT antibodies. GAPDH was used as loading control. (**E**) Nuclear and cytoplasmic fractionation of extracts from control or YB-1 silenced HaCaT, SCC011 and SCC022 cells are shown in Figure 5A. Fractions were analysed by immunoblotting with PTEN antibody. GAPDH and PARP were used as cytoplasmic and nuclear controls, respectively.

Figure 4. Cross-talk of ΔNp63α and YB-1 with EGFR/STAT3 pathway. (A) Immunoblot analysis of SCC022 cells transfected with scramble, YB-1 or p63 siRNA oligos. Whole cell extracts were immunoblotted with, YB-1, p63, EGFR, STAT3 antibodies. Actin was used as a loading control. **(B)** Quantitative Real-time PCR analysis of SCC022 cells transfected with

scrambled or YB-1 siRNA oligos. YB-1, EGFR and STAT3 mRNA levels were analyzed according to the fold-changes compared to scrambled control (value set at 1.0) using the $2^{-\Delta\Delta Ct}$ method. P-value < 0.05 is represented by *; P-value < 0.01 is represented by **. **(C)** Luciferase assay of EGFR-promoter activity in MDA-MB231 cells. Cells were transiently transfected with 1µg of luciferase reporter plasmid and the indicated amounts of ΔNp63α or ΔNp63α F518L plasmids. Luciferase assay was performed at 48 hrs post-transfection. Values are the mean +/- SD of three independent experimental points. **(D**) Representative immunoblotting showing the level of ΔNp63α in transfected MDA-MB231 cell extracts used for the luciferase assay shown in 7C. GAPDH immunodetection was used as loading control. **(E**) MDA-MB231 cells were transfected with empty vector or ΔNp63α plasmids. At 24h post-transfection cells were harvested and whole cell extracts were analyzed by immunoblotting with p63, STAT3 and EGFR antibodies. Actin was used as a loading control.

Supplementary Figures

S1. YB-1 and ΔNp63α coimmunoprecipitation in HaCaT cells. (**A**) Extracts from HaCaT cells were immunoprecipitated with anti-p63 antibodies and the immunocomplexes were blotted and probed with anti-YB-1, as indicated. (**B**) Extracts from HaCaT cells were immunoprecipitated with anti-YB-1 antibodies and the immunocomplexes were blotted and probed with anti-p63. Samples with no antibody (no Ab) or irrelevant α-mouse and α-rabbit antibodies were included as controls. (**C**) Immunoblot analysis of YB-1 level in HaCaT cells treated with proteasome inhibitor MG132 for 6h (5µM final concentration). 36kDa and 43kDa YB-1 forms are reduced with concomitant accumulation of full-length YB-1 50kDa band showing the identity of YB-1 bands.

S2. **YB-1 and p63 knockdown in SCC022 cells. (A)** Immunofluorescence assay in SCC022 cells transfected with scrambled, YB-1 or p63 siRNA oligos. YB1 was detected using anti-YB-1 and secondary anti-rabbit Cy5-conjugated (green) antibodies. p63 was detected using anti-p63 and secondary anti-mouse Cy3-conjugated (red) antibodies. Hoechst was used to stain nuclei**. (B)** (upper panel**)** SCC022 cells were incubated with normal mouse serum and secondary anti-mouse Cy3-conjugated (red) antibodies; (lower panel) SCC022 cells were incubated with normal rabbit serum and secondary anti-rabbit Cy5-conjugated (green) antibodies.

S3. Effect of p63 and YB-1 silencing on SCC022 cells migration speed. (A) Motility assay on SCC022 cells after transient silencing of p63 and YB-1 performed by time-lapse microscopy. After 24 h of incubation with siRNA oligos, cell migration assay was performed. Averaged cell speeds after 16 h of observation are reported. Horizontal lines and boxes and whiskers represent the medians, 25th/75th, and 5th/95th percentile, respectively. P-value < 0.01 is represented by **. Only statistically different doubles are marked. (**B**) Immunoblot analysis of ΔNp63α and YB-1 protein levels in SCC022 cells after 40 h of ΔNp63α or YB-1 silencing and used in cell migration assay. Cell extracts were blotted and probed with anti-p63 or anti-YB-1 antibodies. GAPDH was used as a loading control. ΔNp63α protein band was almost undetectable while YB-1 protein was reduced to 40%, as assed by densitometric scanning.

S4. Proteasome activity is not involved in ΔNp63α up-regulation upon YB-1 silencing. Immunoblot analysis of SCC022 cells transfected with scrambled or YB1-siRNA oligos and treated with MG132 (6 hrs) after 42 hours of YB-1 silencing cells. Whole cell extracts were immunoblotted with YB-1 and p63 antibodies. Actin was used as loading control.

S5. Effect of YB-1 silencing on EGFR/STAT3 mRNA levels in SCC011 and HaCaT cells. Quantitative Real-time PCR analysis of **(A)** SCC011 cells and **(B)** HaCaT cells transfected with scrambled or YB-1 siRNA oligos. YB-1, EGFR and STAT3 mRNA levels were analyzed according to the fold-changes compared to scrambled control (value set at 1.0) using the $2^{-\Delta\Delta Ct}$ method. P-value < 0.05 is represented by *; P-value < 0.01 is represented by **.

Figure 1

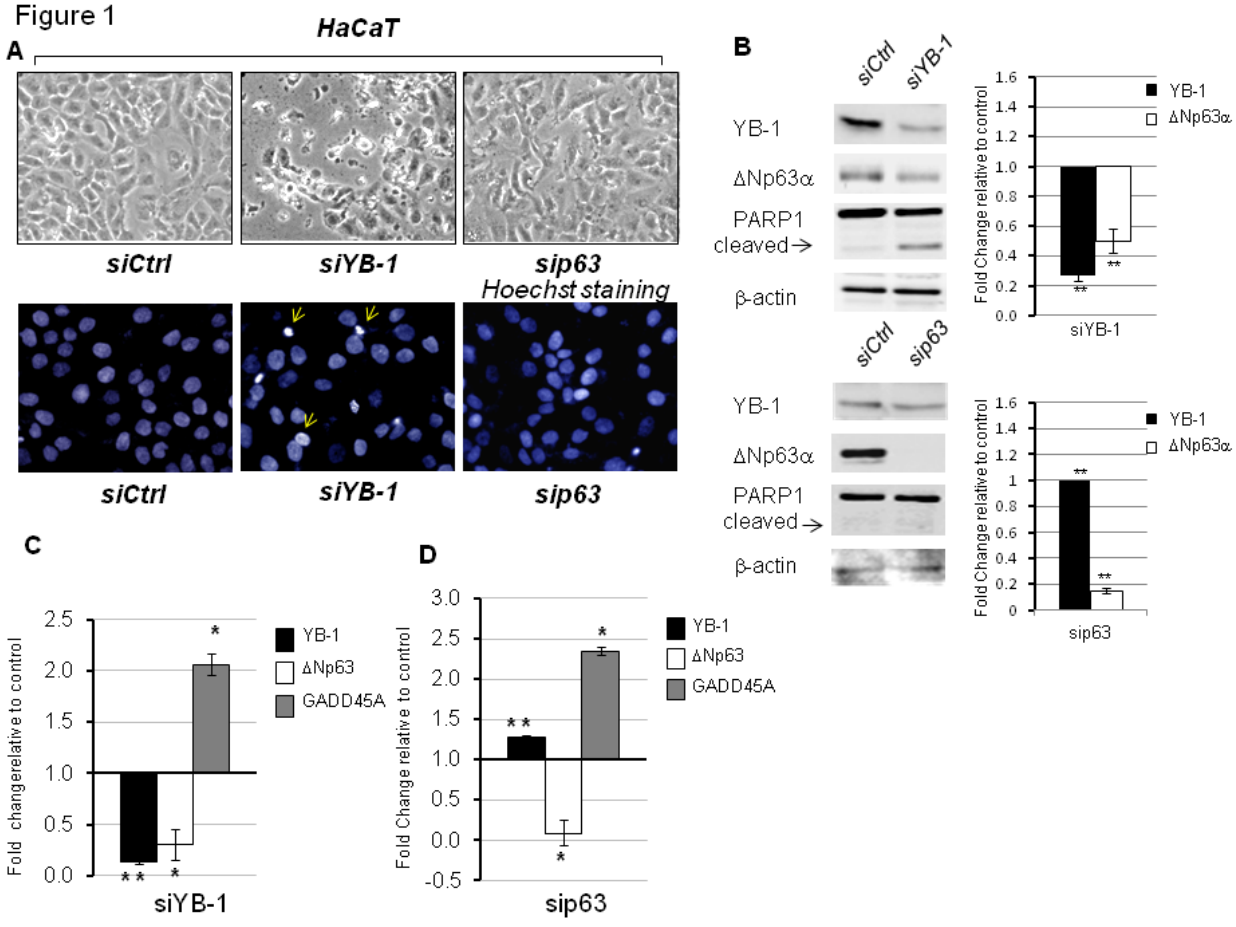

Figure 2

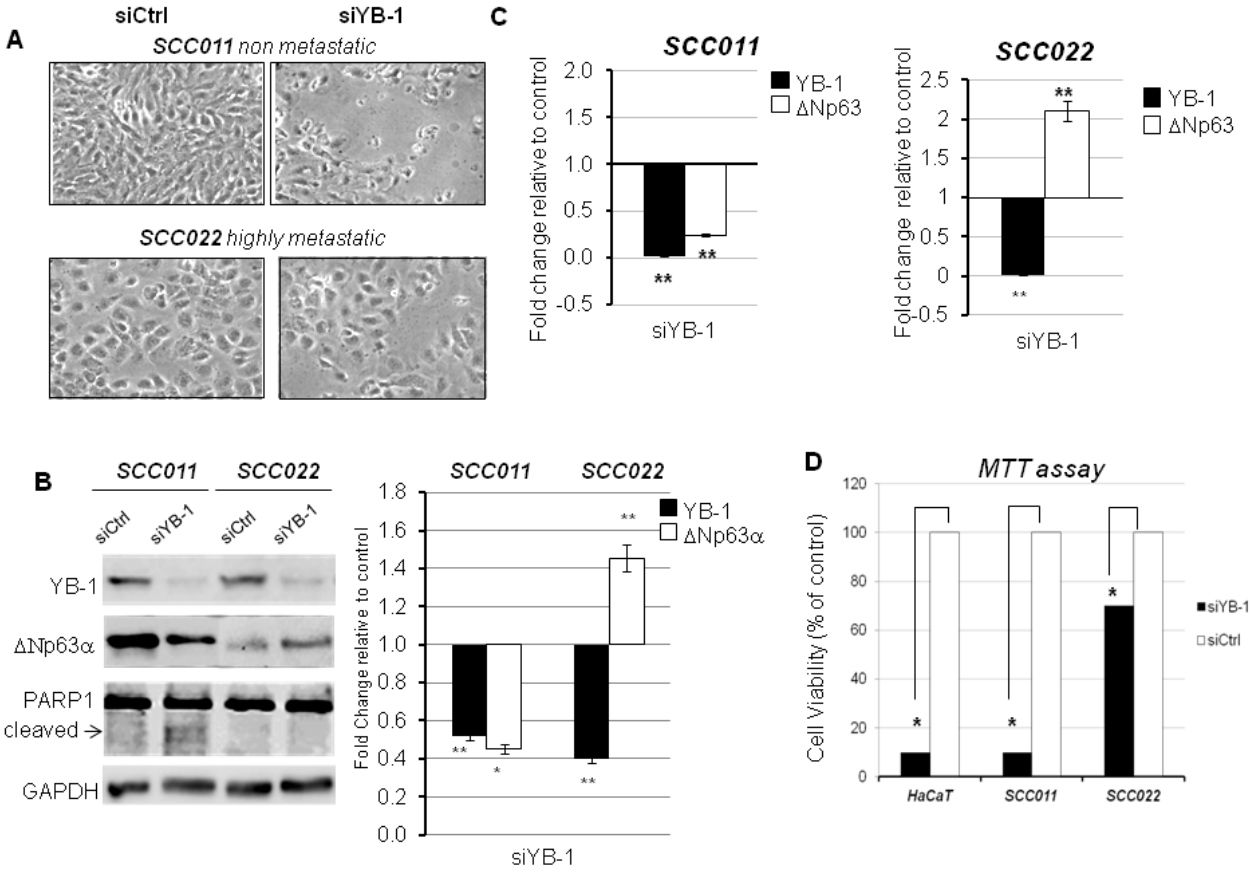

Figure 3

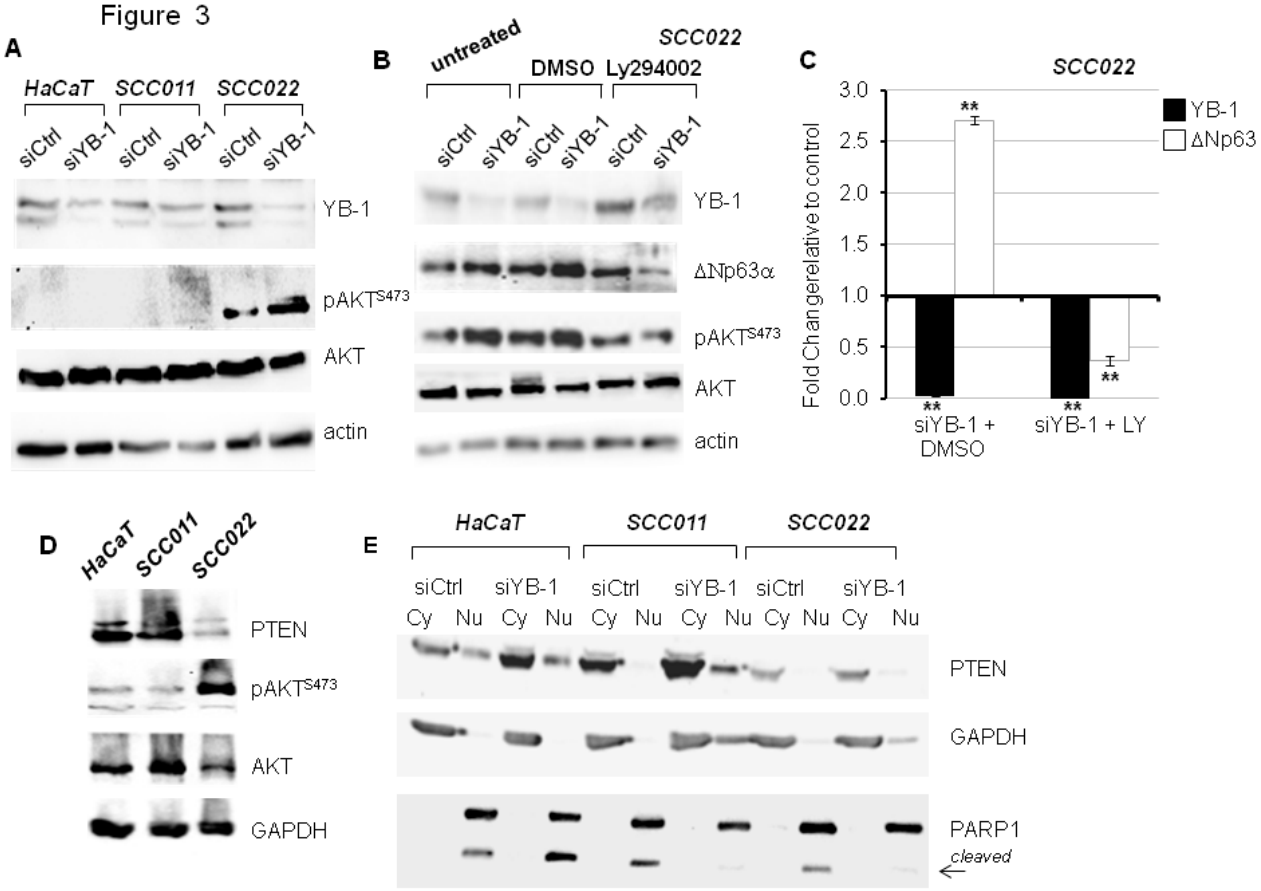

Figure 4

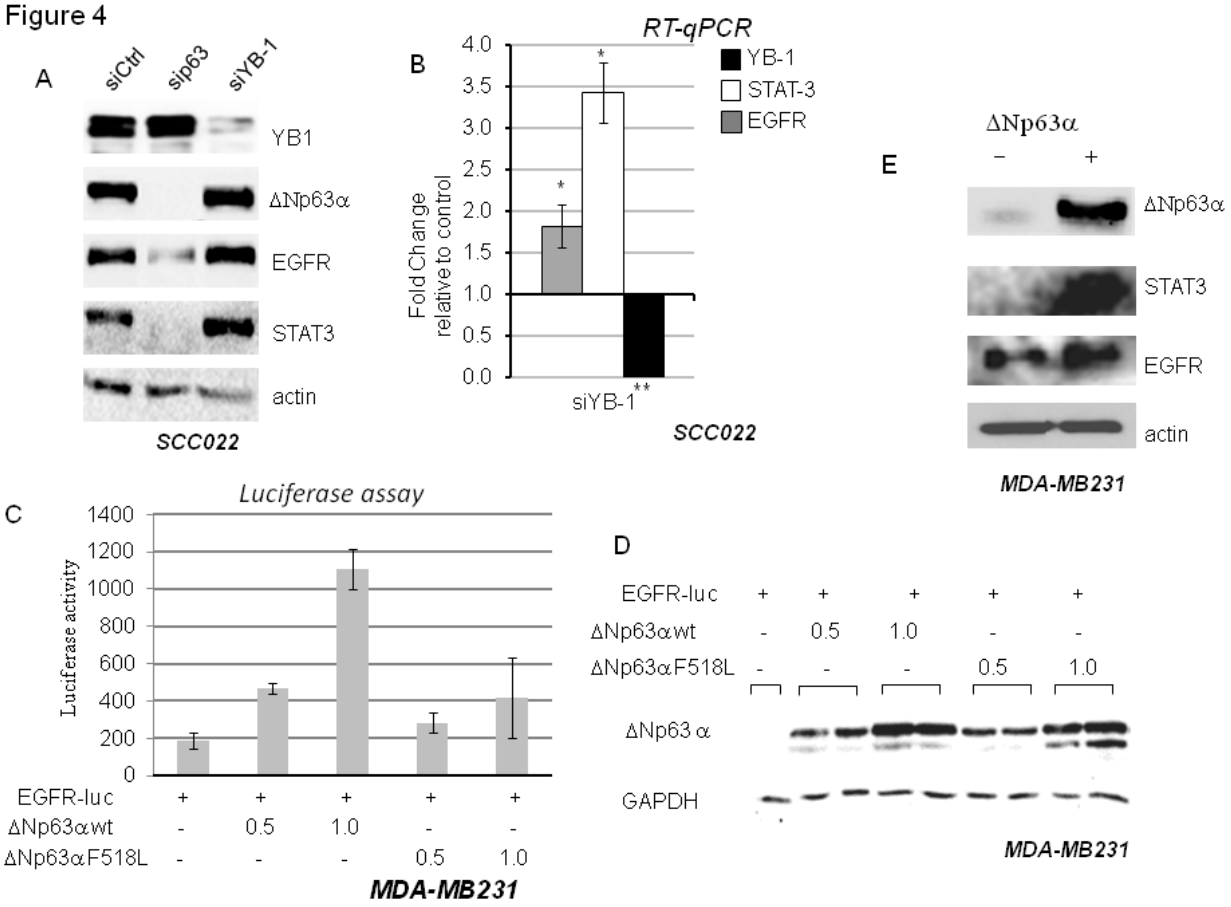

THE JOURNAL OF BIOLOGICAL CHEMISTRY VOL. 287, NO. 36, pp. 30170–30180, August 31, 2012

The p63 Protein Isoform ΔNp63α Modulates Y-box Binding Protein 1 in Its Subcellular Distribution and Regulation of Cell Survival and Motility Genes*

Received for publication, February 5, 2012, and in revised form, July 9, 2012 Published, JBC Papers in Press, July 11, 2012, DOI 10.1074/jbc.M112.349951

Antonella Di Costanzo[‡], Annaelena Troiano[‡], Orsola di Martino[‡], Andrea Cacace[‡], Carlo F. Natale[§], Maurizio Ventre[§], Paolo Netti[§], Sergio Caserta[¶], Alessandra Pollice[‡], Girolama La Mantia[‡], and Viola Calabrò[‡1]

From the [‡]Department of Structural and Molecular Biology and [§]Center for Advanced Biomaterials for Health Care, Istituto Italiano di Tecnologia and Interdisciplinary Research Centre on Biomaterials, University of Naples "Federico II", Naples 80126 and the [¶]Department of Chemical Engineering, University of Naples "Federico II", Naples 80125, Italy

Background: YB-1 is a multifunctional protein that affects transcription, splicing, and translation.
Results: ΔNp63α, the main p63 protein isoform, interacts with YB-1 and affects YB-1 subcellular localization and regulation of cell survival and motility genes.
Conclusion: ΔNp63α and YB-1 interaction inhibits epithelial to mesenchymal transition and tumor cell motility.
Significance: This is the first demonstration of a physical and functional interaction between YB-1 and ΔNp63α oncoproteins.

The Y-box binding protein 1 (YB-1) belongs to the cold-shock domain protein superfamily, one of the most evolutionarily conserved nucleic acid-binding proteins currently known. YB-1 performs a wide variety of cellular functions, including transcriptional and translational regulation, DNA repair, drug resistance, and stress responses to extracellular signals. Inasmuch as the level of YB-1 drastically increases in tumor cells, this protein is considered to be one of the most indicative markers of malignant tumors. Here, we present evidence that ΔNp63α, the predominant p63 protein isoform in squamous epithelia and YB-1, can physically interact. Into the nucleus, ΔNp63α and YB-1 cooperate in *PI3KCA* gene promoter activation. Moreover, ΔNp63α promotes YB-1 nuclear accumulation thereby reducing the amount of YB-1 bound to its target transcripts such as that encoding the SNAIL1 protein. Accordingly, ΔNp63α enforced expression was associated with a reduction of the level of SNAIL1, a potent inducer of epithelial to mesenchymal transition. Furthermore, ΔNp63α depletion causes morphological change and enhanced formation of actin stress fibers in squamous cancer cells. Mechanistic studies indicate that ΔNp63α affects cell movement and can reverse the increase of cell motility induced by YB-1 overexpression. These data thus suggest that ΔNp63α provides inhibitory signals for cell motility. Deficiency of ΔNp63α gene expression promotes cell mobilization, at least partially, through a YB-1-dependent mechanism.

The Y-box binding protein 1 (YB-1), also known as NSEP1, CSBD, and MDR-NF1, is a member of the highly conserved Y-box family of proteins that regulate gene transcription by binding to the TAACC element (the Y-box) contained within many eukaryotic promoters (1). Transcriptional targets of YB-1 include genes associated with cell death, cell proliferation, and multidrug resistance (1, 2). YB-1 protein can also regulate gene transcription by binding to other transcription factors such as p53, AP1, and SMAD3 (2).

YB-1 is an important marker of tumorigenesis and is overexpressed in many malignant tissues, including breast cancer, non-small cell lung carcinoma, ovarian adenocarcinoma, human osteosarcomas, colorectal carcinomas, and malignant melanomas (1). Mostly cytosolic, YB-1 protein shuttles between the nucleus and cytoplasm. Cytoplasmic YB-1 acts as a translation factor of oncogenic/pro-metastatic genes (3). It binds to the mRNA cap structure and displaces the eukaryotic translation initiation factors eIF4E and eIF4G, thereby causing mRNA translational silencing (4). However, cytoplasmic YB-1 activates cap-independent translation of mRNA encoding SNAIL1, a transcription factor that promotes epithelial-mesenchymal transition by suppressing E-cadherin (5). According to those observations, the YB-1 protein level, in breast carcinoma, is positively correlated to the increase of SNAIL1 protein level and reduced expression of E-cadherin (6).

In normal conditions, YB-1 is located in the cytoplasm and transiently translocates to the nucleus at the G_1/S transition of the cell cycle (7). Moreover, nuclear translocation of YB-1 was shown to occur in response to DNA-damaging agents, phosphorylation at Ser-102 by AKT kinase, UV irradiation, TGFβ stimulation, virus infection, hypothermia, and pharmacological compounds (1, 8, 9). Under stress stimuli, YB-1 nuclear translocation requires a physical interaction with wild type p53 (10).

Herein, we report that YB-1 directly interacts with ΔNp63α and accumulates in the nuclear compartment. ΔNp63α is encoded by the *TP63* locus, a homologue of the p53 tumor suppressor gene and the most ancient member of the p53 family (11). Because of the presence of two promoters, the *TP63* gene encodes two major classes of proteins as follows: those containing a transactivating domain homologous to the one present in p53 (*i.e.* TAp63), and those lacking it (*i.e.* ΔNp63) (12). In addition, alternate splicing at the C terminus generates at least three p63 variants (α, β, and γ) in each class. The TAp63γ isoform

* This work was supported by MIUR Grant PRIN 2009KFS94X_003 (to V. C.).
[1] To whom correspondence should be addressed: Dept. Biologia Strutturale e Funzionale, Università Federico II, Via Cinzia Monte S Angelo, 80126 Napoli, Italy. Tel.: 39-081-679069; Fax: 39-081-679033; E-mail: vcalabro@unina.it.

resembles most p53, whereas the α-isoforms include a conserved protein-protein interaction domain named the sterile α motif.

Gene knock-out mice demonstrated that p63 plays a critical role in the morphogenesis of organs/tissues developed by epithelial-mesenchymal interactions such as the epidermis, teeth, hair, and glands (13). In adults, ΔNp63α expression occurs in the basal cells of stratified epithelia. High expression of ΔNp63α is associated with the proliferative potential of epithelial cells (14) and is enhanced at the early stages of squamous cell carcinomas (SCCs)[2] (15). Down-regulation of ΔNp63α by SNAIL transcription factor instead was found to reduce cell-cell adhesion and increase the migratory properties of squamous carcinoma cells (16). Moreover, a partial or complete loss of ΔNp63α expression was associated with tumor metastasis supporting the idea that ΔNp63α plays a relevant role in metastasis suppression (17, 18). Here, we provide experimental evidence that the YB-1 protein associates with ΔNp63α and such interaction plays a critical role in the control of genes involved in cell survival and motility.

EXPERIMENTAL PROCEDURES

Plasmids—cDNAs encoding human FLAG-tagged YB-1 were provided by Dr. Sandra Dunn (Research Institute for Children's and Women's Health, Vancouver, British Columbia, Canada). *PIK3CA* promoter luciferase plasmid was provided by Dr. Arezoo Astanehe (Research Institute for Children's and Women's Health, Vancouver, British Columbia, Canada). cDNA encoding human ΔNp63α and ΔNp63γ were previously described (19). For bacterial expression, ΔNp63γ and ΔNp63α cDNAs were inserted in pRSETA vector in XhoI/ClaI and XhoI/XbaI (filled) sites, respectively. GFP and YB-1-GFP vectors were provided by Dr. Paul R. Mertens (University Hospital Aachen, Germany). PET-YB-1 was from Dr. Jill Gershan (Medical College of Wisconsin, Milwaukee, WI).

Cell Lines, Transfection, and Antibodies—Squamous carcinoma cells (SCC011 and SCC022) were described previously and provided to us by Dr. C. Missero (20).

These cell lines were maintained in RPMI medium supplemented with 10% fetal bovine serum at 37 °C and 5% CO_2. A431, H1299, and MDA-MB-231 cells were obtained from ATCC and maintained in DMEM supplemented with 10% fetal bovine serum at 37 °C and 5% CO_2. Dox-inducible Tet-On H1299/ΔNp63α cells were described previously (21).

Lipofections were performed with Lipofectamine (Invitrogen), according to the manufacturer's recommendations. *YB-1* transient silencing was carried out with ON-TARGET plus SMART pool *YB-1*-siRNA (Dharmacon) and RNAiMAX reagent (Invitrogen). ΔNp63α transient silencing in SCC011 cells was carried out with RIBOXX (IBONI *p63*-siRNA pool) and RNAiMAX reagent (Invitrogen), according to the manufacturer's recommendation. An si-RNA against luciferase (si-Luc) was used as a negative control. Anti-p63 (4A4) and anti-actin(1–19) were from Santa Cruz Biotechnology Inc., and anti-FLAG M2 was from Sigma. PARP, AKT, pAKT (Ser-473) and rabbit polyclonal YB-1 antibody (Ab12148) were from Cell Signaling Technology (Beverly, MA). Mouse monoclonal E-cadherin (ab1416) and SNAIL1 antibodies were from Abcam (Cambridge, UK). Mouse monoclonal N-cadherin (610921) was from BD Transduction Laboratories. Cy3-conjugated anti-mouse IgG and Cy5-conjugated anti-rabbit IgG were from Jackson ImmunoResearch. Doxycycline was from Clontech.

Chromatin Immunoprecipitation (ChIP) Assay—ChIP was performed with chromatin from human MDA-MB-231 cells transfected with ΔNp63γ, ΔNp63α, and/or FLAG YB-1, as described previously (22). Real time PCR was performed with the 7500 Applied Biosystems apparatus and SYBR Green MasterMix (Applied Biosystems) using the following oligonucleotides: *PIK3CA*-For, CCCCCGAACTAATCTCGTTT, and *PIK3CA*-Rev, TGAGGGTGTTGTGTCATCCT.

Sequential ChIP was performed with chromatin from SCC011 cells. Method of chromatin extraction and controls used were previously described (22).

Chromatin samples were subjected to pre-clearing with 80 μl of salmon sperm DNA-saturated agarose A beads for 2 h at 4 °C with rotation. The first immunoprecipitation step was obtained with p63 antibodies (4A4). After several washes, the immunocomplexes were extracted from beads with 100 μl of 2% TE/SDS. The second immunoprecipitation step was obtained with YB-1 (Ab12148) antibodies after a 30-fold dilution in DB buffer (50 mM Tris-HCl, 5 mM EDTA, 200 mM NaCl, 0.5% Nonidet P-40, 15 mM DTT). Samples were incubated overnight at 4 °C with rotation. Immunocomplexes were extracted from beads as described above. Immunoprecipitated protein-DNA complexes were subjected to reverse cross-linking and proteinase K treatment. DNA was purified by phenol/chloroform extraction and resuspended in 40 μl of TE. 2 μl were used for PCR performed with the following primers: *PIK3CA* promoter For, ACAAACCCCTGGAATGTGAG, and *PI3KCA* promoter Rev, TGGAAAAGCGTAGGAGCAGT.

Immunoblot Analyses and Co-immunoprecipitation—Immunoblots and co-immunoprecipitations were performed as described previously (19). To detect p63/YB-1 interaction in SCC011 cells, 5.0×10^5 cells were plated in 60-mm dishes. For co-immunoprecipitations, whole cell extracts, precleared with 30 μl of protein A-agarose (50% slurry; Roche Applied Science), were incubated overnight at 4 °C with anti-YB-1(3 μg) or α-rabbit IgG (3 μg). The reciprocal experiment was performed with anti-p63 (2 μg) or α-mouse IgG.

Far Western Assays—Far Western assays were conducted according to the protocol described by Cui *et al.* (23). Increasing amounts (0.2, 0.5, and 1.5 μg) of ΔNp63α or ΔNp63γ recombinant proteins were subjected to SDS-PAGE and transferred to PVDF membrane (IPVH00010 Immobilon Millipore, Milan, Italy). Bovine serum albumin (0.5 and 1.5 μg; BSA) was used as control of unspecific binding and equal loading of BSA, and recombinant YB-1 or p63 proteins in far Western blotting was verified by Coomassie staining (data not shown).

Luciferase Reporter Assay—MDA-MB-231 cells were co-transfected with ΔNp63α, *PIK3CA* luc promoter, and pRL-TK. *YB-1* gene silencing was carried out 24 h before plasmid

[2] The abbreviations used are: SCC, squamous cell carcinoma; For, forward; Rev, reverse; PARP, poly(ADP-ribose) polymerase; Dox, doxycycline; TRITC, tetramethylrhodamine isothiocyanate; *S*, speed; *P*, persistence time; Ab, antibody; HPRT, hypoxanthine-guanine phosphoribosyltransferase.

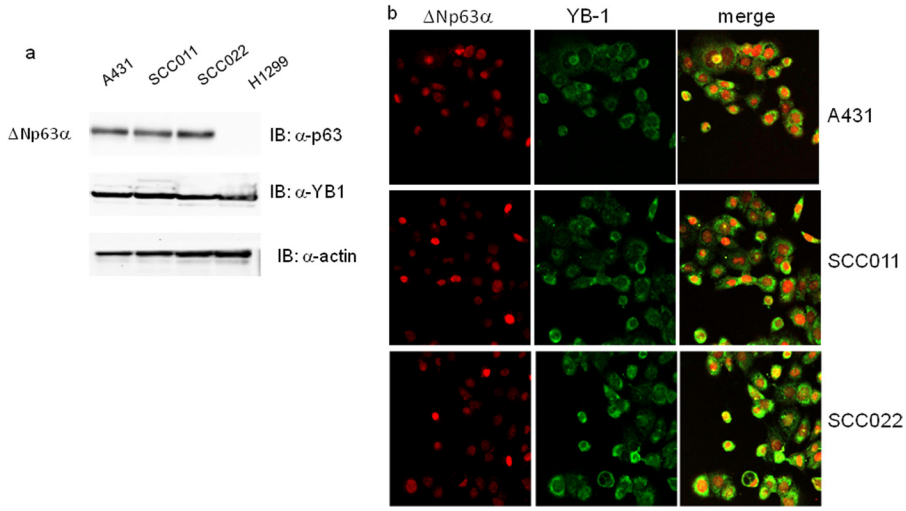

FIGURE 1. **ΔNp63α and YB-1 are co-expressed in squamous carcinoma cell lines.** *a,* whole cell lysates were obtained from H1299 (non-small cell lung carcinoma), A431 (epidermoid carcinoma cell line), and SCC011 and SCC022 (keratinocyte-derived SCC) cells. 30 μg of total protein extracts were separated by SDS-PAGE and subjected to immunoblot (*IB*). Proteins were detected with specific antibodies as indicated. Images were acquired with CHEMIDOC (Bio-Rad) and analyzed with the Quantity-ONE software. *b,* A431, SCC011, and SCC022 cells were seeded (2.5×10^5) on a 35-mm dish and grown on micro cover glasses (BDH). After 24 h at seeding, cells were fixed and subjected to double immunofluorescence using rabbit primary YB-1 antibody and Fitch-conjugated secondary antibodies (*green*). p63 protein was detected using mouse anti-p63 and Cy3-conjugated secondary antibodies (*red*). Images of merge (*yellow*) show the co-expression of two proteins.

transfection. At 24 h after transfection, cells were harvested in 1× PLB buffer (Promega), and luciferase activity was measured using the Dual-Luciferase Reporter system (Promega) using pRL-TK activity as internal control. Firefly-derived luciferase activity was normalized for transfection efficiency. Successful transfection of p63 and silencing of YB-1 was confirmed by immunoblotting.

RNA Immunoprecipitation—1×10^6 MDA-MB-231 cells were seeded in 100-mm plates and transfected with pcDNA3.1 or ΔNp63α expression plasmids. 24 h after transfection, cells were fixed with 1% formaldehyde for 10 min and washed twice in ice-cold PBS. Cell extracts were prepared in RNA immunoprecipitation buffer (0.1% SDS, 1% Triton, 1 mM EDTA, 10 mM Tris, pH 7.5, 0.5 mM EGTA, 150 mM NaCl) supplemented with complete protease inhibitor mixture (Sigma), and sonication was carried out with BANDELINE SONOPULSE HD2200 instrument under the following conditions: 8 pulses of 4 s at 0.250% of intensity. Cell extracts were incubated with anti-YB-1 (3 μg) at 4 °C overnight. The RNA-protein immunocomplexes were precipitated with protein A beads (Roche Applied Science) saturated with tRNA and, after reverse cross-link, subjected to real time PCR.

Semi-quantitative and Real Time PCR—For PCR analysis, total RNA was isolated using the RNA mini extraction kit (Qiagen, GmbH, Hilden, Germany) according to the manufacturer's instructions. Total RNA (1 μg) was used to generate reverse-transcribed cDNA using SuperScript III (Invitrogen). PCR analysis was performed with the following primers: *Twist* (For), 5′-AGAAGTCTGCGGGCTGTG, and *Twist* (Rev), ′-TCTGCAGCTCCTCGTAAGACT; *YB* (For), 5′-CGCAGTG-TAGGAGATGGAGAG, and *YB* (Rev), 5′-GAACACCACCA-GGACCTGTAA; and *HPRT* (For), 5′-CCT GCT GGA TTA CAT TAA AGC, and *HPRT* (Rev), 5′ CTT CGT GGG GTC CTT TTC.

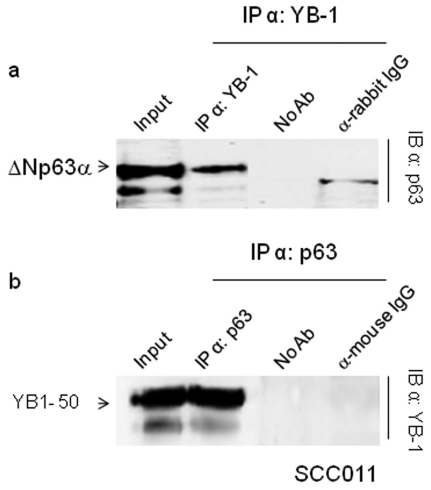

FIGURE 2. **ΔNp63α interacts with YB-1.** *a,* extracts from SCC011 cells were immunoprecipitated (*IP*) with anti-YB-1 antibodies, and the immunocomplexes were blotted and probed with anti-p63 as indicated. *b,* extracts from SCC011 cells were immunoprecipitated with anti-p63 antibodies, and the immunocomplexes were blotted and probed with anti-YB-1. Samples with no antibody (*no Ab*) or irrelevant α-mouse and α-rabbit antibodies were included as controls. *IB*, immunoblot.

SNAIL1 amplification was performed using Quantitect Primers/Hs *SNAIL1* from Qiagen (GmbH, Hilden, Germany). The amplification sequence consisted of 30 cycles of 94 °C for 1 min, 55 °C for 1min, and 72 °C for 1 min. PCR products were resolved by 2% agarose electrophoresis. RT-PCR amplification results were analyzed by Quantity One software (Bio-Rad). Real time PCR was performed with a 7500 RT-PCR Thermo Cycler (Applied Biosystem) as already described (22). *HPRT* was used for normalization. The results were expressed with the value relative to *HPRT* (set at 1) for each mRNA sample.

Immunofluorescence—A431, SCC011, and SCC022 cells (2.5×10^5) were plated in 35-mm dishes and grown on micro cover glasses (BDH). 24 h after seeding, cells were washed with cold phosphate-buffered saline (PBS) and fixed with 4% para-

formaldehyde (Sigma) for 15 min at 4 °C. Cells were permeabilized with ice-cold 0.1% Triton X-100 for 10 min and then washed with PBS. p63 was detected using a 1:200 dilution of the monoclonal antibody 4A4.

YB-1 was detected using 1:100 dilution of the YB-1 antibody (Ab12148). After extensive washing in PBS, the samples were incubated with Cy3-conjugated anti-mouse IgGs and Cy5-conjugated anti-rabbit IgGs at room temperature for 30 min. After PBS washing, the cells were incubated with 10 mg/ml 4′,6′-diamidino-2-phenylindole (DAPI) (Sigma) for 3 min. The glasses were mounted with Moviol (Sigma) and examined under a fluorescence microscope (Nikon). Images were digitally acquired and processed using Adobe Photoshop software CS.

H1299 and MDA-MB-231 cells (5.0×10^5) were plated in 35-mm dishes, grown on micro cover glasses (BDH), and transfected with 0.2 μg of pcDNAYB-1/GFP plasmid with or without 0.6 μg of ΔNp63α or ΔNp63γ plasmid. The GFP empty vector was used as control (data not shown). 24 h after transfection, cells were subjected to the immunofluorescence protocol as described above.

Cytoskeleton Analysis—Actin bundles were stained with TRITC-conjugated phalloidin. Cell fixation was performed with 4% paraformaldehyde for 20 min and then permeabilized with 0.1% Triton X-100 (Sigma) in PBS one time for 10 min. Actin staining was done by incubating sample with TRITC-phalloidin (Sigma) in PBS for 30 min at room temperature. Images of fluorescent cells were collected with a fluorescent inverted microscope (IX81, Olympus, Tokyo, Japan) equipped with an ORCA 2.8 digital camera (Hamamatsu Photonics, Japan).

Time-lapse Microscopy—SCC011 cells were cultured on 35-mm dishes (Corning, NY) at 2×10^4 cells/dish density. ΔNp63α transient silencing was performed as described under "Experimental Procedures." At 48 h from the addition of ΔNp63α si-RNA, the culture dishes were placed in a mini-incubator connected to an automated stage of an optical microscope (Olympus Co., Japan). Images of selected positions of the cell culture were collected in bright field every 10 min for 12 h. The bright field images were mounted to obtain 72-frame time lapse video for each position. Cell trajectories were reconstructed from time lapse video using Metamorph software (Molecular Device, CA). Root mean square speed (*S*) and persistence time (*P*) were chosen as relevant parameters to describe the macroscopic features of cell migration in the different experimental conditions. These parameters were calculated according to the procedure reported by Dunn (24). Briefly, mean-squared displacement of each cell was calculated according to overlapping time interval methods (25). Subsequently, *S* and *P* were estimated by fitting the experimental data of the mean-squared displacement to a linear approximation of the persistent random walk model. The upper limit for the data fitting was set at approximately 200 min for each cell because of the deviation from linearity that was observed at higher time points. The fitting procedure provided (*S*, *P*) pairs for each cell and the statistical significance between *S* and *P* values of the different experimental setups was assessed by performing a nonparametric Kruskal-Wallis test in Matlab (MathWorks, MA). p values < 0.05 were considered significant.

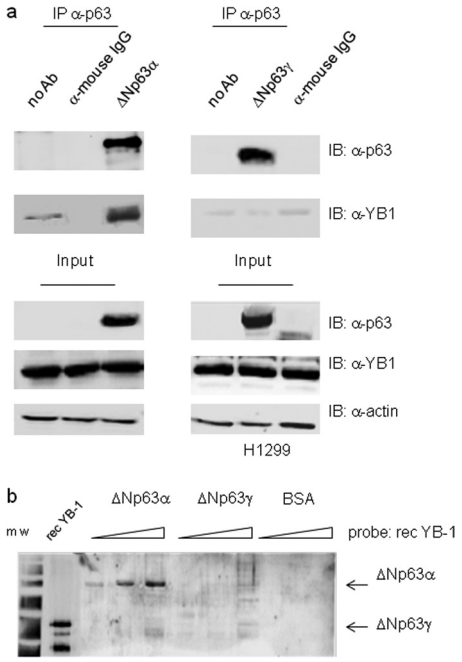

FIGURE 3. **ΔNp63α but not ΔNp63γ interacts with YB-1.** *a,* H1299 cells were transiently transfected with 5 μg of ΔNp63α (*left panel*) or ΔNp63γ (*right panel*) expression vectors. Equal amounts (1 mg) of extracts were immunoprecipitated (*IP*) with anti-p63 antibodies (4A4) or unrelated α-mouse IgG. The immunocomplexes were blotted and probed with anti-p63 and anti-YB-1 antibodies, as indicated. *b,* far Western analysis. Increasing amounts of purified recombinant ΔNp63α (0.2, 0.5, and 1.5), ΔNp63γ (0.2, 0.5, and 1.5), or BSA (0.5 and 1.5) were subjected to SDS-PAGE. After Coomassie staining to monitor equal loading, the proteins were transferred to a PVDF membrane, and the filter was incubated with purified YB-1 recombinant protein (0.8 μg/ml). After extensive washing, the membrane was subjected to immunoblotting (*IB*) with YB-1 antibodies followed by ECL detection. Recombinant YB-1 protein (0.1 μg) was used as positive control. *m.w.,* molecular weight markers.

Cell migration in H1299 cells was evaluated with a similar approach. Briefly, cells were cultured on 35-mm dishes (Corning, NY) at a density of 2×10^4 cells/dish. ΔNp63α expression was induced with 2 μg/ml doxycycline for 48 h. 16 h after transfection, cell dishes were placed in a mini-incubator connected to an automated stage of an optical microscope (Cell[caret]R, Olympus Co., Japan). Time 0 images of selected position were collected in fluorescence to localize transfected cells. Then, at the same positions, images were recorded in bright field every 10 min for 12 h. Data analysis was performed as described above.

RESULTS

YB-1 Interacts with ΔNp63α in Vitro and in Vivo—As a result of a comprehensive screening for ΔNp63α interactors, using affinity purification followed by mass spectrometry, we identified a set of proteins with DNA/RNA binding activity, including YB-1 (26). We decided to confirm the interaction between ΔNp63α and YB-1 in SCC as in this cellular context the *TP63* gene is often amplified and/or overexpressed (27). Immunoblots and immunofluorescence assays performed in A431, SCC022, and SCC011 cell lines showed intense signals for both proteins thus confirming that endogenous YB-1 and ΔNp63α are abundantly co-expressed in human squamous carcinoma cells (Fig. 1, *a* and *b*).

We next performed co-immunoprecipitation experiments in SCC011 cells. Immunocomplexes containing ΔNp63α and

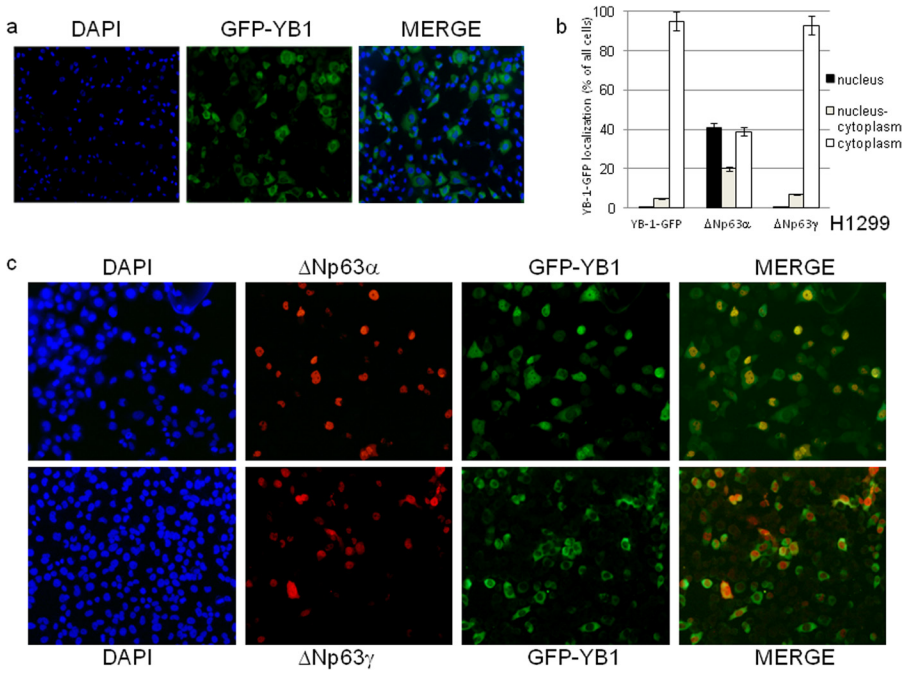

FIGURE 4. **ΔNp63α induces YB-1 nuclear accumulation.** *a*, H1299 cells (2.3×10^5) were seeded at 60% confluency in 24 × 24-mm sterile coverglasses placed in 60-mm dishes and transiently transfected with GFP-YB-1 expression vector (0.3 μg). GFP-YB-1 was detected by direct immunofluorescence. *b*, H1299 cells (2.3×10^5) were seeded as described in *a* and transiently transfected with GFB-YB-1 (0.3 μg) along with 1 μg of ΔNp63α or ΔNp63γ expression vectors. Plot shows the percentage of nuclear (*dark gray*), nucleo-cytoplasmic (*gray*), and cytoplasmic (*white*) GFP-YB-1 in cells transfected with ΔNp63α or ΔNp63γ expression vectors. Each experimental point is the average of counts performed on 100 cells in five independent fields. Each *histogram bar* represents the mean and standard deviation of values from three biological replicates. *c*, H1299 cells (2.3×10^5) were transfected as described in *b*. GFP-YB-1 was detected by direct immunofluorescence (*green*), and p63 was detected using anti-p63 antibodies and secondary anti-mouse Cy3-conjugated (*red*). DAPI was used to stain nuclei.

YB-1 were isolated from total cell lysates, using either antibodies against YB-1 or antibodies against p63 thus confirming the interaction inferred by mass spectrometry (Fig. 2, *a* and *b*). To determine whether YB-1 interacts specifically with the α-isoform of ΔNp63, we transfected p63 null H1299 cells with ΔNp63α or ΔNp63γ to perform co-immunoprecipitation assays. As shown in Fig. 3*a*, YB-1 associates with ΔNp63α but not ΔNp63γ. This result was also confirmed by far Western blot analysis using ΔNp63α, ΔNp63γ, and YB-1 recombinant proteins purified by affinity chromatography (Fig. 3*b*). The obtained results indicate that the α-isoform C-terminal region is involved in the association with YB-1, and the interaction between the two proteins requires no additional factors.

ΔNp63α Induces YB-1 Nuclear Accumulation—It has been reported that YB-1 is ubiquitously expressed and predominantly localized to the cytoplasm (2), ΔNp63α is mainly expressed by basal and myoepithelial cells in skin and glands and is almost completely restricted to the nuclear compartment (29). Because we noticed some overlapping between the p63 and YB-1 immunofluorescence signals in the nucleus of squamous carcinoma cell lines, we sought to determine whether ΔNp63α has an effect on YB-1 subcellular localization. Fusion of YB-1 with the green fluorescent protein (YB-1-GFP) was transfected in H1299 cells. H1299 cells are p63 null and express moderate levels of endogenous YB-1. GFP-positive cells were counted, and 95% showed a strong cytoplasmic signal, although in the remaining 5%, the signal was nuclear or distributed between the nucleus and cytoplasm (Fig. 4, *a* and *b*). A very similar result was observed following ΔNp63γ co-transfection (Fig. 4, *b* and *c*, *lower panel*). Remarkably, combined expression of YB-1-GFP and ΔNp63α caused a dramatic change of YB-1-GFP subcellular localization. In fact, among the GFP-positive cells, more than 40% showed an intense nuclear signal (Fig. 4, *b* and *c*, *upper panel*); an additional 20% exhibited YB-1-GFP almost equally distributed between the nucleus and cytoplasm, and the remaining 40% exhibited exclusively cytoplasmic YB-1-GFP (Fig. 4*b*). As expected, ΔNp63α and ΔNp63γ immunofluorescence signals were almost exclusively nuclear (Fig. 4*c*).

ΔNp63α is a selective nuclear marker of human breast myoepithelial cells. ΔNp63α persists in benign lesions of the breast, although it consistently disappears in invasive carcinomas (30). We transfected ΔNp63α in MDA-MB-231 cells, human metastatic breast carcinoma cells lacking p63 but expressing high level of endogenous YB-1. As shown in Fig. 5, in cells with no detectable p63 signal, YB-1 exhibited a largely prevalent cytoplasmic localization (Fig. 5*a*, *white arrows*), although 95% of ΔNp63α-expressing cells showed a strong YB-1 nuclear staining (Fig. 5*a*, *yellow arrows*). We verified this observation by nuclear/cytoplasmic fractionation of MDA-MB-231 cells transfected with ΔNp63α or ΔNp63γ. Endogenous YB-1 protein, in MDA-MB-231 cells, was detectable as 50- and 36-kDa immunoreactive forms. Both forms of YB-1 appear to accumulate in the nuclear compartment of cells transfected with ΔNp63α but not ΔNp63γ (Fig. 5*b*). Immunoblots with antibodies against PARP-1 (nuclear) and AKT (cytoplasmic) were performed to check for the quality of the fractionation. Interestingly, although the amount of total AKT was comparable, phosphorylated AKT, at serine 473, was enhanced in ΔNp63α but not ΔNp63γ-transfected cells (Fig. 5*b*). This observation was in line with previous data showing the specific

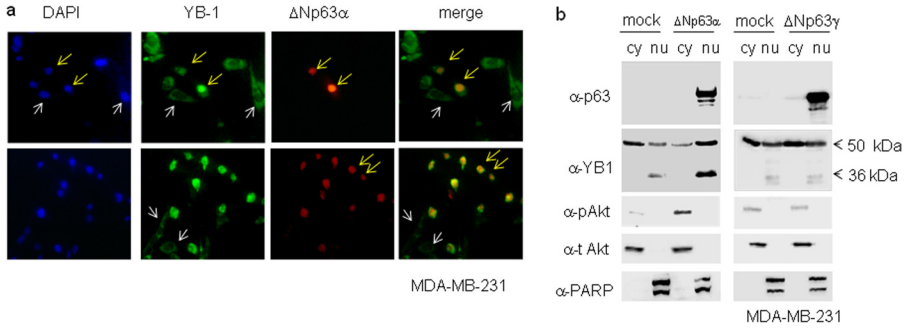

FIGURE 5. **Endogenous YB-1 accumulates in the nucleus of breast cancer cells expressing ΔNp63α.** *a,* MDA-MB-231 cells were seeded at 60% confluency (2.3×10^5) on 24 × 24-mm sterile coverglasses placed in 60-mm dishes and transiently transfected with 1 μg of ΔNp63α expression vector. Cells were fixed and subjected to double indirect immunofluorescence using rabbit primary YB-1 antibody and Fitch-conjugated secondary antibodies (*green*). p63 protein was detected using mouse anti-p63 and Cy3-conjugated secondary antibodies (*red*). DAPI was used to stain nuclei (*blue*). A representative image is given of a cell expressing ΔNp63α and showing nuclear endogenous YB-1 (*yellow arrows*). A representative image is given showing YB-1 cytoplasmic localization in cells bearing no detectable ΔNp63α expression (*white arrows*). *b,* MB-MDA-231 cells were transiently transfected with a fixed amount (5 μg) of an empty vector (*mock*) and ΔNp63α or ΔNp63γ expression vector in 100-mm dishes. 24 h after transfection, cell lysates were fractionated to obtain cytoplasmic (*cy*) and nuclear (*nu*) fractions. 20 μg of nuclear and cytoplasmic extracts were separated by SDS-PAGE and subjected to immunoblot. Proteins were detected with specific antibodies, as indicated. PARP and total AKT were used as nuclear and cytoplasmic controls, respectively, to check for cross-contamination. Images were acquired with CHEMIDOC (Bio-Rad) and analyzed with the Quantity-ONE software.

ability of the ΔNp63α isoform to promote PI3K/AKT pathway activation (31).

We then evaluated the contribution of ΔNp63α to YB-1 subcellular distribution in SCC011 cells expressing both proteins endogenously. To this aim we analyzed YB-1 subcellular distribution by immunoblot on nuclear/cytoplasmic fractions after depletion of ΔNp63α by siRNA. As shown in Fig. 6, *a* and *b*, following p63 knockdown the YB-1 nuclear pool was dramatically reduced, and the 36-kDa form of YB-1 became detectable (Fig. 6*a*).

ΔNp63α and YB-1 Bind to the PIK3CA Gene Promoter and Cooperate in Its Transcriptional Activation—The *PIK3CA* gene encodes the p110α catalytic subunit of the PI3K and is a well characterized YB-1 direct transcriptional target (32). We speculated that ΔNp63α should increase PIK3CA promoter activity because of its ability to cause YB-1 nuclear accumulation. We tested this hypothesis by luciferase assays. As shown in Fig. 7*a*, ΔNp63α transfection in MDA-MB-231 cells caused a relevant increase of the *PIK3CA* promoter activity that was consistently attenuated by YB-1 knockdown. In addition, we observed that ΔNp63α was able to transactivate the *PIK3CA* promoter in a dose-dependent manner, although ΔNp63γ was completely ineffective (Fig. 7*b*).

The role of ΔNp63α and YB-1 in *PIK3CA* promoter activation was thoroughly investigated by chromatin immunoprecipitation (ChIP). We first performed ChIP assays in MDA-MB-231 cells transfected with ΔNp63α or ΔNp63γ using anti-p63 (4A4) antibodies and PIK3CA promoter-specific primers. As shown in Fig. 8*a*, ΔNp63α, but not ΔNp63γ, binds to the genomic sequence of the *PIK3CA* promoter.

Then we evaluated the effect of ΔNp63α expression on the binding of YB-1 to the *PIK3CA* promoter. FLAG-YB-1 was transfected, in MB-MDA-231 cells, with or without ΔNp63α plasmid. ChIP was carried out with anti-FLAG antibodies and coupled with quantitative real time PCR. As show in Fig. 8*b*, FLAG-YB-1 efficiently binds to the *PIK3CA* promoter, and its binding was substantially increased by ΔNp63α. Finally, by using a sequential chromatin immunoprecipitation assay (Re-ChIP) in SCC011 cells, expressing endogenous ΔNp63α and YB-1, we found that both proteins are recruited to the *PIK3CA*

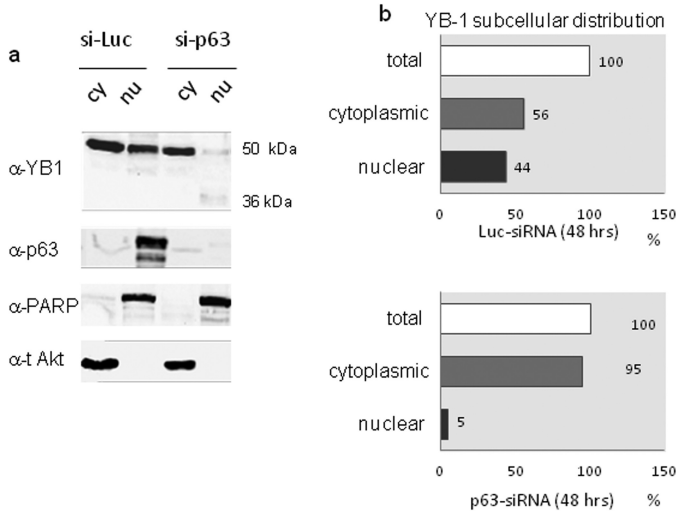

FIGURE 6. **ΔNp63α depletion reduces the pool of nuclear YB-1.** *a,* SCC011 cells were seeded at 60% confluency (1.5×10^6) in 100-mm dishes. 24 h after seeding, cells were transiently silenced with IBONI p63-siRNA pool (20 nm final concentration). 48 h after p63-silencing, cell lysates were fractionated to obtain cytoplasmic (*cy*) and nuclear (*nu*) fractions. Nuclear and cytoplasmic extracts were separated by SDS-PAGE and subjected to immunoblot. Proteins were detected with specific antibodies, as indicated. PARP and total AKT were used as nuclear and cytoplasmic control respectively, to check for cross-contamination. Images were acquired with CHEMIDOC (Bio-Rad) and analyzed with the Quantity-ONE software. *b,* plots show the percentage of YB-1 subcellular distribution in control sample (*upper panel*) and in p63-silenced sample (*lower panel*) considering the total amount of YB-1 between the nucleus and cytoplasm as 100%.

proximal promoter suggesting that they cooperate in *PIK3CA* gene transactivation as a complex (Fig. 8*c*).

ΔNp63α Affects YB-1 Binding to SNAIL and YB-1 mRNAs—Cytoplasmic localization of YB-1 was associated with binding and translational activation of *SNAIL1* mRNA (33). Snail1 protein is a transcriptional repressor of ΔNp63α and E-cadherin and promotes the epithelial-mesenchymal transition in several epithelium-derived cancer cell lines (34). We first observed that ΔNp63α overexpression in MB-MDA-231 caused a reduction of SNAIL1 protein level (Fig. 9*a*). Such a reduction was not associated with a decrease of *SNAIL1* mRNA levels (Fig. 9*b*) thereby suggesting that the SNAIL1 protein was down-regulated at the translational level. We hypothesized that the spe-

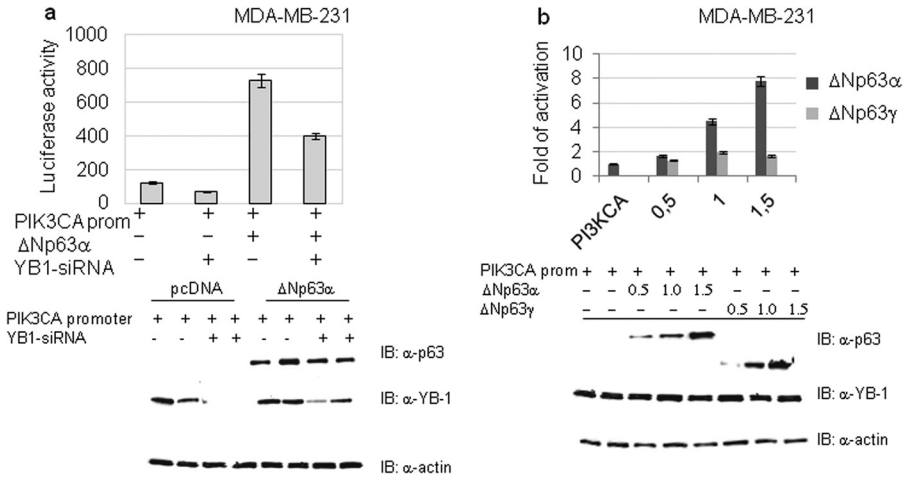

FIGURE 7. **ΔNp63α and YB-1 activates the *PIK3CA* gene promoter.** *a,* MB-MDA− cells were transfected with 1 μg of *PIK3CA* promoter luciferase reporter plasmid. The luciferase activity upon siRNA-mediated knockdown of endogenous YB-1 was measured in the presence or absence of ΔNp63α expression. Values are shown as mean ± S.D. of three biological replicates. The extent of YB-1 knockdown was documented by Western blotting as shown in the *lower panel*. *b,* MB-MDA-231 cells were seeded at 60% confluency (1.2×10^6) in 100-mm dishes and transiently transfected with 1 μg of *PIK3CA* promoter luciferase reporter plasmid and the indicated amounts of ΔNp63α or ΔNp63γ plasmid. Values are the mean ± S.D. of three independent experimental points. *Lower panel,* immunoblotting (*IB*) with indicated antibodies to detect proteins in samples transfected with different amounts of ΔNp63α or ΔNp63γ.

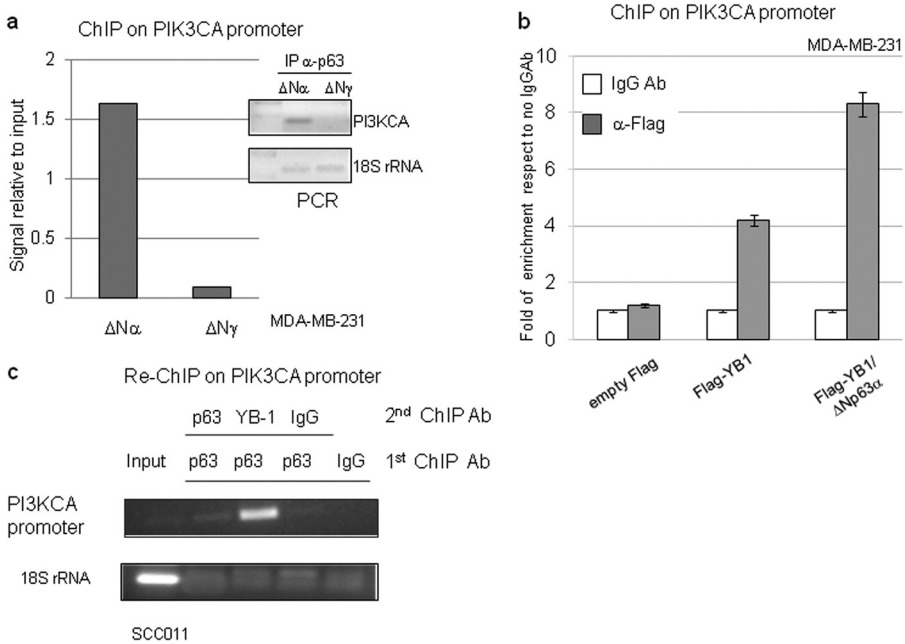

FIGURE 8. **ΔNp63α increases YB-1 binding to the *PIK3CA* gene promoter.** *a,* MDA-MB-231 cells were seeded at 60% confluency (1.2×10^6) in 100-mm dishes and transiently transfected with ΔNp63α or ΔNp63γ plasmid (5 μg). After formaldehyde cross-linking, the DNA-proteins complexes were immunoprecipitated (*IP*) with anti-p63 (4A4) antibody. Immunoprecipitated DNA was PCR-amplified with *PIK3CA* promoter oligonucleotides and 18 S rRNA oligonucleotides (*right*). The data obtained from the ChIP assay were measured by densitometry and are presented as signal relative to the input (*left*). *b,* MDA-MB-231 cells were seeded at 60% confluency (1.2×10^6) in 100-mm dishes and transiently transfected with 3×FLAG empty vector or 3×FLAG-YB-1 (5 μg) plasmid with or without ΔNp63α (2.5 μg) expression vector. The cells were cross-linked with formaldehyde, and DNA-protein complexes were immunoprecipitated with anti-FLAG antibody or irrelevant IgG antibody as negative control. The DNA immunoprecipitates were analyzed by quantitative PCR using *PIK3CA* or *GAPDH* promoter oligonucleotides. Quantitative RT-PCR results were analyzed with the $\Delta\Delta C^T$ method and expressed as fold of enrichment with respect to the IgGAb control samples. Values are represented as the mean of three independent experiments. *c,* SCC011 cells at 85% confluency were fixed with formaldehyde, and the DNA-protein complexes were subjected to sequential ChIP with anti-p63 (4A4), anti-YB-1(Ab12148), or irrelevant IgG antibody as described under "Experimental Procedures." Immunoprecipitated DNA was PCR-amplified with *PIK3CA* promoter primers and 18 S rRNA primers to check the quality of the input chromatin and the cleaning of the other samples.

cific association of ΔNp63α with YB-1 would reduce the amount of YB-1 bound to the *SNAIL1* transcript. To test this hypothesis, we performed RNA-immunoprecipitation coupled with real time PCR to quantitate the amount of *SNAIL1* mRNA bound to endogenous YB-1, in mock and ΔNp63α-transfected MDA-MB-231 cells. The obtained results confirm that ΔNp63α reduces the amount of YB-1 bound to *SNAIL1* transcript (Fig. 9*c*). A similar analysis performed on the *YB-1* transcript gave the same result (Fig. 9*d*).

ΔNp63α Affects Cell Shape and Motility—So far, little attention has been focused on the effects of ΔNp63α on epithelial cancer cell morphology and motility. We have unexpectedly noted a profound change in cell morphology when SCC011 cells were depleted of ΔNp63α by siRNA. SCC011 cells are

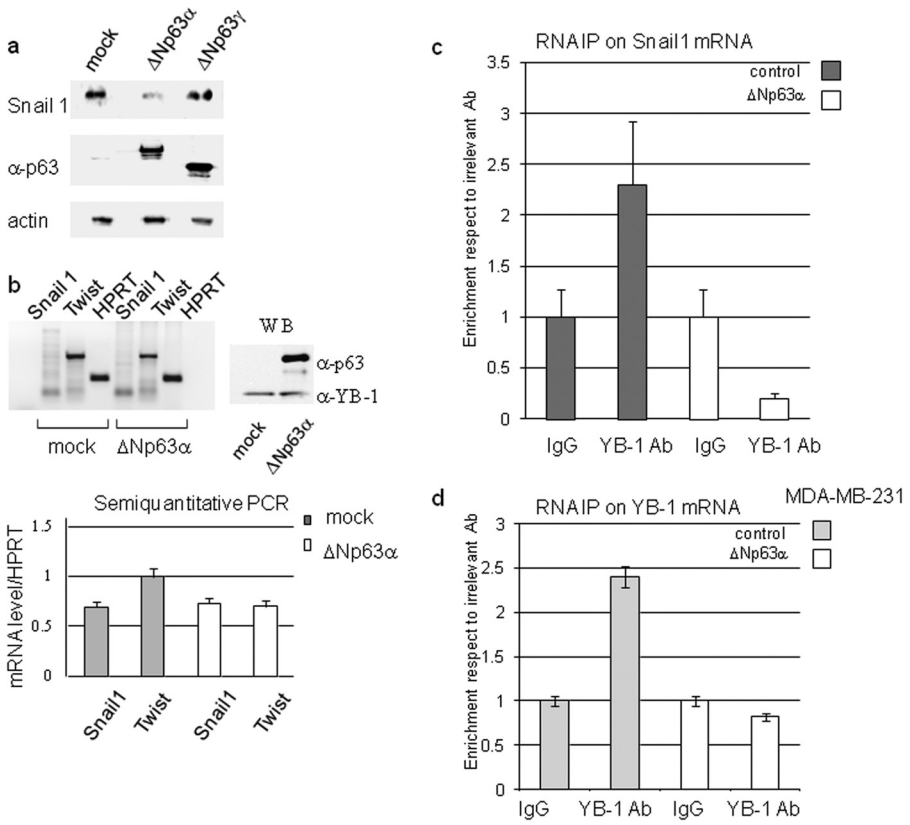

FIGURE 9. **ΔNp63α affects SNAIL1 protein level and YB-1 binding to *SNAIL1* and *YB-1* mRNAs in MDA-MB-231 cells.** *a,* MDA-MB-231 cells were transfected with an empty vector (*mock*) or a fixed amount (1 μg in 60-mm dishes) of ΔNp63α or ΔNp63γ expression vector. 24 h after transfection, cells were harvested, and total extracts were prepared. 20 μg of each extract were loaded on SDS-PAGE and subjected to immunoblot with the indicated antibodies. *b,* MB-MDA-231 cells were transfected with an empty vector or ΔNp63α encoding plasmid. 24 h after transfection, total RNA was purified and retrotranscribed as described under "Experimental Procedures." The expression level of ΔNp63α was checked by immunoblot (*right panel*). *WB,* Western blot. PCR was performed with primers designed to specifically amplify *SNAIL1*, *TWIST*, or *HPRT* transcripts and analyzed by agarose gel electrophoresis (*left panel*). Plot showing the level of *SNAIL1* and *TWIST* transcripts was normalized respect to *HPRT*. Values are the mean of three independent experiments (*lower panel*). Nuclear extracts from ΔNp63α transfected MB-MDA-231 cells were immunoprecipitated with anti-YB-1 antibody. After reverse cross-linking, the YB-1-bound RNA was purified, retrotranscribed, and subjected to quantitative RT-PCR analysis using oligonucleotides designed to specifically amplify *SNAIL1* transcript (*c*) or *YB-1* transcript (*d*). Plots represent the % of enrichment of **SNAIL1/YB-1** transcript normalized as indicated under "Experimental Procedures." 1:50 of the input extract was loaded as control. The values are the means ± S.D. of three biological replicates.

round in shape, and under high density culture conditions, they appear orderly arranged with tight cell-cell contacts. Conversely, ΔNp63α-depleted cells tend to lose their contacts and exhibited an unusual extended phenotype that was distinct from that of the control cells cultured at the same density (Fig. 10*a*). The unusual change in morphology of ΔNp63α-depleted cells indicated possible alterations in actin cytoskeleton organization. Therefore, we examined the status of actin stress fibers at the level of individual cells, in control and ΔNp63α-depleted cells, with TRITC-phalloidin followed by fluorescent microscopy. As shown in Fig. 10*b*, the control cells exhibited a diffuse pattern of actin staining, although ΔNp63α-depleted cells displayed a more substantial enhancement of actin stress fibers suggesting an inhibitory effect of ΔNp63α on cancer cell motility. Remarkably, compared with the control cells, ΔNp63α-depleted SCC011 cells express higher levels of N-cadherin and lower amounts of E-cadherin, suggesting that they were undergoing epithelial to mesenchymal trans-differentiation (Fig. 10*c*).

We determined the influence of ΔNp63α on cell motility by time-lapse microscopy using siRNA-based silencing of endogenous ΔNp63α in SCC011 cells. Silencing efficiency was about 90% as determined by fluorescent staining for p63 protein (data not shown). SCC011 migration was characterized by oscillations of the cells around their initial adhesion site. These oscillations occurred at random directions in space, as reported in the windrose plots of the trajectories (Fig. 10*d*, *inset*). Conversely, ΔNp63α silenced cells display much wider oscillations (Fig. 10*d*). These observations were confirmed by the analysis of the migration parameters "Speed (*S*)" and "persistence time (*P*)" that are computed from cell tracks and are a measure of the frequency of cell steps and of the minimum time that is necessary for a cell to significantly change direction. According to these parameters, SCC011 exhibit lower speeds ($p < 0.05$) and shorter persistence times (0.26 ± 0.03 μm/min and 6.5 ± 0.7 min) with respect to ΔNp63α-depleted cells (0.44 ± 0.05 μm/min and 8.2 ± 2.3 min). These data indicate a role for ΔNp63α in affecting cell motility. In particular, the absence of ΔNp63α causes the cells to migrate faster with less frequent direction changes, which enables the cells to explore larger areas in a fixed time interval.

To gain a better insight into the effects of the interaction of ΔNp63α and YB-1 on cell migration, we used the genetically modified Tet-On-H1299 cells expressing ΔNp63α upon Dox addition (Fig. 11*a*). Cells were transfected with GFP or GFP-

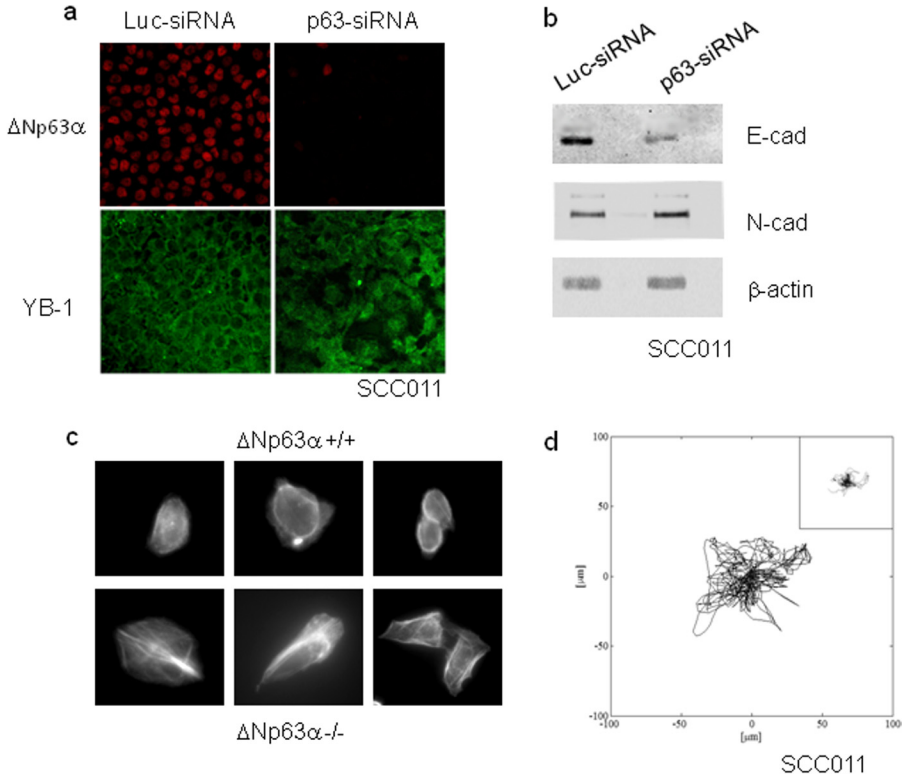

FIGURE 10. **ΔNp63α affects cell shape and motility.** *a,* SCC011 cells were transiently silenced with IBONI p63-siRNA pool (20 nm final concentration). Cells were fixed and subjected to double immunofluorescence 48 h after silencing, as already described. *b,* protein extracts from control and p63-depleted cells were separated by SDS-PAGE and subjected to immunoblot. Proteins were detected with specific antibodies. *c,* actin staining with TRITC-conjugated phalloidin of control and ΔNp63α-depleted SCC011 cells (see "Experimental Procedures"). Cell expressing ΔNp63α displayed a round morphology. Conversely, ΔNp63α-depleted cells had a polarized morphology with more evident lamellipodia and trailing edge. *d,* windrose plot of trajectories described by ΔNp63α depleted SCC011 or SCC011 control cells (*inset*) in 12-h time lapse video. Only 15 cell trajectories were reported in each plot for graphical clarity. *E-cad*, E-cadherin; *N-cad*, N-cadherin.

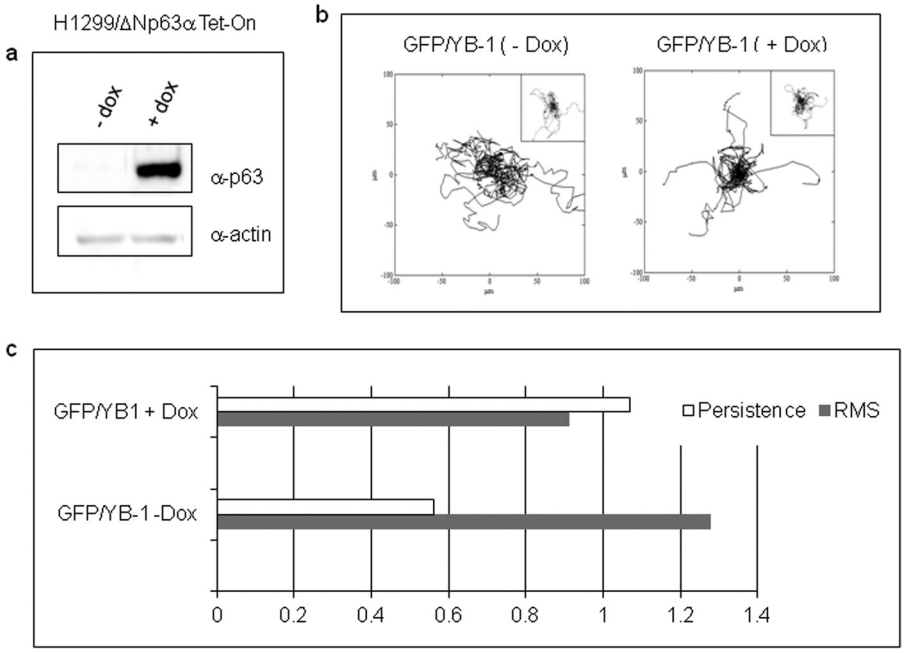

FIGURE 11. **Effects of ΔNp63α and YB-1 on cell migration.** *a,* after being subjected to the migration experiment, extracts from Tet-On H1299 cells, induced (+*dox*) or not (−*dox*) with doxycycline, were prepared and subjected to immunoblot analysis to monitor ΔNp63α induced expression. *b,* trajectories of GFP/YB-1- or GFP (*insets*)-transfected cells. Inducible H1299/ΔNp63α cells were transfected with a fixed amount of GFP-YB-1(1 μg) or GFP empty vector (1 μg). 4 h after transfection, 2 μg/ml doxycycline was added to induce ΔNp63α expression, and 16 h later uninduced (−*Dox*) and induced (+*Dox*) cells were tracked with optical microscopy. Plots represent data from the following number of cells (YB-1/−dox 79; YB−1/+dox 69; control/−dox 44; control/+dox 49). *c*, *bar chart* of speed (*S*; *gray bars*) and persistence ratios (*P*; *white bars*). The ratios are computed by dividing the population average values of speed and persistence for H1299 control cells (− *Dox*) and ΔNp63α-expressing cells (+ *Dox*).

YB-1 plasmid, and unfluorescent and fluorescent cells were tracked separately. Cells migrated describing trajectories that are randomly distributed in plane, as depicted in plots of Fig. 10*b*. In Dox-free medium (−Dox), GFP-YB-1-expressing cells were characterized by a significantly higher *S* and lower *P* (0.69 ± 0.04 μm/min and 8.4 ± 0.5 min) than cells expressing GFP alone (0.54 ± 0.05 μm/min and 15 ± 2.1 min). Remarkably, in Dox-supplemented medium (+Dox), GFP-YB-1-expressing cells exhibited *S* and *P* values (0.62 ± 0.05 μm/min and 9.2 ± 1.0 min), which were not significantly different from those of cells transfected with GFP alone (0.68 ± 0.05 μm/min and 8.6 ± 0.9 min) (Fig. 10*c*). We also noticed that unfluorescent cells were characterized by the highest *S* values suggesting that expression of the green fluorescent protein alters cell migration to some extent (data not shown). However, *S* of unfluorescent cells with or without Dox was comparable. Overall, these data indicate that ΔNp63α expression can revert the increase of cell motility induced by YB-1-enforced expression.

DISCUSSION

In normal epithelium, ΔNp63α protein expression is abundant in basal cells and decreases with differentiation (35). Transient overexpression of ΔNp63α was shown to enhance cell proliferation, inhibit differentiation, and promote malignant conversion of primary keratinocytes (36, 37). However, enhanced and stable expression of ΔNp63α, as seen in human squamous cell carcinomas, is believed to alter skin homeostasis and be directly implicated in the etiology of human cutaneous carcinomas. In normal cells, YB-1 is mainly detected in the cytosol, particularly at the perinuclear region, with a minor pool located in the nucleus (38). Nuclear localization of YB-1 appears to be critical for its role in promoting proliferation. In fact, in the nucleus YB-1 may not only act as a transcription factor of various genes that are closely associated with DNA replication, cell proliferation, and multidrug resistance but also exert SOS signaling against genotoxic factors that could undermine the integrity of highly proliferative basal cells.

This report unveils a novel protein-protein association involving ΔNp63α and YB-1. This specific association results in the accumulation of nuclear YB-1, as shown by immunofluorescence assays and nuclear-cytoplasmic fractionation. Moreover, we have demonstrated that ΔNp63α and YB-1 cooperate in *PIK3CA* gene activation with both being recruited to the *PIK3CA* proximal promoter, thereby supporting the hypothesis that this molecular association can function as a pro-survival mechanism. It's worth mentioning, however, that additional mechanisms have been described to activate and translocate YB-1 to the nucleus (8).

Into the cytoplasm, YB-1 is known to act as a positive translational regulator of SNAIL1, a potent epithelial to mesenchymal transition inducer able to reduce cell-cell adhesion and increase migratory properties of cancer cells (33). Accordingly, we have observed that enforced expression of YB-1 in tumor cells increases their motility and migration speed. Remarkably, we have shown that ΔNp63α-enforced expression reduces the activating binding of YB-1 to the *SNAIL1* transcript and restores a normal migratory behavior to YB-1-overexpressing cells. However, depletion of endogenous ΔNp63α in SCC cells results in SNAIL1 up-regulation, E-cadherin repression, and increased cell motility.

Finally, cytoplasmic YB-1 is known to bind to actin filaments and causes actin fibers to bundle *in vitro* (39). It was also demonstrated that YB-1 plays a relevant role in the organization of the actin cytoskeleton by binding to F-actin and microtubules (40, 41). In normal conditions, SCC011 cells are round in shape and exhibit a more diffuse actin distribution, as determined by phalloidin staining. Here, we show that ΔNp63α depletion in SCC cells promotes morphological changes and causes a profound cytoskeleton reorganization. ΔNp63α-depleted cells had a polarized morphology with more evident lamellipodia and trailing edge. They also exhibited mature stress fibers suggesting a pro-migratory behavior. The alterations in cell morphology and motility of ΔNp63α-depleted SCC cells closely resemble the process of epithelial to mesenchymal transition (28). We can speculate that the absence of ΔNp63α can promote F-actin polymerization by YB-1 thereby promoting the formation of stress fibers.

All together, our data indicate that ΔNp63α-YB-1 association into the nucleus can act as a pro-proliferative/survival mechanism, although the loss of p63 predisposes the acquisition of mesenchymal characteristics at least in part by restoring YB-1 cytoplasmic functions. Moreover, we suggest that the balance between ΔNp63α and YB-1 protein levels could be critical for the transition to a mesenchyme-like phenotype explaining, at least in part, why ΔNp63α depletion promotes cancer cell invasion and spreading (35).

Acknowledgments—We thank Sandra Dunn, Arezoo Astanehe, Karsten Jurchott, and Jill Gershan for kindly providing expression and reporter constructs. We acknowledge Dr. Caterina Missero for providing SCC cell lines.

REFERENCES

1. Matsumoto, K., and Bay, B. H. (2005) Significance of the Y-box proteins in human cancers. *J. Mol. Genet. Med.* **1,** 11–17
2. Homer, C., Knight, D. A., Hananeia, L., Sheard, P., Risk, J., Lasham, A., Royds, J. A., and Braithwaite, A. W. (2005) Y-box factor YB-1 controls p53 apoptotic function. *Oncogene* **24,** 8314–8325
3. Wu, J., Stratford, A. L., Astanehe, A., and Dunn, S. (2007) YB-1 is a transcription/translation factor that orchestrates the oncogenome by hardwiring signal transduction to gene expression. *Translational Oncogenomics* **2,** 49–65
4. Evdokimova, V., Ruzanov, P., Anglesio, M. S., Sorokin, A. V., Ovchinnikov, L. P., Buckley, J., Triche, T. J., Sonenberg, N., and Sorensen, P. H. (2006) Akt-mediated YB-1 phosphorylation activates translation of silent mRNA species. *Mol. Cell. Biol.* **26,** 277–292
5. Sou, P. W., Delic, N. C., Halliday, G. M., and Lyons, J. (2010) Snail transcription factors in keratinocytes. Enough to make your skin crawl. *Int. J. Biochem. Cell Biol.* **42,** 1940–1944
6. Evdokimova, V., Tognon, C., Ng, T., Ruzanov, P., Melnyk, N., Fink, D., Sorokin, A., Ovchinnikov, L. P., Davicioni, E., Triche, T. J., and Sorensen, P. H. (2009) Translational activation of Snail and other developmentally regulated transcription factors by YB-1 promotes an epithelial-mesenchymal transition. *Cancer Cell* **15,** 402–415
7. Jurchott, K., Bergmann, S., Stein, U., Walther, W., Janz, M., Manni, I., Piaggio, G., Fietze, E., Dietel, M., and Royer, H. D. (2003) YB-1 as a cell cycle-regulated transcription factor facilitating cyclin A and cyclin B1 gene expression. *J. Biol. Chem.* **278,** 27988–27996
8. Sutherland, B. W., Kucab, J., Wu, J., Lee, C., Cheang, M. C., Yorida, E., Turbin D., Dedhar, S., Nelson, C., and Pollak, M. (2005) Akt phosphory-

lates the Y-box binding protein 1 at Ser-102 located in the cold shock domain and affects the anchorage-independent growth of breast cancer cells. *Oncogene* **24,** 4281–4292
9. Higashi, K., Tomigahara, Y., Shiraki, H., Miyata, K., Mikami, T., Kimura, T., Moro, T., Inagaki, Y., and Kaneko, H. (2011) A novel small compound that promote nuclear translocation of YB-1 ameliorates experimental hepatic fibrosis in mice. *J. Biol. Chem.* **286,** 4485–4492
10. Zhang, Y. F., Homer, C., Edwards, S. J., Hananeia, L., Lasham, A., Royds, J., Sheard, P., and Braithwaite, A. W. (2003) Nuclear localization of Y-box factor YB-1 requires wild type p53. *Oncogene* **22,** 2782–2794
11. Moll, U. M. (2004) p63 and p73. Roles in development and tumor formation. *Mol. Cancer Res.* **2,** 371–386
12. Yang, A., Kaghad, M., Wang, Y., Gillett, E., Fleming, M. D., Dötsch, V., Andrews, N. C., Caput, D., and McKeon, F. (1998) p63, a p53 homolog at 3q27–29, encodes multiple products with transactivating, death inducing, and dominant-negative activities. *Mol. Cell* **2,** 305–316
13. Yang, A., Schweitzer, R., Sun, D., Kaghad, M., Walker, N., Bronson, R. T., Tabin, C., Sharpe, A., Caput, D., Crum, C., and McKeon, F. (1999) p63 is essential for regenerative proliferation in limb, craniofacial, and epithelial development. *Nature* **398,** 714–718
14. Parsa, R., Yang, A., McKeon, F., and Green, H. (1999) Association of p63 with proliferative potential in normal and neoplastic human keratinocyte. *J. Invest. Dermatol.* **113,** 1099–1105
15. Fukunishi, N., Katoh, I., Tomimori, Y., Tsukinoki, K., Hata, R., Nakao, A., Ikawa, Y., and Kurata, S. (2010) Induction of ΔNp63 by the newly identified keratinocyte-specific transforming growth factor β-signaling pathway with Smad2 and IkB kinase α in squamous cell carcinoma. *Neoplasia* **12,** 969–979
16. Higashikawa, K., Yoneda, S., Tobiume, K., Taki, M., Shigeishi, H., and Kamata, N. (2007) Snail induced down-regulation of ΔNp63α acquires invasive phenotype of human squamous cell carcinoma. *Cancer Res.* **67,** 9207–9213
17. Graziano, V., and De Laurenzi, V. (2011) Role of p63 in cancer development. *Biochim. Biophys. Acta* **1816,** 57–66
18. Adorno, M., Cordenonsi, M., Montagner, M., Dupont, S., Wong, C., Hann, B., Solari, A., Bobisse, S., Rondina, M. B., Guzzardo, V., Parenti, A. R., Rosato, A., Bicciato, S., Balmain, A., and Piccolo, S. (2009) A mutant-p53/Smad complex opposes p63 to empower TGFβ-induced metastasis. *Cell* **137,** 87–98
19. Di Costanzo, A., Festa, L., Duverger, O., Vivo, M., Guerrini, L., La Mantia, G., Morasso, M. I., and Calabrò, V. (2009) Homeodomain protein Dlx3 induces phosphorylation-dependent p63 degradation. *Cell Cycle* **8,** 1185–1195
20. Lefort, K., Mandinova, A., Ostano, P., Kolev, V., Calpini, V., Kolfschoten, I., Devgan, V., Lieb, J., Raffoul, W., Hohl, D., Neel, V., Garlick, J., Chiorino, G., and Dotto, G. P. (2007) Notch1 is a p53 target gene involved in human keratinocyte tumor suppression through negative regulation of ROCK1/2 and MRCKα kinases. *Genes Dev.* **21,** 562–577
21. Lo Iacono, M., Di Costanzo, A., Calogero, R. A., Mansueto, G., Saviozzi, S., Crispi, S., Pollice, A., La Mantia, G., and Calabrò, V. (2006) The Hay Wells syndrome-derived TAp63αQ540L mutant has impaired transcriptional and cell growth regulatory activity. *Cell Cycle* **5,** 78–87
22. Radoja, N., Guerrini, L., Lo Iacono, N., Merlo, G. R., Costanzo, A., Weinberg, W. C., La Mantia, G., Calabrò, V., and Morasso M. I. (2007) Homeobox gene Dlx3 is regulated by p63 during ectoderm development. Relevance in the pathogenesis of ectodermal dysplasia. *Development* **134,** 13–18
23. Cui, S., Arosio, D., Doherty, K. M., Brosh, R. M., Jr., Falaschi, A., and Vindigni, A. (2004) Analysis of the unwinding activity of the dimeric RECQ1 helicase in the presence of human replication protein. *Nucleic Acid Res.* **32,** 2158–2170
24. Dunn, G. A. (1983) Characterizing a kinesis response. Time averaged measures of cell speed and directional persistence. *Agents Actions Suppl.* **12,** 14–33
25. Dickinson, R. B., and Tranquillo, R. T. (1993) Optimal estimation of cell movement indices from the statistical analysis of cell tracking data. *AIChE J.* **39,** 1995–2010
26. Amoresano, A., Di Costanzo, A., Leo, G., Di Cunto, F., La Mantia, G., Guerrini, L., and Calabrò, V. (2010) Identification of ΔNp63α protein interactions by mass spectrometry. *J. Proteome Res.* **9,** 2042–2048
27. Hibi, K., Trink, B., Patturajan, M., Westra, W. H., Caballero, O. L., Hill, D. E., Ratovitski, E. A., Jen, J., and Sidransky, D. (2000) AIS is an oncogene amplified in squamous cell carcinoma. *Proc. Natl. Acad. Sci U.S.A.* **97,** 5462–5467
28. Lee, J. M., Dedhar, S., Kalluri, R., and Thompson, E. W. (2006) The epithelial-mesenchymal transition. New insights in signaling, development, and disease. *J. Cell Biol.* **172,** 973–981
29. Di Como, C. J., Urist, M. J., Babayan, I., Drobnjak, M., Hedvat, C. V., Teruya-Feldstein, J., Pohar, K., Hoos, A., and Cordon-Cardo, C. (2002) p63 expression profiles in human normal and tumor tissues. *Clin. Cancer Res.* **8,** 494–501
30. Barbareschi, M., Pecciarini, L., Cangi, M. G., Macrì, E., Rizzo, A., Viale, G., and Dogliosi, C. (2001) p63, a p53 homologue, is a selective nuclear marker of myoepithelial cells of the human breast. *Am. J. Surg. Pathol.* **25,** 1054–1060
31. Danilov, A. V., Neupane, D., Nagaraja, A. S., Feofanova, E. V., Humphries, L. A., DiRenzo, J., and Korc, M. (2011) ΔNp63α-mediated induction of epidermal growth factor receptor promotes pancreatic cancer cell growth and chemoresistance. *PLoS One* **6,** e26815
32. Astanehe, A., Finkbeiner, M. R., Hojabrpour, P., To, K., Fotovati, A., Shadeo, A., Stratford, A. L., Lam, W. L., Berquin, I. M., Duronio, V., and Dunn, S. E. (2009) The transcriptional induction of PIK3CA in tumor cells is dependent on the oncoprotein Y-box binding protein-1. *Oncogene* **28,** 2406–2418
33. Evdokimova, V., Tognon, C., Ng, T., Ruzanov, P., Melnyk, N., Fink, D., Sorokin, A., Ovchinnikov, L. P., Davicioni, E., Triche, T. J., and Sorensen, P. H. (2009) Reduced proliferation and enhanced migration: Two sides of the same coin? Molecular mechanisms of metastatic progression by YB-1. *Cancer Cell* **15,** 402–415
34. Peiró, S., Escrivà, M., Puig, I., Barberà, M. J., Dave, N., Herranz, N., Larriba, M. J., Takkunen, M., Francí, C., Muñoz, A., Virtanen, I., Baulida, J., and García de Herreros, A. (2006) Snail1 transcriptional repressor binds to its own promoter and controls its expression. *Nucleic Acids Res.* **34,** 2077–2084
35. Barbieri, C. E., Tang, L. J., Brown, K. A., and Pietenpol, J. A. (2006) Loss of p63 leads to increased cell migration and up-regulation of genes involved in invasion and metastasis. *Cancer Res.* **66,** 7589–7597
36. King, K. E., Ponnamperuma, R. M., Yamashita, T., Tokino, T., and Lee, L. A. (2003) ΔNp63α functions as a positive and negative transcriptional regulator and blocks *in vitro* differentiation of murine keratinocytes. *Oncogene* **22,** 3635–3644
37. Ha, L., Ponnamperuma, R. M., Jay, S., Ricci, M. S., and Weinberg, W. C. (2011) Dysregulated ΔNp63α inhibits expression of Ink4a/arf, blocks senescence, and promotes malignant conversion of keratinocytes. *PLoS One* **6,** e21877
38. Koike, K., Uchiumi, T., Ohga, T., Toh, S., Wada, M., Kohno, K., and Kuwano, M. (1997) Nuclear translocation of the Y-box binding protein by ultraviolet irradiation. *FEBS Lett.* **417,** 390–394
39. Ruzanov, P. V., Evdokimova, V. M., Korneeva, N. L., Hershey, J. W., and Ovchinnikov, L. P. (1999) Interaction of the universal mRNA-binding protein, p50, with actin. A possible link between mRNA and microfilaments. *J. Cell Sci.* **20,** 3487–3496
40. Uchiumi, T., Fotovati, A., Sasaguri, T., Shibahara, K., Shimada, T., Fukuda, T., Nakamura, T., Izumi, H., Tsuzuki, T., Kuwano, M., and Kohno, K. (2006) Yb-1 is important for an early stage embryonic development. Neural tube formation and cell proliferation. *J. Biol. Chem.* **281,** 40440–40449
41. Chernov, K. G., Mechulam, A., Popova, N. V., Pastre, D., Nadezhdina, E. S., Skabkina, O. V., Shanina, N. A., Vasiliev, V. D., Tarrade, A., Melki, J., Joshi, V., Baconnais, S., Toma, F., Ovchinnikov, L. P., and Curmi, P. A. (2008) Yb-1 promotes microtubules assembly *in vitro* through interaction with tubulin and microtubules. *BMC Biochem.* 9–23

Gene Regulation:

The p63 Protein Isoform ΔNp63α Modulates Y-box Binding Protein 1 in Its Subcellular Distribution and Regulation of Cell Survival and Motility Genes

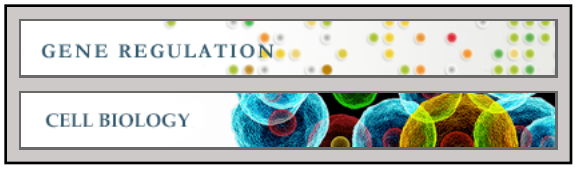

Antonella Di Costanzo, Annaelena Troiano, Orsola di Martino, Andrea Cacace, Carlo F. Natale, Maurizio Ventre, Paolo Netti, Sergio Caserta, Alessandra Pollice, Girolama La Mantia and Viola Calabrò

J. Biol. Chem. 2012, 287:30170-30180.
doi: 10.1074/jbc.M112.349951 originally published online July 11, 2012
